Universitat Politècnica de Catalunya

Programa de Doctorat:

Automàtica, Robòtica i Visió

Tesis Doctoral

Health-aware Predictive Control Schemes Based on Industrial Processes

Fatemeh Karimi Pour

Directors: Prof. Vicenç Puig Cayuela i Prof. Gabriela Cembrano Gennari

June 2020

In memory of my father

To my mother

To my siblings

To my love

Acknowledgement

Reaching to the end of doctoral journey is an exciting moment. It has been a period of my life full of anecdotes and experiences. I have experienced failure, depression and hope to learn the pattern of success. While doing research, there are a number of people with whom I always received support and encouragement. I do want to express my gratitude to those who participated in this moment of my life.

First, I would like to deeply thank my supervisors, Prof. Vicenç Puig Cayuela, Prof. Gabriela Cembrano and Prof. Carlos Ocampo-Martinez from Universitat Politècnica de Catalunya (UPC) whom I received many supports during this research journey. They have contributed in my professional training with their critiques and persistent questioning, being always available for academic discussions. They have also given me the possibility to begin this challenging and wonderful journey from which I have learned plenty of things.

Second, I want to thank Prof. Didier Theilliol from Université de Lorraine to accept me as a visitor researcher in Laboratoire Le Centre de Recherche en Automatique de Nancy (CRAN) and for his time to discuss and make me analyse interesting issues regarding LMI and battery's life and for giving me the opportunity to interact with excellent researchers.

Third, I sincerely thank Agència de Gestió de Ajust Universitaris i de Recerca AGAUR for having granted the FI scholarship for me to study the doctoral degree at Universitat Politècnica de Catalunya (UPC). I would also like to thank the projects DEOCS (ref. DPI2016-76493-C3-3-R) and HARCRICS (ref. DPI2014-58104-R) for partially supporting me.

Fourth, I want to thank all the people at Institut de Robótica i Informàtica Industria (IRI), especially office No. 7, to provide me a friendly atmosphere, which allows me to focus on my research and enjoy my life in Barcelona.

Finally, *but being the most important acknowledgment*, I owe my gratitude to my dear mother Samireh and to my beloved father Ghaleb who died years ago... I miss you daddy. Essential aspects that are not learned in the academic environment, but that without them, the successful culmination of this journey would not have been possible. I do thank them for having taught me to have perseverance and to pursue goals in an honest manner. Likewise, I would like to thank my siblings, for being exemplar of discipline and who played such important roles along my life journey. I also express my thankfulness to Masoud Pourasghar-Lafmejani for his eternal support and understanding. He has always made me smile in stressful moments, and has provided a lot of happiness to my days with his love.

Fatemeh Karimi Pour
Barcelona, Spain, 2019

Abstract

This thesis intends to provide theoretical and practical contributions on safety and control of industrial systems, especially in the mathematical form of uncertain systems. The research is motivated by real applications, such as pasteurization plant, water networks and autonomous systems. All of them require a specific control system to provide proper management able to take into account their particular features and operating limits in presence of uncertainties related to their operation and failures from component breakdowns.

Most of the real systems present nonlinear behaviors. One promising approach to deal with non-linear systems is representing them by means of Linear Parameter Varying (LPV) and Takagi-Sugeno (TS) models. In this thesis, an Economic Model Predictive Control (MPC) approach based on LPV/TS models is proposed and the stability of the proposed approach is guaranteed by using a region constraint on the terminal state. Besides, the MPC-LPV strategy is extended to deal with systems with varying delays affecting states and inputs. The control approach allows the controller to accommodate the scheduling parameters and delay change. By computing the prediction of the state variables and delay along a prediction time horizon, the system model can be modified according to the evaluation of the estimated state and delay at each time instant.

To increase the system reliability, anticipate the appearance of faults and reduce the operational costs, actuator health monitoring should be considered. Different strategies are studied for assessing the system health. First, the damage is assessed with the rainflow-counting algorithm that allows estimating the component fatigue and control objective is modified by adding an extra criterion that takes into account the accumulated damage. Besides, two different health-aware economic predictive control strategies that aim to minimize the damage of components are presented.

Then, an economic health-aware MPC approach is developed to determine the components and system reliability in the MPC model using an LPV modeling approach that maximizes the availability of the system by considering system reliability. Then, another approach is proposed using chance-constraint programming to compute an optimal list replenishment policy based on a desired risk acceptability level and aiming to dynamically determine safety stocks in flow-based networks to satisfy non-stationary flow demands. Finally, an innovative health-aware control approach for autonomous racing vehicles allowing to simultaneously control them at the driving limits and to follow the desired path based on maximization of the battery RUL. The control design is divided into two layers with different time scale, path planner and controller. The proposed approach is formulated as an optimal on-line robust LMI based MPC driven from Lyapunov stability. The controller gain are determined by solving an LPV-LQR problem using LMIs and including an integral action for improving trajectory tracking.

Keywords: Model predictive control, economic optimization, linear parameter varying, Takagi-Sugeno, time-varying delay, health-aware control, reliability, remaining useful life, autonomous system, industrial process.

Resumen

Esta tesis presenta diversas contribuciones teóricas y prácticas sobre seguridad y control de sistemas industriales con dinámicas no lineales. La investigación está motivada por diversas aplicaciones reales (una planta de pasteurización, redes de agua y sistema autónomos). Cada uno de las cuales requiere un sistema de control específico para conseguir una gestión adecuada capaz de tener en cuenta sus características particulares y límitesó de operación en presencia de incertidumbres relacionadas con su operación y fallas de averías de componentes.

De acuerdo con que la mayoría de los sistemas reales tienen comportamientos no lineales, puede aproximarse a ellos mediante modelos inciertos lineales politópicos como los modelos de Lineal Variación de Parámetros (LPV) y Takagi-Sugeno (TS). Por lo tanto, se propone un nuevo enfoque de Control Predictivo del Modelo (MPC) económico basado en modelos LPV/TS y la estabilidad del enfoque propuesto se certifica mediante el uso de una restricción de región en el estado terminal. Además, la estrategia MPC-LPV se extiende en función del sistema con diferentes demoras que afectan los estados y las entradas. El enfoque de control permite al controlador acomodar los parámetros de programación y retrasar el cambio. Al calcular la predicción de las variables de estado y el retraso a lo largo de un horizonte de tiempo de predicción, el modelo del sistema se puede modificar de acuerdo con la evaluación del estado estimado y el retraso en cada instante de tiempo.

Para aumentar la confiabilidad del sistema, anticipar la aparición de fallas y reducir los costos operativos, se debe considerar el monitoreo del estado del actuador. Con respecto a varios tipos de fallas del sistema, se estudian diferentes estrategias para obtener fallas del sistema. Primero, el daño se evalúa con el algoritmo de conteo de flujo de lluvia que permite estimar la fatiga del componente y el objetivo de control se modifica agregando un criterio adicional que tiene en cuenta el daño acumulado. Además, se presentan dos estrategias diferentes de control predictivo económico que

tienen en cuenta la salud y tienen como objetivo minimizar el daño de los componentes.

Luego, se desarrolla un controlador MPC económico con conciencia de salud para calcular los componentes y la confiabilidad del sistema en el modelo MPC utilizando un enfoque de modelado LPV y maximiza la disponibilidad del sistema mediante la estimación de la confiabilidad del sistema. Además, otra mejora considera la programación de restricción de posibilidades para calcular una política óptima de reposición de listas basada en un nivel de aceptabilidad de riesgo deseado, logrando designar dinámicamente existencias de seguridad en redes basadas en flujo para satisfacer demandas de flujo no estacionarias. Finalmente, un enfoque innovador de control consciente de la salud para vehículos de carreras autónomos para controlarlo simultáneamente hasta los límites de conducción y seguir el camino deseado basado en la maximización de la batería RUL. El diseño del control se divide en dos capas con diferentes escalas de tiempo, planificador de ruta y controlador. El enfoque propuesto está formulado como un MPC robusto en línea óptimo basado en LMI impulsado por la estabilidad de Lyapunov y la síntesis de ganancia del controlador resuelta por el problema LPV-LQR en la formulación de LMI con acción integral para el seguimiento de la trayectoria.

Palabras clave: Control predictivo del modelo, optimización económica, variación lineal de parómetros, takagi-sugeno, retraso variable en el tiempo, control consciente de la salud, confiabilidad, vida útil restante, sistema autónomo, proceso industrial.

Resum

Aquesta tesi vol proporcionar aportacions teóriques i próctiques sobre seguretat i control dels sistemes industrials, especialment en la forma matemática de sistemes incerts. La investigació està motivada per aplicacions reals, com la planta de pasteurització, les xarxes daigua i el sistema autónom, que cadascuna dfelles requereix un sistema de control específic per proporcionar una gestió adequada capaç de tenir en compte les seves característiques i límits operatius particulars davant díncerteses relacionades amb la seva funcionament i fallades per avaries en components.

Segons que la majoria dels sistemes reals tenen comportaments no lineals, es poden aproximar-los mitjançant models polítics lineals i incerts com els models Lineals Parameter Varying (LPV) i Takagi-Sugeno (TS). Per tant, es proposa un nou enfocament de model de control predictiu (MPC) econòmic basat en models LPV / TS i l'estabilitat de l'enfocament proposat està certificada mitjançant l'ús d'una restricció de regió a l'estat terminal. A més, l'estratègia MPC-LPV s'estén en funció del sistema, amb diferents retards que afecten estats i entrades. L'enfocament de control permet al controlador acomodar els paràmetres de programació i retardar el canvi. Si es calcula la predicció de les variables déstat i el retard al llarg dún horitzó de predicció, el model del sistema es pot modificar segons lávaluació de léstat estimat i el retard en cada moment.

Per augmentar la fiabilitat del sistema, preveure l'aparició de falles i reduir els costos operatius, s'ha de tenir en compte la vigilància de la salut de l'actuador. Quant a diversos tipus de fallades del sistema, séstudien diferents estratègies per obtenir fallades del sistema. Primer, el dany es valora amb l'algoritme de recompte de fluxos de pluja que permet estimar la fatiga del component i l'objectiu de control es modifica afegint un criteri addicional que tingui en compte el dany acumulat. A més, es presenten dues estratègies de control predictiu econòmic diferents que tenen per objectiu minimitzar els danys dels components.

A continuació, es desenvolupa un controlador MPC econòmic que té la salut econòmica per calcular els components i la fiabilitat del sistema en el model MPC mitjançant un enfocament de modelat LPV i maximitza la disponibilitat del sistema mitjançant l'estimació de la fiabilitat del sistema. Addicionalment, una altra millora considera que la programació de restricció d'atzar calcula una política òptima de reposició de llistes basada en un nivell d'acceptabilitat del risc desitjat, aconseguint designar dinàmicament les existències de seguretat a les xarxes basades en fluxos per satisfer les demandes de flux no estacionàries. Finalment, un innovador enfocament de control de salut per als vehicles de cursa autònoms per controlar-lo simultàniament fins als límits de conducció i seguir el camí desitjat basat en la maximització del RUL de la bateria. El disseny del control es divideix en dues capes amb escala de temps diferent, planificador de ruta i controlador. L'enfocament proposat es formula com un MPC òptim en línia basat en LMI basat en LMI impulsat des de l'estabilitat de Lyapunov i la síntesi de guanys del controlador resolts pel problema LPV-LQR en la formulació de LMI amb acció integral de seguiment de la trajectòria.

Paraules clau:Control de predicció del model, optimització econòmica, variació lineal de paràmetres, takagi-sugeno, retard variable en el temps, control conscient de la salut, fiabilitat, vida útil permanent, sistema autònom, procés industrial.

Notation

Throughout the thesis...

$\{.,...\}$	set or sequence
$\emptyset$	empty set
$i \in X$	i is an element of the set X
$\mathbb{R}$	set of real numbers
$\mathbb{R}_+$	set of non-negative real numbers, defined as $\mathbb{R}_+ \triangleq \mathbb{R} \setminus (-\infty, 0]$
$\mathbb{R}_{\geq c}$	$\mathbb{R}_{\geq c} := \{x \in \mathbb{R}_+ \vert x \geq c\}$ for some $c \in \mathbb{R}_+$
$\mathbb{R}_{>c}$	$\mathbb{R}_{>c} := \{x \in \mathbb{R} \vert x > c\}$ for some $c \in \mathbb{R}$
$\mathbb{R}^{m \times n}$	space of n by m matrices with real entries
$\mathbb{Z}$	set of integer numbers
$\mathbb{Z}_+$	set of non-negative integer numbers
$\mathbb{Z}_{\geq c}$	$\mathbb{Z}_{\geq c} := \{x \in \mathbb{Z}_+ \vert x \geq c\}$ for some $c \in \mathbb{Z}_+$
$\mathbb{Z}_{>c}$	$\mathbb{Z}_{>c} := \{x \in \mathbb{Z} \vert x > c\}$ for some $c \in \mathbb{Z}$
$> (<)$	positive (negative) definite
$\geq (\leq)$	positive (negative) semi-definite
X^{-1}	inverse of the matrix $X \in \mathbb{R}^{m \times n}$
$\mathbb{X}(\subset) \subseteq \mathbb{Y}$	set $\mathbb{X}$ is a (strict) subset of $\mathbb{Y}$
$\mathbb{X} \times \mathbb{Y}$	Cartesian product of the sets $\mathbb{X}$ and $\mathbb{Y}$, i.e., $\mathbb{X} \times \mathbb{Y} = \{(x, y) \vert x \in \mathbb{X}, y \in \mathbb{Y}\}$
$\mathbb{X}^n$	n-dimensional Cartesian product $\mathbb{X} \times \mathbb{X} \times ... \times \mathbb{X}$, for some $n \in \mathbb{Z} \geq 0$
$x^\top (X^\top)$	transpose of a vector$x \in \mathbb{R}^n (matrix X \in \mathbb{R}^{m \times n})$
X_{ij}	element in the i-th row and j-th column of the matrix $X \in \mathbb{R}^{m \times n}$
$\|.\|$	the spectral norm for matrices
$\|x\|_2$	2-norm of a vector x is defined by $\|x\|_2 = \sqrt{x^\top x}$
$\mathbb{P}[\cdot]$	probability measure
$\mathbb{E}[\cdot]$	expectation with respect to probability measure $\mathbb{P}[\cdot]$
$\oplus$	direct sum of matrices (block diagonal concatenation)

$\text{diag}(\cdot)$	operator that builds a diagonal matrix with the elements of its argument
$\mathcal{N}(\overline{x}, \sum x)$	multivariate normal distribution of x with mean $\overline{x}$ and covariance $\sum x$
$*$	a term induced by (Hermitian) symmetry in a block matrix
$\prod_{k=1}^{n}$	product of all values in range of series $\prod_{k=1}^{n} x_k$ means $x_1 x_2 ... x_n$
x_k	the sub-index k indicates the discrete time
$x_{k+j\|k}$	prediction of x made at time instant k for the time instant $k+j$, where $k, j \in \mathbb{Z}_{\leq} 0$ .In the argument $k+j\|k$, the first element $k+j$ indicates discrete time prediction, whereas the second element k indicates the actual discrete time

Acronyms

MPC	Model Predictive Control
EMPC	Economic Model Predictive Control
NEMPC	Nonlinear Economic Model Predictive Control
RMPC	Robust Model Predictive Control
CC-MPC	Chance-Constrained MPC
PHM	Prognosis and Health Management
LPV	Linear parameter varying
LTI	Linear Time Invariant
LTV	Linear Time Varying
TS	Takagi-Sugeno
RUL	Remaining Useful Life
HAC	Health- Aware Control
LMI	linear matrix inequalitie
LQR	Linear Quadratic Regulator
DWN	Drinking Water Network
OCP	Optimal Control Problem
QP	Quadratic Programming
Co	Convex hull
RFC	Rainflow Counting Algorithm
FHOP	Finite-time Horizon Optimization Problem
SoC	State of Charge
HTST	High-Temperature Short-Time

Contents

Acknowledgement 5

Abstract 7

Resumen 9

Resum 11

Notation 13

Acronyms 15

List of Tables 23

List of Figures 24

1 Introduction **1**

1.1 Motivation 1

1.2 Thesis Objectives 3

1.3 Outline of the Thesis 4

I Background and case studies **9**

2 Research Background **11**

2.1 Model Predictive Control 11

2.1.1 General Consideration of MPC and EMPC 11

2.1.2 MPC and EMPC Strategies Descriptions 13
2.2 LPV/TS Modeling 16
2.2.1 Linear Parameter Varying Modeling 16
2.2.2 Takagi-Sugeno Modeling 19
2.3 Prognostics and Health Management 21
2.3.1 Reliability analysis methods 23
2.3.2 Health-aware control 25
2.4 Summary 27

3 Case studies **29**

3.1 Pasteurization Process 29
3.1.1 Introduction 29
3.1.2 Pasteurization model 1 31
3.1.3 Pasteurization model 2 35
3.2 Drinking Water Networks 53
3.2.1 Introduction 53
3.2.2 Control-oriented modeling of water transport network 54
3.2.3 System management criteria 57
3.3 Autonomous Racing Vehicle 59
3.3.1 Introduction 59
3.3.2 System description and modeling 59
3.4 Summary 61

II Economic MPC approaches based on LPV/TS **63**

4 Economic Model Predictive Control for LPV/TS Systens **65**

4.1 Introduction 65

4.2 Problem statement 66

4.3 Proposed LPV/TS-based EMPC approach 68

4.3.1 General approach of LPV-based EMPC 68

4.3.2 Adaptation to the TS-EMPC case 71

4.4 Stability and convergence analysis 73

4.4.1 Computation of the Terminal Components 77

4.5 Numerical results 81

4.5.1 Cost function parameters 81

4.5.2 Simulation results 83

4.6 Summary 89

5 MPC for LPV systems with parameter-varying delays **91**

5.1 Introduction 91

5.2 Problem statement 92

5.3 Proposed approach 93

5.4 Numerical results 95

5.4.1 Simulation results and discussion 96

5.5 Summary 99

III Health-Aware Control **101**

6 Multi-Layer Health-Aware Economic Predictive Control based on Components Fatigue **103**

6.1 Introduction 103

6.2 Problem statement 104

6.2.1 Operational Control 105

6.3 Rainflow Counting Algorithm (RFC) 106

6.4 Health-aware MPC 111

6.4.1 Design of Single-layer Health-aware MPC Controllers 111

6.4.2 Design of Multi-layer Health-aware MPC Controllers 115

6.5 Simulation Results 117

6.5.1 Design of an MPC Controller with Health-aware Capabilities and Economic Objectives 117

6.5.2 Results and Comparison Assessment 120

6.6 Summary 122

7 Health-aware MPC-LPV based on system Reliability **123**

7.1 Introduction 123

7.2 EMPC Formulation of DWN 125

7.3 Chance-constrained Model Predictive Control 126

7.4 Reliability Assessment 130

7.4.1 Failure Rate and Reliability Concept 130

7.4.2 Overall Reliability 131

7.4.3 System Reliability Modeling 131

7.5 Economic health-aware MPC-LPV 132
7.5.1 General approach of economic health-aware MPC-LPV 132
7.5.2 Enhancing system reliability using chance constraints 135
7.6 Application to the water network case study 138
7.6.1 Water transport Network (3-Tanks) 138
7.6.2 Chance-constraints health-aware EMPC-LPV for water transport network of Barcelona (17-Tanks) 141
7.7 Summary 150

8 Health-aware optimization-based control design for autonomous racing vehicle 153

8.1 Introduction 154
8.2 System Modeling 156
8.2.1 LPV modeling 157
8.3 Problem Statements 158
8.4 Proposed approach 159
8.4.1 LPV MPC Planner 159
8.4.2 LMI control design of Planner including health management . . 160
8.4.3 Tracking Controller 165
8.5 Simulation results and discussion 166
8.6 Summary 174

IV Conclusions and perspectives 175

9 Concluding Remarks 177

9.1 Conclusions 177

9.2 Future Research 180

V Appendices **181**

Pasteurization Plant 183

Racing Vehicle 187

Some Lemma 189

Bibliografia **190**

List of Tables

4.1 Comparison of control performance. 89

5.1 Physical properties and process data 98

5.2 Comparison of each strategies timing performance. 98

7.1 Success minimal paths of the water transport network of Barcelona (3-Tanks) 139

7.2 Simulation parameters. 140

7.3 Structural actuators (towards tanks). 145

7.4 Structural actuators (towards demands). 145

7.5 Success minimal paths of the DWN case study. 145

7.6 Comparison of control performance. 150

7.7 Comparison of daily average costs of the MPC approaches. 151

8.1 Model parameters value. 173

A.1 Time constants and gains of the hot-water tank 183

A.2 Time constants of the G_{ij} transfer functions 183

A.3 Gains of the G_{ij} transfer functions 184

A.4 The adjusted parameters 184

List of Figures

2.1 Control theory and health monitoring combination. 26

3.1 Pasteurization plant scheme. 32

3.2 Block diagram of the pasteurization model 1. 33

3.3 The pasteurization Plant 2. 36

3.4 The pasteurization Plant scheme of model 2. 37

3.5 Experimental relationship between the flow F_1 and N_1. 38

3.6 Experimental relationship between the flow F_2 and N_2. 39

3.7 Scheme of the hot-water tank 40

3.8 Verifying the simulation model of hot-water tank T_2 41

3.9 Error achieved during the simulation. 41

3.10 Scheme of the holding tube. 43

3.11 Verifying the simulation model of holding tube T_1 44

3.12 Error achieved during the simulation. 44

3.13 Verifying the simulation model of delay 45

3.14 Scheme of the heating phase 46

3.15 Verifying the simulation model of heating phase T_4 47

3.16 Error achieved during the simulation. 47

3.17 Scheme of the Regeneration phase 48

3.18 Verifying the simulation model of regeneration phase T_{in} 49

3.19 Error achieved during the simulation. 49

3.20 Verifying the simulation model of temperature T_{2r} 51

3.21 Error achieved during the simulation. 52

3.22 Barcelona DWN aggregate diagram 55

3.23 DWN sector diagram 56

3.24 Racing vehicle variables along the road 60

4.1 Evolution of controlled temperature of TMPC strategy and the EMPC based on TS model 84

4.2 Evolution of controlled hot-water tank temperature of TMPC strategy and EMPC based on TS model 85

4.3 Evolution of control inputs of TMPC strategy and EMPC based on T-S model 88

5.1 Evaluation of the output temperatures (Delay is constant during the prediction horizon) 96

5.2 Evaluation of the output temperatures (Delay is varied during the prediction horizon) 97

5.3 Evaluation of the control inputs (Delay is constant during the prediction horizon) 99

5.4 Evaluation of the control inputs (Delay is varied during the prediction horizon) 100

5.5 Comparison of delay during the prediction horizon 100

6.1 Rainflow counting damage procedure. 107

6.2 Rainflow counting damage estimation. 107

6.3 Accumulated Damage Comparison. 109

6.4 Accumulated damage RFC as a function of time and z fatigue damage state. 110

6.5 Representative block diagram of single-layer MPC with fatigue model and linear regulator. 113

6.6 Representative block diagram of two-layer MPC with fatigue model. . . 115

6.7 Evolution of pasteurization temperature T_{past} with and without the health-aware objective in the MPC. 118

6.8 Evolution of accumulated damages with and without health-aware objective in the MPC. 119

6.9 Evolution of power the electrical heater P in the single-layer and two-layer MPC. 121

6.10 Trade-off between the health and cost in the single-layer and two-layer MPC over the normalization. 121

7.1 Digram of the new proposed control model approach. 133

7.2 Drinking water network diagram (Three-tanks). 138

7.3 Drinking water demand for the three tanks example. 139

7.4 Evaluation of the control actions results of 3-tanks. 141

7.5 Results of the evolutions of storage tanks for 3-tanks. 142

7.6 Evaluation of system reliability and accumulated economic cost for 3-tanks. 142

7.7 Barcelona drinking water network (17-Tanks). 143

7.8 Case study based on the DWN case study. 143

7.9 Drinking water demand for several sinks. 144

7.10 Evaluation of the control actions results. 146

7.11 Results of the evolutions of control action. 148

7.12 Results of the evolutions of control action in 48 h. 149

7.13 Evaluation of system reliability and accumulated economic cost. 150

8.1 Block diagram of control approach 159

8.2 Comparison of planner racing laps with and without RUL objective. . . 167

8.3 The reference and response of racing lap without RUL objective. 168

8.4 The reference and response of racing lap with RUL objective. 168

8.5 Comparison of the velocity with and without the RUL objective. 169

8.6 Error achieved during the simulation racing laps. 170

8.7 Comparison of the battery RUL. 171

8.8 Comparison of the Response with and without the disturbance and noise with RUL objective 171

8.9 Comparison of the velocity with and without the disturbance and noise with RUL objective. 172

8.10 Friction force disturbance. 172

8.11 Poles positions of the planner and controller in a particular operating point.173

Chapter 1

Introduction

This chapter presents the introduction of this thesis document. The aim of this chapter is to describe the main motivations which have originated this thesis as described in Section 1.1. Then, the thesis objectives are presented in Section 1.2. Finally, in Section 1.3, a brief outline of the structure of this dissertation is introduced, providing an abstract of each chapter.

1.1 Motivation

In modern times of industrialization, the investigation of advanced control algorithms for complex dynamic systems is still very active. Controlling these complex systems is one of the most important problems in control engineering, but also one of the most challenging. Another essential but just as a demanding topic is including robustness against uncertainties in the design of the control system. On the other hand, regularly, the time delay arises in the dynamics of the systems, such as communication systems, chemical processes, and transportation systems [82, 179, 23]. One of the main successful and widespread advanced control methodologies in industrial processes is Model Predictive Control (MPC). MPC is quite popular in the process industry for the automatic control of process units under operating constraints and has attracted a considerable research effort in the last three decades. MPC based on linear models is typically used in process control where the on-line optimization problem can be formulated as a convex optimization problem by either using Linear Programming (LP) or Quadratic Programming (QP). However, most of the real-time processes are nonlinear. Thus, when the

operating conditions undergo significant changes, the performance of linear MPC can deteriorate drastically. However, most of the real systems show nonlinear behaviors that can be approximated by polytopic linear uncertain models. In order to reduce the conservativeness, the idea of controlling nonlinear systems considering linear parameter varying (LPV) and Takagi-Sugeno (TS) models have been widely investigated in the literature [147, 191, 207, 33]. In particular, the LPV and the TS paradigms have provided an elegant way to apply linear techniques to nonlinear systems with theoretical guarantees of stability and performance.

The application of control strategies by considering the system and components reliability becomes necessary to ensure the quality of service. In order to increase the system reliability, anticipate the appearance of faults and reduce the operational costs, actuator health monitoring should be considered. Recently, system reliability has been taken into account in the control algorithm through a Prognosis and Health Management (PHM) framework using reliability. Reliability is the ability of a system or component to perform its expected functions. On the one hand, it a systematic strategy that is utilized to assess the state-of-health of a system in its actual life-cycle conditions, predict failure progression, and decrease damage via control actions. And, on the other hand, it is principal process in maintenance strategies based on the remaining useful life of the equipment, which makes it possible to avoid critical damages and reducing costs. The Remaining Useful Life (RUL) is the useful life that remains on an asset at a particular time of operation. Its estimation is fundamental for condition based maintenance, health management and prognostics. Therefore, it can be noted that the reliability estimation of equipment as well as its RUL prediction is necessary to establish if the mission goals can be achieved. Since the prediction of RUL is critical for operations and decision making, it is imperative that the RUL is determined accurately.

Merging the LPV/TS modeling, the MPC strategy, and the PHM opens up a new view to control engineering of industrial process. In this case, open issues that motivate further research regarding how to design the control algorithm in the MPC framework for considering the information about system health in order to extend the useful life of the system. Therefore, the motivation of this PhD thesis is to develop the new MPC strategies, specifically, economic MPC based on the LPV/TS models of the industrial process and as well as a methodology for the design of a Health-Aware Control (HAC) strategy that takes into account the system and actuators state-of-health in order to extend its useful life.

1.2 Thesis Objectives

The overall objective of this thesis is to design predictive controllers based on LPV/TS models for complex industrial systems subject to delays, constraints, and uncertainty in order to improve the performance of the closed-loop process from the energy point of view. Moreover, the controller will be upgraded such that the system health is considered in the control objective. In this way, the control methodology will provide major benefits such as decreasing maintenance costs, avoiding incipient and catastrophic failures and extending equipment uptime.

Moreover, some specific objectives of this thesis have been proposed as follows:

Objective I Develop an economic MPC strategy for nonlinear systems that can be represented by means of LPV/TS models.

Objective II Investigate the MPC strategies for LPV/TS models in order to guarantee the stability and performance.

Objective III Design an MPC controller for nonlinear systems with varying delays affecting states and inputs using LPV framework.

Objective IV Modeling the degradation of actuators and reliability of system/actuators as a function of affected by control actions.

Objective V Design and Develop a health-aware strategy for a complex system to extend the components and system reliability and RUL of the system by using the model predictive control and LPV LQR approaches.

Objective VI Design and develop an economic health-aware MPC for a complex system to extend the components and system reliability based on a finite horizon stochastic optimization problem with joint probabilistic (chance) constraints in order to manage dynamically designate safety stocks in the system.

Objective VII Validate the proposed approaches is complex systems as a industrial process (pasteurization plant and water network) and complex systems (autonomous vehicle).

1.3 Outline of the Thesis

The structure of this thesis is reported in this section mentioning different parts and chapters. Thereby, a short abstract and related published papers are provided for each chapter.

This dissertation is organized into four parts:

Part I entitled ***Background and case studies***, presents the previous results that establish a contribution to the state-of-the-art of control strategies based on LPV /TS models and description of application used in this thesis. It is made up of two chapters:

- **Chapter 2: Research Background**
  This chapter background on classical and economic MPC controller with particular emphasis on LPV and TS systems is recalled. Known results about analysis, modeling, and control of LPV/TS models are presented and discussed. Moreover, the fundamental concepts and definitions of PHM and HAC by providing bibliographical references to the main contributions in this area are introduced.
- **Chapter 3: Case studies**
  This chapter presents case studies considered in this dissertation. Firstly, a non-linear model of the pasteurization plant its validation with real data and its embedding in the LPV/TS models. Then, a part of the drinking water network of the city of Barcelona (Spain) is described as another case study. Finally, the model of autonomous racing vehicle is presented in detail.

Part II, entitled ***Economic MPC approaches based on LPV/TS***, proposes an economic MPC based on LPV /TS models with and without delays and guaranteeing their stability. It is made up of three chapters:

- **Chapter 4: A new design of economic model predictive control based on LPV/T-S Models**
  This chapter proposes an EMPC strategy based on an LPV/T-S models. Moreover, for solving the economic optimization problem by using a series of QP problems at each time instant, a new iterative approach is introduced that reduces the computational load compared to the solution of a non-linear optimization problem. The stability of the proposed approach is analyzed presenting the conditions to be

satisfied. The proposed algorithm for EMPC strategy based on the quasi-LPV/T-S is illustrated through a pasteurization plant as a case study that is described by a quasi-LPV model/ T-S models. This chapter is based on the following papers:

F. Karimi Pour, V. Puig and C. Ocampo-Martinez. Comparative assessment of LPV-based predictive control strategies for a pasteurization plant. 4^{th} *International Conference on Control, Decision and Information Technologies (CoDIT)*, (pp. 0821-0826). IEEE, Spain, 2017.

F. Karimi Pour, V. Puig and C. Ocampo-Martinez. Economic predictive control of a pasteurization plant using a linear parameter varying model. *In Computer Aided Chemical Engineering*, (Vol. 40, pp. 1573-1578). Elsevier, 2017.

F. Karimi Pour, C. Ocampo-Martinez and V. Puig . Output-feedback model predictive control of a pasteurization pilot plant based on an LPV model. *In Journal of Physics: Conference Series* (Vol. 783, No. 1, p. 012029), France, 2017.

F. Karimi Pour, V. Puig and C. Ocampo-Martinez . A new Design of Economic model Predictive Control based on LPV systems. To be submitted *Journal of Process control.*

F. Karimi Pour, V. Puig and C. Ocampo-Martinez . Takagi-Sugeno based Economic Predictive Control of a Pasteurization Plan. To be submitted *International Journal of Computer Applications in Chemical Engineering.*

- **Chapter 5: Economic model predictive control based on LPV models with parameter varying delays**

  This chapter presents an MPC strategy based on LPV models with varying delays affecting states and inputs. By computing the prediction of the state variables and delay along a prediction time horizon, the system model can be modified according to the evaluation of the estimated state and delay at each time instant. Moreover, the solution of the optimization problem associated with the MPC design is achieved by solving a series of QP problem at each time instant.The pasteurization plant system is used as a case study to demonstrate the effectiveness of the proposed approach. This chapter is based on the following papers:

  F. Karimi Pour, V. Puig and C. Ocampo-Martinez. Comparison of Set-membership and Interval Observer Approaches for State Estimation of Uncertain Systems. 18^{th} *European Control Conference (ECC)*, (pp. pp. 3644-

3649) IEEE, Denmark, 2019.

Part III, entitled ***Health-Aware Control***, present the contributions to the state of the art on Health Aware Control (HAC). It is made up of four chapters:

- **Chapter 6: Multi-layer health-aware economic predictive control based on Components Fatigue**
  This chapter proposes a multi-layer health-aware economic predictive control strategy that aims to minimize the damage of components in a pasteurization plant. The damage is assessed with the rainflow-counting algorithm that allows estimating the components fatigue. In order to achieve the best minimal accumulated damage and operational costs, a multi-layer control scheme is proposed, where the solution of the dynamic optimization problem is obtained from the model in two different time scales. Finally, to achieve the advisable trade-off between minimal accumulated damage and operational costs, both control strategies are compared in simulation over for the pasteurization case study. This chapter is based on the following papers:

  F. Karimi Pour, V. Puig and C. Ocampo-Martinez. Multi-layer health-aware economic predictive control of a pasteurization pilot plant. *International Journal of Applied Mathematics and Computer Science*,28(1), 97-110), 2018.

  F. Karimi Pour, V. Puig and C. Ocampo-Martinez. Health-aware model predictive control of pasteurization plant. *In Journal of Physics: Conference Series*,(Vol. 783, No. 1, p. 012030), 2017.

- **Chapter 7: Economic health-aware LPV-MPC based on a system reliability and remaining useful life assessment**

  This chapter presents a new strategy of health-aware MPC for industrial processes. The new approach is based on an economic health-aware MPC that involves an extra objective: to extend the components and system reliability. The components and system reliability are incorporated in the MPC model using an LPV modelling approach. To exhibit the advantage of taking into account system and component reliability, computed on-line in an LPV-based MPC algorithm. Moreover, this approach is improved to extend the components and system reliability

based on a finite horizon stochastic optimization problem with joint probabilistic (chance) constraints. The improvement is that the considered chance-constraint programming allows computing an optimal tank storage value based on a desired risk acceptability level, managing to dynamically designate safety stocks in flow-based networks to satisfy non-stationary flow demands. A case study based on a part of the drinking water transport network of Barcelona is used for illustrating the performance of the proposed approach. This chapter is based on the following papers:

- F. Karimi Pour, V. Puig, and G. Cembrano. Economic Health-Aware LPV-MPC Based on System Reliability Assessment for Water Transport Network. *Energies, 12(15), 3015*,2019.
- F. Karimi Pour, V. Puig, and G. Cembrano. Economic Health-aware MPC-LPV based on DBN Reliability model for Water Transport Network. 6^{th} *International Conference on Control, Decision and Information Technologies (CoDIT)*,(pp. 1408-1413). IEEE, France,2019.
- F. Karimi Pour, V. Puig, and G. Cembrano. Health-aware LPV-MPC based on system reliability assessment for drinking water networks. *IEEE Conference on Control Technology and Applications (CCTA)*,(pp. 187-192). IEEE, Denmark, 2018.
- F. Karimi Pour, V. Puig, and G. Cembrano. Health-aware LPV-MPC based on a reliability-based remaining useful life assessment. 10^{th} *IFAC Symposium on Fault Detection, Supervision and Safety for Technical Processes, (SAFEPROCESS)*,IFAC-Papers OnLine,51(24), 1285-1291, Poland, 2018.
- F. Karimi Pour, V. Puig, and G. Cembrano. Economic MPC-LPV Control for the Operational Management of Water Distribution Networks. *IFAC Workshop on Control Methods for Water Resource Systems (CMWRS 2019)*, IFAC-PapersOnLine, 52(23), 88-93, Netherlands, 2019.
- F. Karimi Pour, V. Puig, and G. Cembrano. Economic Reliability-Aware MPC-LPV for Operational Management of Flow-based Water Networks including Chance-Constraints Programming. Submitted to *Processes*.
- F. Karimi Pour and V. Puig. Reliable Aware Model Predictive Control including Fault tolerant ability for Drinking Water Transport Networks. Submitted to 10^{st} *IFAC World Congress, 2020*.

- **Chapter 8: Health-aware optimization-based control design for autonomous racing vehicle**
  This chapter proposes an innovative health-aware control approach using the Linear Matrix Inequality (LMI), where the objective consists in preserving the state of charge (SoC) and maximizing the battery RUL based on optimizing the lap time to obtain the best trajectory under the constraints of the circuit. The proposed approach is solved by an optimal online robust LMI based Model Predictive Control (MPC) driven from Lyapunov stability. The proposed approach is evaluated in a simulation of autonomous vehicles. This chapter is based on the following papers:

  F. Karimi Pour, D. Theilliol, V. Puig, and G. Cembrano. Health-aware Optimization-based Control Design: Application to Autonomous Racing based State of Charge. 4^{th} *In 2019 4th Conference on Control and Fault Tolerant Systems (SysTol)*, (pp. 244-249), IEEE. Morocco, 2019.

  F. Karimi Pour, D. Theilliol, V. Puig, and G. Cembrano. Health-aware Control Design based on Remaining Useful Life Estimation for Autonomous Racing Vehicle. Submitted to *ISA Transactions*.

Part IV, entitled ***Conclusions and perspectives***, is the final part of this thesis that is concluded by:

- **Chapter 9: Conclusions and future research**
  This chapter summarizes the contributions provided in this thesis and presents the main concluding ideas and open issues for future research.

Part I

Background and case studies

Chapter 2

Research Background

This chapter presents a literature review related to the main topics treated in this doctoral dissertation. Firstly, a review and the formulations of model predictive control (MPC) and economic model predictive control (EMPC) are discussed. Secondly, a literature review for the Linear Parameter Varying (LPV) and Takagi-Sugeno (TS) models and control strategies, with a special emphasis on the MPC strategy, based both paradigms is presented. Then, preliminary concepts regarding Prognostics and Health Management (PHM), damage and reliability, which are used throughout the thesis, are presented. Finally, some relevant works related to improve system reliability and prevent the occurrence of system failures are mentioned.

2.1 Model Predictive Control

2.1.1 General Consideration of MPC and EMPC

Model Predictive Control (MPC) is an effective control methodology widely used in both the academic and industrial fields and treated as a powerful approach with proven ability to deal with a lot of industrial problems. MPC refers to a class of control algorithms that use an explicit dynamic process model to predict the future response of the plant and optimize its performance [179]. At each control interval, the MPC algorithm computes an open-loop sequence of manipulated variable adjustments in order to optimize the future plant behavior. The MPC problem is formulated as a finite-horizon open-loop optimal control problem, subject to system dynamics and constraints involving

physical bounds for system variables (inputs, states, outputs), exogenous disturbances and operational policies [130]. According to [138], there are several specific variants of predictive control that are listed as follows: dynamic matrix control (DMC), extended prediction self-adaptive control (EPSAC), generalized predictive control (GPC), model algorithmic control (MAC), predictive functional control (PFC), quadratic dynamic matrix control (QDMC), sequential open-loop optimization (SOLO) and model predictive heuristic control (MPHC). For more detailed information about those algorithms and their developments, see [32, 151, 178, 138]. MPC includes three essential structures: an explicit internal model, the receding horizon idea, and computation of the control signal by optimizing the predicted plant behavior. The core of MPC consists of the receding horizon idea; in fact, only the first control action of the optimal sequence is applied to the plant. At the next sampling instant, the optimization problem is solved again with new measurements, and the control input is updated. Due to its ability to handle constraints on inputs, states, uncertainty and output, the method has received much interest in both academic community and industry over the last three decades [144, 179].

- It handles multi-variable problem naturally, being quite well adapted to the majority of industrial system that present the multi-variable characteristic.
- It can take into account the actuator limitations and cope with input, state and output constraints in a systematic way.
- It allows the system operation closer to constraints, which frequently leads to more profitable operation.
- Control update rates in predictive control are relatively low, so that there is plenty of time for a necessary on-line computation.
- Because of the use of the receding horizon principle, it has satisfactory accommodation ability to several kinds of disturbances and noise.

For more details, [32, 216] could be referred.

Conventionally, standard tracking MPC is formulated as an optimization problem that penalizes the tracking error [179, 183]. Although this method ensures that the set-point is achieved in a reasonable amount of time, it does not guarantee that the transition between set-points is achieved in an economically efficient way. To overcome

this problem, MPC has been adapted to solve Optimal Control Problem (OCP) with general cost functions. In this way, Economic MPC (EMPC) contributes a systematic approach for optimizing an economic performance [55, 47]. EMPC has received much attention because of its capability of integrating real-time process economic optimization and feedback control into an optimal control framework. The optimization problem of EMPC includes three principal parts: a cost function with a stage cost that considers the economic goals to be optimized, system constraints containing state and input constraints as well as other constraints such as stability and performance constraints, and a nonlinear dynamic model to predict the future evolution of the system (and thus, being able to select the optimal input profile with respect to the economic cost over a finite-time prediction horizon) [54]. Unlike tracking MPC, that minimizes a positive definite error cost function, EMPC can consider economic functions as stage costs.

2.1.2 MPC and EMPC Strategies Descriptions

Although there exist some applications of MPC with continuous-time models, [216], it is more general to design MPC controllers in discrete time [183, 140, 138], and by using a state space model of the system. Hence, consider a system whose discrete-time model is given by

$$x_{k+1} = f(x_k, u_k, d_k) \tag{2.1}$$

where the discrete-time variable is denoted by $k \in \mathbb{I}_{\geq 0}$. The vectors $x \in \mathbb{X} \subseteq \mathbb{R}^{n_x}$, $u \in \mathbb{U} \subseteq \mathbb{R}^{n_u}$, and $d \in \mathbb{R}^{n_d}$. Besides, the sets $\mathbb{X}$ and $\mathbb{U}$ are defined as feasible sets according to physical and/or operational constraints for the system states and control inputs:

$$x \in \mathbb{X} \triangleq \{x_k \in \mathbb{R}^{n_x} \,|\, \underline{x} \leq x_k \leq \overline{x}\}, \quad \forall k, \tag{2.2a}$$

$$u \in \mathbb{U} \triangleq \{u_k \in \mathbb{R}^{n_u} \,|\, \underline{u} \leq u_k \leq \overline{u}\}, \quad \forall k, \tag{2.2b}$$

where vectors $\underline{x} \in \mathbb{R}^{n_x}$ and $\overline{x} \in \mathbb{R}^{n_x}$ establish the minimum and maximum possible state values of the system, respectively. Analogously, $\underline{u} \in \mathbb{R}^{n_u}$ and $\overline{u} \in \mathbb{R}^{n_u}$ determine the minimum and maximum possible value of manipulated variables, respectively. The function $f : \mathbb{R}^{n_x} \times \mathbb{R}^{n_u} \longrightarrow \mathbb{R}^{n_x}$ is an arbitrary system state function. Let

$$\tilde{u}_k \triangleq \big(u_{0|k}, u_{1|k}, ..., u_{N_p-1|k}\big), \tag{2.3}$$

be a feasible control input sequence over a fixed-time prediction horizon denoted by $N_p \in \mathbb{I}_{>0}$. Notice that (2.3) depends on the initial condition $x_{0|k} \triangleq x_k$. Moreover, the predictive control approach involves the solution of an open-loop optimization problem of the following general form:

$$\min_{\tilde{u}_k} J(x_k, \tilde{u}_k) = J_f(x_{N_p|k}) + \sum_{i=0}^{N_p-1} J_l(x_{i|k}, u_{i|k}), \tag{2.4a}$$

subject to

$$x_{i+1|k} = f(x_{i|k}, u_{i|k}, d_{i|k}), \qquad \forall i \in [0, N_p], \tag{2.4b}$$

$$x_{i|k}, \in \mathbb{X} \qquad \forall i \in [0, N_p], \tag{2.4c}$$

$$u_{i|k}, \in \mathbb{U} \qquad \forall i \in [0, N_p - 1], \tag{2.4d}$$

where the function $J_l : \mathbb{R}^{n_x} \times \mathbb{R}^{n_u} \longrightarrow \mathbb{R}$ allows to determine the cost throughout the prediction horizon N_p, and the function $J_f : \mathbb{R}^{n_x} \longrightarrow \mathbb{R}$ denotes the terminal cost. Moreover, functions in (2.4a) must be suitably chosen in order to guarantee the stability of the closed-loop system as discussed in [183, 216].

Assuming that the optimization problem in (2.4) has a solution there will be an optimal sequence of control inputs

$$\tilde{u}_k^* \triangleq \big(u_{0|k}^*, u_{1|k}^*, ..., u_{N_p-1|k}^*\big). \tag{2.5}$$

Then, according to the receding horizon philosophy, $u_{0|k}^*$ is applied to the system, and the whole process is repeated for the next time instant $k \in \mathbb{I}_{\geq 0}$. Algorithm 2.1 presents the MPC strategy.

Algorithm 2.1 General procedure for the computation of the MPC law

1: Measure the state x_k at time k
2: Compute $\tilde{u}_k^* \triangleq \big(u_{0|k}^*, u_{1|k}^*, ..., u_{N_p-1|k}^*\big)$ by solving the optimization problem (2.4)
3: Apply only the first element $u_k \triangleq u_{0|k}^*$ to the system
4: $k \leftarrow k + 1$. Go to 1

Conventionally, standard tracking MPC is formulated as an optimization problem that penalizes the tracking error [179, 183]. Although this method ensures that the set-point is achieved in a reasonable amount of time, it does not guarantee that the

transition between set-points is achieved in an economically efficient way. To overcome this problem, MPC has been adapted to solve OCPs with general cost functions. In this way, Economic MPC (EMPC) contributes a systematic approach for optimizing an economic performance [55, 47]. In the EMPC, the operational costs are directly considered as the objective function instead of penalising the tracking error with respect to the targets [181]. The controller design problem is based on obtaining a control law that minimizes a specific performance cost index

$$L(x_k, \tilde{u}_k) = \sum_{i=0}^{N_p-1} \ell(x_{i|k}, u_{i|k}), \qquad \ell : \mathbb{X} \times \mathbb{U} \longrightarrow \mathbb{R}. \tag{2.6}$$

where $\ell(x_k, u_k)$ is an economic stage cost. Given the economic stage cost, the economic controller should conduct the system to the optimal reachable steady state, that is determined by using the implicit form of the optimization as next definition follows:

Definition 2.1. [63] The optimal reachable steady state and input, (x_s, u_s), satisfy

$$(x_s, u_s) = arg \min_{(x,u)} \ell(x, u), \tag{2.7a}$$

subject to:

$$\begin{aligned} x &= f(x, u, d), \\ x &\in \mathbb{X}, \quad u \in \mathbb{U}. \end{aligned}$$

□

In the case of tracking MPC, the stage cost is typically designated as a positive definite function with regard to (x_s, u_s). In EMPC, $\ell(x, u)$ is chosen according to some economic criteria such as production cost, energy saving and efficiency, etc [143, 78]. These economic criteria have to be minimized or maximized in terms of profits and environmental issues according to the particular system. Therefore, in EMPC, $\ell(x, u)$ is not necessarily positive definite with regards to (x_s, u_s). The EMPC control law is derived from the solution of the optimization problem

$$\min_{x_k, \tilde{u}_k} L(x_k, \tilde{u}_k) = \sum_{i=0}^{N_p-1} \ell(x_{i|k}, u_{i|k}), \tag{2.8a}$$

subject to:

$$x_{i+1|k} = f(x_{i|k}, u_{i|k}, d_{i|k}), \qquad \forall i \in [0, N_p], \tag{2.8b}$$

$$u_{i|k}, \in \mathbb{U} \qquad \forall i \in [0, N_p - 1], \tag{2.8c}$$

$$x_{i|k}, \in \mathbb{X} \qquad \forall i \in [0, N_p], \tag{2.8d}$$

$$x_{N_p} = x_s, \tag{2.8e}$$

and, according to the receding horizon form, the same procedure of the MPC strategy is applied for the EMPC controller.

2.2 LPV/TS Modeling

Most of the real systems show nonlinear behaviours that can be approximated by polytopic linear uncertain models [196]. In order to reduce the conservativeness of controlling the nonlinear system and increasing the systematic analysis of gain-scheduled controllers, two most successful approaches, Linear Parameter Varying (LPV) and the Takagi-Sugeno (TS) paradigms, have been widely studied in the literature [175, 176, 191, 207].

2.2.1 Linear Parameter Varying Modeling

The LPV paradigm was introduced by Shamma [195] for the analysis of the control design practice of *gain-scheduling* [196]. In brief, gain-scheduling is a control design approach that constructs a nonlinear controller for a nonlinear plant by patching together a collection of linear controllers. Specifically, LPV models are a particular class of LTV systems, where the time-varying elements depend on measurable parameters that can vary over time [220]. The LPV framework is proved to be suitable for controlling nonlinear systems by embedding the nonlinearities in the varying parameters, that will depend on some endogenous signals, e.g. states, inputs or outputs. In this case, the system is referred to as quasi-LPV, to make a further distinction with respect to pure LPV systems, where the varying parameters only depend on exogenous signals [141]. The general state-space representation for discrete-time LPV model is described as

$$x_{k+1} = A(\theta_k)x_k + B(\theta_k)u_k, \tag{2.9a}$$

$$y_k = C(\theta_k)x_k + D(\theta_k)u_k, \tag{2.9b}$$

where the system matrices $A(\theta_k) \in \mathbb{R}^{n_x \times n_x}$, $B(\theta_k) \in \mathbb{R}^{n_x \times n_u}$, $C(\theta_k) \in \mathbb{R}^{n_y \times n_x}$ and $D(\theta_k) \in \mathbb{R}^{n_y \times n_u}$ are varying matrices of appropriate dimensions.

Among the available analysis approaches, the most widely-used, at least taking into account the number of publications, is the polytopic approach [81]. An LPV system is called *polytopic* when it can be represented by matrices $A(\theta_k)$, $B(\theta_k)$, $C(\theta_k)$ and $D(\theta_k)$, that are assumed to depend linearly on the parameter vector $\theta_k := [\theta_{1,k}, \theta_{2,k}, ..., \theta_{n_\theta,k}]^T \in \mathbb{R}^N$, which belongs to a convex polytope Θ defined by

$$\Theta := \left\{ \theta_k \in \mathbb{R}^{n_\theta} | \sum_{j=1}^{N} \theta_{j,k} = 1,\ \theta_{j,k} \geq 0 \right\}, \tag{2.10}$$

where N is the number of vertices of the polytope. Hence, as θ_k varies inside the convex polytope Θ, the matrices of the system (2.9) vary inside a corresponding polytope Ψ, which is defined by the convex hull (Co) of N local matrix vertices $[A_j, B_j, C_j, D_j]$, $j \in [1, .., N]$,

$$\Psi := Co \left\{ \begin{bmatrix} A_1 & B_1 \\ C_1 & D_1 \end{bmatrix}, \begin{bmatrix} A_2 & B_2 \\ C_2 & D_2 \end{bmatrix}, ... \begin{bmatrix} A_N & B_N \\ C_N & D_N \end{bmatrix} \right\}. \tag{2.11}$$

and the matrices of the (2.9) can be rewritten as

$$\begin{aligned} A(\theta_k) &= \sum_{j=1}^{N} \theta_{j,k} A_j, \qquad B(\theta_k) = \sum_{j=1}^{N} \theta_{j,k} B_j, \\ C(\theta_k) &= \sum_{j=1}^{N} \theta_{j,k} C_j, \qquad D(\theta_k) = \sum_{j=1}^{N} \theta_{j,k} D_j. \end{aligned} \tag{2.12}$$

The polytopic LPV model is an appropriate choice for addressing the nonlinear system control. Not only it can describe the inherent nonlinearity and time-varying characteristics of the system, but it also allows controller designers to use linear-like control theory for nonlinear system control. Therefore, it is suitable for the design of MPC controllers that are scheduled based on some measurable variables. For this reason, in recent years, the use of this type of system is extended for MPC applications (see, e.g., [124][198]).

However, in real processes, the precise model parameters are seldom available and hence Robust Model Predictive Control (RMPC) is more practical for real applications.In RMPC, the model parametric uncertainty can be dealt with within the frame

of LPV systems. For the online RMPC, at each time, a min-max optimization problem is frequently exploited to minimize the performance function of LPV systems, which evaluates all the possible realization of model parametric uncertainty [115]. However, this approach can lead to conservative results. To reduce the conservativeness, a class of linear parameter-dependent Lyapunov functions has been introduced [215]. Then, a linear controller is computed at every time instant. The control performance improvements are remarkable at the price of an increased number of LMI conditions. In [49], the RMPC method with the help of norm-bounding technology to restrict the states affected by disturbances into the invariant ellipsoid is presented. In addition, in [65] the special class of non-linear parameter-dependent Lyapunov functions is used and a non-linear scheduled control law is obtained, which leads to further improvement of the control performance. More recently, a less conservative RMPC controller was presented based on polytopic LPV model when the input matrix is unique [29].

As highlighted in the previous subsection, in LPV systems, parameters take values in prespecified sets and the dynamic characteristics involve time-varying parameters. In the real world, many non-linear systems of practical interest can be represented as quasi-LPV systems, where *quasi* is added since the scheduling parameters do not depend only on external signals, but also on a system variable [188]. In other words, the model parameters are exactly known at the current time, but their future evolutions are uncertain and contained in the prescribed bounded sets. In some practical applications, the varying parameters (such as the atmospheric temperature) can be measured and their change rates are limited, i.e. the current parameters can be known and the rates of parameter changes are bounded. For this category of LPV systems, if the information about the parameters can be used properly, then the system model in the future can be accurately predicted. By using the predicted future system behavior in the RMPC scheme, a better control performance could be achieved. This inspires the works of [134], [35], [136], [167]. In [126], [91], the controller design considers the time-varying parameters of quasi-LPV systems having the bounds on their rate of variation. [226] considers the quasi-LPV systems with a parameter-dependent control law. In this way, LPV models allow applying powerful linear-like design tools to complex non-linear models.

A Lyapunov-based EMPC (LEMPC) scheme for nonlinear systems that it is able to manage asynchronous and delayed measurements and can be extended to distributed MPC is proposed in [79, 39]. However, much of the research up to now on EMPC

and stability issue for nonlinear systems has not considered the use of LPV models. Moreover, nonlinear economic MPC (NEMPC) is computationally quite expensive and, in general, there is no guarantee that the solution of the nonlinear optimization problem is the global optimum. Alternatively, the optimization problem based on a nonlinear system may be converted into a QP problem by using linearizing the non-linear model at each iteration. [117]. However, in this method, it is not only required to update online the system matrices applying the linearization method but also the equilibrium points should be updated when the operating point changes, which is increases computational time.

2.2.2 Takagi-Sugeno Modeling

A nonlinear system can be approximated through the TS fuzzy models. The TS models, as introduced by Takagi and Sugeno [206], is described by fuzzy IF–THEN rules which represent local linear input-output relations of a nonlinear system [207]. The main feature of a TS fuzzy model is to express the local dynamics of each fuzzy implication (rule) by a linear system model [38, 197]. TS fuzzy models are universal approximators, since they can approximate any smooth nonlinear function to any degree of accuracy [62, 90, 207, 227], so that they can represent complex nonlinear systems. TS models are described by local models combined together by utilizing fuzzy IF–THEN rules as follows:

$$\text{IF } \theta_1(k) \text{ is } M_{i1} \text{ and } ... \text{ and } \theta_p(k) \text{ is } M_{ip},$$

$$\text{THEN} \begin{cases} x_{k+1} &= A_i x_k + B_i u_k, \\ y_k &= C_i x_k + D_i u_k \quad i = 1, 2, ..., r, \end{cases} \tag{2.13}$$

where r is the number of model rules, M_{ij} $(j = 1, 2, ..., p)$ are the fuzzy sets and $\theta_1(k), ..., \theta_p(k)$ are premise variables that can be functions of the state variables, external disturbances and/or time. Every linear model denoted by $A_i x_k + B_i u_k$ is named a *subsystem*. The TS systems can be modeled by means of sector-nonlinearity methodology [106, 160], which ensures that, the interpolated models are an exact formulation of the nonlinear system, in a limited local region on the state space. Evidently, the models are interpolated by membership functions. Then, the state and output equations of the

TS models can be expressed as follows:

$$\begin{aligned} x_{k+1} &= \frac{\sum_{i=1}^{r} w_i(\theta_k)\{A_i x_k + B_i u_k\}}{\sum_{i=1}^{r} w_i(\theta_k)}, \\ &= \sum_{i=1}^{r} h_i(\theta_k)\{A_i x_k + B_i u_k\}, \end{aligned} \tag{2.14}$$

$$\begin{aligned} y_k &= \frac{\sum_{i=1}^{r} w_i(\theta_k)\{C_i x_k + D_i u_k\}}{\sum_{i=1}^{r} w_i(\theta_k)}, \\ &= \sum_{i=1}^{r} h_i(\theta_k)\{C_i x_k + D_i u_k\}, \end{aligned} \tag{2.15}$$

where $\theta_k = [\theta_i(k), ..., \theta_p(k)]$ is the vector comprising all the singular premise variables. In addition, $w_i(\theta_k)$ and $h_i(\theta_k)$ are written as follows:

$$w_i(\theta_k) = \prod_{j=1}^{p} M_{ij}(\theta_j(k)), \tag{2.16}$$

$$h_i(\theta_k) = \frac{w_i(\theta_k)}{\sum_{i=1}^{r} w_i(\theta(k))}, \tag{2.17}$$

for all k. The term $M_{ij}(\theta_j(k))$ is a degree of membership of $\theta_j(k)$ in M_{ij} and $h_i(\theta_k)$ is such that

$$\begin{cases} \sum_{i=1}^{r} h_i(\theta(k)) = 1, \\ h_i(\theta_k) \geq 0, \quad i = 1, 2, ..., r. \end{cases} \tag{2.18a}$$

One of the first references based on fuzzy MPC with a certain entity is found in [46] where the TS models are introduced in the MPC due to the capacity of these models to be obtained online. A multi-step prediction is implemented where a fuzzy controller obtained as a set. In the same line, there exist some works such as [139, 221]. Other

interesting applications of the MPC to TS fuzzy models are shown in [190], in this article the authors treat predictive control with all its basic ingredients. The optimization problem is obtained with the linearized model in a plausible prediction of the model. Moreover, in [128, 2, 204] the authors are used the same method. In [105] is used a linear MPC by freezing the memberships at a particular instant and assuming that they will be constant in the future; it might work in practice, but it lacks theoretical justification in fast transients. The work [135] presents an interesting approach in which a sequence of quadratic cost bounds and state-feedback gains solves (sub-optimally) the MPC problem. The great advantage is its computational tractability; however, it is well known that even for the linear case, under constraints, the optimal value function is not quadratic in the state, so the approach is conservative.

An output-feedback MPC controller based on the TS model that includes bounded disturbance is designed in [48]. Killian et al. [114] investigated a fuzzy MPC controller based on TS fuzzy models. In this approach, a linear controller is intended for each rule of the general TS framework. At that point, the general MPC law is obtained by the fuzzy combination of those controllers. In [133], an MPC controller is designed based on the interval type-2 TS fuzzy models. The membership functions of the Parallel Distributed Compensation (PDC) controller can be separated from those of the TS fuzzy model that implements relaxation by using the PDC controller. One fuzzy MPC controller is presented for discrete-time TS framework based on piecewise Lyapunov functions (PLF) in [230]. Nevertheless, the PLF are not suitable for a TS model obtained by the sector nonlinearity approach [192].

Most of the previous studies have been only carried out in the standard tracking MPC framework that it is formulated as an optimization problem which penalizes the tracking error [179, 183]. The present thesis provides an EMPC approach based on TS model providing stability guarantees.

2.3 Prognostics and Health Management

During the last decade, important improvements in safety, performance, availability, and effectiveness of industrial systems have been achieved through prognostics and health management (PHM) paradigm [168]. PHM is a systematic strategy that is utilized to

assess the reliability of a system in its actual life-cycle conditions, predict failure progression, and decrease damage via control actions. PHM involves the application of three concepts: diagnostics, prognostics and health management. Diagnostics identifies the state of the system during its functioning, providing an accurate fault detection and isolation capability with low false alarm rate [170]. Prognostic is now identified as a principal process in maintenance strategies based on the remaining useful life of the equipment, that it makes possible to avoid critical damages and reducing costs. The Remaining Useful Life (RUL) is the useful life time that remains on an asset at a particular time of operation [53, 169]. The principal aim of PHM is to increase safety and decrease maintenance cost. To obtain this objective, some tasks, such as failure prognosis, system monitoring, and RUL calculation, may be required. Therefore, some operations like logistics requirements, maintenance performance, components replacement or controller reconfiguration, among others, should be used in order to manage the health of the system [92].

The generic structure of PHM is based on three steps: observation, analysis, and decision-making [53, 170]. The observation step consists of data acquisition, processing, storage or collection. The analysis step prepares the acquired data and extracting the diagnostics, and prognosis information. In this step, the monitoring of the system is performed based on the data acquired in the previous step. Next, the appropriate decisions about logistics actions, maintenance, mission or control reconfiguration are taken based on the information presented by the previous data analysis. In the analysis step, various methods and algorithms are used in order to estimate the remaining useful life of the asset. This process provides the diagnosis and prognosis results. In the literature, there is a certain consensus about the distribution of these methodologies, for instance, in [4] they are classified into four categories, such as physically based, data-driven, hybrid and experimental based. The next step is the decision-making, that consists in applying the convenient action based on the analyzed data to extend the useful life of the system or components.

Research on PHM methodologies, motivated by the benefits it brings, has advanced considerably in the last decade. For instance, a literature review on prognosis can be found in [170], and a particular review of data-driven methods for PHM can be observed in [210], a PHM study in the manufacturing process can be found in [214]. A review on machinery PHM implementing CBM which summarizes the recent research with emphasis on models, algorithms, and technologies for data processing and maintenance

decision-making is presented in [86]. In [69] a diagnosis and prognostic method for power electronic drives and electric machines (AC/DC, DC/DC and DC/AC systems) are presented. This approach incorporates a low-cost monitoring using the power electronics such as power MOSFETs and IGBTs. The proposed HAC strategy consists in reducing the performance of the control accomplishing the mission with reduced performance.

2.3.1 Reliability analysis methods

The beginning of a reliable-control concept was introduced in [201], where the author proposed the use of redundant controllers to improve the reliability of the control system based on a decentralized control scheme. In this case, the *reliability* concept is related to the control structure that included two or more independent controllers. Such a structure guarantees stability under controller failures and perturbations in the plant interconnection structure [202]. Reliability analysis of dynamical systems helps to prevent failures which could be costly and sometimes disastrous. In complex systems or in safety-critical systems, it is imperative to identify the key components of the system and prevent the system failure. Regularly, this is done by implementing Conditioned-Based Maintenance (CBM) methods, where decisions are supported by the reliability analysis information [3, 86].

In the literature [20, 213, 19, 152], authors refer to the concepts of reliability, degradation, deterioration, etc. In general, *reliability* directs to the concept of dependability, successful operation or performance, and the absence of failures, whereas unreliability leads to the opposite [20]. Hence, it is convenient now to give a clear definition of these concepts.

Definition 2.2. Reliability is characterized as the probability that components, units, types of equipment and systems will perform their predesignated function for a certain period of time under some operating conditions and specific environments [68].

More specifically, reliability is the probability of success in performing a task or reaching a desired property in the process, based on right operation of components. Mathematically, reliability $R(t)$ is the probability that a system will be successful in the interval from time 0 to time t:

$$R(t) = P(T > t), \qquad t \geq 0 \tag{2.19}$$

where T is a nonnegative random variable which represents time-to-failure or failure time. Moreover, the definition of unreliability of actuators or a system is defined as

Definition 2.3. The unreliability of a component (or system) $F(t)$ is defined as the probability that the component or system experiences the first failure or has failed one or more times during the time interval 0 to time t [7].

Since the component is always in one of the two possible states (operational or failed), the following relation is satisfied

$$F(t) + R(t) = 1. \tag{2.20}$$

On the other hand, the degradation can be viewed as a damage that the system accumulates over time and eventually leads to a failure when the accumulated damage reaches a failure threshold.

Definition 2.4. Degradation is the reduction in performance, reliability and lifespan of assets [71].

From these definitions, note that reliability is reduced when assets degrade or deteriorate. The failure threshold provides a link between degradation and assets failure. Therefore, it is possible to use the degradation signals to estimate the failure rate time distribution, the RUL, etc [200]. The degradation signals are obtained by a proper degradation model, which consists in developing a good probability model that is capable of describing the degradation process.

Reliability is the ability of a system to operate successfully long enough to complete its assigned mission under stated conditions. In reliability theory, various types of probability distributions are used; for example, an exponential function [64, 223], a Weibull function [89, 17], a Gamma function [122, 132, 211] or log-normal [40, 121], among others. The exponential distribution is one of the most widely used in reliability engineering because it is relatively easy to handle in performing reliability analysis, and many engineering items exhibit constant hazard rate during their useful life [45]. In the case of the Weibull distribution which is used to represent several physical phenomena and the popularity of this distribution stands on the fact that, depending on the parameters, it may describe both increasing and decreasing failure rates [219]. The gamma distribution is especially useful for reliability modeling of those asset lifetimes which

degradation can be explained by the shock accumulation [209]. The log-normal distribution is a continuous probability distribution of a random variable whose logarithm is normally distributed. The log-normal distribution is applied to the description of the dispersion of the component failure rate data [146].

Reliability can also be expressed as a stochastic process [161]. For example, it is common to use Markov Chains (MC) to model the reliability of components [163]. However, in practice, the complexity of the system steer to a combinatorial explosion of states resulting in an MC with a quite large size. The reliability information achieved with the MC is generated using a Dynamic Bayesian Network (DBN) to the system which includes temporal information to calculate the impact of the component reliability on the system reliability [218].

2.3.2 Health-aware control

Health-aware Control (HAC) is a concept that connects the health monitoring and prognostics with the control theory [80, 58]. HAC technique assesses the health system while performing control over the system in a non-faulty situation. Furthermore, it avoids faulty scenarios by mitigating health degradation via appropriate control actions considering health indicators in the control objectives [92]. This is done by regularly evaluating the system health indicators and making corrections through the control actions based on those indicators.

In this paradigm, the information provided by the prognosis module about the component system health should allow the modification of the controller so that the system health is considered in the control objectives [92, 59]. In this way, the control actions will be obtained to fulfill these objectives and, at the same time, to extend the life of the system components. The prognosis module will estimate on-line the component ageing for the specific operating conditions. In the non-faulty situation, the control efforts are distributed in the system based on the proposed health indicator [60]. Figure 2.1 represents the different techniques involved in HAC paradigm found in the literature.

In recent years, there has been an increasing interest in combining control approaches with reliability methods to develop system monitoring. For instance, in [171] the authors propose to model the degradation process in terms of asset usage and then use

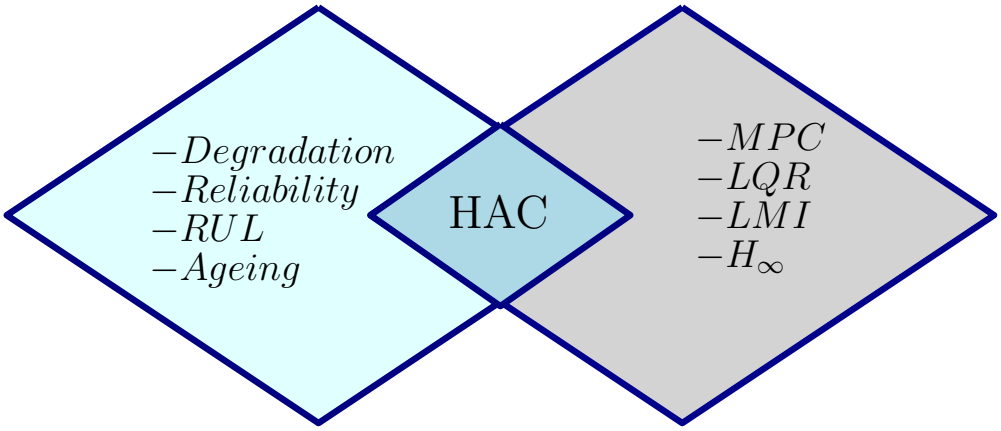

Figure 2.1: Control theory and health monitoring combination.

it to redistribute the control effort in a two-tank system by means of an MPC algorithm which solves a quadratic optimization problem and a linear optimization problem [171, 96]. In [77], the robust control methods are applied for maintaining the stability and performance of the system near to the desired performance in case of component faults is possible and in certain circumstances reduce the performance requirements to achieve the objective. In [112, 111], the authors propose the integration of reliability and reconfigurability analysis in an Fault-Tolerant Control (FTC) system for a tank system and aircraft model, respectively. These works have in common the use of components reliability as indexes to perform the control reconfiguration after the occurrence of failures. In [113], the authors propose an FTC system based on a feedback controller which guarantees the highest system reliability. This controller is synthesized using linear matrix inequalities (LMIs) and incorporating a reliability indicator. This reliability indicator is the well known Birnbaum measure which indicates those system components whose reliability are critical for the reliability of the system. Note that in the mentioned works, the asset reliabilities are modeled using the exponential distribution function.

In [17, 16], a control problem is solved by combining reliability importance measures to redistribute the control effort among the available actuators of a hydraulic system. The reliability is modeled using a Weibull distribution function and it is computed by a Dynamic Bayesian Network (DBN). In [129], the authors provide a reliable robust tracking controller against actuator faults and control surface deterioration for aircraft

bases on a mixed linear-quadratic (LQ)/H_∞ performance indexes and multi-objective optimization using LMIs.

In [110], the authors provide a reconfigurable control allocation problem for an over-actuated system in which the redistribution factor is defined in terms of the actuator reliabilities modeled by using the Weibull distribution function. Then, the control allocation problem consists in assigning more control effort to those actuators whose reliabilities are higher and to relieve those actuators whose reliabilities are lower.

In [184], the authors present an overview of modeling and control strategies including fault-tolerant capabilities for wind turbines and wave energy devices. In these systems, the reliability improvement is achieved by a significant reduction of periods of null or very low power production.

2.4 Summary

In this chapter, a literature review on a Linear Parameter Varrying (LPV) and Takagi-Sugeno (TS) modeling frameworks and Model Predictive control based on these approaches has been presented. Moreover, a literature review on prognosis and Health Management, particularly in the historical development of Health-Aware Control methodologies has been presented. Besides the attempts to address the problem of HAC, a list of applications and control techniques used were given.

Chapter 3

Case studies

In this chapter,case studies of the thesis are presented. The system descriptions and mathematical preliminaries about the pasteurization process are presented. A nonlinear model of the pasteurization plant and validation it by real data and how to embedding in the LPV models in details are specified. Besides, a selected part of the drinking water network of the city of Barcelona (Spain) is described as another case study. Finally, the nonlinear model of autonomous racing vehicle is presented in details.

3.1 Pasteurization Process

3.1.1 Introduction

One of the important food preservation techniques is pasteurization, which is widely used in food industries. The pasteurization process implies applying heat to some products such as milk, cream, beer and others at a specified temperature for a specified period of time [94]. The pasteurization process is divided into three phases that involve heating, regeneration and cooling treatments. The most significant treatment is heating, which contains heat exchanger devices to warm up the temperature of the product at the desired setpoint, and afterward keeping up this temperature during a stable time.[148].

Among many pasteurization approaches, the High-Temperature Short-Time (HTST) approach is generally accepted as the industry standard [5]. In this process, the time temperature compound can change depending on the product and some of its properties

as viscosity, fat percentage, solid residues, etc. Controlling and maintaining the temperature of the process is an important key in pasteurization. Accordingly, a suitable control system to control product temperature needs to be designed for keeping the desired product quality [94]. The necessity of a significant control for the process arises from the saving in energy, product and time if accurate tractability of the pasteurization temperature is achieved from the specified value.

Furthermore, a pasteurization system includes typical behaviors of relevant processes, such as complex dynamical models with nonlinearities [186]. Therefore, mathematical modeling and process simulation are important tools for the design, evaluation and control of continuous pasteurization processes, mainly to determine the thermal effect of the process on quality and safety attributes of the product [72, 13, 107]. A dynamic model of a continuous pasteurization process presents a virtual system that can be useful for the design and tuning of controllers, the study of the influence of the fouling, the scheduling of production and cleaning, and for personnel training [137, 41]. In the literature, there are different modeling approaches and controller strategies for pasteurization systems. The development of dynamic models of a pasteurization unit was driven by the need to design process controllers. In [153], author developed an empirical model based on ARX type time series modeling to represent a pilot scale HTST (high temperature short time) pasteurization system that consists of a PHE with two sections (regeneration and heating), a holding tube and a hot water generator unit that uses steam injection as heat source. In [109], an artificial neural network (ANN) used to empirically model a milk pasteurization plant to design linear and nonlinear model. In the AAN, the pasteurization temperature of the plant was expressed as a function of the rate of steam injection in the two heating circuits.

In [84], the complete process model leads to a multi-variable first order with pure delay transfer functions with variable parameters after decomposing the system into functional subsystems. In [22], authors used a modular process simulator for the simulation and optimization of a milk pasteurization process with three PHEs and a holding tube, but the dynamics of the process were not investigated. Other models from the whole system and/or some subsystems are obtained in [1, 148].

Motivated by the need of dynamic models to simulate pasteurization processes, one of the objectives of this dissertation is to develop and to validate a nonlinear model of a pasteurization process consisting of a heat exchanger, hot-water tank, pumps and a holding tube for the HTST processing of a liquid food. Two dynamic models of the

pasteurization plant based on different approaches and experimental data are presented in this thesis.

- **Pasteurization model 1**: The block diagram of the pasteurization model and experimental data are used for creating the first dynamic model are presented in [85].
- **Pasteurization model 2**: The dynamical model is obtained based on physical principles and fundamental laws such as energy balances and heat exchanger design, which the validation of this model is confirmed with the experimental data from the pasteurization benchmark.

3.1.2 Pasteurization model 1

System description

The pasteurization process considered is the utility-scale plant PCT-23MKII, manufactured by Armfield (UK) [12].This laboratory system is the small version (1.2m, 0.6m, 0.6m) of the real-time industrial pasteurization process. The system represents an industrial High-Temperature Short-Time (HTST) process. In this process, the goal is to warm and maintain the product at a prearranged temperature for a minimum time. This procedure is accomplished by flowing the heated fluid through a holding tube [102]. During the pasteurization process, as it can be seen in Figure 3.1, the fluid is pumped at a prearranged flow speed from the storage tank to the heat exchanger. The heat is transported to the product inward the first section of the heat exchanger, which is named regenerator. By applying lost energy of the pasteurized product, the raw product is heated to an average temperature. Later, in the second section, while utilizing a hot-water flow F_h arising from a closed circuit with a heater, the product is heated from that intermediate temperature to the complete pasteurization temperature. The T_{past} temperature is related to the output of the holding tube to monitor the temperature of the product after the pasteurization procedure. Eventually, the product temperature is reduced in the third section of the heat exchanger, where the resting heat is recuperated from the incoming product. Briefly, from a control viewpoint, the pasteurization processes can be regarded as a multiple-input-multiple-output (MIMO) system with the power of the electrical heater, P, and the water pump speed, N, as inputs, and temperatures of hot-water tank and pasteurization T_{ow}, and T_{past}, respectively, as outputs.

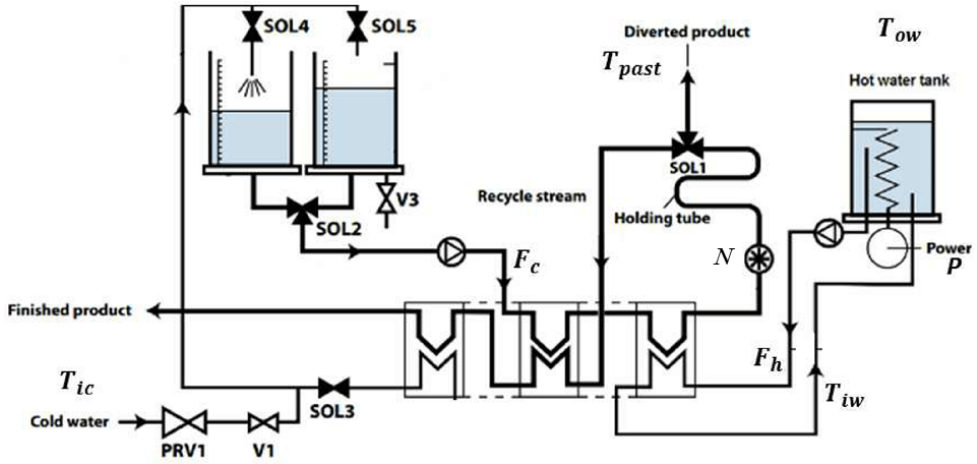

Figure 3.1: Pasteurization plant scheme.

In addition, T_{iw} and T_{ic} are disturbances of the plant, where T_{iw} is the temperature of the water heater inflow and T_{ic} is the temperature of cold water as input for the heat exchanger.

Mathematical Model

The block diagram of the pasteurization model utilized in this paper is presented in [85], whenever the ratio of hot/cold-water flow ($R = F_h/F_c$) is modified as a function of hot-water flow F_h. The modified block diagram of the pasteurization plant is exposed in Figure 3.2.

Hot-water tank model: The hot-water tank subsystem is an electric heat storage that is coated in order to decrease heat losses. In this subsystem, the water is heated by using the power resistor, while the water pump including an upper limit of 700 ml/min moves the heated water [94]. The flow is introduced as hot-water flow F_h, transmitting heat to the pasteurization product in the heat exchanger, before returning product to the water heater. In general, the hot-water flow varies over time in order to keep running of the pasteurization process. The temperature T_{iw} and the power of the electrical heater P are recognized as the inputs and the T_{ow} temperature is the output of the hot-water tank subsystem, that it is shown in Figure 3.2 (dotted red box).

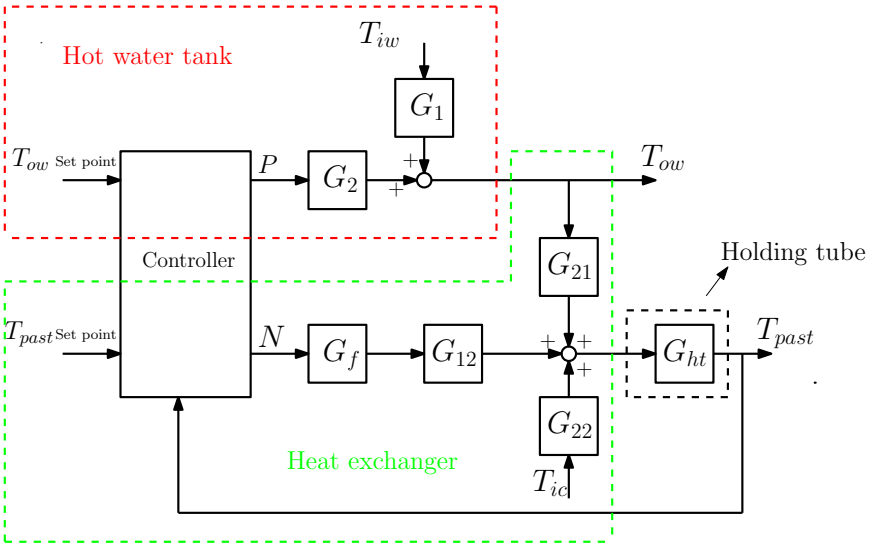

Figure 3.2: Block diagram of the pasteurization model 1.

Heat exchanger model: This part involves two sections. The first section is related to the regeneration section and the second one is based on the heating section. The heating section (second section) is more complicated than the regeneration section (first section), while the first section is obtained as a simplification of the second one, hence, the heating section is studied first.

Heating section (*second section*). The block diagram from the heat exchanger is presented in Figure 3.2 (dotted green box). As reported in [85], the transfer functions are presented as

$$G_{ij}(s) = \frac{K_{ij}(R)}{1 + \tau_{ij}(F_c, F_h)s}, \tag{3.1}$$

where τ and K are the time constant and static gain of the transfer functions, respectively. The transfer function G_{21} mainly depends on the hot-water flow, while G_{12} and G_{22} express the variations induced by the cold water flow. The pasteurization time (or holding time) is fixed during the real pasteurization process. Hence, the cold water flow should be preserved as a fixed value. Thus, G_{12} and G_{22} are transfer functions with varying gain, changing with R as stated in (3.1). Note that the parameters of (3.1) were obtained experimentally in [85] (see Appendix A. Tables A.2 and A.3).

Regeneration section (*first section*). In the regeneration phase of the heat exchanger, both cold-water and hot-water flows are the same, thus the relation $R = F_h/F_c$ is constant and of unitary value.

Holding tube model: The holding tube model is not just a transport delay since there are some heat losses. The model of the holding tube can be represented as a single-input single-output system. According to [85], the estimated parameters of the transfer function G_{ht} (in Figure 3.2) are set as static gain $K_{ht} = 0.91$ and time constant $\tau_{ht} = 21$s.

LPV modeling

Collecting all the information above, the state-space LPV model can be written as (2.9), where $x \in \mathbb{R}^{n_x}$ is the state vector composed of hot-water flow, F_h, hot-water tank temperature, T_{ow} and pasteurization temperature, T_{past}, $u \in \mathbb{R}^{n_u}$ is the vector of manipulated variables that includes the electrical power of the heater P and the water pump speed N, $y \in \mathbb{R}^{n_y}$ is the vector of controlled variables that include of the hot-water tank temperature T_{ow} and pasteurization temperatures T_{past} also the system matrices of the pasteurization system including the varying parameters in function of the scheduling variables (F_h and R) can be expressed in the discrete-time state-space form as follows:

$$A = \begin{bmatrix} 1+\frac{-T_s}{\tau_1(F_h(t))} & 0 & 0 & 0 & 0 & 0 & 0 \\ 0 & 1+\frac{-T_s}{\tau_2(F_h(t))} & 0 & 0 & 0 & 0 & 0 \\ \frac{T_s K_{21}(R(t))}{\tau_{21}(F_h(t))} & \frac{T_s K_{21}(R(t))}{\tau_{21}(F_h(t))} & 1+\frac{-T_s}{\tau_{21}(F_h(t))} & 0 & 0 & 0 & 0 \\ 0 & 0 & 0 & 1+\frac{-T_s}{\tau_{12}(F_h(t))} & 0 & \frac{T_s K_{12}(R(t))}{\tau_{12}(F_h(t))} & 0 \\ 0 & 0 & 0 & 0 & 1+\frac{-T_s}{\tau_{22}(F_h(t))} & 0 & 0 \\ 0 & 0 & 0 & 0 & 0 & 1+\frac{-T_s}{\tau_f} & 0 \\ 0 & 0 & 0 & \frac{T_s K_{ht}}{\tau_{ht}} & \frac{T_s K_{ht}}{\tau_{ht}} & \frac{T_s K_{ht}}{\tau_{ht}} & 1+\frac{-T_s}{\tau_{ht}} \end{bmatrix},$$

$$B = \begin{bmatrix} 0 & 0 & \frac{T_s K_1(R(t))}{\tau_1} & 0 \\ \frac{T_s K_2(R(t))}{\tau_2(F_h(t))} & 0 & 0 & 0 \\ 0 & 0 & 0 & 0 \\ 0 & 0 & 0 & 0 \\ 0 & 0 & 0 & \frac{T_s K_{22}(R(t))}{\tau_{22}} \\ 0 & \frac{T_s K_f}{\tau_f} & 0 & 0 \\ 0 & 0 & 0 & 0 \end{bmatrix}, \qquad C = \begin{bmatrix} 1 & 1 & 0 & 0 & 0 & 0 & 0 \\ 0 & 0 & 0 & 0 & 0 & 0 & 1 \end{bmatrix}, \tag{3.2}$$

where K is the static gain and τ is the time constant of the transfer functions of the subsystems, that the indices of K and τ are related to the transfer functions of the each subsystem from the whole pasteurization system (see Figure 3.2).

3.1.3 Pasteurization model 2

System description

In this part, the dynamical model is obtained based on physical principles and fundamental laws such as energy balances and heat exchanger design, which the validation of this model is confirmed with the experimental data from the pasteurization benchmark in laboratory. The system has the same information as previous part, a small-scale pasteurization plant PCT23 MKII that manufactured by Armfield. In this case of obtaining the model, the pasteurization plant divides to five main section such as source tank, hot-water tank, heat exchanger and peristaltic pumps (see Figure 3.3). The product to be pasteurized is filled within tank A or B (the valve SOL2 allows to choose the tank). The peristaltic pump N_1 impulses the pro duct from these tanks to the regeneration phase of the heat exchanger. In this phase, the product is preheated by the effluent of the holding tube. Then, it moves through the heating phase in the same heat exchanger where the product accomplishes the pasteurization temperature. The product quits the exchanger at high temperature T_4 and flows through the holding tube to maintain the high temperature (pasteurization temperature) during a particular time. At the end of the holding tube, there is a valve (SOL1) that opens in case that the temperature at this point T_1 is higher than the wanted. When the valve is open the fluid returns to the

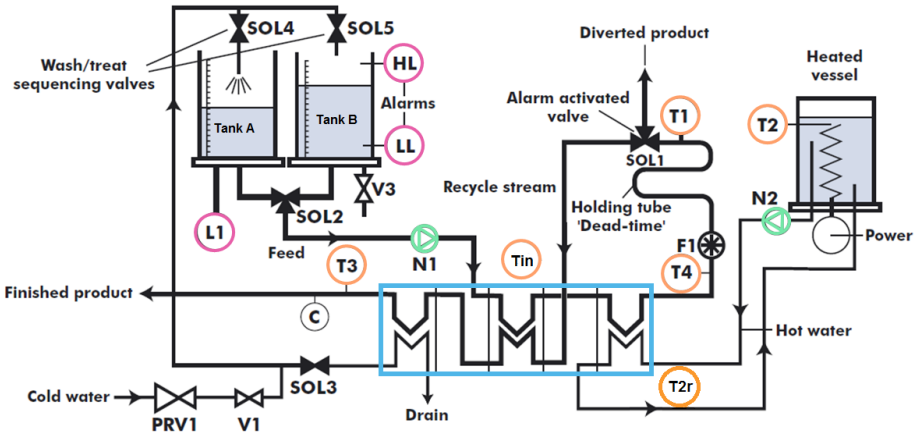

Figure 3.3: The pasteurization Plant 2.

exchanger and moves through two phases. The first one is the regeneration, where its temperature reduces by preheating the product from tank A and B. The second phase is cooling, where the goal is to cool the final product using water as a cooling fluid. On the other hand, when the product temperature is not high enough (T_1 is lower than the requested temperature), the valve SOL1 is closed and it sends the product to the feeding tank again.

Nonlinear modeling and experimental validation

The information of the dynamic response of each one of the components of the pasteurization plant is significant in order to control it. According to the number of variables of the system and by describing a physical process, it can be proposed a parametric model. For developing the pasteurization model, the plant is divided into five parts such as feeding pump, hot-water pump, hot-water tank, holding tube and heat exchanger. Physical principles based on fundamental laws such as energy balances and heat exchanger design are utilized to describe the main processes of the plant. The scheme of all the parts of the pasteurization system is presented in Figure 3.4. In this part, the model based on each element is presented. Moreover, the identification procedure to estimate the constant parameters of the pasteurization plant is presented. The idea of the method

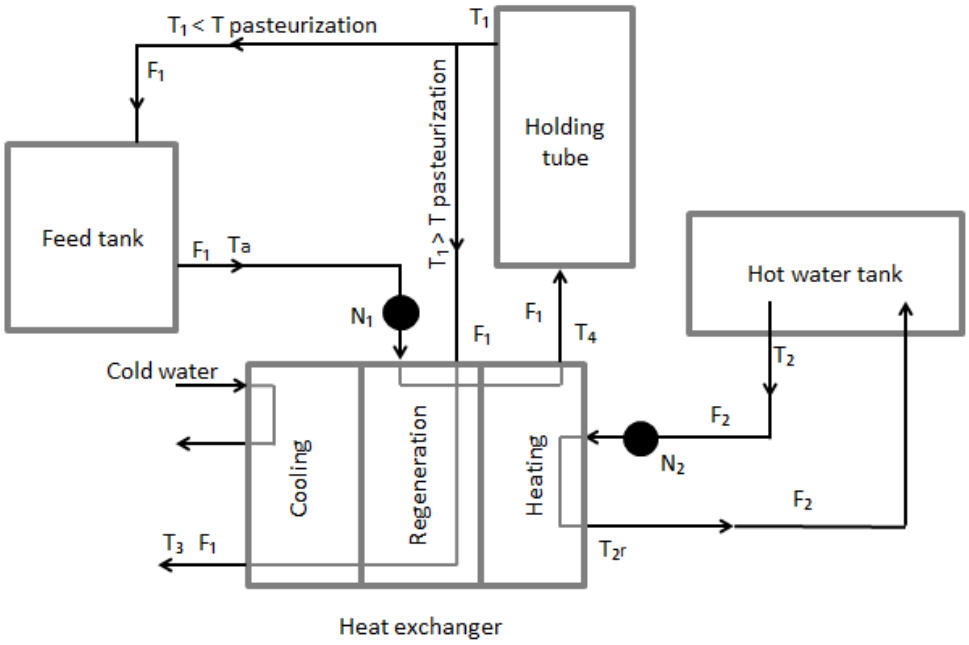

Figure 3.4: The pasteurization Plant scheme of model 2.

is to compare, the data obtained from the real set-up with the data obtained by simulating part of the continuous time non-linear model of the pasteurization process. This is formulated as an optimization problem that allows finding the parameter values that better approximate the real system in the least squares sense. Finally, in order to validate the values obtained by identification, the simulation of the non-linear model has been compared by the data obtained from the real system.

Feeding pump: The feeding pump, N_1, is the one that arouses the product to be managed from the feeding tank to the heat exchanger (Figure 3.4). The pump model connects the speed of the pump N_1 with the fluid flow through the tube F_1. This model is based on experimental data extracted from a flow meter installed in the plant. Figure 3.5 displays the flow rate F_1 for different values of rotor speed N_1, in percentage. The blue line represents the experimental flow increasing the pump speed in steps of 5% and the red line the experimental flow decreasing 5% the pump speed. Finally, the green line represents the fitting curve. The figure shows a linear correlation for speeds

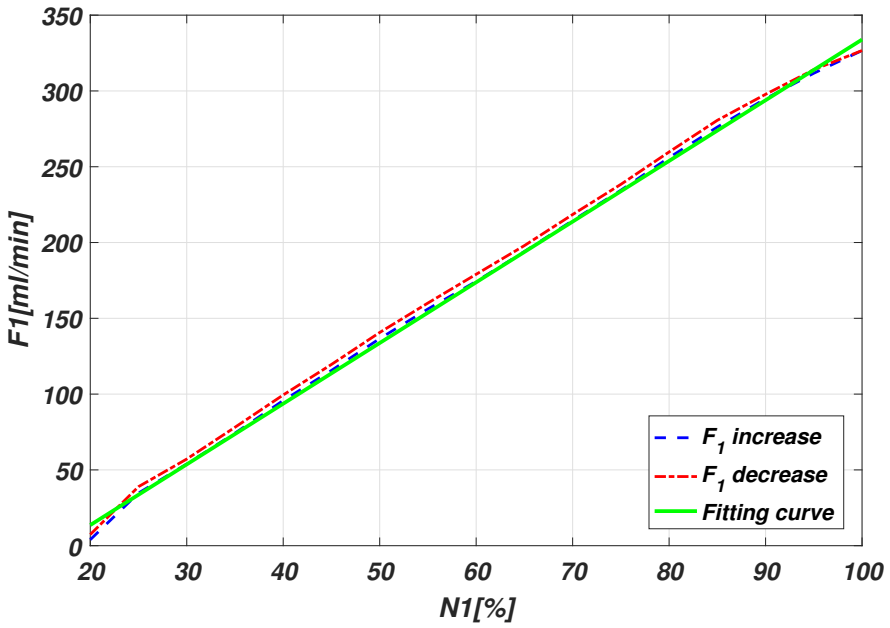

Figure 3.5: Experimental relationship between the flow F_1 and N_1.

higher than 20 % described by the following equation:

$$F_1 = K_{N_1}(N_1 - 20), \tag{3.3}$$

where F_1 represent the mass flow circulating in the plant and K_{N_1} is static gain of the pump. Moreover, the flow (in ml/min) obtained in (3.3) is the same of the mass flow expressed in g/min taking into account the density (water).

Hot-water pump: The hot-water pump pushes the hot-water from the hot-water tank to the heat exchanger (Figure 3.4). The same method as pump N_1 has been followed to determine the relationship between the speed of the pump N_2 and the flow F_2. However, in this case, a flow meter is not established hence the flow has been experimentally determined at each speed. Figure 3.6 shows the flow rate F_2 for different values of rotor speed N_2, in percentage. The blue line describes the experimental flow increasing the pump speed in steps of 5% and the red line the experimental flow decreasing a 5 % the pump speed. Finally, the green line represents the fitting curve. The equation in

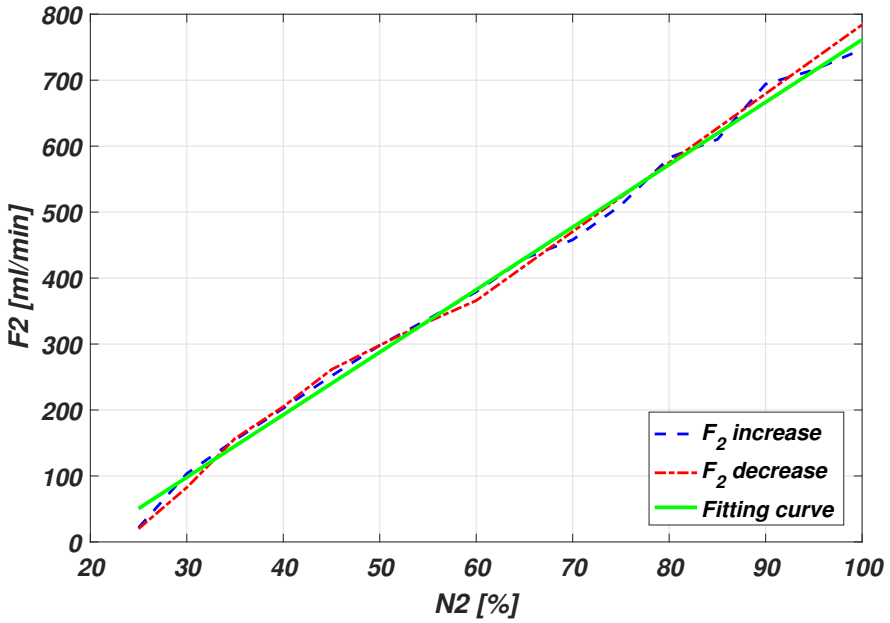

Figure 3.6: Experimental relationship between the flow F_2 and N_2.

the range 20 % to 100 % of speed is defined as:

$$F_2 = K_{N_2}(N_1 - 20), \tag{3.4}$$

As with the feeding pump, it can be considered that the change of the speed immediately exhibited the change of flow. The flow obtained in this equation (in ml/min) is the same of the mass flow expressed in g/min taking into account the density (water).

Hot-water tank: In general, the hot water tank is a plastic cylindrical recipe, with an internal radius of 7.5 cm and 20 cm length and thickness are 0.5 cm. The hot-water tank keeps the water in high-temperature T2. This thermal energy is used in the heat exchanger to the pasteurization process. Hot-water leaves the tank at a temperature $T2$ and goes to the heat exchanger. When the exchange is fulfilled, water returns to the tank at a lower temperature T_{2_r}. The value of this temperature depends on the speed of the hot-water pump $N2$. Three different heat transfer processes are considered in Hot-water tank subsystem Figure 3.7.

- The transferred heat (Q_0) depends on the power resistance utilized P. The power

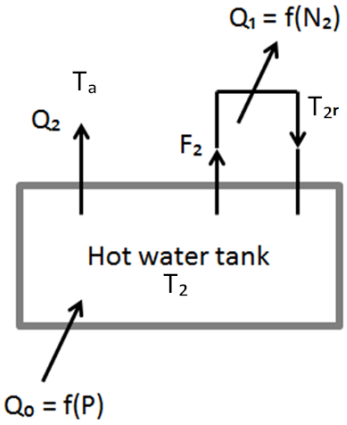

Figure 3.7: Scheme of the hot-water tank

is varied from 0 W up to 1600 W.

- The loss of heat due to the rotational flow in the heat exchanger (Q_1), represented by the following equation:

$$Q_1 = F_2 C_p (T_2 - T_{2r}) \tag{3.5}$$

where F_2 is the mass flow of hot water that flows to the heat exchanger and returns and C_p (J/K) is the particular heat of the water. T_2 is the temperature inside the reactor and T_{2r} is the returned water temperature from the heat exchanger.

- The heat loss by the environment (Q_2) defined by the convection equation [208]

$$Q_2 = U\ A(T_2 - T_a) \tag{3.6}$$

where T_a (°C) is the room temperature, A (m2) is the area of the tank and U (Wm^2/K) is the convective heat transfer.

Then, by applying an energy balance, the model of hot-water tank can be defined as:

$$C_A \frac{dT_2(t)}{dt} = P - F_2 C_p (T_2 - T_{2r}) - \alpha_{T_2}(T_2 - T_a) + \beta_{T_2} \tag{3.7}$$

where, C_A(J/K) is the calorific capacity of hot-water tank, $\alpha_{T_2} = UA$ and β_{T_2} is offset variable that are obtained by experimental data. The actuators are the power of the

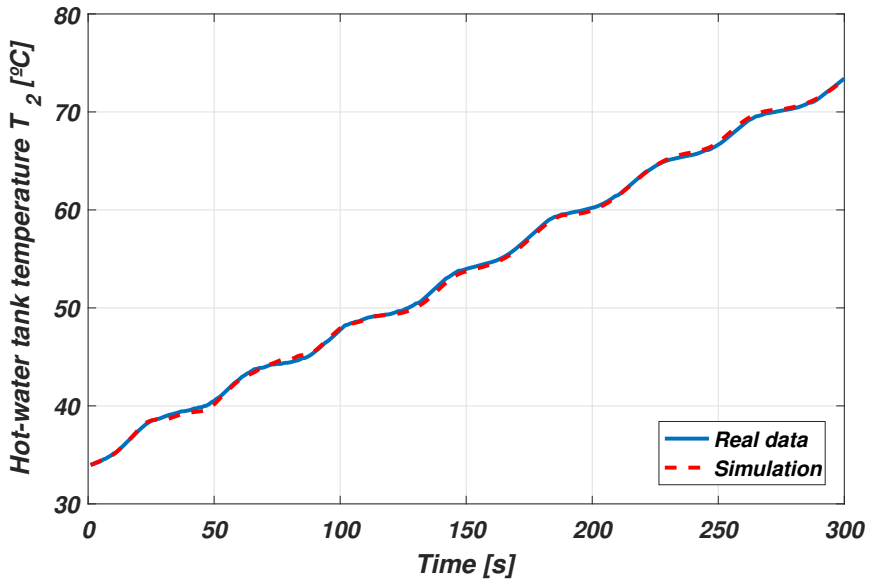

Figure 3.8: Verifying the simulation model of hot-water tank T_2

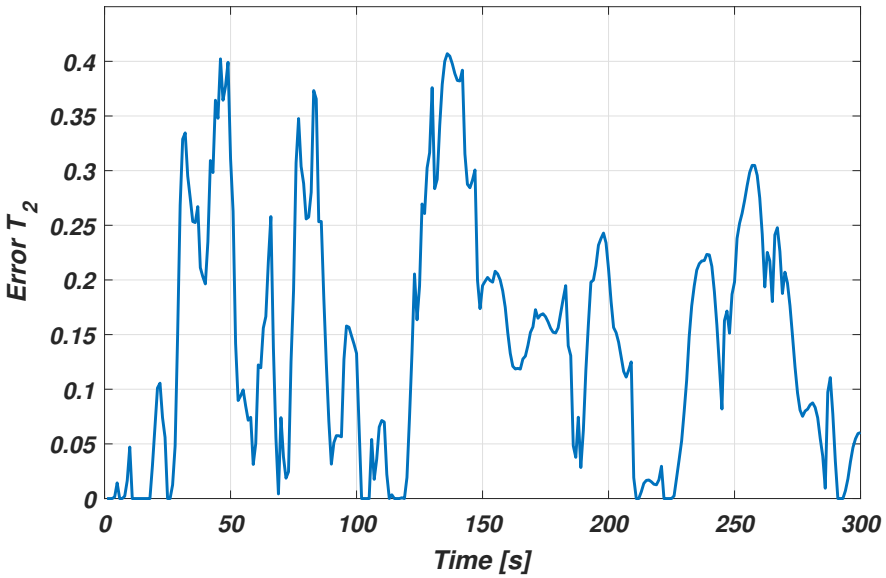

Figure 3.9: Error achieved during the simulation.

electrical resistance P and speed of the hot-water pump N_2. Moreover,(3.7) involve three temperatures T_2, T_{2r} are output and input of the hot-water tank and T_a is the room temperature that are measurable variables. The hot-water model can be rewrite as:

$$\frac{dT_2(t)}{dt} = \alpha_{1,T_2} P - F_2 C_p (T_2 - T_{2r}) - \alpha_{2,T_2} T_2 + \alpha_{3,T_2}, \tag{3.8}$$

where can be only illustrated by estimating unknown parameters of the hot-water tank temperature where the identification procedure is based on the knowledge of the non-linear model of the hot-water tank temperature. It is assumed to have at access N_{T_2} sets of data $P^j(k)$, $N_2^j(k)$ for the hot-water tank temperature where $j = 1, ..., N_{T_2}$ and $k = 1, ..., K_j$ where K_j is the number of samples of the $j-$th set of data. The identification process determines the minimum of the following objective function over the unknown parameters $\alpha_{1,T_2}, \alpha_{2,T_2}$ and α_{3,T_2}:

$$J_{T_2} = \sum_{j=1}^{N_{T_2}} \sum_{k=1}^{K_j} \left(T_2^j(k) - \hat{T}_2^j(k) \right)^2, \tag{3.9}$$

where $\hat{T}_2^j(k)$ is the simulation provided by (3.7). The comparison between the simulation data and the real data of the hot-water tank temperature is shown in Figure.3.8. The error between the real data and simulation data of hot-water tank is presented in Figure.3.9. The validation shows the model approximates the behavior of the hot-water tank in a quite perfect behavior.

Holding Tube: The holding tube is an S-shaped thermal insulated tube. The influent comes from the first stage of the heating exchanger (heating phase, Figure 3.4) at a flow rate $F1$ and high-temperature T_4. The input temperature has been considered the same that at the output of the heat In spite that the tube is isolated, the heat loss is expected. Small flow heat (Figure 3.10) is transferred to the environment producing a lessening of the effluent temperature.

The energy balance can be described by:

$$Q = F_1 C_p \Delta T + M_1 C_p \frac{dT_{in}}{dt}, \tag{3.10}$$

where T_{in} is the variation of the internal mean temperature inside the tube ($T_{in} = (T_1(t) + T_4(t))/2$) and $\Delta T = T_1(t) - T_4(t - \tau)$ is the temperature between the output (T1) at the instant t and the input (T_4) at the instant $t - \tau$, where τ is denoted the

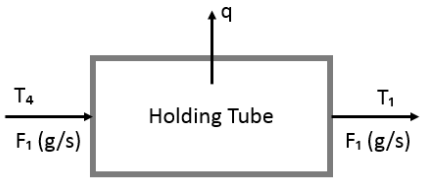

Figure 3.10: Scheme of the holding tube.

delay. M_1 is the mass of liquid. To describe the heat lost in the system Q, the general design equation for head exchanged is considered as :

$$Q = -AU\Delta T_{ml}, \tag{3.11}$$

where A is the internal area in contact with the isolated material and U is the global head transfer coefficient. Beside, ΔT_{ml} is the logarithmic mean temperature. As the mean temperature T_{in} is considered inside the whole tube, (3.11) can be rewrite as:

$$\begin{aligned} Q &= -AU\Delta T, \\ &= -AU(T_{in} - T_a), \\ &= -AU\left(\frac{T_1(t) - T_4(t-\tau)}{2} - T_a\right). \end{aligned} \tag{3.12}$$

The model of holding tube taking into account the delay, (3.10) and (3.12) can be expressed as:

$$F_1C_p(T_1(t) - T_4(t-\tau)) + M_1C_p\frac{dT_{in}}{dt} = -AU(T_{in} - T_a), \tag{3.13}$$

where holding tube model can be rewrite as:

$$\frac{dT_1}{dt} = \frac{2}{M_1C_P}(-UA\frac{T_1 + T_4(t-\tau)}{2} - T_a) - F_1C_p(T_1 - T_4(t-\tau)) - \frac{dT_4(t-\tau)}{dt}. \tag{3.14}$$

The delay τ in the holding tube can be obtained according the different behaviour between the T_4 and T_1. It consists in changing the temperature T_4 and determine the effect over T_1. To vary the temperature T_4 the speed of the feeding pump N_1 has been

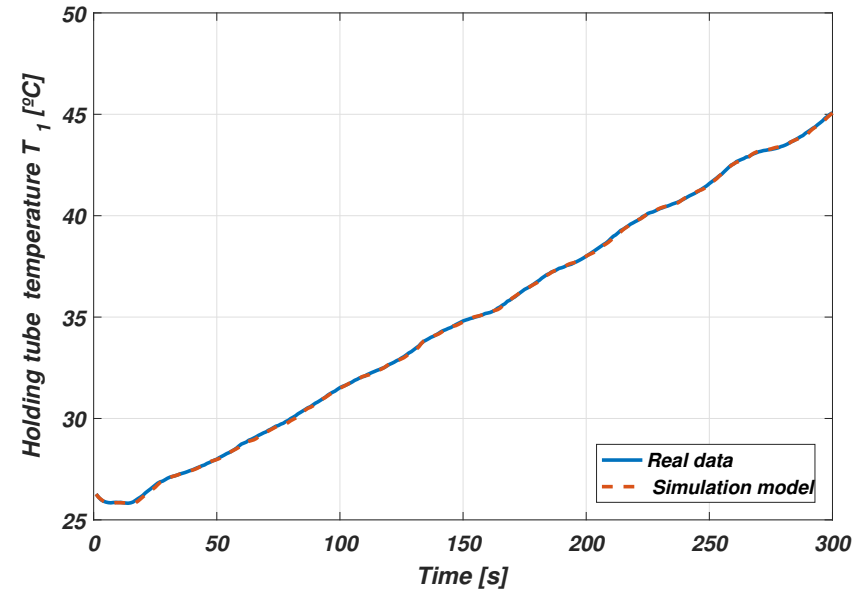

Figure 3.11: Verifying the simulation model of holding tube T_1

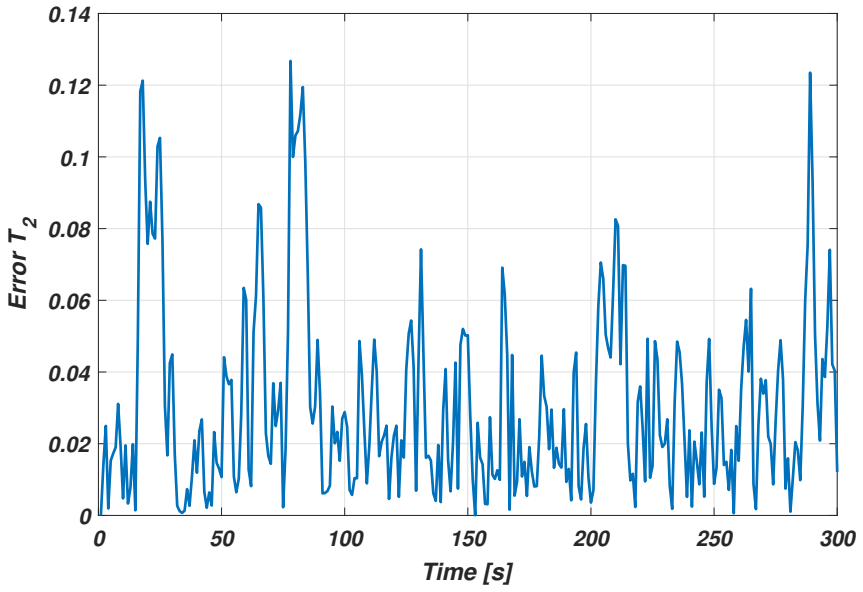

Figure 3.12: Error achieved during the simulation.

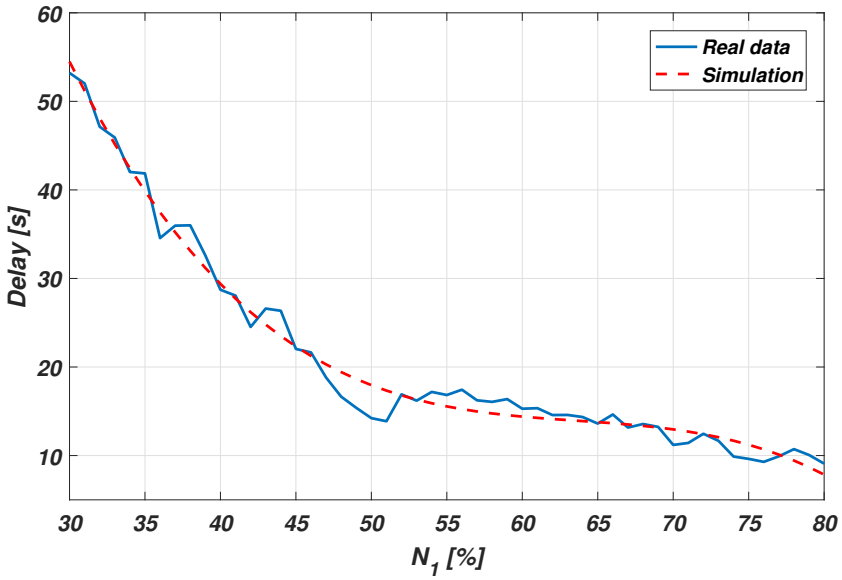

Figure 3.13: Verifying the simulation model of delay

increased from 30 to 80. Finally, the relation between the delay and N_1 is obtained as:

$$\tau(t) = -\alpha_{1,\tau}(N_1(t))^3 + \alpha 2, \tau(N_1(t))^2 - \alpha_{3,\tau}N_1(t) + \alpha_{4,\tau}, \tag{3.15}$$

where $\alpha_{1,\tau}, \alpha_{2,\tau}, \alpha_{3,\tau}$ and $\alpha_{4,\tau}$ are unknown parameters and obtained by identification procedure. It is assumed to have at access N_τ sets of data $N_1^j(k)$ for the pump where $j = 1, ..., N_\tau$ and $k = 1, ..., K_j$ where K_j is the number of samples of the $j-$th set of data. The identification process determines the minimum of the following objective function over the unknown parameters:

$$J_\tau = \sum_{j=1}^{N_\tau} \sum_{k=1}^{K_j} \left(\tau^j(k) - \hat{\tau}^j(k) \right)^2, \tag{3.16}$$

where $\hat{\tau}^j(k)$ is the simulation provided by (3.15). The comparison between the simulation data and the real data of the temperature of holding tube and the delay are shown in Figures.3.11 and 3.13, respectively. Moreover, the error between the real data and simulation data of holding tube is shown in Figure.3.12. The validation show the model approximates the behaviors of the temperature of holding tube and the delay are in a quite perfect behavior.

Heat exchanger: The heat exchanger is the system that provides the thermal energy exchange without joining the liquids. Heat exchange is controlled by the influent temperature of the fluids and their mass flow. The heat exchanger of the pasteurization system includes three phases with a different finality: heating, regeneration and cooling. As mentioned before, the main goal in the pasteurization process is to control the pasteurization temperature that is T_1. Hence, only heating and regeneration phases are considered. Moreover, the model of each phase is developed separately because each phase operates have different conditions

Heating phase: An experimental assay is performed to obtain a model of the heating phase. With this objective, the regeneration phase is stopped (closing the valve SOL1) hence, the effluent of the feeding tank is the influent of the heating phase at the same temperature ($T_{in} = T_a$, see Figures 3.3 and 3.14). Furthermore, for monitoring T_{2r} (water temperature that returns to the hot water tank), the sensor of the product temperature (T_3) are moved to that point.

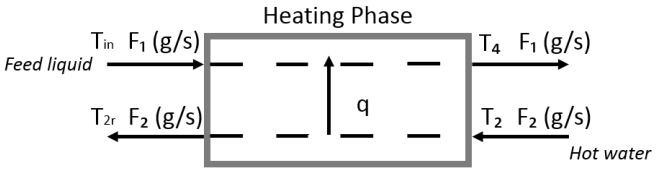

Figure 3.14: Scheme of the heating phase

To present the model of the heating phase, an energy balance in dynamic conditions is proposed as:

$$\begin{aligned} \text{Feeding} - \text{product} : q &= \bar{m}C_a(T_4 - T_{in}) + M_2C_a\frac{dT_{in2}}{dt}, \\ \text{Hot} - \text{water} : q &= \bar{m}C_a(T_2 - T_{2r}), \\ F_1C_a(T_4 - T_{in}) + M_2C_a\frac{dT_{in2}}{dt} &+ Q_{loss1} = F_2C_a(T_2 - T_{2r}) \end{aligned} \tag{3.17}$$

where $\bar{m}$ is the mass flow (F_1 corresponding to the feed product and F_2 to the hot-water) in g/s, M2 is the product mass inside the exchanger and $T_{in2} = ((T_4 + T_{in})/2)$. T_2 is the temperature inside the hot-water tank and T_{2r} the temperature of the water when it returns to the hot-water tank. The heat exchanger is not isolated therefore a heat loss to the environment Q_{loss1} should be considered, which is obtained by identification

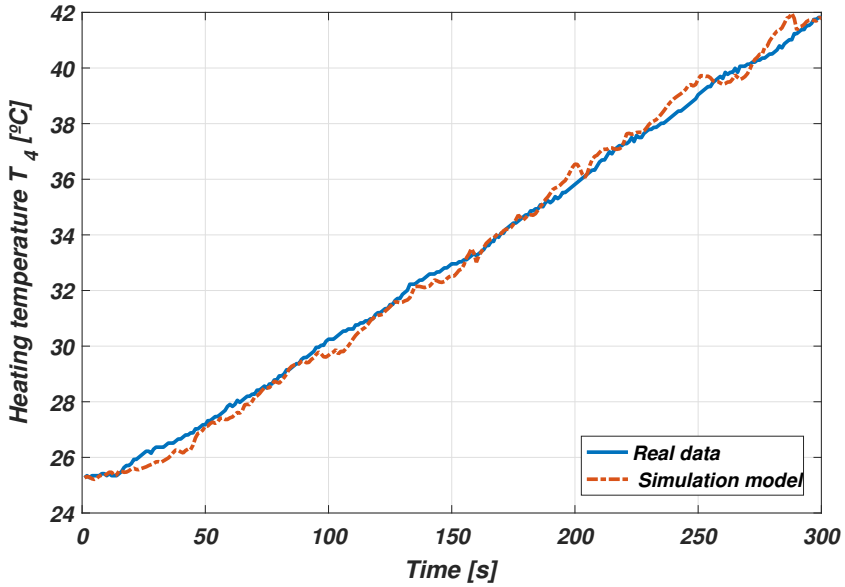

Figure 3.15: Verifying the simulation model of heating phase T_4

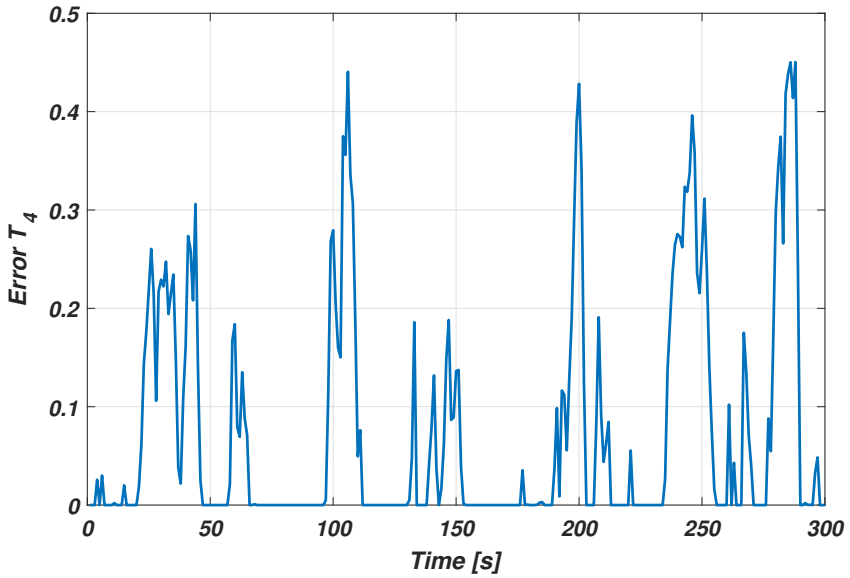

Figure 3.16: Error achieved during the simulation.

procedure. Finally, by using the experimental data and 3.17 the heating section model is proposed as:

$$\frac{dT_4}{dt} = -F_1(T_4 Tin) + \alpha_{1,T_4} F_2(T_2 - T2r) - \alpha_{2,T_4} - \alpha_{3,T_4} N_1(T_4 - Tin) + \alpha_{4,T_4} N_2(T_2 - T_{2r}). \tag{3.18}$$

For obtaining the unknown parameters, it is assumed to have at access N_{T_4} sets of data $T_{in}^j(k)$, $T_{2r}^j(k)$, $N_1^j(k)$, $N_2^j(k)$ for the heating temperature where $j = 1, ..., N_{T_4}$ and $k = 1, ..., K_j$ where K_j is the number of samples of the $j-$th set of data. The identification process determines the minimum of the following objective function over the unknown parameters $\alpha_{1,T_4}, \alpha_{2,T_4}, \alpha_{3,T_4}$ and α_{4,T_4}:

$$J_{T_4} = \sum_{j=1}^{N_{T_4}} \sum_{k=1}^{K_j} \left(T_4^j(k) - \hat{T}_4^j(k) \right)^2, \tag{3.19}$$

where $\hat{T}_4^j(k)$ is the simulation provided by (3.18). The comparison between the simulation data and the real data of the heating temperature is shown in Figure.3.15. The error between the real data and simulation data of heating phase is presented in Figure.3.16. The validation show the model approximates the behaviors of the heating temperature is in a quite perfect behavior.

Regeneration section: In the regeneration phase, the product from the feeding tank at a temperature T_a is preheated to reach T_{in} using as liquid heater the final pasteurized product (Figure 3.17). Part of the energy applied in the pasteurization process is reused in the own system. For extracting experimental data of this phase, the heating phase of the heat exchanger is stopped during the experiment. The water of the hot-water tank is applied as the pasteurized product in order to have a determined value of T_1.

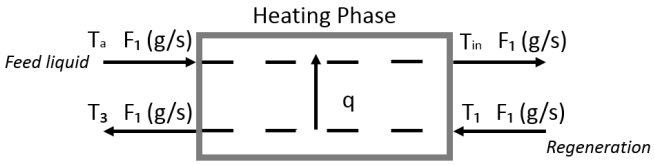

Figure 3.17: Scheme of the Regeneration phase

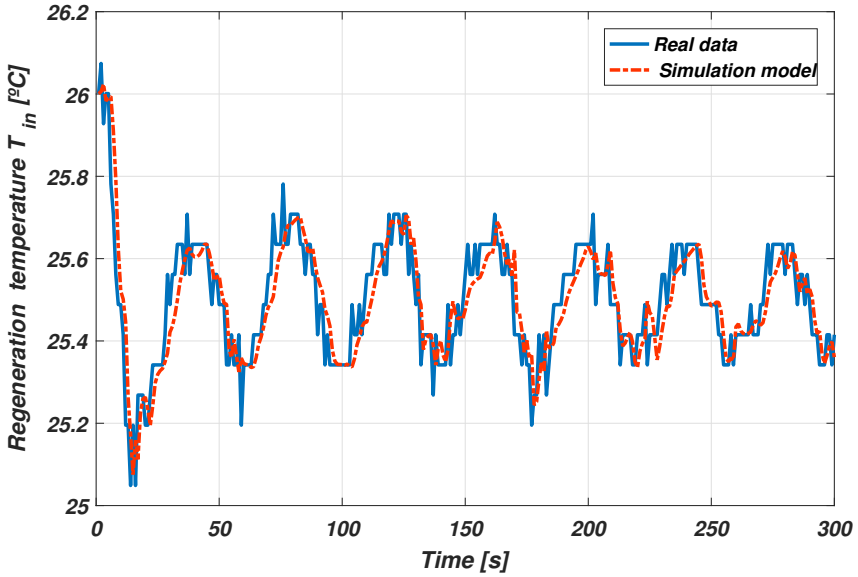

Figure 3.18: Verifying the simulation model of regeneration phase T_{in}

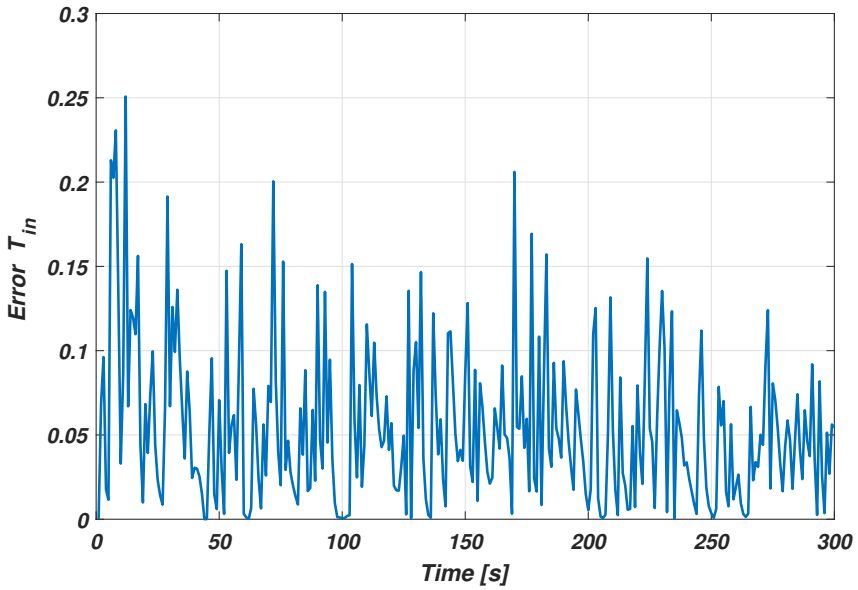

Figure 3.19: Error achieved during the simulation.

By using the energy balance, the regeneration phase model can be described as :

$$\begin{aligned} \text{Feeding} - \text{product} : q &= \bar{m}C_a(T_{in} - T_a) + M_2C_a\frac{dT_{in3}}{dt}, \\ \text{Pasteurized} - \text{product} : q &= \bar{m}C_a(T_1 - T_3), \\ F_1C_a(T_{in} - T_a) + M_2C_a\frac{dT_{in3}}{dt} &+ Q_{loss2} = F_2C_a(T_1 - T_3) \end{aligned} \tag{3.20}$$

where M_2 is the product mass inside the exchanger and $T_{in3} = ((T_a + T_{in})/2)$. T_{2r} is the temperature inside the hot-water tank and T_{2r} the temperature of the water when it returns to the hot-water tank. As explained before, the heat exchanger is not isolated therefore a heat loss to the environment Q_{loss2} should be considered, which is obtained by identification procedure. Finally, by using the experimental data and 3.20 the regeneration phase model is proposed as:

$$\frac{dT_{in}}{dt} = \frac{\alpha_{1,T_{in}}(N_1 - \alpha_{2,T_{in}})(T_1 - T_{in}) - \alpha_{3,T_{in}}(T_{in} - T_a)}{M_2}. \tag{3.21}$$

For obtaining the unknown parameters, it is assumed to have at access $N_{T_{in}}$ sets of data $T_1^j(k)$, $N_1^j(k)$ for the heating temperature where $j = 1, ..., N_{T_{in}}$ and $k = 1, ..., K_j$ where K_j is the number of samples of the $j-$th set of data. The identification process determines the minimum of the following objective function over the unknown parameters $\alpha_{1,T_{in}}, \alpha_{2,T_4}$ and $\alpha_{3,T_{in}}$:

$$J_{T_{in}} = \sum_{j=1}^{N_{T_{in}}} \sum_{k=1}^{K_j} \left(T_{in}^j(k) - \hat{T}_{in}^j(k) \right)^2, \tag{3.22}$$

where $\hat{T}_{in}^j(k)$ is the simulation provided by (3.21). The comparison between the simulation data and the real data of the regeneration temperature is shown in Figure.3.18. The error between the real data and simulation data of heating phase is presented in Figure.3.16. The validation show the model approximates the behaviors of the regeneration temperature is in a quite perfect behavior.

State T_{2r}: The model of temperature that is going back to the hot water tank (T_{2r}) is required to obtain a correct energy balance of the heat exchanger. Moreover, this temperature is not measurable due to lack of sensor in this part, then a model is required in order to estimate it in future when the plant will run normally. Therefore, sensor T_3 is moved to T_{2r} and then start the process with the production valve manually

set on divert position.

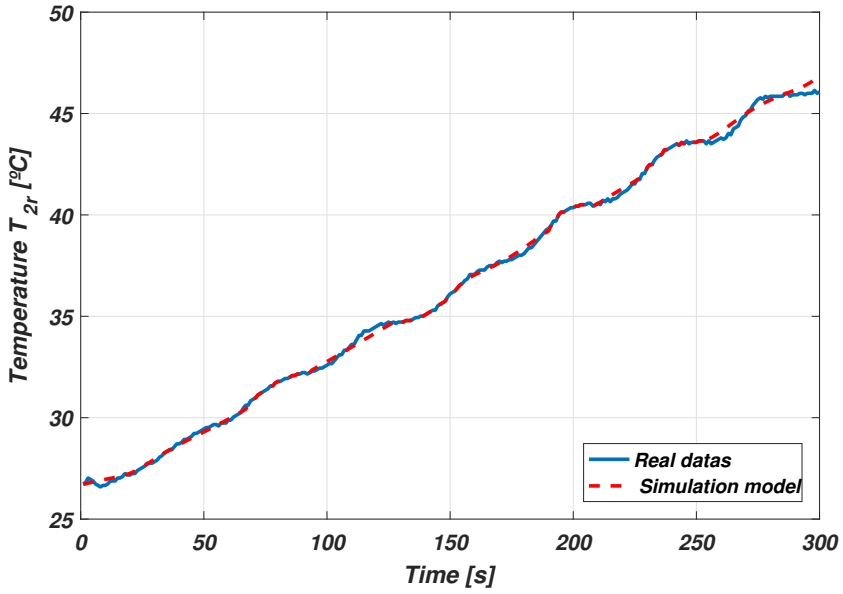

Figure 3.20: Verifying the simulation model of temperature T_{2r}

According to the above discussion, the model of this temperature are obtained as

$$\begin{aligned}\frac{dT_{2r}}{dt} =& F_1(T_4 - T_{in}) + \alpha_{1,T_{2r}} F_2(T_2 - T_{2r}) - \alpha_{2,T_{2r}}(T_2 - T_a) - \alpha_7 N_1(T_4 - T_{in}) \\ &+ \alpha_{3,T_{2r}} N_2(T2 - T_{2r}) - \alpha_{4,T_{2r}}(T_4 - T_{in}) + \alpha_{5,T_{2r}}(T_2 - T_{2r}) - \alpha_{1,T_{2r}},\end{aligned} \tag{3.23}$$

where $(\alpha_{1,T_{2r}} - \alpha_{6,T_{2r}})$ are unknown parameters and obtained by identification procedure. For obtaining the unknown parameters, it is assumed to have at access $N_{T_{2r}}$ sets of data $T_{in}^j(k),\ T_4^j(k),\ T_2^j(k),\ F_1^j(k),\ N_2^j(k)$ for the heating temperature where $j = 1, ..., N_{T_{2r}}$ and $k = 1, ..., K_j$ where K_j is the number of samples of the $j-$th set of data. The identification process determines the minimum of the following objective function over the unknown parameters $(\alpha_{1,T_{2r}} - \alpha_{6,T_{2r}})$:

$$J_{T_{2r}} = \sum_{j=1}^{N_{T_{in}}} \sum_{k=1}^{K_j} \left(T_{2r}^j(k) - \hat{T}_{2r}^j(k) \right)^2, \tag{3.24}$$

where $\hat{T}_{2r}^j(k)$ is the simulation provided by (3.23). The comparison between the simulation data and the real data of the temperature T_{2r} is shown in Figure.3.20. The error

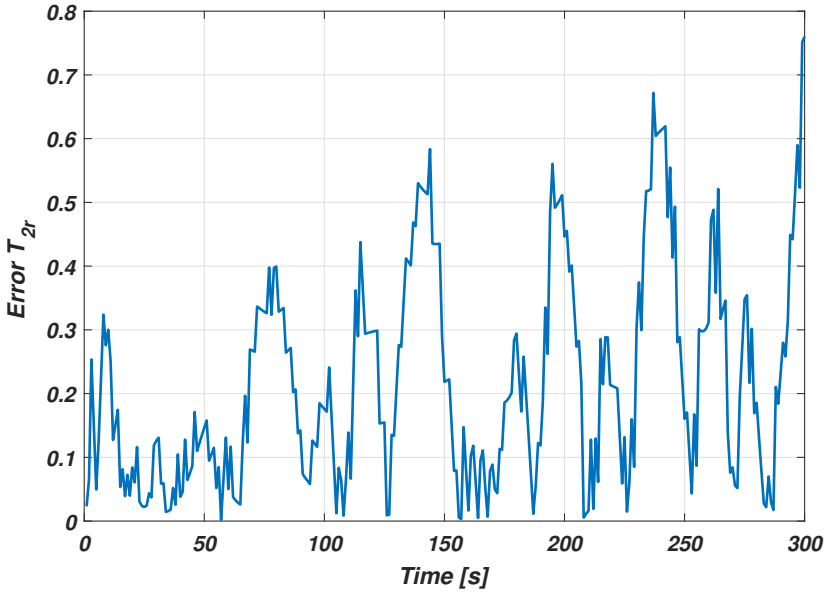

Figure 3.21: Error achieved during the simulation.

between the real data and simulation data is presented in Figure.3.21. The validation show the model approximates the behaviors of the temperature T_{2r} is in a quite perfect behavior.

LPV modeling

According to nonlinear model of each subsystem and the delay inside the system nonliner model of the pasteurization system is considered as:

$$\dot{x} = f(x, x(t-\tau), u, u(t-\tau), \omega(t)), \tag{3.25}$$

where, $x = [T_1\ T_2\ T_{2r}\ T_4\ T_{in}]^\top \in \mathbb{R}^5$, $u = [N_1\ N_2\ P]^\top \in \mathbb{R}^3$ and $\omega = [T_a] \in \mathbb{R}^1$ are states, inputs and disturbance of the pasteurization system, respectively. In addition, state equation $f : \mathbb{X} \times \mathbb{U} \longrightarrow \mathbb{X}$ and $\mathbb{X} \subseteq \mathbb{R}^5$ is presented in Appendix A. (A.1). The physical properties, process data and parameters related of the pasteurization model in the identification process are described in Table A.4 in Appendix A.

Then, by using the non-linear embedding approach [119], the state-space LPV model

of the pasteurization plant according to non-liner models of each subsystem can be expressed as follows

$$A = \begin{bmatrix} a_{11} & 0 & 0 & 0 & 0 \\ 0 & a_{22} & a_{23} & 0 & 0 \\ 0 & a_{32} & a_{33} & a_{34} & a_{35} \\ 0 & a_{42} & a_{43} & a_{44} & a_{45} \\ 0 & 0 & a_{53} & 0 & a_{55} \end{bmatrix}, \; B = \begin{bmatrix} b_{11} & 0 & 0 \\ 0 & b_{22} & b_{23} \\ b_{31} & b_{32} & 0 \\ b_{41} & b_{42} & 0 \\ b_{51} & 0 & 0 \end{bmatrix}, \; B_d = \begin{bmatrix} b_{d,11} \\ b_{d,21} \\ b_{d,31} \\ b_{d,41} \\ 0 \end{bmatrix},$$

$$A_\tau = \begin{bmatrix} 0 & a_{\tau,12} & a_{\tau,13} & a_{\tau,14} & a_{\tau,15} \\ 0 & 0 & 0 & 0 & 0 \\ 0 & 0 & 0 & 0 & 0 \\ 0 & 0 & 0 & 0 & 0 \\ 0 & 0 & 0 & 0 & 0 \end{bmatrix}, \; B_\tau = \begin{bmatrix} b_{\tau,11} & b_{\tau,12} & 0 \\ 0 & 0 & 0 \\ 0 & 0 & 0 \\ 0 & 0 & 0 \\ 0 & 0 & 0 \end{bmatrix},$$

$$C = \begin{bmatrix} 1 & 0 & 0 & 0 & 0 \\ 0 & 1 & 0 & 0 & 0 \end{bmatrix}, \tag{3.26}$$

where the value of matrix parameters are introduced in Appendix A. (A.2).

3.2 Drinking Water Networks

3.2.1 Introduction

Some approaches presented in this thesis will be assessed with a case study of a large-scale real system reported in [158], specifically a case study based on the Barcelona drinking water network (DWN). DWNs are large-scale multisource/multi-node systems which must be reliable and flexible to deal with continuously varying conditions, as for example, unexpected changes in the demands or faults in some of the components [177, 73]. DWN are multivariable dynamic constrained systems that are characterized by the interrelationship of several subsystems (actuators, tanks, intersection nodes, sources and consumer sectors). The general goal of this system is the temporal re-allocation of water sources from nature to human society, maintaining in mind the quantitative

and qualitative aspects of water accessibility and human needs. This network is currently managed by AGBAR[1] and it supplies potable water to the Metropolitan Area of Barcelona (Catalunya, Spain). Generally, the water network operates as an interconnected system driven by flow demands; different hydraulic elements are used to collect, store, distribute and supply drinking water to the associated population. In the DWN case study, the water is applied from both superficial (i.e., rivers) and underground sources (i.e., wells), contributing together with a flow of around 7 m^3/s.

According to the geographical terrain, the water supply area is subdivided into 113 pressure levels, called tiers, and the DWN is structured in two management layers: the transport network, which links the water treatment plants with the tanks established all over the city, and the distribution network, which is sectorised in sub-networks that link tanks to consumers. This thesis is focused on the transport network. Therefore, each sector of the distribution network will be recognized as a pooled demand to be served by the transport network. These demands are characterized by patterns of water usage and can be predicted by time-series models, neural networks, among other methods [205, 18].

Throughout this thesis, three different network examples extracted from the original graph of the DWN case study Barcelona DWN are used to present the numerical results. The models related to each example are denoted as *aggregate* model and *sector* model. The aggregate model is a simplification of the original graph, where groups of elements have been aggregated (not discarded) in single nodes to reduce the size of the original problem (see Figure 3.22). The sector model considers only a sector of the DWN (see Figure 3.23).

3.2.2 Control-oriented modeling of water transport network

Several control-oriented modeling approaches dealing with DWNs have been proposed in the literature (see, e.g., [145], [97]). A water transport and distribution system regularly includes a number of flow- or pressure-control elements, established at the inlets to the network; usually water production/treatment plants. Likewise, it involves flow and pressure control elements within the network, such as valves and booster pumps. A suitable description of the dynamic model of a water network is realized by counting the set of flows through these control elements (pumps and valves) as the vector of

[1] Aguas de Barcelona, S.A. Company that manages the drinking water transport and distribution in Barcelona (Spain)

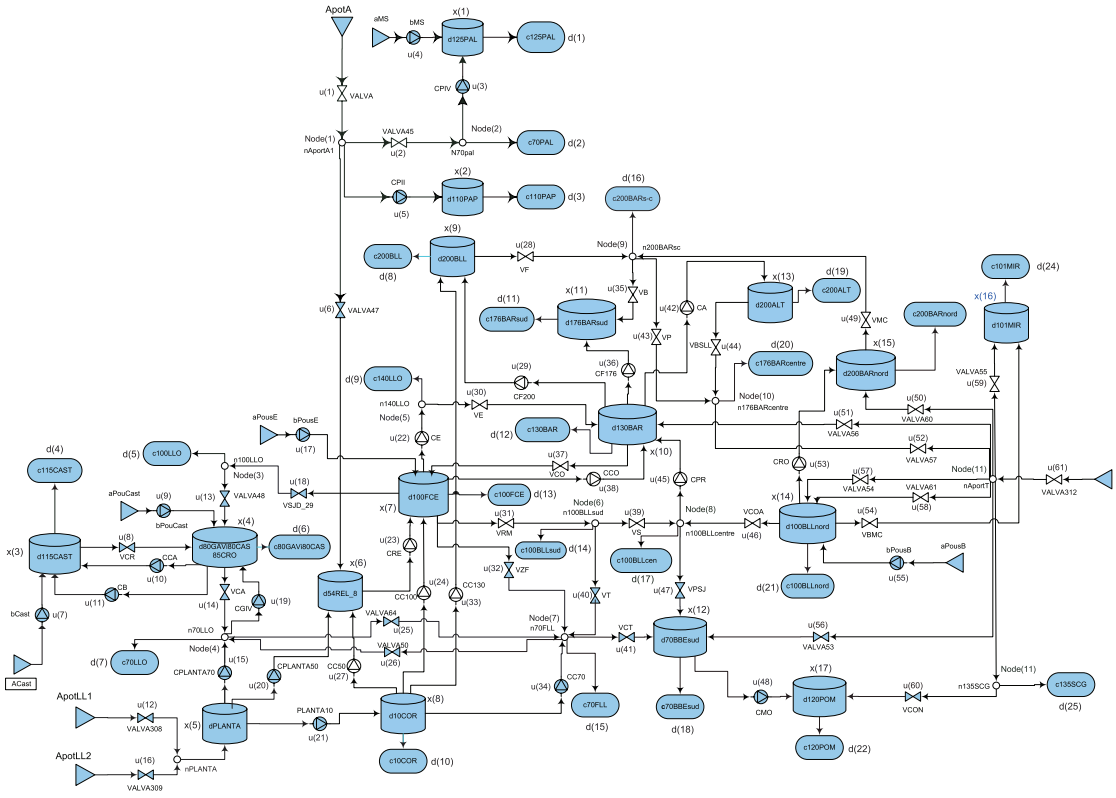

Figure 3.22: Barcelona DWN aggregate diagram

control variables $u \in \mathbb{R}^{n_u}$. The state of the network or the effect of control actions can be considered in passive elements, such as water storage tanks. Therefore, the set of n_x tank volumes observed through a telemetry system is a vector of state variables $x \in \mathbb{R}^{n_x}$. Water demand at consumer nodes can be considered a stochastic disturbance in the model. Hence, $d \in \mathbb{R}^{n_d}$ is a vector of stochastic disturbances including the values of the demands at the n_d consumer nodes in the network. Because the model is used for predictive control, d will usually be a vector of demand forecasts, achieved by suitable demand prediction models. The generalized dynamic model of the network in discrete-time can be written as follows:

$$x(k+1) = f(x(k), u(k), d(k)), \tag{3.27}$$

while the effect on the network is described at time $k+1$, produced by certain control action u, at time k, when the network is described by $x(k)$. Function f represents the mass and energy balance in the water network and k denotes the instant values at

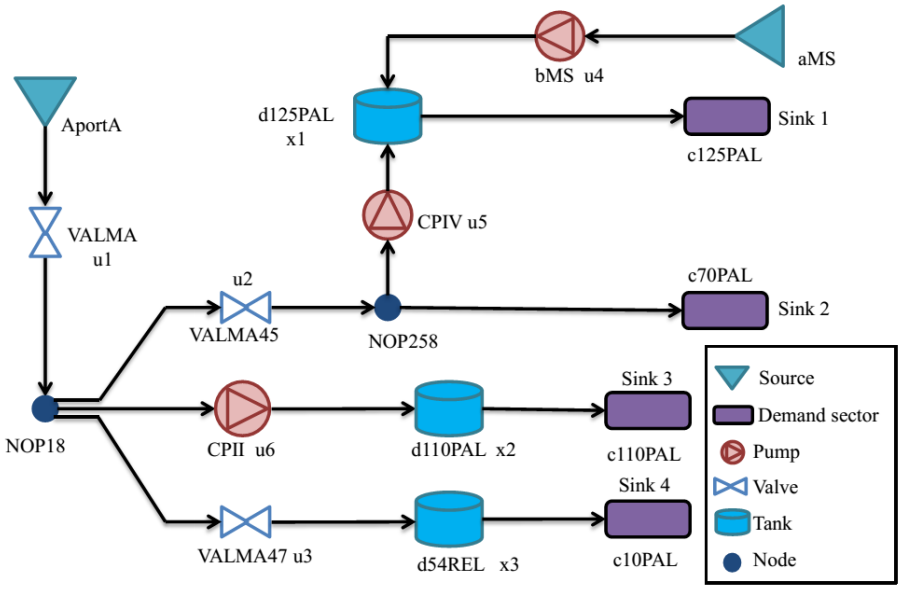

Figure 3.23: DWN sector diagram

sampling time, $d(k)$ is the demand prediction at time k.

Considering the set of compositional elements and the modeling methodology of each component in the DWN (see [37] for more details), the network is dependent on several capacity and operational constraints, and on measured stochastic flows driven by customers water demand. The control-oriented model of DWN can be described by the following set of linear discrete-time difference-algebraic equations for all time instant $k \in \mathbb{Z}_+$:

$$x(k+1) = Ax(k) + Bu(k) + B_d d_m(k), \tag{3.28a}$$

$$0 = E_u u(k) + E_d d_m(k), \tag{3.28b}$$

$$y(k) = Cx(k), \tag{3.28c}$$

where the difference equations in (3.28a) correspond to the dynamics of the storage tanks, and the algebraic equations in (3.28b) come from the static relations in the network (i.e., mass balance at junction nodes). Furthermore, $x(k) \in \mathbb{R}^{n_x}$ is the volume of the storage tanks, $u(k) \in \mathbb{R}^{n_u}$ is the manipulated inputs, $y \in \mathbb{R}^{n_y}$ denotes the output of the system and $d_m(k) \in \mathbb{R}^{n_m}$ is the demanded flow that can be as measured (or estimated) disturbances. $A \in \mathbb{R}^{n_x \times n_x}, B \in \mathbb{R}^{n_x \times n_u}, B_d \in \mathbb{R}^{n_x \times n_d}, E_u \in \mathbb{R}^{n_d \times n_u}, E_d \in$

$\mathbb{R}^{n_d \times n_d}$ and $C \in \mathbb{R}^{n_y \times n_x}$ are time-invariant matrices of suitable dimensions dictated by the network topology.

3.2.3 System management criteria

The general aim in the management of the DWN case study is to control the hydraulic performance and to minimize the economic investments of water provision as presented in [97]. Hence, the control task for the operation of this system can be formulated as a multi-objective optimization problem, which includes three operational goals in the management of DWN with different nature such as:

- Economic: To provide the required amount of water minimizing water production and transport costs.
- Safety: To guarantee the safety levels in each storage tanks that guarantee the water supply under unexpected changes in the demand up to some level.
- Smoothness: To operate actuators in the DWN under smooth control actions to avoid overpressure in pipes and damage in actuators.

Minimization of water production and transport cost

The main control objective of the DWN is to minimize the water distribution costs that are related to water production costs and electrical costs associated to pumping. Transferring drinking water to suitable pressure levels through the network includes important electricity costs in booster pumping. Hence, the cost function associated to this objective can be formulated as

$$\ell_e(k) \triangleq \alpha(k)^\top W_e u(k), \tag{3.29}$$

where $\alpha(k) \triangleq (\alpha_1 + \alpha_2(k)) \in \mathbb{R}^{n_u}$, which $\alpha_1 \in \mathbb{R}^{n_u}$ is a fixed water-production cost which is constant and a time-varying water pumping electrical cost is presented by $\alpha_2 \in \mathbb{R}^{n_u}$ that changes at each time instant k according to the dynamic electricity tariff. W_e denotes the weighting term that indicates the prioritisation of the economic control objective.

Guarantee safety management of water storage

With the aim of the preserving water supply in spite of the variation of water demands between two consecutive MPC iterations, a suitable safety volume for each storage tank must be maintained. A possible mathematical expression for this objective can be expressed as follows

$$\ell_s(k) \triangleq \begin{cases} \|x(k) - x_s\|_p, & if x(k) \leq x_s \\ 0, & otherwise \end{cases} \tag{3.30}$$

where x_s denotes the vector of the safety volumes for all the tanks. To avoid the piecewise linear form of this formulation, this cost function can be also formulated by means of a soft constraint by adding a slack variable ξ that can be expressed as

$$\ell_s(k) \triangleq \xi^\top(k) W_s \xi(k), \tag{3.31}$$

where W_s is diagonal positive definite matrix and the following soft constraint is included

$$x(k) \geq x_s - \xi(k). \tag{3.32}$$

Smoothing of control actions

The actuators in the DWN include valves and pumps. Thus, the flow-based control actions determined by the MPC controller should be smooth in order to extend the component lifespan. To ensure the smoothing effect, the slew rate of the control actions between two consecutive time instants is penalized according to

$$\ell_{\Delta u}(k) \triangleq \Delta u(k)^\top W_{\Delta u} \Delta u(k), \tag{3.33}$$

where the $\ell_{\Delta u}(k)$ corresponds to the penalization of control signal variations $\Delta u(k) \triangleq u(k) - u(k-1)$, and $W_{\Delta u}$ is a diagonal positive definite matrix. The controller should also operate actuators and tanks inside their bounds and extend the reliability of the system as will be presented later.

3.3 Autonomous Racing Vehicle

3.3.1 Introduction

Some strategies proposed in this thesis will be evaluated with a case study of a mobile system such as an autonomous vehicle. A mobile object can be presented by using equations that describe the dynamic and kinematic behaviours. Unlike general mobile robots, urban autonomous vehicles are systems with a larger mass and operating at a higher velocity. Therefore, the use of dynamic models becomes necessary. In dynamic models, the sum of forces existing over the vehicle is taken into account for computing the vehicle acceleration. The motion is generated by applying forces over the driven wheels and mass, inertial and tire parameters are considered. On the other hand, the kinematic model is based on the velocity vector movement to compute longitudinal and lateral velocities referenced to a global inertial frame.

3.3.2 System description and modeling

In racing, the race car driver's goal is to win a race, which means finishing the race with the quickest time. A race car driver has to drive the car as fast as possible without losing control of the vehicle at the limits. Moreover, it has to keep and control consistently the energy of the vehicle for keeping in the race. Therefore, a racing controller has to robustly track the desired path and stabilize the vehicle. For obtaining an optimal response in terms of tractability, it is required the vehicle to work in the dynamic limits established. The dynamic model of the vehicle used in this paper is a standard bicycle model version obtained from [166], such as:

$$\begin{aligned} \dot{v}_x &= \alpha + \frac{-F_{yf}\sin(\delta) - \mu m\, g}{m} + \omega v_y, \\ \dot{v}_y &= \frac{F_{yf}\cos(\delta) + F_{yr}}{m} - \omega v_x, \\ \dot{\omega} &= \frac{F_{yf} l_f \cos(\delta) - F_{yr} l_r}{I}, \end{aligned} \tag{3.34}$$

where v_x , v_y and ω are the body frame velocities linear in x, linear in y in (m/s) and angular velocity in (rad/s), respectively. δ is the steering angle in (rad) and α is longitudinal acceleration in (m/s^2), while both of them are control inputs of the system (see Fig.3.24).

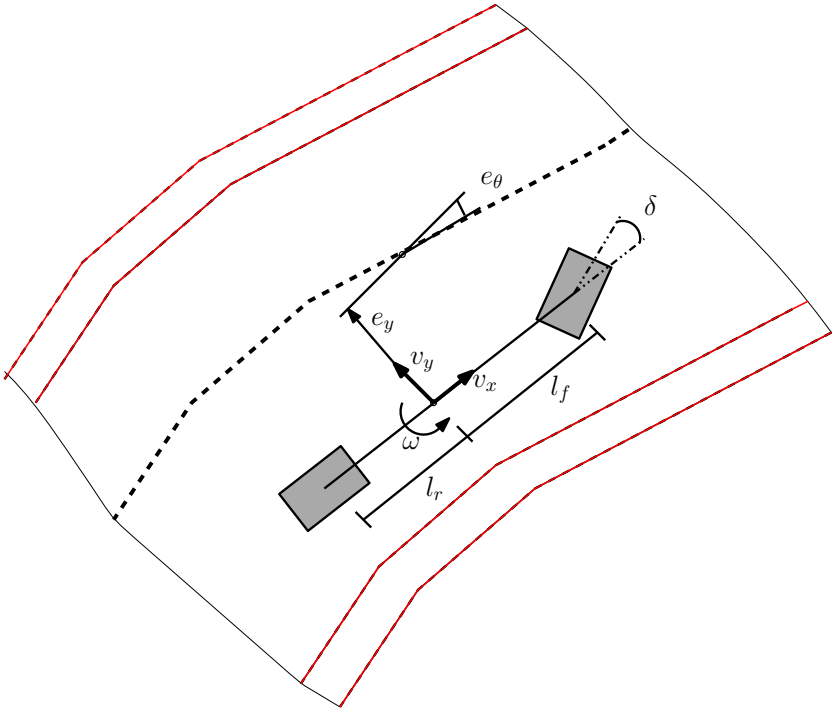

Figure 3.24: Racing vehicle variables along the road

Moreover, F_{yf} and F_{yr} are the lateral forces produced in front and rear tires in (N), respectively, given by

$$F_{yf} = C_f\left(\delta - \frac{v_y}{v_x} - \frac{l_f\omega}{v_x}\right), \tag{3.35}$$

$$F_{yr} = C_r\left(-\frac{v_y}{v_x} - \frac{l_r\omega}{v_x}\right). \tag{3.36}$$

where variables C_f and C_r are the tire stiffness coefficient for the front and rear wheels. m and I represent the vehicle mass and inertia. l_f and l_r are the distances from the center of gravity to the front and rear wheel axes, respectively. μ and g are the friction coefficient and the gravity value, respectively.

On the other hand, the kinematic model is based on the velocity vector movement in order to obtain longitudinal and lateral velocities referenced to a global inertial frame [6]. Kinematic based model has generally used because its low parameter dependency. The kinematic model used in this paper is based on the error model which is obtained

as the difference between the real position orientation states and their references. These kinematic equations are determined by the following curvature-based equations:

$$\begin{aligned} \dot{e}_y &= \sin(e_\theta)v_x + \cos(e_\theta)v_y, \\ \dot{e}_\theta &= \omega - \frac{\cos(e_\theta)v_x - \sin(e_\theta)v_y}{1 - e_y\kappa}\kappa, \\ \dot{s} &= \frac{\cos(e_\theta)v_x - \sin(e_\theta)v_y}{1 - e_y\kappa}, \end{aligned} \tag{3.37}$$

where $\dot{e}_y$ and $\dot{e}_\theta$ are the heading lateral distance and angle error between the vehicle and the path and s indicates the distance traveled along the centerline of the road. κ is the circuit curvature and presents the lateral behaviour reference. The vehicle model is concisely expressed in state space representation as

$$\dot{x}(t) = f(x(t), u(t)), \tag{3.38}$$

where at time t the vectors x and u represent the state and input,

$$x = [v_x \; v_y \; \omega \; e_y \; e_\theta]^\top, \quad u = [\delta \; \alpha]^\top. \tag{3.39}$$

3.4 Summary

This chapter presents the system descriptions and mathematical model of some case studies used in this thesis. A nonlinear model of the pasteurization plant and validation it by real data and how to embedding in the LPV models in details are specified. A case study network bases on the Barcelona DWN is described as another case study. Moreover, the nonlinear model of autonomous racing vehicle is presented in details for evaluated other approaches.

Part II

Economic MPC approaches based on LPV/TS

Chapter 4

Economic Model Predictive Control for LPV/TS Systens

This chapter proposes an EMPC strategy for LPV/TS systems. Furthermore, the economic optimization problem is solved by using a series of Quadratic Programming (QP) problems at each time instant. The new approach reduces the computational load avoiding the solution of a non-linear optimization problem. The stability of the proposed approach is analyzed and the corresponding conditions are established. The proposed algorithm for the EMPC strategy based on the LPV/TS approach is illustrated using as a case study the pasteurization plant described in Chapter 3.

4.1 Introduction

Model predictive control (MPC) based on linear models is typically used in process control when operated around a particular set-point, since the on-line optimization problem can be formulated as a convex problem by either linear or quadratic programming approaches. Nevertheless, for some systems, the nonlinear behavior can not be handled in this manner. One way to deal with non-linear system is to represent the process behavior by means of LPV/TS models [30]. The main advantage of LPV/TS models is that it embeds the system nonlinearities in the varying parameters, which make the nonlinear system become a linear-like system with varying parameters [94]. According to Section 2.2, LPV/TS models allow applying powerful linear design tools to complex non-linear models [189, 94].

Nonlinear economic MPC (NEMPC) involves optimization with nonlinear constraints, which may be computationally expensive and, in some cases, there may be no guarantee that the solution of the nonlinear optimization problem is the global optimum. Alternatively, a way of solving the optimization problem for a nonlinear system is to transform the nonlinear problem into QP problem by linearizing the model at each iteration. [117]. This method requires updating online the system matrices, applying the linearization method and also the equilibrium points when the operating point changes, which increases computational time.

The main contribution of this chapter is to provide an EMPC strategy based on quasi-LPV/TS models, in order to formulate an optimization problem that exploits the functional dependency of scheduling variables and state vector to develop a prediction strategy with numerically suitable solution. This solution is iteratively forced to an accurate solution, thereby avoiding worst-case optimization. Additionally, this chapter provides a rigorous analysis of using terminal penalties and terminal regions instead of a terminal equality constraint for guarantying the stability of EMPC control scheme based on the LPV/TS models. In comparison to other strategies mentioned above, the proposed approach is less conservative and computationally quite effective because the problem turns into solving a series of QP at each time instant. Finally, the small-scale pasteurization plant is used in order to test the effectiveness of the proposed approach.

4.2 Problem statement

Generally the nonlinear dynamics of a plant could be modeled as the fallowing discrete-time system:

$$x_{k+1} = f(x_k, u_k), \tag{4.1}$$

where the discrete-time variable is denoted by $k \in \mathbb{I}_{\geq 0}$. The state $x \in \mathbb{X} \subset \mathbb{R}^{n_x}$, input $u \in \mathbb{U} \subset \mathbb{R}^{n_u}$ and state-transition map $f : \mathbb{X} \times \mathbb{U} \longrightarrow \mathbb{X}$. Besides, the sets $\mathbb{X}$ and $\mathbb{U}$ are defined as (2.2). It is assumed that the system has an equilibrium point (x_s, u_s) such that $x_s = f(x_s, u_s)$, and the function model $f(x, u)$ is continuous. The solution of the system for a presented sequence of control inputs u and initial state x_0 is denoted as $x_k = \phi(k; x_0, u)$ for k where $x_0 = \phi(0; x_0, u)$. Additionally, the system is subject to

the state and control constraints

$$(x_k, u_k) \subset \mathbb{Z}, \qquad k \in \mathbb{I}_{\geq 0}, \tag{4.2}$$

for some compact set $\mathbb{Z} \subseteq \mathbb{X} \times \mathbb{U}$.

As mentioned before, for obtaining the optimal solution based on the nonlinear model, the optimization problem should be solved as a nonlinear problem which may be computationally expensive and/or may have convergence problems. Then, the discrete-time LPV/TS models are considered, as (2.9) and (2.13), respectively.

The controller design problem involves obtaining a control law that minimizes a specific performance cost index

$$L(\tilde{\mathbf{x}}, \tilde{\mathbf{u}}) = \sum_{i=0}^{N_p-1} \ell(x_{i|k}, u_{i|k}) \qquad \ell(x, u) : \mathbb{X} \times \mathbb{U} \longrightarrow \mathbb{R}. \tag{4.3}$$

where $\ell(x, u)$ characterized as an economic stage cost. Given the economic stage cost, the economic controller should conduct the system to the optimal reachable steady state, that is determined by using the implicit form of the optimization as follows:

Definition 4.1. The optimal reachable steady state and input, (x_s, u_s), of the system (4.1) satisfy

$$(x_s, u_s) = arg \min_{(x,u)} \ell(x, u) \tag{4.4a}$$

subject to:

$$x = f(x, u), \tag{4.4b}$$

$$x \in \mathbb{X}, \tag{4.4c}$$

$$u \in \mathbb{U}. \tag{4.4d}$$

□

As mentioned in Chapter 2, in the case of tracking MPC, $\ell(x, u)$ is typically designed as a positive definite function with regard to (x_s, u_s), i.e. In other words, $\ell(x, u) \geq 0$ for all $(x, u) \in \mathbb{X} \times \mathbb{U}$ and $\ell(x, u) = 0$ if and only if $(x, u) = (x_s, u_s)$. Hence, the optimal operation often steers to closed-loop stability of x_s by using the standard MPC stability

scheme [143]. In EMPC, $\ell(x,u)$ is arranged pursuant to some economic criteria such as production cost, energy saving and efficiency, etc. These economic criteria have to be minimized or maximized in terms of profits and environmental issues for systems. Therefore, in EMPC $\ell(x,u)$ is not necessarily positive definite with regards to (x_s,u_s). Accordingly, stability properties and convergence in the optimal economic operation are not guaranteed by using the standard MPC stability designs since these designs belong on the positive definiteness of $\ell(x,u)$.

4.3 Proposed LPV/TS-based EMPC approach

4.3.1 General approach of LPV-based EMPC

In order to derive an EMPC formulation based on LPV models, some basic assumptions are required, as follows

Assumption 4.1. *It assumed that* $\theta_k = \psi(x_k,u_k) \in \mathbb{R}^{n_\theta}$ *and* $\theta_k \in \Theta \forall k \geq 0$, *where* Θ *is a compact set.*

Assumption 4.2. *It assumed that* $(A(\theta),B(\theta))$ *is stabilizable for all* $\theta \in \Theta$.

The focus in the predictive control framework is on minimizing the economic stage cost

$$L_k = \sum_{i=0}^{N_p-1} \ell_k(x_{i|k},u_{i|k}), \tag{4.5}$$

and at each time instant k, the initial value of state and input are known and the optimization problem

$$\min_{\tilde{\mathbf{u}}_k,\tilde{\mathbf{x}}_k} L_k(\tilde{\mathbf{x}}_k,\tilde{\mathbf{u}}_k) \tag{4.6a}$$

subject to:

$$x_{i+1|k} = A(\theta_{i|k})x_{i|k} + B(\theta_{i|k})u_{i|k}, \qquad \forall i \in [0, N_p - 1], \tag{4.6b}$$

$$\theta_{i+1|k} = \psi(x_{i|k}, u_{i|k}), \qquad \forall i \in [0, N_p - 1], \tag{4.6c}$$

$$u_{i|k}, \in \mathbb{U} \qquad \forall i \in [0, N_p - 1], \tag{4.6d}$$

$$x_{i|k}, \in \mathbb{X} \qquad \forall i \in [0, N_p], \tag{4.6e}$$

$$\theta_{0|k} = \theta_k, \tag{4.6f}$$

$$x_{0|k} = x_k, \tag{4.6g}$$

$$x_{N_p} = x_s, \tag{4.6h}$$

is solved online for

$$\tilde{\mathbf{u}}_k = \begin{bmatrix} u_{0|k} \\ u_{i+1|k} \\ \vdots \\ u_{N_p-1|k} \end{bmatrix} \in \mathbb{U}. \tag{4.6i}$$

The control law is obtained by applying a receding horizon strategy, i.e., at time instant k, only the first control action in the sequence (4.6i) is applied. Then, at time $k+1$, a new optimization problem L_{k+1} is solved considering as the initial states x_{k+1} and producing the control sequence $\tilde{\mathbf{u}}_{k+1}$ such that again only the first control in the new sequence is applied.

It is not possible to solve the optimization problem (4.6) using LPV modelling, because the future state sequence cannot be predicted. Indeed the predicted states depend not only on the future control inputs u_k (the decision variables), but also on the future scheduling parameters, which for a pure LPV model are not assumed to be known a priori but only to be measurable online. On the contrary, for a quasi-LPV model, where the scheduling parameters θ_k are determined by x_k and/or u_k, the state trajectory can be predicted. Lemma 4.1 is introduced according to Lemma 1 [44] which will be used in the following parts of this chapter.

Lemma 4.1. *[44]. In the quasi-LPV model* (4.6b)*, the predicted varying parameter vector* $\theta_{i+1|k}$ *in* (4.6c) *can be determined for each* i *in the prediction horizon* N_p *knowing some estimation of* $x_{i|k}$ *and* $u_{i|k}$ *as follows:* $\hat{\theta}_{i+1|k} = \psi(\hat{x}_{i|k}, \hat{u}_{i|k})$.

Thus, instead of solving the optimization problem (4.6) by using (4.6c) that will provide the exact solution, the proposed solution is to use an approximation based on using the $\hat{\theta}$ estimation instead of θ in (4.6c). This means that the varying parameters along the prediction horizon are estimated and considered in the EMPC controller as known. Therefore, the vector

$$\Theta_k = \begin{bmatrix} \hat{\theta}_{0|k} \\ \hat{\theta}_{i+1|k} \\ \vdots \\ \hat{\theta}_{N_p-1|k} \end{bmatrix} \in \mathbb{R}^{N_p,n_\theta}, \tag{4.7}$$

contains the sequence of estimated parameters in the prediction horizon N_p. Then, by using (4.7), the predicted states can be conveniently written in vector form as

$$\mathbf{x}_k = \mathfrak{A}(\Theta_k)x_k + \mathfrak{B}(\Theta_k)\tilde{\mathbf{u}}_k, \tag{4.8}$$

where $\mathfrak{A} \in \mathbb{R}^{n_x \times n_x}$ and $\mathfrak{B} \in \mathbb{R}^{n_x \times n_u}$ are given by (4.9) and (4.10).

$$\mathfrak{A}(\Theta_k) = \begin{bmatrix} I \\ A(\hat{\theta}_k) \\ A(\hat{\theta}_{k+1})A(\hat{\theta}_k) \\ \vdots \\ A(\hat{\theta}_{k+N_p-1})A(\hat{\theta}_{k+N_p-2})\dots A(\hat{\theta}_k) \end{bmatrix} \tag{4.9}$$

and

$$\mathfrak{B}(\Theta_k) = \begin{bmatrix} 0 & 0 & 0 & \dots & 0 \\ B(\hat{\theta}_k) & 0 & 0 & \dots & 0 \\ A(\hat{\theta}_{k+1})B(\hat{\theta}_k) & B(\hat{\theta}_{k+1}) & 0 & \dots & 0 \\ \vdots & \vdots & \ddots & \ddots & \vdots \\ A(\hat{\theta}_{k+N_p-1})\dots A(\hat{\theta}_{k+1})B(\hat{\theta}_k) & A(\hat{\theta}_{k+N_p-1})\dots A(\hat{\theta}_{k+2})B(\hat{\theta}_{k+1}) & \dots & B(\hat{\theta}_{k+N_p-1}) & 0 \end{bmatrix} \tag{4.10}$$

Hence, the optimization problem (4.6) now can be rewritten as

$$\min_{\tilde{\mathbf{u}}_k, \tilde{\mathbf{x}}_k} L_k(\tilde{\mathbf{u}}_k, \mathfrak{A}(\Theta_k)x_k + \mathfrak{B}(\Theta_k)\tilde{\mathbf{u}}_k) \tag{4.11a}$$

subject to:

$$u_{i|k} \in \mathbb{U}, \qquad \forall i \in [0, N_p - 1], \tag{4.11b}$$

$$x_{i|k} \in \mathbb{X}, \qquad \forall i \in [0, N_p], \tag{4.11c}$$

$$\theta_{0|k} = \theta_k, \tag{4.11d}$$

$$x_{0|k} = x_k, \tag{4.11e}$$

$$x_{N_p} = x_s. \tag{4.11f}$$

In this way, the online optimization problem can be solved as a QP problem, which is significantly easier than solving a general nonlinear optimization problem. The parameter varying estimation will be done by means of the following approach at each discrete time k:

- In the first iteration ($k = 0$), the optimization problem (4.6) is solved as a linear problem since the quasi-LPV model (4.6b) is replaced by the LTI model that is obtained considering $\theta_{0|i} \simeq \theta_{1|i} \simeq \theta_{2|i} \simeq ... \simeq \theta_{N_p-1|i}$ along the prediction horizon N_p and where $\theta_{0|0} = \psi(x_{0|0}, u_{0|0})$.
- In the next iterations, the sequence of the estimated varying parameters Θ_k in (4.7) according to Lemma 4.1 is obtained using as estimation for the states $\hat{x}^*_{k-1}$ and controls $\hat{u}^*_{k-1}$ that are the state and input sequences obtained from the optimal solution (4.11) in the previous iteration $k - 1$.

4.3.2 Adaptation to the TS-EMPC case

As mentioned in section 2.2.2, nonlinear systems can be approximated through the TS fuzzy models. Modeling the process behavior by means of the TS model is one way to deal with nonlinear systems.Hence, the general formulation of EMPC deals with discrete-time TS fuzzy models of the following form:

$$x(k+1) = \sum_{i=1}^{r} h_i(\theta(k))(A_i x(k) + B_i u(k)). \tag{4.12}$$

where the sets $\mathbb{X}$ and $\mathbb{U}$ are defined as (2.2). Besides, the system is subject to the control constraint and state (4.2). The task of control is to satisfy constraints whilst the economic stage cost function is represented as $\ell : \mathbb{X} \times \mathbb{U} \longrightarrow \mathbb{R}$.

Considering the economic stage cost (4.5), the economic controller aims to drive the system to the optimal accessible steady state, that is defined by using the implicit form of the optimization

as: The optimal accessible steady state and input, (x_s, u_s) for TS model, satisfy

$$(x_s, u_s) = arg \min_{(x,u)} \ell(x, u) \tag{4.13a}$$

subject to:

$$x = \sum_{i=1}^{r} h_i(\theta)(A_i x + B_i u), \tag{4.13b}$$

$$x \in \mathbb{X}, \tag{4.13c}$$

$$u \in \mathbb{U}. \tag{4.13d}$$

Analogously to the LPV-based EMPC controller presented in the previous section, the EMPC controller based on the TS fuzzy model (4.12) is obtained by solving a finite-time horizon optimization problem (FHOP).

By considering the same economic objective function (4.5), the system initial conditions and assuming premise variables are dependent on the function of states and inputs, the optimization problem associated to the TS-MPC can be formulated as

$$\min_{\tilde{\mathbf{x}}, \tilde{\mathbf{u}}} L(\tilde{\mathbf{x}}, \tilde{\mathbf{u}}) \tag{4.14a}$$

subject to:

$$x(l+1) = \sum_{i=1}^{r} h_i(\theta(l))(A_i x(l|k) + B_i u(l|k)), \qquad \forall l \in [0, N_p - 1], \tag{4.14b}$$

$$\theta(l|k) = f(x(l|k), u(l|k)), \qquad \forall l \in [0, N_p - 1], \tag{4.14c}$$

$$u(l|k) \in \mathbb{U}, \qquad \forall l \in [0, N_p - 1], \tag{4.14d}$$

$$x(l|k) \in \mathbb{X}, \qquad \forall l \in [0, N_p], \tag{4.14e}$$

$$\theta(0|k) = \theta(0), \tag{4.14f}$$

$$x(0|k) = x(0), \tag{4.14g}$$

$$x(N_p) = x_s, \tag{4.14h}$$

is solved online for

$$\tilde{\mathrm{u}}(k) = \big[u(l|k), u(l+1|k), ..., u(N_p - 1|k)\big] \in \mathbb{U}. \tag{4.14i}$$

Similarly to the LPV case, when using the TS model (4.12) in the optimization problem (4.14), the future premise variables sequence (4.14c) is not known. In fact, the structure (4.14b) is linear but because of (4.14c), the problem becomes nonlinear. Actually, this issue makes the problem (4.14) not easy to solve. Then, by using the same

approach proposed for the LPV case, (4.14) is solved as a QP problem which consists in transforming the exact NEMPC into an approximate linear EMPC.

Hence, by using a vector that contains the sequence of the estimated premise variables Θ_k in a similar way that (4.7) in the LPV case, the predicted states can be conveniently written in vector form as (4.8) by defining

$$A(\theta_k) = \sum_{i=1}^{r} h_i(\theta(k))A_i, \tag{4.15}$$

$$B(\theta_k) = \sum_{i=1}^{r} h_i(\theta(k))B_i, \tag{4.16}$$

The predicted states can be formulated in vector form as (4.8), where $\mathfrak{A} \in \mathbb{R}^{N_p,\, n_x \times N_p,\, n_x}$ and $\mathfrak{B} \in \mathbb{R}^{N_p,\, n_x \times N_p,\, n_u}$ are given by (4.9) and (4.10). Then, the optimization problem (4.14) can be represented as

$$\min_{\tilde{\mathbf{u}}, \tilde{\mathbf{x}}} L(\mathcal{A}(\Theta(k))x(k) + \mathcal{B}(\Theta(k))\tilde{\mathbf{u}}(k), \tilde{\mathbf{u}}) \tag{4.17a}$$

subject to:

$$u(l|k) \in \mathbb{U}, \qquad \forall l \in [0, N_p - 1], \tag{4.17b}$$

$$x(l|k) \in \mathbb{X}, \qquad \forall l \in [0, N_p], \tag{4.17c}$$

$$\theta(0|k) = \theta(0), \tag{4.17d}$$

$$x(0|k) = x(0), \tag{4.17e}$$

$$x(N_p) = x_s. \tag{4.17f}$$

As in the LPV case, the sequence of the estimated premise variables Θ_k in (4.8) according to Lemma 4.1 is obtained using as estimation for the states $\hat{x}^*_{k-1}$ and controls $\hat{u}^*_{k-1}$ that are the state and input sequences obtained from the optimal solution (4.17) in the previous iteration $k-1$.

4.4 Stability and convergence analysis

For the first time in control research, asymptotic stability of the EMPC was established in [182] with an assumption of linear plant dynamic and stringently convex cost functional. In Section 4.3, the propose EMPC approach is provided by considering terminal equality constraints $x(N_p) = x_s$. However, this constraint can not guarantee the stability of EMPC based on the LPV model because the terminal constraint is just around a point. In this section, it will be shown that by considering the terminal state belongs to a compact set the stability of the approach can be improved and ensured.

In this chapter, by following [8, 9], the main proof of stability strongly relies on imposing a region constraint on the terminal state instead of a point constraint and

adding a penalty on the terminal state to the regulator the cost. Moreover, the stability analysis is adjusted for terminal constraint EMPC taking into account that the strict dissipativity is sufficient for guaranteeing asymptotic stability of the closed-loop system. Hence, the economic objective function defined as

$$L(\tilde{\mathbf{x}}, \tilde{\mathbf{u}}) := \sum_{i=0}^{N_p-1} \ell(x_i, u_i) + V_f(x_{N_p}), \tag{4.18}$$

where $V_f : \mathbb{X}_f \longrightarrow \mathbb{R}$ is the penalty on the terminal state, and $\mathbb{X}_f \subseteq \mathbb{X}$ is a compressed terminal region including the steady-state operating point in its interior. For LPV models, one can ofter determine $\mathbb{X}_f$ when a control Lyapunov function is available. In this formulation, the system using EMPC is stabilized by adding the requirement that the terminal state extends in this terminal region, rather than at the optimal steady state. According to [10] and for simplifying the method of improving the stability of EMPC, the following definition and some assumptions are presented.

Definition 4.2. A control system (2.9) is dissipative regarding by stock rate $s : \mathbb{X} \times \mathbb{U} \longrightarrow \mathbb{R}$ whereas there exists a function $\gamma : \mathbb{X} \longrightarrow \mathbb{R}$

$$\gamma(A(\theta_k)x_k + B(\theta_k)u_k) - \gamma(x) \leq s(x, u), \tag{4.19}$$

for all $(x, u) \in \mathbb{Z} \subseteq \mathbb{X} \times \mathbb{U}$. Additionally, if $\rho : \mathbb{X} \longrightarrow \mathbb{R}_{\geq 0}$ is definite positive[1] then

$$\gamma(A(\theta_k)x_k + B(\theta_k)u_k) - \gamma(x) \leq -\rho(x - x_s) + s(x, u), \tag{4.20}$$

finally, it can be said the system is stringently dissipative.

□

Assumption 4.3. *(Strict dissipativity) System model* (2.9) *is strictly dissipative with respect to the supply rate that defined as* $s(x, u) := \ell(x, u) - \ell(x_s, u_s)$.

Assumption 4.4. *The stage cost and model are continuous on* $\mathbb{Z}$. *The terminal cost function* $V_f(.)$ *is continuous on* $\mathbb{X}_f$.

Assumption 4.5. *The storage function* $\gamma(.)$ *is continuous on* $\mathbb{Z}$.

Assumption 4.6. *(Stability assumption) A compact terminal region* $\mathbb{X}_f \subseteq \mathbb{X}$, *containing the point* x_s *in its interior and control law* $K_f(\theta_k) : \mathbb{X}_f \longrightarrow \mathbb{U}$ *are exist, in such a way that the following holds*

$$V_f\big((A(\theta_k) + B(\theta_k)K_f(\theta_k))x_k\big) \leq V_f(x) - \ell(x, K_f(\theta_k)x_k) + \ell(x_s, u_s) \tag{4.21}$$

Remark 4.1. Assumption 4.6 implies the set for $\mathbb{X}_f(x_s^*)$ for all $k \in \mathbb{Z}_+$ to be invariant under the control law $u_k = K_f(\theta_k)x_k$. ◊

[1] A function is positive definite according to some points $x_s \in \mathbb{X}$ if it is continues, $\rho(x_s) = 0$ and $\rho(x) \geq 0$ for all $x \neq x_s$.

Remark 4.2. Considering Assumption 4.6 is the only condition on V_f, it can be assumed without loss of generality that $V_f(x_s) = 0$ for all $k \in \mathbb{I}_+$. It should be remarked that unlike the standard MPC problem, $V_f(x)$ is not significantly positive definite with respect to x_s. $\Diamond$

In order to analyse the asymptotic stability of the closed-loop model, the following rotated regulator cost functions with terminal costs are considered:

$$\mathcal{L}(x,u) := \ell(x,u) - \ell(x_s,u_s) + \gamma(x) - \gamma(A(\theta_k)x_k + B(\theta_k)u_k), \tag{4.22a}$$

$$\bar{V}_f(x) := V_f(x) - V_f(x_s) + \gamma(x) - \gamma(x_s), \tag{4.22b}$$

with the costs $\bar{V}_f$and $\mathcal{L}$, the following auxiliary optimal control problem is introduced:

$$\min_{\tilde{\mathbf{u}},x} \bar{L}(x,\tilde{\mathbf{u}}) := \sum_{i=0}^{N_p-1} \mathcal{L}(x_i,u_i) + \bar{V}_f(x_{N_p}), \tag{4.23}$$

subject to (4.11b)-(4.11f).

The constraints in problem $\bar{L}(x,\tilde{\mathbf{u}})$ are the same as in problem $L(x,\tilde{\mathbf{u}})$. Therefore, solutions exist for both problems for $x \in \mathbb{X}_{N_p}$ .Consequently, both problems have an identical feasible set for all $k \in \mathbb{I}_+$.

Remark 4.3. According to Assumption 4.6, it can be assumed that $\gamma(x_s) = 0$ for all $k \in \mathbb{I}_+$ without loss of generality. $\Diamond$

Lemma 4.2. *Considering Assumptions 4.4, 4.5 and 4.6 hold. The solution of the auxiliary problem $\bar{L}(x,\tilde{\mathbf{u}})$ is identical to the solution of the original problem $L(x,\tilde{\mathbf{u}})$.*

Proof. By considering that both problems only differ in the cost function, expanding the rotated regulator cost function yields

$$\begin{aligned}
\bar{L}(x,\tilde{\mathbf{u}}) &= \sum_{i=0}^{N_p-1} \mathcal{L}(x_i,u_i) + \bar{V}_f(x_{N_p}) \\
&= \sum_{i=0}^{N_p-1} \ell(x_i,u_i) - \ell(x_s,u_s) \\
&+ \gamma(x) - \gamma(A(\theta_i)x_i + B(\theta_i)u_i) + V_f(x_{N_p}) - V_f(x_s) + \gamma(x_{N_p}) - \gamma(x_s) \\
&= L(x,\tilde{\mathbf{u}}) - V_f(x_s) + \gamma(x_{N_p})) - \gamma(x_s) + \gamma(x) - \gamma(x_{N_p}) - \sum_{i=0}^{N_p-1} \ell(x_s,u_s).
\end{aligned}$$

Subsequently, according to Remark 4.3, it is obtained that

$$\bar{L}(x,\tilde{\mathbf{u}}) = L(x,\tilde{\mathbf{u}}) + \gamma(x) - \sum_{i=0}^{N_p-1} \ell(x_s,u_s). \tag{4.25}$$

Since $\sum_{i=0}^{N_p-1} \ell(x_s, u_s)$ and $\gamma(x)$ are independent of the decision variable $\tilde{\mathbf{u}}$ for a provided initial state $x \in \mathbb{X}$, the two cost functions $\bar{L}(x, \tilde{\mathbf{u}})$ and $L(x, \tilde{\mathbf{u}})$ are different only by a constant. Therefore, the two optimization problems have the same identical solutions at all time steps $k \in \mathbb{I}_+$. □

Now, it can be seen that the modified terminal cost obtains the basic stability condition of the original terminal cost, due to the equivalence of the problems is improved.

Lemma 4.3. *The modified costs $\mathcal{L}$ and $\bar{V}_f$ satisfy the following property if and only if $V_f(.), \ell(.)$ satisfies Assumption 4.6.*

$$\bar{V}_f\big((A(\theta_k) + B(\theta_k)K_f(\theta_k))x_k\big) \leq \bar{V}_f(x) - \mathcal{L}(x, K_f(\theta_k)x) \tag{4.26}$$

Proof. The proof follows from the results presented in [8]. By considering Remark 4.3, Remark 4.2 and proper manipulation of (4.22b) by adding the term $\gamma(x) + \gamma((A(\theta_k) + B(\theta_k)K_f(\theta_k))x_k)$ to both sides. □

Lemma 4.4. *[108] Let $\rho(x) : \mathcal{C} \longrightarrow \mathbb{R}_{\geq 0}$ be a positive definite function that defined on the compact set $\mathcal{C}$. Then, there exists a class $\mathcal{K}$ function $\zeta(.)$ such that*

$$\rho(x) \geq \zeta(|x|), \qquad \forall x \in \mathcal{C}. \tag{4.27}$$

Lemma 4.5. *Let Assumptions 4.3 to 4.6 hold. The terminal cost $\bar{V}_f$ and rotated stage cost $\mathcal{L}$ are satisfied for following inequalities:*

$$\mathcal{L}(x, u) \geq \zeta(\|x - x_s\|) \geq 0, \qquad \forall (x, u) \in \mathbb{Z} \tag{4.28}$$

$$\zeta(\|x - x_s\|) \leq \bar{V}_f \leq \hat{\zeta}(\|x - x_s\|), \qquad \forall (x) \in \mathbb{X}_f \tag{4.29}$$

where functions $\zeta(.)$ and $\hat{\zeta}(.)$ are class $\mathcal{K}$.

Proof. From (4.20), (4.22a) and Assumption 4.3, it holds that $\mathcal{L}(x, u) \geq \rho(\|x - x_s\|)$ for all $(x, u) \in \mathbb{Z}$, which according to Lemma 4.4, leads to (4.28). By following [8], it can be shown from (4.26) and (4.28) that $\bar{V}_f(x) \geq \sum_{i=0}^{\infty} \mathcal{L}(x_i, K_f(\theta_k)x_i)$. Moreover, from Assumption 4.4, $\bar{V}_f(x(k))$ is bounded and by $\bar{V}_f(x_s) = 0$, thus, it can be upperbounded by a class $\mathcal{K}$ function, i.e., $\bar{V}_f(x) \leq \hat{\zeta}(\|x - x_s\|)$ for all $x \in \mathbb{X}_f$. □

Theorem 4.1. *Let Assumptions 4.3 to 4.6 hold. Then, the steady state solution is asymptotically for all feasible initial states. The candidate Lyapunov function is $\bar{L}^0(x_k)$, and satisfies*

$$\bar{L}^0(x_k) \leq \zeta(\|x - x_s^*\|), \tag{4.30}$$

$$\bar{L}^0(x_{k+1}) - \bar{L}^0(x_k) \leq -\underline{\zeta}(\|x - x_s^*\|), \tag{4.31}$$

for all $x_k \in X(N_p)$, where $\underline{\zeta}(.)$ being a class $\mathcal{K}$ functions.

Proof. The lower and upper bounds that imposed by inequality (4.30) follow from Lemma 4.5. Condition (4.31) can be proved by following analysis that considers the optimal modified cost functions

$$\bar{L}(x, \tilde{\mathbf{u}}) = \sum_{i=0}^{N_p-1} \mathcal{L}(x(i), u(i)) + \bar{V}_f(x_{N_p})). \qquad x \in \mathbb{X}(N_p) \tag{4.32}$$

There is feasible solution for the current state which gives optimal input and state sequences denoted respectively as $\mathbf{u}^*(k) = \{u^*(k+i|k)\}_{i\in\mathbb{I}_{[0,N_p-1]}}$ and $\mathbf{x}^*(k) = \{x^*(k+i|k)\}_{i\in\mathbb{I}_{[0,N_p]}}$. A candidate input sequence and a associated state sequence for the next time step are chosen as following:

$$\begin{aligned}
\bar{\mathbf{u}}(k+1) &= \{u^*(k+1|k), ..., u^*(k+N_p|k), K_f(x^*(k+N_p|k))\},\\
\bar{\mathbf{x}}(k+1) &= \{x^*(k+1|k), ..., x^*(k+N_p|k), x^*(k+N_p+1|k)\},
\end{aligned}$$

where $x^*(k+N_p+1|k) = ((A(\theta_k)+B(\theta_k)K_f(\theta_k)))x^*(k+N_p|k)$. Because of the terminal constraint and Assumption 4.6, it holds $x^*(k+N_p+1|k) \in \mathbb{X}_f(x^*(k+N_p))$. Furthermore, the cost is given by

$$\begin{aligned}
\bar{L}(x^*(k+1|k), \bar{\mathbf{u}}(k+1)) = &\sum_{l=1}^{N_p-1} \mathcal{L}(x^*(k+i|k), u^*(k+i|k))\\
&+ \mathcal{L}(x^*(k+N_p|k), K_f(x^*(k+N_p|k)))\\
&+ \bar{V}_f(x^*(k+N_p+1|k))\\
=&\bar{L}^0(x_k) - \mathcal{L}(x(k), u^*(k|k))\\
&+ \mathcal{L}(x^*(k+N_p|k), (\theta(k))K_f(x^*(k+N_p|k)))\\
&- \bar{V}_f(x^*(k+N_p|k)) + \bar{V}_f(x^*(k+N_p+1|k)).
\end{aligned}$$

From Assumption 4.6 and Lemma 4.3, it follows that

$$\bar{L}(x^*(k+1|k), \bar{\mathbf{u}}(k+1)) \leq \bar{L}^0(x_k) - \mathcal{L}(x_k, u^*(k|k)). \tag{4.35}$$

Since $\bar{L}^0(x^*(k+1|k), \bar{\mathbf{u}}(k+1)) \leq \bar{L}(x^*(k+1|k))$, hence, from (4.35) and Lemma 4.5 it follows that

$$\bar{L}^0(x_{k+1}) - \bar{L}^0(x_k) \leq -\underline{\zeta}(\|x - x_s^*\|), \tag{4.36}$$

which completes the proof. ■

4.4.1 Computation of the Terminal Components

For completely determining the stabilizing of the proposed EMPC controller based on LPV model, it is necessary to compute the terminal components. By following [8], a systematic procedure is presented where a fixed terminal region around the optimal steady state was used. Then, terminal sets and quadratic cost functions are computed based on the LPV model in a stabilizing MPC context.

Assumption 4.7. *There exist* $K_k \in \mathbb{R}$, $k \in \mathbb{I}_{[1,N_p-1]}$, *such that the matrices* $\tilde{A}_k := A_k + B_k K_k$ *are Schur.*

The computation of the terminal components of (4.6) needs in addition the presence of a terminal control law, which is determined as follows:

$$K_f = K_k(x - x_s^*(k)) + u_s^*(k), \tag{4.37}$$

where K_k is the feedback gain satisfying Assumption 4.7, and the pair $(x_s^*(k), u_s^*(k))$ are elements of the optimal steady state and input trajectories.

The terminal penalty is introduced based on the ellipsoidal level sets correlated to quadratic functions of the form

$$V_f(x) := \frac{1}{2}(x - x_s^*(k))^\top \mathcal{P}_k (x - x_s^*(k)), \tag{4.38}$$

for all $k \in \mathbb{Z}_+$. Therefore, the terminal regions are centered around the nominal trajectory and defined as

$$\mathbb{X}_f(x_s^*(k)) := \{x \in \mathbb{R} | (x - x_s^*(k))^\top \mathcal{P}_k (x - x_s^*(k)) \leq \delta\}, \tag{4.39}$$

where $\delta \in \mathbb{R}_+$. The scaler δ must ensure that the state and input constraints are perpetually satisfied under the use of terminal controller (4.37), i.e., $x(k) \in \mathbb{X}_f(x_s^*(k)) \subset \mathbb{X}$ and $K_f(\theta_k)x_k \in \mathbb{U}$ for all $k \in \mathbb{I}_+$. To derive an appropriate terminal function V_f for the economic cost based on the LPV model, the procedure in [8] is suitably modified. First, assume that the economic costs $\ell(.)$ are twice continuously differentiable and let $\bar{\ell}(x_k) := \ell(x_k, K_f(\theta_k)x_k) - \ell(x_s^*(k), u_s^*(k))$. Then, from [8], for all $x \in \mathbb{X}$, $(x_s^*(k), u_s^*(k)) \in \mathbb{Z}$ and $k \in \mathbb{I}_{[0,N_p-1]}$, there exists a matrix Q_k such that $Q_k - \bar{\ell}_{xx}(x_k) \geq 0$. Moreover, the quadratic cost functional

$$\ell_q(x) := \frac{1}{2}(x - x_s^*(k))^\top Q_k (x - x_s^*(k)) + q^\top (x - x_s^*(k)), \tag{4.40}$$

where $q := \bar{\ell}_x(x_s^*(k), u_s^*(k))$ for all $k \in \mathbb{I}_+$, is such that for all $x \in \mathbb{X}$ the inequality $\ell_q(x) \geq \bar{\ell}(x_k) + (1/2)(x - x_s^*(k))^\top (x - x_s^*(k))$ holds. Hence, the candidate terminal function is defined as

$$V_f(x) := \sum_{i=0}^{\infty} \ell_q(x(i)), \tag{4.41}$$

where $x(k+1+i) = A_{k+i}x(k+i) + B_{k+i}\big(K_{k+i}(x - x_s^*(k+i)) + u_s^*(k+i)\big)$ fo all $i \in \mathbb{I}_+$. To obtain an explicit definition of (4.41), it can use $x_s^*(k+1) = A_k x_s^*(k) + B_k u_s^*(k)$. From Assumption 4.7 and (4.37), the error dynamics are given by

$$(x(k+1) - x_s^*(k+1)) = \tilde{A}_k(x(k) - x_s^*(k)), \qquad \forall k \in \mathbb{I}_+. \tag{4.42}$$

The so-called monodromy matrix of system (4.42) with N_P models, is given by

$$\Psi_k := \prod_{l=0}^{N_p-1} \tilde{A}_{k+l}, \qquad \forall k \in \mathbb{I}_+. \tag{4.43}$$

Then, according to (4.40), (4.42) and (4.43), the terminal function (4.41) can be written as follows

$$\begin{aligned}V_f(x) &= \frac{1}{2}\sum_{l=0}^{N_p-1}(x(k+l)-x_s^*(k+l))^\top\Bigg(\sum_{i=0}^{\infty}(\Psi_{k+l}^i)^\top Q_{k+l}(\Psi_{k+l}^i)\Bigg)(x(k+l)-x_s^*(k+l))\\ &\quad+\bar{\ell}_x(x_s^*(k+l),u_s^*(k+l))^\top\sum_{i=0}^{\infty}(\Psi_{k+l}^i)(x(k+l)-x_s^*(k+l))\\ &= \frac{1}{2}\sum_{l=0}^{N_p-1}(x(k+l)-x_s^*(k+l))^\top\mathcal{P}_{k+l}(x(k+l)-x_s^*(k+l))+p_{k+l}^\top(x(k+l)-x_s^*(k+l)),\end{aligned} \tag{4.44}$$

with $x(k+1+l) = A_{k+l}x(k+l)+B_{k+l}\big(K_{k+l}(x(k+l)-x_s^*(k+l))+u_s^*(k+l)\big)$ fo all $l\in\mathbb{I}_{[0,N_p-1]}$ and $p_k^\top = \bar{\ell}_x(x_s^*(k+l),u_s^*(k+l))^\top(I-\Psi_{k+l})^{-1}$. For the given k and each $l\in\mathbb{I}_{[0,N_p-1]}$, matrices $\mathcal{P}_{k+l}$ are the solutions to the discrete Lyapunov equations $\Psi_{k+l}^\top\mathcal{P}_{k+l}\Psi_{k+l}-\mathcal{P}_{k+l} = -Q_{k+l}$. Through (4.41), it follows that the candidate function V_f satisfies condition Assumption 4.6. In fact, from Assumption 4.7 and suitable manipulation of (4.41)-(4.44) the following balance may be derived:

$$\begin{aligned}&V_f((A(\theta_k)+B(\theta_k)K_f(\theta_k))x_k)-V_f(x(k))\\ &\quad=\frac{1}{2}(x(k)-x_s^*(k))^\top(\tilde{A}_k^\top\mathcal{P}_k\tilde{A}_k-\mathcal{P}_k)(x(k)-x_s^*(k))-\bar{\ell}_x(x_s^*(k),u_s^*(k))^\top(x(k)-x_s^*(k)).\end{aligned} \tag{4.45}$$

Hence, (4.41) and (4.45) yield the following Lyapunov equation

$$\Psi_k^\top\mathcal{P}_k\Psi_k-\mathcal{P}_k = -Q_k,\qquad \forall k\in\mathbb{I}_{[0,N_p-1]}. \tag{4.46}$$

It is important to express that matrices $\mathcal{P}_k$ and K_k must provide in addition the following condition:

$$\tilde{A}_k^\top\mathcal{P}_k\tilde{A}_k-\mathcal{P}_k\leq 0,\qquad \forall k\in\mathbb{I}_{[0,N_p-1]}. \tag{4.47}$$

The main problem to do so is that the matrices in (4.43) lead to non-linear matrix inequalities that cannot be solved directly. Despite the mentioned difficulty for solving (4.46), it is still conceivable to obtain a set of matrices satisfying Assumption 4.7. To do so, relax condition (4.46) and consider instead $\tilde{A}_k^\top\mathcal{P}_k\tilde{A}_k-\mathcal{P}_k\leq -Q_k$ for all $k\in\mathbb{I}_{[0,N_p-1]}$. This theory is formalized with the following result.

Theorem 4.2. *Consider the system function $x(k+1) = (A(\theta_k)+B(\theta_k)K_f(\theta_k))x_k$ satisfying Assumption 4.4, control low (4.37) and the pair $(x_s^*(k),u_s^*(k))\in\mathbb{Z}$ for all $k\in\mathbb{I}_{[0,N_p-1]}$. Let $X_k\in\mathbb{S}_{++}^{n_x}, Y_k\in\mathbb{R}^{n_u\times n_x}$ and $\delta\in\mathbb{R}_+$ be decision variables, and solve*

$$\max_{X_k\succ 0, Y_k\in\mathbb{R}^{n_u\times n_x},\delta\in\mathbb{R}_+} -logdet(X_0) \tag{4.48a}$$

subject to

$$\begin{bmatrix} X_k & * & * \\ A_k X_k + B_j Y_k & X_{k+1} & * \\ Q^{1/2} X_k & 0_{n\times n} & \delta I_n \end{bmatrix} \geq 0, \tag{4.48b}$$

for all $k \in \mathbb{I}_{[0,N_p-1]}$ *while,* $X_{opt,k}, Y_{opt,k}$ *and* δ_{opt} *indicate the solution of* (4.48)*. Moreover,*

$$\mathcal{P}_k := X_{opt,k}^{-1}\delta_{opt}, \quad K_k := Y_k X_k^{-1}, \quad \forall k \in \mathbb{I}_{[N_p-1]}. \tag{4.49}$$

If problem (4.48) *can be solved, then Assumption 4.6 is satisfied.*

Proof. At first, it should be indicated that the solution of (4.48) presents the terminal sets defined in (4.39) for system $x(k+1) = (A(\theta_k) + B(\theta_k)K_f(\theta_k))x_k$ with K_f as defined in (4.37). To do so, remark that for $k \in \mathbb{I}_+$ the the terms $x(k) \in \mathbb{X}_f(x_s^*(k))$ is equal to the following quadratic functional condition

$$F_0 = (x(k) - x_s^*(k))^\top \mathcal{P}_k (x(k) - x_s^*(k)) - \delta \leq 0.$$

Similarly, the requirement that $x(k+1) \in \mathbb{X}_f(x_s^*(k+1))$ is equivalent to

$$F_1 = (x(k+1) - x_s^*(k+1))^\top \mathcal{P}_{k+1} (x(k+1) - x_s^*(k+1)) - \delta \leq 0.$$

According to Lemma C.1, the term that $x(k) \in \mathbb{X}_f(x_s^*(k))$ signifies $x(k+1) \in \mathbb{X}_f(x_s^*(k+1))$, is equal to the existence of $\omega_k \succ 0$, such that

$$(x(k+1)-x_s^*(k+1))^\top \mathcal{P}_{k+1}(x(k+1)-x_s^*(k+1)) - \delta - \omega_k((x(k)-x_s^*(k))^\top \mathcal{P}_k (x(k)-x_s^*(k)) - \delta) \leq 0. \tag{4.50}$$

From (4.42), the mentioned inequality can be edited as a quadratic functional of $(x(k) - x_s^*(k))$ for all $k \in \mathbb{I}_+$. Therefore, by Lemma C.2, an equivalent linear matrix inequality condition can be established, i.e.,

$$\begin{bmatrix} \tilde{A}_k^\top \mathcal{P}_{k+1} \tilde{A}_k - \omega_k \mathcal{P}_k & 0 \\ 0 & \omega_k - \delta \end{bmatrix} \leq 0.$$

The above inequality can be decoupled to obtain, $0 \prec \omega_k \leq \delta$, and

$$\tilde{A}_k^\top \mathcal{P}_{k+1} \tilde{A}_k - \omega_k \mathcal{P}_k \leq 0. \tag{4.51}$$

As reviewed in [21], there exists a ω_k such that (4.51) is equivalent to

$$\tilde{A}_k^\top \mathcal{P}_{k+1} \tilde{A}_k - \mathcal{P}_k \leq -Q_k. \tag{4.52}$$

By recovering X_k and Y_k according to (4.49) and applying the Schur complement to (4.48b), and pre- and post-multiplying the result with $\mathcal{P}_k$, it can be indicated that

(4.48b) is equal to (4.51) with $k \in \mathbb{I}_{[0,N_p-1]}$. Finally, for proving (4.21), (4.52) is pre- and post-multiplied with $(x(k) - x_s^*(k))^\top$ and $(x(k) - x_s^*(k))$ and yields the following inequality

$$(x(k) - x_s^*(k))^\top (\tilde{A}_k^\top \mathcal{P}_{k+1} \tilde{A}_k - \mathcal{P}_k)(x(k) - x_s^*(k)) \leq -(x(k) - x_s^*(k))^\top Q_k (x(k) - x_s^*(k)) \tag{4.53}$$

for all $k \in \mathbb{I}_+$. By using (4.42), (4.43) and summing up (4.53) from $k = 0$ to $k = N_p - 1$, (4.53) can be written as

$$(x(k)-x_s^*(k))^\top (\Psi_k^\top \mathcal{P}_{k+1} \Psi_k - \mathcal{P}_k)(x(k)-x_s^*(k)) \leq -\sum_{k=0}^{N_p-1} (x(k)-x_s^*(k))^\top Q_k (x(k)-x_s^*(k)). \tag{4.54}$$

Then, by multiplying (4.53) with (1/2) and adding $-\bar{\ell}(x_s^*(k), u_s^*(k))^\top (x(k) - x_s^*(k))$ to both sides of its, lead to

$$\begin{aligned}
&\frac{1}{2}(x(k) - x_s^*(k))^\top (\Psi_k^\top \mathcal{P}_{k+1} \Psi_k - \mathcal{P}_k)(x(k) - x_s^*(k)) - \bar{\ell}(x_s^*(k), u_s^*(k))^\top (x(k) - x_s^*(k)) \\
&\qquad \leq -\frac{1}{2} \sum_{k=0}^{N_p-1} (x(k) - x_s^*(k))^\top Q_k (x(k) - x_s^*(k)) - \bar{\ell}(x_s^*(k), u_s^*(k))^\top (x(k) - x_s^*(k)) \\
&\qquad \leq -\frac{1}{2}(x(k) - x_s^*(k))^\top Q_k (x(k) - x_s^*(k)) - \bar{\ell}(x_s^*(k), u_s^*(k))^\top (x(k) - x_s^*(k)) \\
&\qquad \leq \bar{\ell}(x(k)) = \ell(x(k), K_f(x(k))) - \ell(x_s^*(k), u_s^*(k)),
\end{aligned} \tag{4.55}$$

for all $k \in \mathbb{I}_+$. The second inequality comes from the positive definiteness of Q_k, and the last inequality is obtained from the description of $\ell_q(x)$ in (4.40). Hence, according to (4.44) and (4.55), condition (4.21) is satisfied. Furthermore, Theorem 4.2 can be proved by solving (4.48) to obtain terminal components considering Assumption 4.6. ■

4.5 Numerical results

In this part, application results in simulation of the proposed EMPC strategy based TS/LPV model for the pasteurization process are presented and analyzed in detail.

4.5.1 Cost function parameters

One of the important objectives of the pasteurization process is to ensure that the pasteurization temperature is attained and preserved close to the set-point temperature for a pre-established time. However, the set-point is different for several products. Simultaneously, the decrease of energy consumption of the system considered an economic target should be achieved by minimizing the power of the resistor of the hot-water tank for reducing the cost of the heater. The control aim is to minimize a convex multiobjective stage cost function that probably anticipates each functional connection to the

economic aspect and to achieve a suitable temperature for maintaining the performance of the system.

The EMPC objective function for the pasteurization process involves three operational purposes with several characteristics, i.e., minimizing energy cost, maintaining safety bounds for temperature, and control input smoothness.

Minimization of energy costs

One of the main control objective in the pasteurization process is to minimize the cost energy consumption of the system that includes minimizing the power of the hot-water tank for reducing the energy cost of the heater. Then, the cost function related to this objective can be formulated as

$$\ell(k) \triangleq \alpha(k) W_e u(k) \Delta t, \tag{4.56}$$

where $\alpha(k)$ is time-varying electricity cost that changes in each time instate k according the dynamic electricity tariff. Moreover, W_e denotes the weighting term that indicates the prioritisation of the economic control objective and Δt is the sampling time in second.

Guarantee of safety temperature

For preserving the value of the pasteurization temperature T_{past}, and the hot-water tank temperature T_{ow} between the pre-specified minimal and maximal of the suitable output temperatures, a appropriate safety bounds for each output temperature must be maintained. The mathematical expression for this objective is formulated as

$$\ell^t(k) = \begin{cases} ||Cx(k+1) - y_S||_2, & \text{if } Cx(k+1) \leq y_S. \\ 0, & \text{otherwise.} \end{cases} \tag{4.57}$$

where y_S is the safety output temperatures of the pasteurization temperature T_{past}, and the hot-water tank temperature T_{ow} and $||.||_2$ is the squared 2-norm symbol. The safety cost function can be also obtained by means of a soft constraint, adding a slack variable ξ, which can be reformulated as

$$\ell^t(k) \triangleq \xi(k)^\top W_t \xi(k), \tag{4.58}$$

where $\xi > 0$ is a slack variable that it is presented for preserving the feasibility of the optimization problem by considering the following soft constraint:

$$Cx(k+1) \geq y_S - \xi(k), \tag{4.59}$$

and W_t is a diagonal positive definite matrix that shows the prioritisation of the safety objective.

Smoothness of control actions

Pumps and electric heater resistor are known as the actuators of the pasteurization plant. The control actions found by the EMPC controller are should be smooth in order to extend the lifespan of physical components. The objective function for this part can be written as

$$\ell^{\Delta}(k) \triangleq \Delta u(k)^{\top} W_{\Delta u} \Delta u(k), \tag{4.60}$$

where the $\ell^{\Delta}(k)$ indicates the penalization of control signal variations $\Delta u(k) \triangleq u(k) - u(k-1)$ and $W_{\Delta u}$ is weighting term for smoothness of control actions as a diagonal positive definite matrix.

Multi-objective cost function

According to the previous explanation about the different control objectives, the multi-objective cost function for the operational management of the pasteurization plant can be rewritten as

$$L_G(k) = [\ell(k) + \ell^t(k) + \ell^{\Delta}(k)]. \tag{4.61}$$

4.5.2 Simulation results

As mentioned before, one of the most important goal of the pasteurization process is to guarantee that the pasteurization temperature is reached and maintained as close as possible to the desired thermal temperature margin. At the same time, the reduction of energy consumption of the system expressed as a economic objective should be achieved by minimizing the power of the hot-water tank for reducing the cost consumption based on power of heater. For this purpose, the input temperature of hot-water tank T_{iw} and the cold temperature T_{ic} are maintained constant at 40°C and 30°C, respectively. Furthermore, the power of the electrical heater P can take values in the range $[0, 1.5]$ kW. The states are constrained to be $[0, 0, 0, 0, 0, 0, 0]^{\top} \leq x_k \leq [120, 120, 120, 120, 120, 800, 120]^{\top}$. The states of the model are arranged by the initial states $x_0 = [28, 0, 0, 0, 0, 155, 22]^{\top}$ and sampling time is chosen $\Delta t = 1$ second. The control objective is to preserve the principle temperatures for products pasteurization such that the constraints are always satisfied while minimizing an economic cost function given by (4.61), where weighting matrices are $W_e = 10$, $W_t = [80, 0; 0, 20]$, $W_{\Delta u} = 0.001$ and the prediction horizon has been selected as $N_p = 5$.

In addition, the range of hot water flow is considered as $F_h \in [150, 695]$ and by applying the well-known sector nonlinearity approach [160], the nonlinear model of the pasteurization plant can be expressed by a T-S fuzzy model with $r = 2^{n_\theta}$ fuzzy If-Then rules as follows:

Rule 1: If $\theta(k)$ is M_{11} Then $x(k+1) = A_1 x(k) + B_1 u(k)$,
Rule 2: If $\theta(k)$ is M_{12} Then $x(k+1) = A_2 x(k) + B_2 u(k)$,

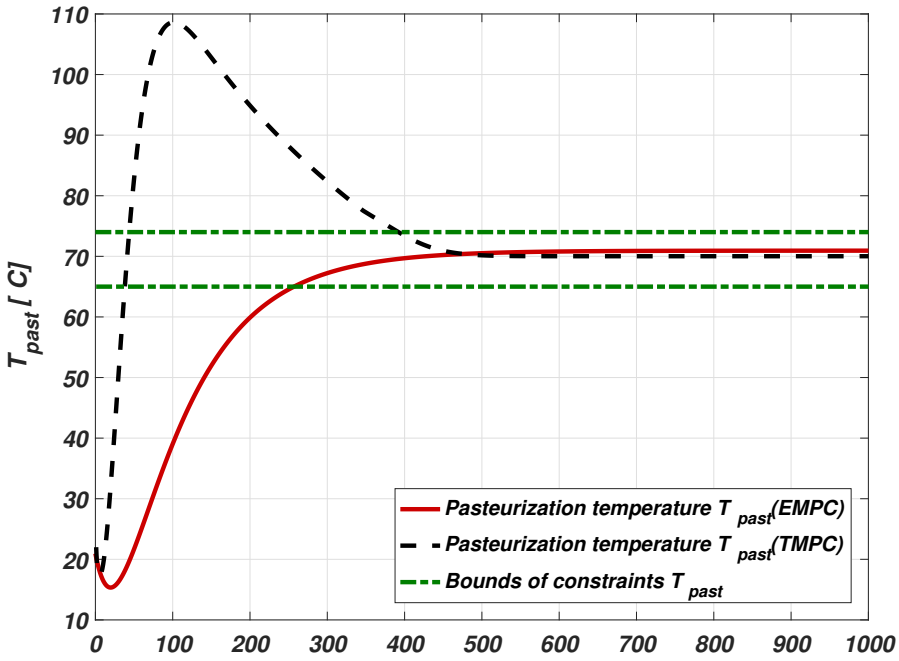

Figura 4.1: Evolution of controlled temperature of TMPC strategy and the EMPC based on TS model

where $\theta(k) = F_h(k)$ is the premise variable, M_{11} and M_{12} are the membership functions which can be defined as:

$$M_{11} = \frac{F_h(k) - \underline{F_h}}{\overline{F_h} - \underline{F_h}}, \quad M_{12} = 1 - M_{11}. \tag{4.62}$$

According to (**??**) and cost function (4.61), the optimal steady-state of the pasteurization system is obtained as $x_s = [42.35,\ 38.58,\ 58.17,\ 0,\ 33.49,\ 0,\ 73.41]^\top$ and $u_s = [623.37,\ 0]^\top$. Moreover, the stability issue of approach based on TS model is satisfied same as section 4.4 for LPV model. Then, the convergence of the system to the optimal circuit (if desired) can be ensured due to the pasteurization system is strictly dissipative with respect to the supply rate $s(x,u) := \ell(x,u) - \ell(x_s,u_s)$ while the storage function is $\gamma = (1/2)x$. By solving (4.48), it is obtained a sub-level $\delta = 1444.6196$ and

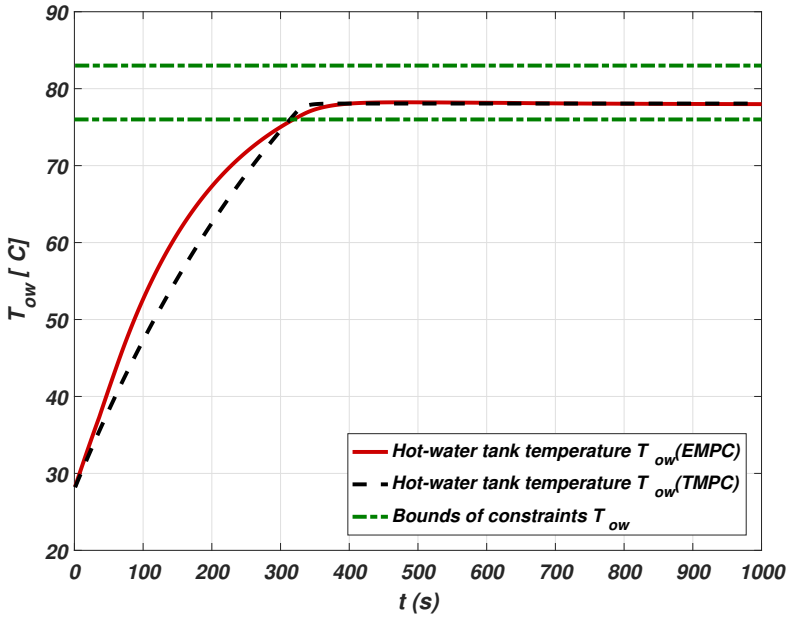

Figura 4.2: Evolution of controlled hot-water tank temperature of TMPC strategy and EMPC based on TS model

matrices $\mathcal{P}_k$, K_k as:

$$\mathcal{P}(0) = \begin{bmatrix} 560.65 & 0.0530 & 0.5636 & -0.0001 & -0.0001 & 0.0000 & -0.0021 \\ 0.0530 & 567.51 & 0.5107 & -0.0001 & -0.0001 & 0.0000 & -0.0017 \\ 0.5636 & 0.5107 & 566.41 & 0.0118 & 0.0128 & -0.0000 & 0.2833 \\ -0.0001 & -0.0001 & 0.0118 & 567.54 & 0.0127 & 0.0536 & 0.2793 \\ -0.0001 & -0.0001 & 0.0128 & 0.0127 & 561.35 & -0.0000 & 0.3056 \\ 0.0000 & 0.0000 & -0.0000 & 0.0536 & -0.0000 & 561.34 & -0.0002 \\ -0.0021 & -0.0017 & 0.2833 & 0.2793 & 0.3056 & -0.0002 & 569.53 \end{bmatrix},$$

$$K(0) = \begin{bmatrix} 0 & 0 & -631.07 & 0 \\ -1362.50 & 0 & 0 & 0 \\ 0 & 0 & 0 & 0 \\ 0 & 0 & 0 & 0 \\ 0 & 0 & 0 & -11.83 \\ 0 & -0.0263 & 0 & 0 \\ 0 & 0 & 0 & 0 \end{bmatrix},$$

$$\mathcal{P}(1) = \begin{bmatrix} 560.62 & 0.0234 & 0.3806 & -0.0001 & -0.0001 & 0.0000 & -0.0014 \\ 0.0234 & 567.49 & 0.3449 & -0.0001 & -0.0001 & 0.0000 & -0.0011 \\ 0.3806 & 0.3449 & 566.59 & 0.0118 & 0.0128 & -0.0000 & 0.2826 \\ -0.0001 & -0.0001 & 0.0118 & 567.27 & 0.0127 & 0.2119 & 0.2802 \\ -0.0001 & -0.0001 & 0.0128 & 0.0127 & 561.35 & -0.0000 & 0.3056 \\ 0.0000 & 0.0000 & -0.0000 & 0.2119 & -0.0000 & 561.35 & -0.0008 \\ -0.0014 & -0.0011 & 0.2826 & 0.2802 & 0.3056 & -0.0008 & 569.54 \end{bmatrix},$$

$$K(1) = \begin{bmatrix} 0 & 0 & -631.29 & 0 \\ -1368.50 & 0 & 0 & 0 \\ 0 & 0 & 0 & 0 \\ 0 & 0 & 0 & 0 \\ 0 & 0 & 0 & -11.51 \\ 0 & -0.0263 & 0 & 0 \\ 0 & 0 & 0 & 0 \end{bmatrix}$$

$$\mathcal{P}(2) = \begin{bmatrix} 560.62 & 0.0191 & 0.3448 & -0.0000 & -0.0001 & 0.0000 & -0.0013 \\ 0.0191 & 567.49 & 0.3125 & -0.0000 & -0.0001 & 0.0000 & -0.0010 \\ 0.3448 & 0.3125 & 566.63 & 0.0118 & 0.0128 & -0.0000 & 0.2825 \\ -0.0000 & -0.0000 & 0.0118 & 567.22 & 0.0127 & 0.2418 & 0.2804 \\ -0.0001 & -0.0001 & 0.0128 & 0.0127 & 561.36 & -0.0000 & 0.3056 \\ 0.0000 & 0.0000 & -0.0000 & 0.2418 & -0.0000 & 561.35 & -0.0009 \\ -0.0013 & -0.0010 & 0.2825 & 0.2804 & 0.3056 & -0.0009 & 569.54 \end{bmatrix},$$

$$K(2) = \begin{bmatrix} 0 & 0 & -631.33 & 0 \\ -1369.73 & 0 & 0 & 0 \\ 0 & 0 & 0 & 0 \\ 0 & 0 & 0 & 0 \\ 0 & 0 & 0 & -11.45 \\ 0 & -0.0263 & 0 & 0 \\ 0 & 0 & 0 & 0 \end{bmatrix}$$

$$\mathcal{P}(3) = \begin{bmatrix} 560.63 & 0.0183 & 0.3378 & -0.0000 & -0.0001 & 0.0000 & -0.0013 \\ 0.0183 & 567.4906 & 0.3062 & -0.0000 & -0.0001 & 0.0000 & -0.0010 \\ 0.3378 & 0.3062 & 566.63 & 0.0118 & 0.0128 & -0.0000 & 0.2825 \\ -0.0000 & -0.0000 & 0.0118 & 567.21 & 0.0127 & 0.2475 & 0.2805 \\ -0.0001 & -0.0001 & 0.0128 & 0.0127 & 561.36 & -0.0000 & 0.3056 \\ 0.0000 & 0.0000 & -0.0000 & 0.2475 & -0.0000 & 561.35 & -0.0009 \\ -0.0013 & -0.0010 & 0.2825 & 0.2805 & 0.3056 & -0.0009 & 569.54 \end{bmatrix},$$

$$K(3) = \begin{bmatrix} 0 & 0 & -631.33 & 0 \\ -1369.65 & 0 & 0 & 0 \\ 0 & 0 & 0 & 0 \\ 0 & 0 & 0 & 0 \\ 0 & 0 & 0 & -11.44 \\ 0 & -0.0263 & 0 & 0 \\ 0 & 0 & 0 & 0 \end{bmatrix}$$

$$\mathcal{P}(4) = \begin{bmatrix} 560.64 & 0.0427 & 0.5083 & -0.0001 & -0.0001 & 0.0000 & -0.0019 \\ 0.0427 & 567.50 & 0.4606 & -0.0001 & -0.0001 & 0.0000 & -0.0015 \\ 0.5083 & 0.4606 & 566.46 & 0.0118 & 0.0128 & -0.0000 & 0.2831 \\ -0.0001 & -0.0001 & 0.0118 & 567.46 & 0.0127 & 0.1026 & 0.2796 \\ -0.0001 & -0.0001 & 0.0128 & 0.0127 & 561.35 & -0.0000 & 0.3056 \\ 0.0000 & 0.0000 & -0.0000 & 0.1026 & -0.0000 & 561.34 & -0.0004 \\ -0.0019 & -0.0015 & 0.2831 & 0.2796 & 0.3056 & -0.0004 & 569.53 \end{bmatrix},$$

$$K(4) = \begin{bmatrix} 0 & 0 & -631.16 & 0 \\ -1364.84 & 0 & 0 & 0 \\ 0 & 0 & 0 & 0 \\ 0 & 0 & 0 & 0 \\ 0 & 0 & 0 & -11.73 \\ 0 & -0.0263 & 0 & 0 \\ 0 & 0 & 0 & 0 \end{bmatrix}$$

Then, according to matrices $\mathcal{P}$, terminal penalty may be defined as (4.38). While this $V_f(x)$ can be satisfied (4.21) for all $x \in \mathbb{X}_f \subset \mathbb{X}$ and $k_f = K_k(x - x_s^*) + u_s^*$.

To evaluate the advantage and economic efficiency of the presented strategy for EMPC controller based on the TS fuzzy model, the tracking MPC (TMPC) strategy is implemented on the TS model of pasteurization system. The TMPC based on the TS fuzzy model is done solving the following optimization problem:

$$\min_{\mathrm{u}(k)} \sum_{l=0}^{N_p-1} \|Cx(l+1|k) - y_{ref}(l+1)\|_{p,w_1} + \|\Delta u(l+1|k)\|_{p,w_2}, \tag{4.64}$$

subject to (2.14) and (2.15) and same constraints in (4.61). Moreover, p denotes the norm used for this chapter is squared norm and the weighting matrices $w_1 \in \mathbb{R}^{n_x \times n_x}$ and $w_2 \in \mathbb{R}^{n_u \times n_x}$ are applied to verify the priority of the several control objectives.

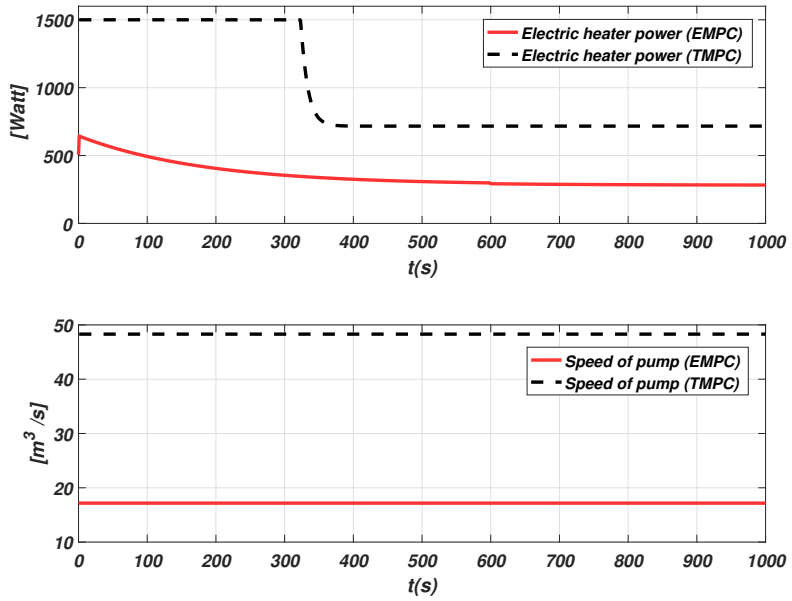

Figura 4.3: Evolution of control inputs of TMPC strategy and EMPC based on T-S model

All tests were done using the same weights, initial conditions and prediction horizon as mentioned above. All simulation and computations have been carried out on an i7 2.40-GHz Intel core processor with 12 GB of RAM running MATLAB R2016b, and the optimization problem is solved by using YALMIP toolbox with Cplex solver. In addition, the numeric assessment of the above-mentioned controllers is carried through different key performance indicators (KPIs), which are detailed as follows:

$$KPI_e := \frac{1}{n_s+1}\sum_{k=0}^{n_s} \alpha^\top u_k \, \Delta t, \tag{4.65a}$$

$$KPI_{\Delta u} := \frac{1}{n_s+1}\sum_{i=1}^{n_u}\sum_{k=0}^{n_s} (\Delta_u(i,k))^2, \tag{4.65b}$$

where KPI_e denotes the average economic performance of the pasteurization process and $KPI_{\Delta u}$ evaluates the smoothness of the control actions. Moreover, $n_s \in \mathbb{I}_+$ is the number of seconds considered in the simulations and Δt is the sampling time in seconds. It should be noted that in KPI_e and KPI_{Δ_u} lower values signified better performance results.The comparison results of different key performance indicators (KPIs) plus the simulation time between EMPC and TMPC strategies based on T-S model are presented in Table 4.1.

Taula 4.1: Comparison of control performance.

Controller	KPI_e	KPI_{Δ_u}	Simulation Time
EMPC	12177	6824	3562
TMPC	44339	15430	3025

Figures 4.1 and 4.2 provide the evaluation of the controlled output temperature results that include the pasteurization temperature, T_{past} and hot-water tank temperature, T_{ow}. These output temperatures obtained under the new strategy of the EMPC based on the T-S fuzzy model with hard constraints in input and output temperature in order to save energy and avoid overheating the product. In Figure 4.1, it can be seen that the pasteurization temperature, T_{past} and hot-water tank temperature, T_{ow} from EMPC approach are within expected ranges $T_{past} \in [65°C,\ 74°C]$ and $T_{ow} \in [76°C,\ 83°C]$, respectively.

The TMPC is designed just for reaching the predefined references where their references are the mean values of the expected ranges of the output temperatures. The results of output temperature behaviour from the TMPC controller based on the T-S fuzzy model that designed to achieve the references are presented in Figure 4.1. From Figure 4.1, it can be observed that the pasteurization temperature T_{past} and hot-water tank temperature T_{ow} are tracked the predetermined references and achieved them. However, T_{past} has overshoot behaviour.

Figure 4.3 shows the simulation results of the power of the electrical heater and speed of pump based on the EMPC and TMPC strategies. By analyzing theses results from economic point of view, it can be observed that the appropriate pasteurization temperature T_{past} and hot-water tank temperature T_{ow} are obtained with the EMPC controller while the power of the electrical heater is decreased and the value of the power is less than the TMPC strategy. The output temperatures of both strategies achieve the suitable temperature according to the economic objective. In the meantime, the performance of products is kept, it means the product is pasteurized in a suitable temperature and not burnt while the economic cost in EMPC is almost reduced three times compared to the TMPC.

4.6 Summary

This chapter focused on the design of an economic model predictive control algorithm for a class of LPV/TS models. The constrained optimization problem for LPV/TS model are solved iteratively by a series of QP problems while the scheduling parameters are calculated at each time instant. The model is predicted in the horizon by using the previous sequence of scheduling variable and state of the model. The proposed approach

is extended based on the TS model. The asymptotic stability of EMPC based on LPV models is provided by satisfying a strong dissipativity assumption to prove stability. The proposed approach is attractive because the implementation of this method is basically the same algorithm as for LTI systems. Finally, the EMPC strategy based on TS model has been satisfactorily designed and tested in a simulation of a small-scale pasteurization system. The TS model of the pasteurization system has been obtained by considering the hot-water flow F_h as premise variable. Then, the comparison between the EMPC approach and the classic tracking MPC is done and the results show the advantages of EMPC for decreasing the economistic cost. Moreover, this approach will be extended in the next chapter by considering the time delay in the system.

The content of this chapter was based on the following works:

F. Karimi Pour, V. Puig and C. Ocampo-Martinez. Comparative assessment of LPV-based predictive control strategies for a pasteurization plant. 4^{th} *International Conference on Control, Decision and Information Technologies (CoDIT)*, (pp. 0821-0826). IEEE, Spain, 2017.

F. Karimi Pour, V. Puig and C. Ocampo-Martinez. Economic predictive control of a pasteurization plant using a linear parameter varying model. *In Computer Aided Chemical Engineering*, (Vol. 40, pp. 1573-1578). Elsevier, 2017.

F. Karimi Pour, C. Ocampo-Martinez and V. Puig . Output-feedback model predictive control of a pasteurization pilot plant based on an LPV model. *In Journal of Physics: Conference Series* (Vol. 783, No. 1, p. 012029), France, 2017.

F. Karimi Pour, V. Puig and C. Ocampo-Martinez . A new Design of Economic model Predictive Control based on LPV systems. To be submitted *Journal of Process control.*

F. Karimi Pour, V. Puig and C. Ocampo-Martinez . Takagi-Sugeno based Economic Predictive Control of a Pasteurization Plan. To be submitted *International Journal of Computer Applications in Chemical Engineering.*

Capítol 5

MPC for LPV systems with parameter-varying delays

This chapter presents MPC strategy for LPV systems with varying delays affecting states and inputs. The proposed control approach allows the controller to accommodate the scheduling parameters and delay change. By computing the prediction of the state variables and delay along a prediction time horizon, the system model can be modified according to the evaluation of the estimated state and delay at each time instant. Moreover, the solution of the optimization problem associated with the MPC design is achieved by solving a series of Quadratic Programming (QP) problems at each time instant. The pasteurization plant system is used as a case study to demonstrate the effectiveness of the proposed approach.

5.1 Introduction

The effect of time delay in a process increases the complexity of the control problem. The delays can affect the states, inputs or/and outputs, and they can be time-varying or constant, unknown or known, deterministic or stochastic depending on the systems under study.

Recently, many researchers focus on robust model predictive control (RMPC) based on linear models with constant or varying delays [66, 123]. In [34], a RMPC with constant state delay by using linear matrix inequalities (LMIs) is proposed. The work of [87] proposes an MPC algorithm for uncertain time varying systems with state delays. Besides, a synthesis strategy for predictive control based on LPV models with state delays was provided in [87]. However, there exist only a few MPC methods that consider time-delayed LPV models [222, 229]. In [222], authors proposed a parameter-dependent state-feedback controller based on LPV model with parameter-varying time delay and proved the stability by using parameter-dependent Lyapunov functionals. However, there exists a limitation to apply input constraints which are required when controlling

many practical plants. Also, an RMPC based on LPV model with state delay was presented in [229] by using a Lyapunov function augmented with the current state and the time-delayed states. But, still delay is considered to be constant in the RMPC. Therefore, an MPC controller that can overcome the drawbacks mentioned above is needed to enable handling effects of varying delays and constraints.

In this chapter, an MPC controller based on the LPV models with varying parameters delays is provided. The main contribution consists of designing an improved LPV-based MPC strategy in order to formulate an optimization problem that exploits the functional dependency of scheduling variables and varying delays to develop a prediction strategy with a numerically suitable solution. This solution is iteratively forced to an accurate solution, thereby avoiding the use of non-linear optimization. In addition, the optimization problem is decomposed into a series of QP problems that are solved at each time instant. Finally, the small-scale pasteurization plant that presents nonlinear behavior with varying delays is used in order to test the effectiveness of the proposed approach.

5.2 Problem statement

Consider the following discrete-time state-space LPV model with parameter-varying delays in inputs and states:

$$\begin{aligned} x(k+1) =& A(\theta(k))x(k) + A_\tau(\theta(k))x(k-\tau(\theta(k))) \\ &+ B(\theta(k))u(k) + B_\tau(\theta(k))u(k-\tau(\theta(k))), \\ y(k) =& C(\theta(k))x(k) + C_\tau(\theta(k))x(k-\tau(\theta(k))), \end{aligned} \tag{5.1}$$

where $x \in \mathbb{R}^{n_x}$, $u \in \mathbb{R}^{n_u}$ and $y \in \mathbb{R}^{n_y}$ are the state vector, input vector and output vector, respectively. Moreover, $A(\theta(k)) \in \mathbb{R}^{n_x \times n_x}$, $B(\theta(k)) \in \mathbb{R}^{n_x \times n_u}$ and $C(\theta(k)) \in \mathbb{R}^{n_y \times n_x}$ are system matrices with the appropriate dimensions, which depend affinely on the varying parameter $\theta(k) \in \Theta \ \forall k \geq 0$ where Θ is a given compact set. Moreover, τ is a scalar function representing the parameter-varying delay and satisfies $0 \leq \tau_m \leq \tau(\theta(k)) \leq \tau_M$, where τ_M and τ_m are the upper bound and lower bound of $\tau(\theta(k))$. Throughout this paper, it is assumed that $(A(\theta), B(\theta))$ is stabilizable for all $\theta \in \Theta$.

The MPC controller design with a quadratic objective function subject to input and states constraints based on the LPV model (5.1) can be formulated as follows:

$$\min_{\tilde{u}(k)} \ J(k) = \sum_{i=0}^{N_p-1} \|x(i|k)\|^p_{w_1} + \|u(i|k)\|^p_{w_2}, \tag{5.2a}$$

subject to

$$\begin{aligned} x(i+1|k) =& A(\theta(i|k))x(i|k) \\ &+ A_\tau(\theta(i|k))x(i-\tau(\theta(i|k))|k) \\ &+ B(\theta(i|k))u(i|k) \\ &+ B_\tau(\theta(i|k))u(i-\tau(\theta(i|k))|k), \end{aligned} \tag{5.2b}$$

$$u(i|k) \in \mathbb{U}, \tag{5.2c}$$

$$x(i|k) \in \mathbb{X}, \tag{5.2d}$$

$$x(0|k) = x(k) \tag{5.2e}$$

$$\theta(0|k) = \theta(i|k), \tag{5.2f}$$

and for all $i \in \mathbb{Z}_{[0,N_p-1]}$, it is solved online for

$$\tilde{u}(k) = \left[u(i|k), u(i+1|k), ..., u(N_p-1|k)\right]^\top \in \mathbb{U}, \tag{5.3}$$

where $\tilde{u}(k)$ is the decision sequence of N_p predicted control inputs. Moreover, $w_1 \in \mathbb{R}^{n_x \times n_x}$ and $w_2 \in \mathbb{R}^{n_u \times n_u}$ are positive definite weighting matrices that establish the trade-off between state and the control input effort, respectively. The super-index p is the squared norm. Furthermore, the sets $\mathbb{X}$ and $\mathbb{U}$ are defined as (2.2).

The control law is applied in a receding horizon manner. Also, $x(i|k)$ is the predicted state at time i, with $i = 1, ..., N_p$, obtained by starting from the state $x(0|k) = x(k)$.

The LPV model can not be evaluated before solving the optimization problem (5.2) because the future state sequence is not known. Indeed $x(i|k)$ depends not only on the future control inputs $u(k)$, but also on the future scheduling parameters $\theta(k)$ and delay, which for a general LPV system, are not assumed to be known a priori, but only to be measurable online at current time k. In addition, in the case of a system with varying delay, the delay varies with the scheduling variables. Hence, predicting the future states regarding the dynamic of the system is more difficult. But, for a quasi-LPV system, where the scheduling parameters $\theta(k)$ are defined by $x(k)$ and $u(k)$, the delay and state trajectory can be predicted.

5.3 Proposed approach

This section proposes an MPC controller design in order to solve the optimization problem of an LPV model with parameter-varying delay where the parameters and delays change along the prediction horizon. The solution for this problem is based on the estimation of the scheduling variables and subsequently the delays into the prediction horizon and then, using them to update the system matrices of the model used by the MPC controller. In fact, the sequence of the control input is used to modify the delay and system matrices of the model used along the prediction horizon. Therefore, the sequence of states and predicted parameters can be obtained from the control sequence

$\tilde{u}(k)$ as

$$\tilde{\mathbf{x}}(k) = \begin{bmatrix} x(i+1|k) \\ x(i+2|k) \\ \vdots \\ x(N_p|k) \end{bmatrix} \in \mathbb{R}^{N_p,\, n_x}, \quad \Theta(k) = \begin{bmatrix} \hat{\theta}(i|k) \\ \hat{\theta}(i+1|k) \\ \vdots \\ \hat{\theta}(N_p-1|k) \end{bmatrix} \in \mathbb{R}^{N_p,\, n_\theta}. \tag{5.4}$$

Since the delays depend on the scheduling parameters, the delays can be estimated based on the sequence of predicted parameters as

$$\tilde{\tau}(k) = \begin{bmatrix} \tau(i|k) \\ \tau(i+1|k) \\ \vdots \\ \tau(N_p-1|k) \end{bmatrix} \in \mathbb{R}^{N_p,\, ,n_\tau}. \tag{5.5}$$

Thus, with slight abuse of notation, ψ and ϕ can be used as: $\Theta(k) = \psi([x^\top(k) \;\; \tilde{\mathbf{x}}^\top(k)]^\top, \tilde{u}(k))$ and $\tilde{\tau}(k) = \phi([x^\top(k) \;\; \tilde{\mathbf{x}}^\top(k)]^\top, \tilde{u}(k))$, respectively. The vector $\Theta(k)$ includes parameters from time k to $k+N_p-1$ whilst the state prediction is accomplished for time $k+1$ to $k+N_p$.

Consequently, by using the vectors (5.4) and (5.5), the $\tilde{\mathbf{x}}(k)$ can be simply formulated as follows:

$$\begin{aligned} \tilde{\mathbf{x}}(k) = {} & \mathcal{A}(\Theta(k))x(k) + \mathcal{A}_\tau(\Theta(k))x(k-\tilde{\tau}(\Theta(k))) \\ & + \mathcal{B}(\Theta(k))\tilde{u}(k) + \mathcal{B}_\tau(\Theta(k))\tilde{u}(k-\tilde{\tau}(\Theta(k))), \end{aligned} \tag{5.6}$$

where $\mathcal{A}$ and $\mathcal{A}_\tau \in \mathbb{R}^{n_x \times n_x}$ and $\mathcal{B}$ and $\mathcal{B}_\tau \in \mathbb{R}^{n_x \times n_u}$ are given by (4.9) and (4.10).

By using (5.6) and augmented block diagonal weighting matrices $\tilde{w_1} = diag_{N_p}(w_1)$ and $\tilde{w_2} = diag_{N_p}(w_2)$, the cost function (5.2a) can be represented in vector form as

$$\min_{\tilde{u}(k)} J(k) = \big(\tilde{\mathbf{x}}(k)^\top \tilde{w_1} \tilde{\mathbf{x}}(k) + \tilde{u}(k)^\top \tilde{w_2} \tilde{u}(k)\big), \tag{5.7a}$$

subject to

$$u(i|k) \in \mathbb{U}, \tag{5.7b}$$
$$x(i|k) \in \mathbb{X}, \tag{5.7c}$$
$$x(0|k) = x(k) \tag{5.7d}$$
$$\theta(0|k) = \theta(i|k), \tag{5.7e}$$

for all $i \in \mathbb{Z}_{[0,N_p-1]}$. Since the predicted states $\tilde{\mathbf{x}}(k)$ in (5.6) are linear in control inputs $\tilde{u}(k)$, the optimization problem can be solved as a QP problem, which is significantly easier than solving a nonlinear optimization problem.

However, the variation of delays at each iteration and inside the prediction horizon makes it difficult to solve the optimization problem considering a specific value of the

Algorithm 5.1 LPV-MPC based on LPV models with varying delay

$k \longleftarrow 0$
repeat
$i \longleftarrow 0$
if $k = 0$ **then**
  Solve the optimization problem (5.7) by considering $\theta(0|k) \simeq \theta(1|k) \simeq \theta(2|k) \simeq ... \simeq \theta(N_p - 1|k)$
  Calculate $\Theta(k)$ and $\tilde{\tau}(k)$ using $\tilde{\mathbf{x}}(k)$ and $\tilde{u}(k)$
else
  Determine $\Theta(k) = \{\hat{\theta}(i|k)\}_{i=0}^{N_p-1}$ and $\tilde{\tau}(k) = \{\tau(i|k)\}_{i=0}^{N_p-1}$, where $\hat{\theta}(i|k) = \psi(x(i|k-1+1), u(i|k-1))$ and $\tau(i|k) = \phi(x(i|k-1+1), u(i|k-1)$
  Compute the difference value $g = \tilde{\tau}(k) - \tilde{\tau}(k-1)$
  if $g \leq 0$ **then**
    $\tilde{\mathbf{x}}(k) = \{x(i|k)\}_{i=0}^{N_p-|g|}$ and $\tilde{u}(k) = \{u(i|k)\}_{i=0}^{N_p-1-|g|}$
  else
    $\tilde{\mathbf{x}}_g(k) = repmat(\tilde{\mathbf{x}}(N_p - 1), [1, g])$
    $\tilde{\mathbf{x}}(k) = \{\tilde{\mathbf{x}}(k), \tilde{\mathbf{x}}_g(k)\}$
  end if
  Solve the optimization problem (5.7)
  $i \longleftarrow i + 1$
end if
Apply the first value of the optimal input sequence to the system
Define $\Theta_0(k+1) = \psi(\tilde{\mathbf{x}}_1(k), \tilde{u}_0(k))$ and $\tilde{\tau}_0(k+1) = \phi(\tilde{\mathbf{x}}_1(k), \tilde{u}_0(k))$
Modify the size of N_p, $N_p > \tau$
$k \longleftarrow k + 1$
until end

prediction horizon length because this should include the (varying) delay [101]. Hence, when solving MPC optimization problem the prediction horizon length should be adapted considering the delay value. Thus, because of the change of the prediction horizon, the size of states and inputs vectors should be adapted accordingly. This procedure is summarized in Algorithm 5.1.

5.4 Numerical results

According to Section 3.1, the pasteurization model is represented using the equations of each subsystem, namely, holding tube, power, water pump, heat exchanger and hot water tank. In this chapter, the second model (3.25) of the pasteurization process is used due to the delay in the model. The non-linear model of the pasteurization system is considered as

$$\dot{x} = f(x, x(t-\tau), u, u(t-\tau), \omega(t)), \tag{5.8}$$

where, $x = [T_1\ T_2\ T_{2r}\ T_4\ T_{in}]^\top \in \mathbb{R}^5$, $u = [N_1\ N_2\ P]^\top \in \mathbb{R}^3$ and $\omega = [T_a] \in \mathbb{R}^1$ are states, inputs and disturbance of the pasteurization system, respectively. Then, by using the non-linear embedding approach [119], the state-space LPV model of the pasteurization

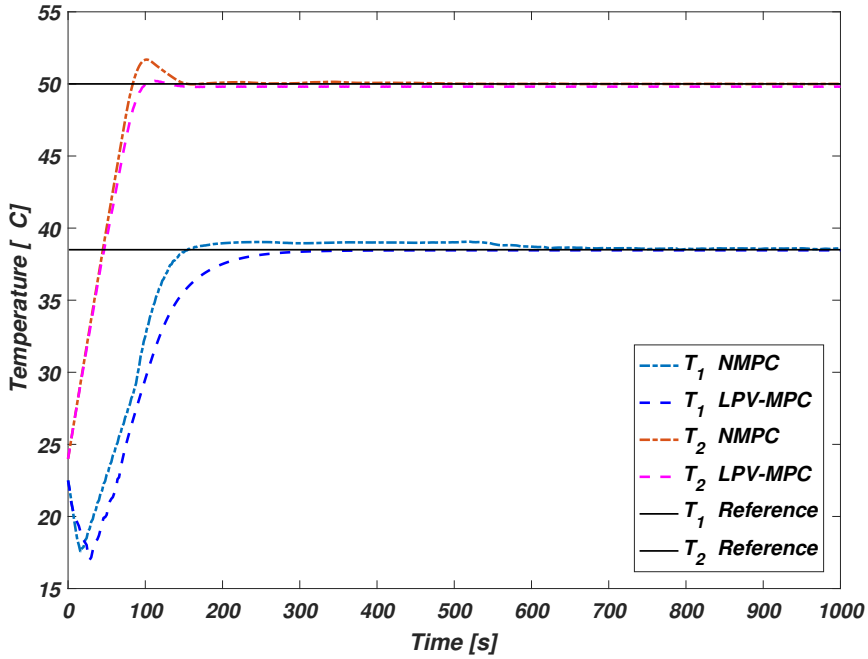

Figura 5.1: Evaluation of the output temperatures (Delay is constant during the prediction horizon)

plant is expressed as (3.26). The pasteurization temperature must be kept as close as possible to the set-point value for a pre-established time. According to this, temperature T_1 is the output of the holding tube for monitoring the temperature of the product after the pasteurization procedure, so that controlling T_1 to track set-points is one of the main objectives. On the other hand, the hot-water tank is the thermal energy source used to heat the product and proper system operation, T_2 should always be greater than T_1 to achieve the final temperature desired. Hence, in order to guarantee the energy for the process, T_2 should be controlled.

5.4.1 Simulation results and discussion

In this section, the proposed algorithm based on the system with constant delay and varying delay is compared with the state-of-the-art NMPC approach based on the system with the same information. The comparison is made both in terms of closed-loop performance and computational timing performance.

All simulation and computations have been carried out using a commercial computer with i7 2.40-GHz Intel core processor with 12 GB of RAM running MATLAB R2016b. Optimization problems (5.7) and (5.2) are solved by using the linear and nonlinear

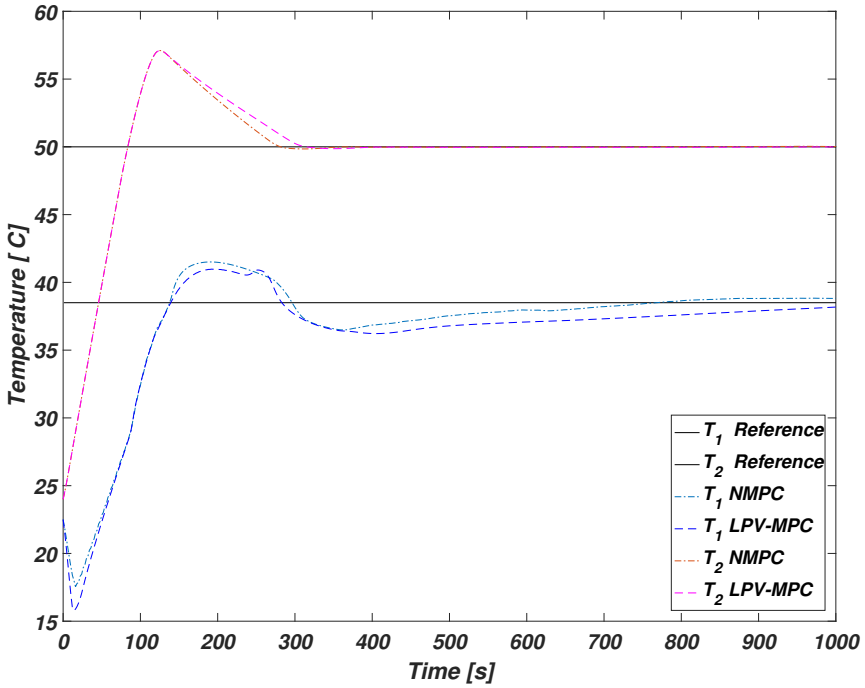

Figura 5.2: Evaluation of the output temperatures (Delay is varied during the prediction horizon)

programming solvers available in YALMIP [131]. All tests were done using the same prediction horizon, parameters and constraints as mentioned in Table 5.1.

Figures 5.1 and 5.2 present the comparison of the tracking response results obtained under the LPV-based MPC approach and the NMPC controller based on the pasteurization model with constant and varying delay during the prediction horizon, respectively. Moreover, the responses to the control actions using a controller based on the proposed approach and on NMPC, with constant and varying delay, are provided in Figures 5.3 and 5.4, respectively. The comparison of computation time of LPV-based MPC and NMPC is summarized in Table 5.2. Actually, in the pasteurization process, the delay of the system depends on the control action. Therefore, in the constant delay case, the delays of the system are varied at each time instant k, but during the prediction horizon, delays are considered as constant delays, where the value of delay in the next iteration $k+1$ is computed by the first elements of the optimal input. For more clarity of how the delay is varied in the new proposed approach during prediction horizon, Figure.5.5 shows the evolution of delay when it is considered constant and varying during the prediction horizon.

According to these results, it can be observed that the proposed LPV-based MPC

Taula 5.1: Physical properties and process data

Parameter	Description	Value	Unit
U	constant of convective heat transfer	10	[Wm^2/K]
A	area of the tank	0.0248	[m^2]
C_p	specific heat of the hot-water	4.186	[J/g°C]
M_1	mass of liquid inside the tank	82	[g]
M_2	mass product inside the regeneration section	24.85	[g]
T_a	room temperature	24.5	[°C]
T_1	temperature at the end of holding tube	[0,80]	[°C]
T_2	temperature inside hot water tank	[0,80]	[°C]
T_{2r}	returned water temperature from the heat exchanger	[0,80]	[°C]
T_4	temperature at the exit of heat exchanger	[0,80]	[°C]
T_{in}	temperature after regeneration section	[0,80]	[°C]
N_1	percentage speed of feeding pump	[40-80]	[%]
N_2	percentage speed of hot-water pump	[20-80]	[%]
P	power of the electric resistor	[0-1500]	[W]

controller is tracked and reached the set-point and the performance of the proposed algorithm is almost the same as the NMPC one. In terms of computational time, there is a quite clear difference: although the average time shows that the LPV-based MPC is on average four times faster than NMPC, in fact, the algorithms are only as good as their worst-case performance, in which case it is clear that the proposed approach is approximately an order of magnitude faster. To sum up, the simulation results show that the proposed LPV-based MPC controller is able to control LPV time-delay systems while improving the performance of the closed-loop system and achieving the specified set-point.

Taula 5.2: Comparison of each strategies timing performance.

Configuration	Maximum time	Average time	Standard deviation	r.m.s. error (T_1)	r.m.s. error (T_2)
NMPC constant delay into N_P	4.4540	2.0091	0.9071	4.9703	4.3479
LPV-MPC constant delay into N_P	0.1640	0.0785	0.0078	5.243	4.425
NMPC varying delay into N_P	24.887	6.9558	3.9441	5.117	4.7791
LPV-MPC varying delay into N_P	0.8771	0.2480	0.1409	5.402	4.820

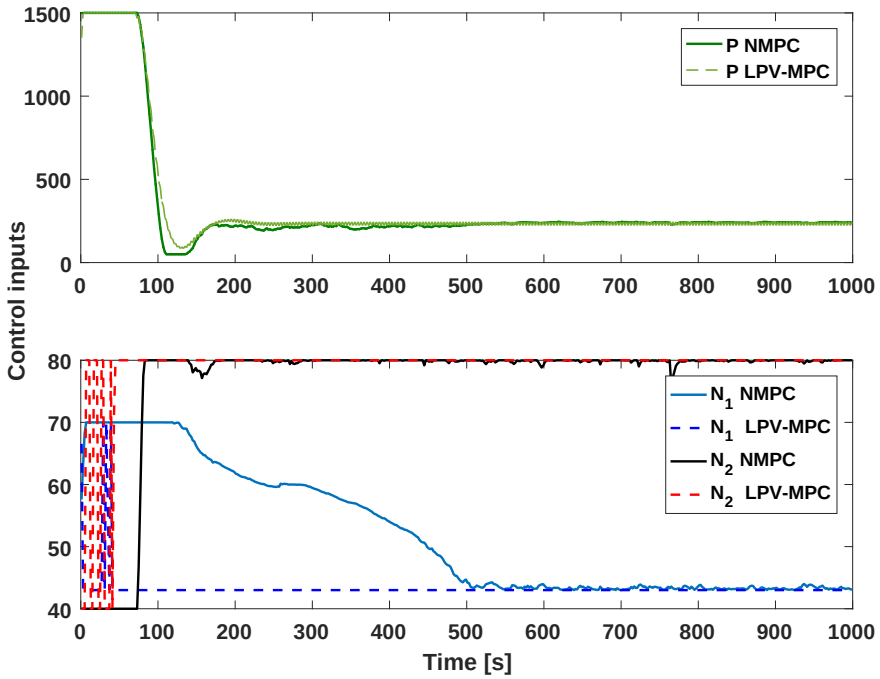

Figura 5.3: Evaluation of the control inputs (Delay is constant during the prediction horizon)

5.5 Summary

This chapter focused on the design of a model predictive control algorithm based on a class of Linear Parameter Varying (LPV) models with varying parameters delay. The constrained optimization problem for an LPV model with parameter varying and constant delay is solved iteratively by a series of QP problems while the scheduling parameters and delay are calculated at each time instant. The model with varying delay is predicted in the horizon by using the previous sequence of scheduling variable and state of the model. Based on the variation of the delay, the prediction horizon length is changed during the simulation. The proposed approach is easier to implement than NMPC, because the implementation of this method is basically the same algorithm as for linear systems. Also, as shown, the computation time required for the proposed approach has appreciably faster than other mentioned approach.

The content of this chapter was based on the following works:

F. Karimi Pour, V. Puig and C. Ocampo-Martinez. Model predictive control based on LPV models with parameter-varying delays 18^{th} *European Control Conference (ECC)*, (pp. pp. 3644- 3649) IEEE, Denmark, 2019.

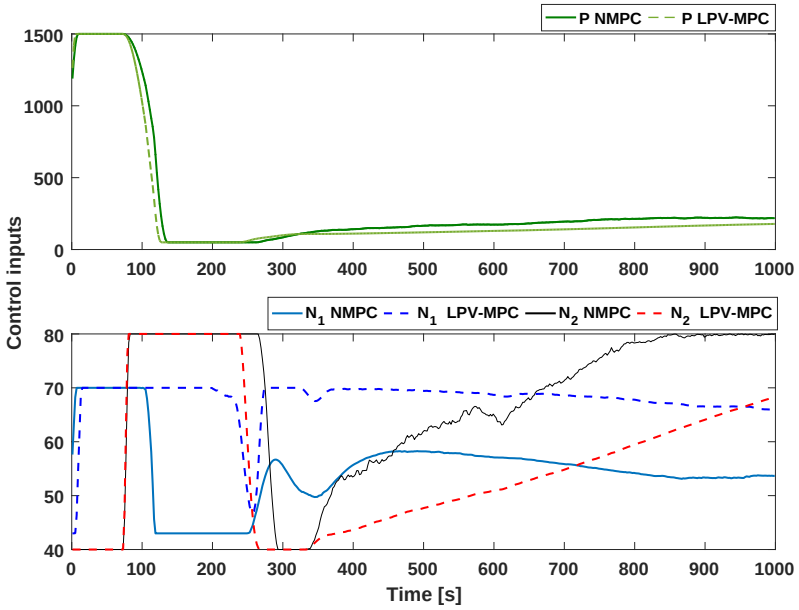

Figura 5.4: Evaluation of the control inputs (Delay is varied during the prediction horizon)

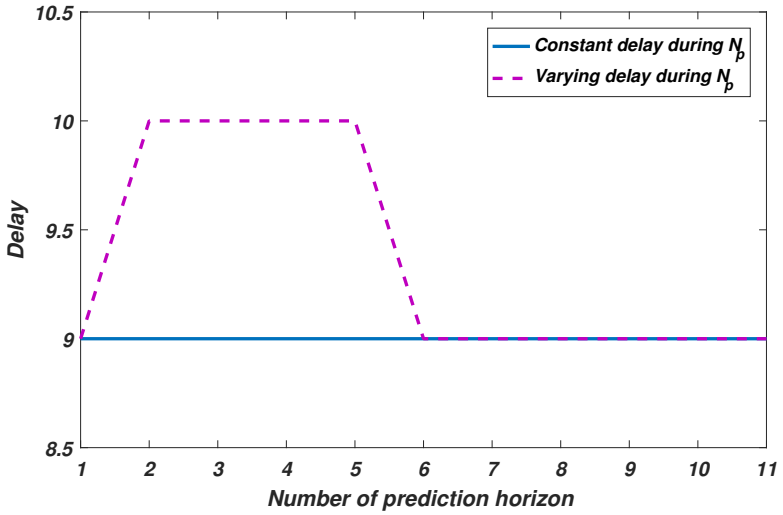

Figura 5.5: Comparison of delay during the prediction horizon

Part III

Health-Aware Control

Capítol 6

Multi-Layer Health-Aware Economic Predictive Control based on Components Fatigue

This chapter proposes two different health-aware economic predictive control strategies to minimize the damage of components in a pasteurization plant. The damage is assessed with the rainflow-counting algorithm that allows estimating the components fatigue. By using the results obtained from this algorithm, a simplified model that characterizes the health of the system is developed and integrated into the predictive controller. The overall control objective is modified by adding an extra criterion that takes into account the accumulated damage. The first strategy is a single-layer predictive controller with integral action to eliminate the steady-state error that appears when adding the extra criterion. In order to achieve the best minimal accumulated damage and operational costs, the single-layer approach is improved with a multi-layer control scheme, where the solution of the dynamic optimization problem is obtained from the model in two different time scales. Finally, to achieve the advisable trade-off between minimal accumulated damage and operational costs, both control strategies are compared in simulation over a utility-scale pasteurization plant.

6.1 Introduction

As mentioned in Section3.1, pasteurization implies that a food product is exposed to some temperature profile during a predetermined period of time, in order to reduce the proportion of microorganisms. Controlling and maintaining the temperature of the process are key aspects in the pasteurization process. Hence, a suitable control strategy for the system needs to be designed in order to manage the product temperature for keeping the desired product quality. The necessity of a significant control of the process arises from the savings in energy, product and time if an accurate tracking of the setpoint is performed. On the other hand, due to the high number of load

cycles that occur during the life of a pump within a pasteurization process, its fatigue estimation is an important factor for the proper control of such processes. For this reason, research regarding the integration of control with a fatigue-based prognosis of components has been developed in recent years. Fatigue leads to the breakdown of the material subject to stress, especially when frequent series of stresses are applied [162]. Damage has been widely and exhaustively studied from different perspectives [149]. In this chapter, the Palmgren-Miner linear damage rule is used to perform fatigue analysis [100]. This rule, commonly called the Miner's rule, is being currently used throughout the industry and in academia [142]. On the other hand, MPC has been recently proved as an adequate strategy for implementing health-aware control schemes. Several economic-oriented controllers have recently been proposed within the MPC framework [55, 74] but without considering safety issues of the system components. In fact, both safety stock and actuator lifetime are competing with the economic performance of the system. For this reason, it is required to have a flexible control strategy that allows to trade off the economic optimization and the safety of the system.

This chapter presents a health-aware control (HAC) with economic objectives that considers the information about the system health to adapt the objectives of the control law to extend the remaining useful life (RUL) of the considered system. Thus, the control inputs are generated to fulfill the control objectives/constraints but at the same time to extend the lifespan of the system components. In this way, the HAC makes an effort to attain maximum performance while not degrading the system too much. In case that the controller is implemented using MPC, the trade-off is based on modifying the control objective including new terms that take care of the system health. This leads to solving a multi-objective optimization problem where a trade-off between system health and performance should be established [171].

The main contribution of this chapter consists in the design of an improved health-aware economic MPC strategy. This strategy minimizes the damage of the pasteurization components and reduces the power consume of the electrical heater as economic objective, while still the pasteurization temperature tracks the suitable references related to the products, extending the result presented in [102]. The novelty is a multi-layer scheme including the health-aware and economic operation that extends and improves the preliminary ideas presented in [102]. The upper layer solves an optimization problem with an economic cost function and a new objective to minimize the accumulated damage at slow time scales. In the lower layer, a linear MPC controller forces the process dynamics to track the trajectory provided by the upper layer. Finally, a comparison between the multi-layer and single-layer control schemes is performed by using a high-fidelity simulator of a utility-scale pasteurization plant.

6.2 Problem statement

According to section 3.1.2, the control-oriented pasteurization model is represented in terms of behavioral equations of each subsystem, consisting of power, water pump, heat exchanger and hot water tank. The controlled inputs are the power of the electrical

heater, P, and the pump rotational speed of the second pump, N, respectively. The input temperature of the water heater, T_{iw}, and the temperature of cold water, T_{ic}, are measured non-controlled inputs (disturbances). Therefore, the matrix B in model (3.2) is separated to the matrices B and E. In this chapter, the LTI model of pasteurization plant is used based on a operating point of model (3.2). Finally, to design the MPC controller, this model is discretized and expressed in state space form

$$x_{k+1} = Ax_k + Bu_k + Ed_k, \tag{6.1a}$$

$$y_k = Cx_k, \tag{6.1b}$$

where $x \in \mathbb{R}^{n_x}$ is the state vector including hot-water flow, F_h, hot-water tank temperature, T_{ow} and pasteurization temperature, T_{past}, $u \in \mathbb{R}^{n_u}$ is the vector of manipulated variables that includes the electrical power of the heater P and the pump rotational speed N, $d \in \mathbb{R}^{n_d}$ is the vector of measured disturbances that include input temperature of the water heater, denoted by T_{iw}, and the temperature of cold water, denoted by T_{ic}. Finally, $y \in \mathbb{R}^{n_y}$ is the vector of controlled variables that include pasteurization temperature, denoted by T_{past}. Moreover, the input matrix B and disturbance matrix E of the model in (6.1) can be represented in the discrete-time domain as

$$B = \begin{bmatrix} 0 & 0 \\ \frac{T_s K_2}{\tau_2} & 0 \\ 0 & 0 \\ 0 & 0 \\ 0 & \frac{T_s K_{12}}{\tau_{12}} \\ 0 & 0 \\ 0 & 0 \end{bmatrix}, \qquad E = \begin{bmatrix} \frac{T_s K_1}{\tau_1} & 0 \\ 0 & 0 \\ 0 & 0 \\ 0 & 0 \\ 0 & \frac{T_s K_{22}}{\tau_{22}} \\ 0 & 0 \\ 0 & 0 \end{bmatrix}, \tag{6.2}$$

where K and τ are a static gain and a time constant, respectively.

6.2.1 Operational Control

As previously mentioned, the main goal is to guarantee that the pasteurization temperature is reached and maintained as close as possible to the set-point value for a per-established time. At the same time, reduction of energy consumption and health management of the system expressed should be achieved by formulating a multi-objective control problem. This optimization problem should be solved considering as constraints the mathematical model of the pasteurization system (6.1) and the operational constraints defined by (2.2).

Thus, the MPC controller design is based on the solution of the following FHOP:

$$\min_{\mathbf{u}_k} \sum_{i=0}^{N_p-1} \|x_{k+i|k}\|_{w_1}^p + \|u_{k+i|k}\|_{w_2}^p + \|\Delta u_{k+i|k}\|_{w_3}^p, \tag{6.3a}$$

subject to:

$$x_{k+i+1|k} = Ax_{k+i|k} + Bu_{k+i|k} + Ed_{k+i|k}, \tag{6.3b}$$

$$u_{k+i|k} \in \mathbb{U}, \tag{6.3c}$$

$$x_{k+i|k} \in \mathbb{X}, \tag{6.3d}$$

$$(x_{k|k}, u_{k-1|k}, d_{k|k}) = (x_k, u_{k-1}, d_k), \tag{6.3e}$$

for all $i \in \mathbb{Z}_{[0,N_p-1]}$, where $\mathbf{u}_k = \{u_{k+i|k}\}_{i\in\mathbb{Z}_{[0,N_p-1]}}$ is the decision sequence, with $\mathbf{u}_k$ being the sequence of controlled inputs. Furthermore, p denotes the norm used for this chapter is squared norm, $\Delta u_{k+i|k} = u_{k+i|k} - u_{k+i-1|k}$ are the input increments and the weighting matrices $w_1 \in \mathbb{R}^{n_x\times n_x}$, $w_2 \in \mathbb{R}^{n_u\times n_u}$ and $w_3 \in \mathbb{R}^{n_u\times n_u}$ are used to establish the priority of the different control objectives.

Moreover, $\mathbf{u}_k^\star$ denotes the optimal solution of (6.3) at time step k. According to the MPC receding horizon philosophy, only the first optimal control input is applied, i.e., $u_k = u_{k|k}^\star$. Then, the new measurements are used to update the initial conditions (6.3e) and then the optimization problem (6.3) is solved again using the receding horizon principle, as described in subsection 2.1.2.

6.3 Rainflow Counting Algorithm (RFC)

The damage accumulation process on a component produced by cyclic loading is known as *fatigue*. Fatigue is as frequent cause of failure in industrial machinery such as pumps [157]. In reality, fatigue failure occurs because of the application of fluctuating stresses that are much lower than the stress required causing failure during a single application of stress [100]. The commonly recognized and used measure for fatigue damage estimation is the so-called rainflow counting (RFC) method. RFC algorithm, first introduced by [56], has a complex consecutive and nonlinear structure in order to analyze ideal sequences of loads into cycles. Ordinarily, to compute a lifetime estimate from a given structural stress input signal, the RFC method is exerted by computation cycles and maxima, jointly with the Palmgren-Miner rule to calculate the expected damage. The input signal is received from time signal of the loading parameter of interest, such as torque, force, strain, stress, acceleration, or deflection [125]. Figure 6.1 shows the rain-flow counting procedure.

There are several types of RFC algorithms with different rules proposed by [56] and [156], which, at the end, yield in quite similar results. The RFC algorithm used in this chapter is presented in [156]. This algorithm computes the stress for each rainflow cycle in four steps:

- the stress history is converted to an extremum sequence of alternating maxima and minima of stress;
- for each local maximum M_j, the left (m_j^-) and right (m_j^+) regions where all stress values are below M_j are identified;

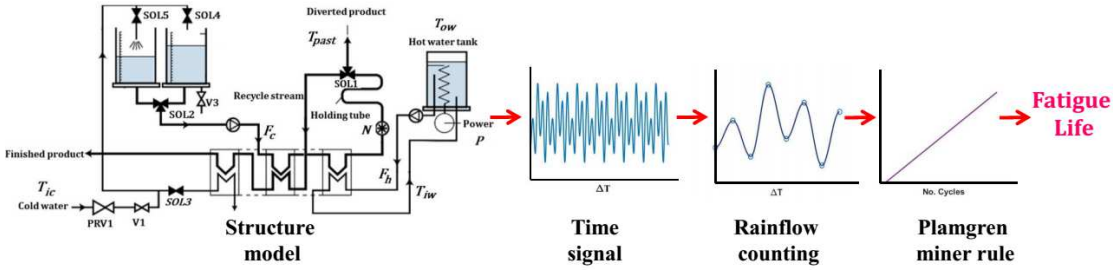

Figura 6.1: Rainflow counting damage procedure.

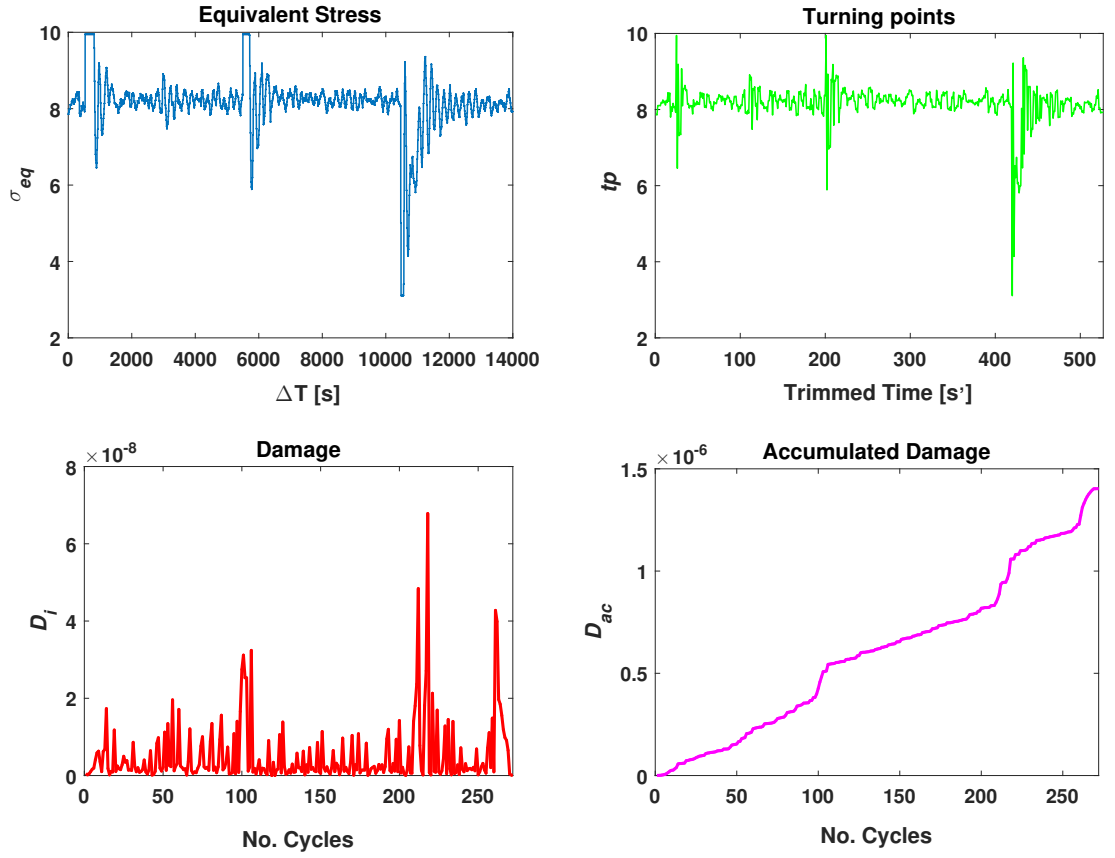

Figura 6.2: Rainflow counting damage estimation.

- the minimum stress value is $m_j = min\{m_j^-, m_j^+\}$;
- the equivalent stress per rainflow cycle s_j related to M_j is granted by either the amplitude $s_j = M_j - m_j$ or the mean value $s_j = \frac{M_j - m_j}{2}$.

In most of the materials, there is an explicit relationship between the number of cycles and cycles of failure, which is known as $S-N$ or Wöhler curves, whereas the damage D is calculated by using the $S-N$ curve at each stress cycle [120]. An often-used model for $S-N$ curve is

$$s^{c_w} N = K_{sp}, \tag{6.4}$$

where c_w and K_{sp} are material-specific parameters and N is the number of cycles to failure at a given stress amplitude s. The damage imposed by a stress cycle with a range s_j is computed as

$$D_j \equiv \frac{1}{N_j} = \frac{1}{K_{sp}} s_j^{c_w}. \tag{6.5}$$

Then, the total damage under the linear accumulation damage (Palmgren-Miner) rule is given as

$$D_{ac} = \sum_{j=1}^{\lambda} \frac{1}{N_j} = \sum_{j=1}^{\lambda} \frac{1}{K_{sp}} s_j^{c_w}, \tag{6.6}$$

for damage increments D_{ac} associated to each counted cycle, where N_j is the number of cycles of failure associated to the stress amplitude s_j and the number of all counted cycles λ. These sequences are presented in Figure 6.2. On the top-left and top-right part of Figure 6.2, the input stress and the same signal converted into a sequence of maxima and minima are shown, respectively. The instantaneous damage and the accumulated damage are displayed in the bottom part of Figure 6.2.

For real-time systems, applying the customary rainflow counting algorithm is quite challenging and computationally demanding. Considerable amounts of data must be stored and provided periodically to obtain a quantity of data in equivalent regular cycles. Besides, the algorithm must be applied to a stored set of data. One of the objectives of this chapter is to analyze the fatigue due to pump load of the pasteurization system. Loads in the pump structure arise from several factors, the typical reason for pump failure is bearing damage. However, pressure and pump rotational speed are two damage factors that have the greatest influence on the shaft bearing life. Both variables could be chosen as stress indicators for the pasteurization pump. In this chapter, the rotational speed of the pump is used as stress for RFC damage estimation.

Utilizing the RFC algorithm, the accumulated damage is obtained as a function of the cycles of the pump rotational speed stress signal. In order to have available an accumulated damage variable that can be integrated with a linear MPC model, a simplified approach to compute fatigue on time series signal is proposed based on the RFC theory. The outcome of this approach is that the accumulated damage is obtained as a function of time instead of the number of cycles. The proposed approach finds the changes of the sign that correspond to a cycle in the stress time signal. The obtained function at each time instant k is the following:

$$D_k = \begin{cases} 0 & \text{if} \quad I_k = I_{k-1}, \\ \frac{1}{K_{sp}} s_k^{c_w} & \text{if} \quad I_k \neq I_{k-1}, \end{cases} \tag{6.7}$$

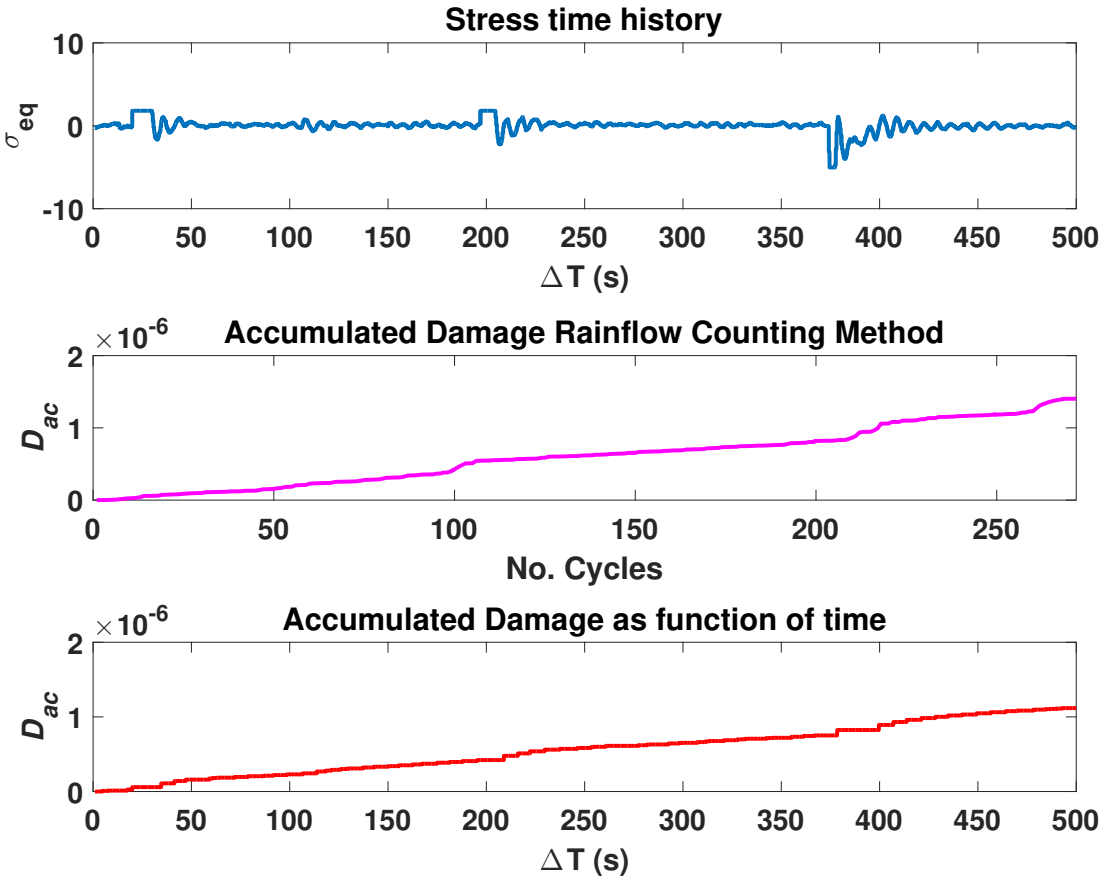

Figura 6.3: Accumulated Damage Comparison.

where s_k is a stress at time k defined as

$$s_k = \frac{1}{L} \sum_{q=k-L}^{k} N_{s,q}, \tag{6.8}$$

L is the number of samples per cycle, N_s is the pump rotational speed moment, q is the difference between the number of samples per cycle and time instant and I_k is the signal adapted to indicate cycle, i.e.,

$$I_k = N_{s,k} - s_k. \tag{6.9}$$

Then, the accumulated damage is calculated by

$$D_{acc,k} = D_{acc,k-1} + D_k. \tag{6.10}$$

Note that, at the end of the scenario, the accumulated damage based on the function of time and rainflow-counting method is practically the same. Figure 6.3 indicates the

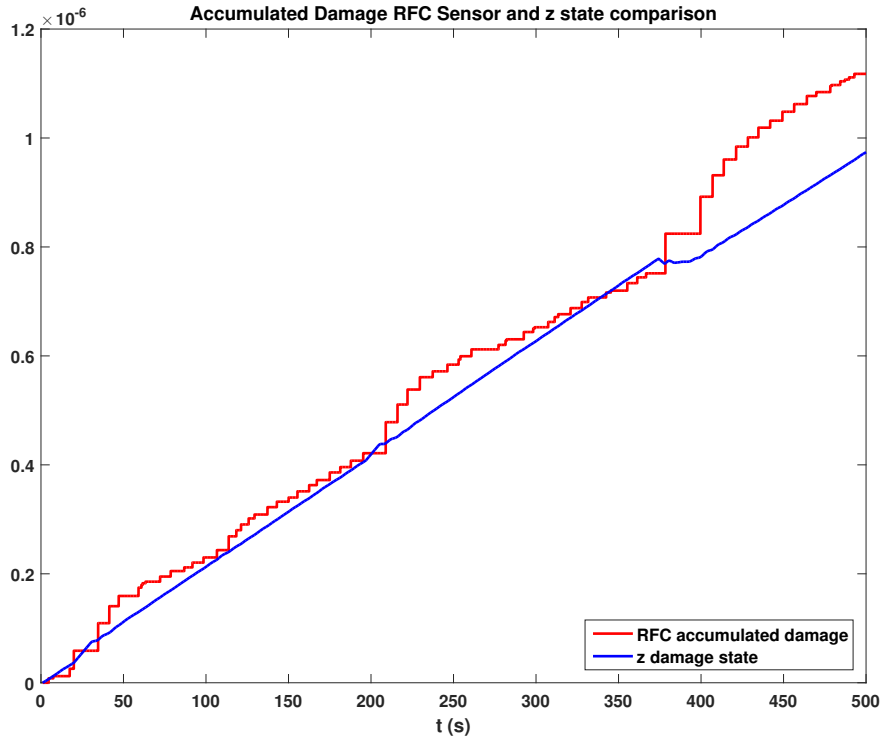

Figura 6.4: Accumulated damage RFC as a function of time and z fatigue damage state.

accumulated damage value obtained with each one. The small difference depends on the fact that the damage obtained by the RFC technique is represented in terms of the cycles while the other is a function of time. The degradation procedure of the pasteurization pump can be characterized by using the water pump rotational speed sensor information. In order to decrease the accumulated damage, a new objective is included in the MPC controller that aims at minimizing the pump degradation assessed by means of a linearized RFC model. The slope m of the accumulated damage curve in function of time is computed and then employed as one of the parameters in the linear fatigue damage model. According to [186], an experimental model that relates the values of the pump rotational speed and flow in steady state is used. The model for the pump rotational speed is a linear model with a slope α_1 and a constant value α_0

$$\bar{N}_{s,k} = \alpha_1 u_{F,k} + \alpha_0, \tag{6.11}$$

where u_F is the hot-water flow. To sum up, a linear fatigue damage model is considered as a relationship between the accumulated damage of the pump and the control signal

$$z_{k+1} = z_k + \frac{m}{L}(\alpha_1 u_{F,k} + \alpha_0), \tag{6.12}$$

where z_{k+1} is the accumulated damage of the pump. Then, (6.12) can be included into the control-oriented model of the MPC as a new state and an additional objective is

added into the MPC cost function (6.3) to minimize the accumulated damage. The degree of fitting between the RFC approximation as a function of time presented in (6.10) and the linear damage model in (6.12) can be compared in Figure 6.4.

6.4 Health-aware MPC

In this section, two MPC structures are proposed for adding the health-aware objective into the MPC cost function in order to minimize the accumulated damage.

6.4.1 Design of Single-layer Health-aware MPC Controllers

First, a health-aware MPC controller based on a single-layer scheme is proposed. In this approach, a single-layer MPC that includes a new objective that assesses the system health by means of (6.12) is considered. The problem formulation of this controller is similar to (6.3). Taking into account (6.12), the proposed approach relies on solving the following optimization problem at each time instant k:

$$\min_{\mathbf{u}_k} \sum_{i=0}^{N_p-1} \|e_{k+i|k}\|_{w_1}^p + \|u_{k+i|k}\|_{w_2}^p + \|\Delta u_{k+i|k}\|_{w_3}^p + \|z_{k+i|k}\|_{w_4}^p + \|\xi_{k+i|k}\|_{w_5}^p, \tag{6.13a}$$

subject to:

$$x_{k+i+1|k} = Ax_{k+i|k} + Bu_{k+i|k} + Ed_{k+i|k}, \tag{6.13b}$$

$$e_{k+i+1|k} = r_{k+i+1|k} - Cx_{k+i|k} \tag{6.13c}$$

$$z_{k+1} = z_k + \frac{m}{L}(\alpha_1 u_{F,k} + \alpha_0), \tag{6.13d}$$

$$T_{ow(k+i|k)} - T_{past(k+i|k)} \geq \zeta + \xi_{k+i|k} \tag{6.13e}$$

$$u_{k+i|k} \in \mathbb{U}, \tag{6.13f}$$

$$x_{k+i|k} \in \mathbb{X}, \tag{6.13g}$$

for all $i \in \mathbb{Z}_{[0,N_p-1]}$, where $e_{k+i|k}$ is the tracking error and $r_{k+i|k}$ is the set-point for the controlled variables while the weighting matrix w_5 is used to manage the penalization of slack variable $\xi \in \mathbb{R}$ that is used for softening the output constraints and ζ is temperature differences between T_{ow} and T_{past} [186]. The value of ζ is considered as a design parameter, which was specified by iterative simulations to have a safety temperatures difference. The health-aware objective with the corresponding weight w_4 is appended in the MPC cost function to minimize the accumulated damage. However, the new state in the model of the MPC controller can lead to steady-state offset. Different mechanisms for steady-state offset elimination have been proposed in the literature [70][150]. The strategy used in this chapter is introduced in [150]. This method is based on augmenting the process model that includes a constant step disturbance to eliminate the steady-state

offset. This disturbance, which is estimated from the measured process variables, is usually considered to be constant in the future and its effect on the controlled variables is eliminated by shifting the steady-state target for a controller. Thus in order to remove the steady state error, the process state-space model is augmented with an integrator as follows:

$$\begin{bmatrix} x_{k+1} \\ e_{k+1} \end{bmatrix} = \begin{bmatrix} A & G_e \\ 0 & I \end{bmatrix} \begin{bmatrix} x_k \\ e_k \end{bmatrix} + \begin{bmatrix} B \\ 0 \end{bmatrix} u_k, \tag{6.14a}$$

$$y_k = \begin{bmatrix} C & 0 \end{bmatrix} \begin{bmatrix} x_k \\ e_k \end{bmatrix}, \tag{6.14b}$$

where G_e is a matrix that determines the effect of the disturbances on the states. In this chapter, considering (6.1) and (6.14a), $G_e = E$. The states of the process model and the unmeasured disturbance model must be estimated simultaneously using the augmented system model (6.14). The state estimation can be performed either within a stochastic framework using a Kalman filter or within a deterministic framework using a Luenberger observer. In both cases, a gain $L_G = [L_x, L_e]^T$ can be determined using standard methods provided the augmented system is detectable [118]. Thus, the steady-state observer equation for a time k is given by

$$\begin{aligned} \hat{x}_{k+1} =& A\hat{x}_k + Bu_{\bar{k}} + G_e\hat{e}_k + L_x[y_k - C(A\hat{x}_k + Bu_k \\ &+ G_e\hat{e}_k)], \end{aligned} \tag{6.15}$$

$$\hat{e}_{k+1} = \hat{e}_k + L_e \left[y_k - C(A\hat{x}_k + Bu_k + G_e\hat{e}_k) \right], \tag{6.16}$$

where L_x and L_e are the observer gains that correspond to the states estimation $\hat{x}_k$, and the tracking error $\hat{e}_k$. In this chapter, the observer gain L_G that includes L_x and L_e is obtained with the Linear Matrix Inequalities (LMI) pole placement technique [174], which allows to place the eigenvalue of the $A - L_G C$ inside the unit circle using an LMI region

$$\begin{bmatrix} -rX & qX + X^T A - W^T C \\ qX + A^T X - C^T W & -rX \end{bmatrix} < 0, \tag{6.17}$$

where q and r denote the center and the radius of a circular LMI region, respectively, X is the unknown symmetric matrix and $W = L_G X$. Finally, L_G is obtained as

$$L_G = WX^T. \tag{6.18}$$

Then, $A - L_G C$ is Schur hence the convergence of the observer in (6.15) and (6.16) is guaranteed.

The control scheme presented in Figure 6.5 shows the integration of the control with the estimation scheme. In this scheme, there is an MPC regulator block that forces the system to a steady state (x_s and u_s), which represents the accessible steady-state input and state target, respectively. Moreover, a Target Calculus block is in charge to compute these steady-state values, while the variables u_{sp} and y_{sp} correspond to the input and output set-points. Note that the Target Calculus stage does not take into account any economic criterion to be optimized. Moreover, the dynamic control is detached from the

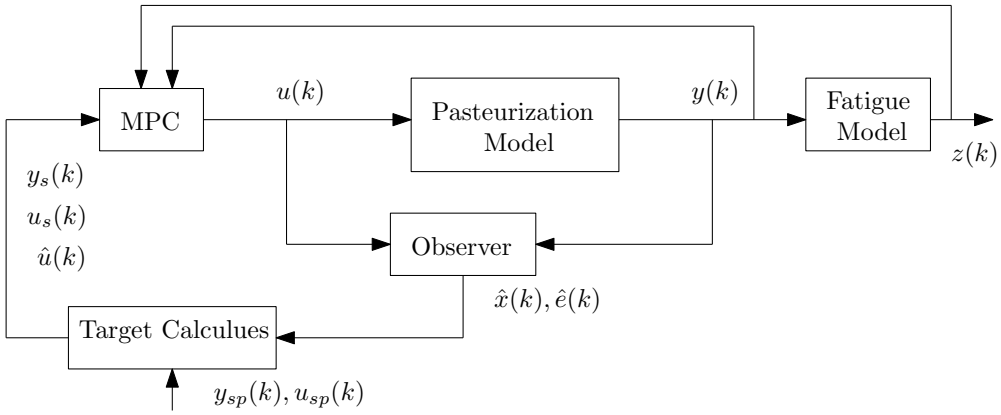

Figura 6.5: Representative block diagram of single-layer MPC with fatigue model and linear regulator.

set-point calculation: the Targets Calculus block is completely dedicated to obtaining the constant values, while the MPC regulator block is devoted to leading the states $\hat{x}_k$ to its corresponding targets. Then, the optimization problem that must be solved in the regulatory block is as follows:

$$\min_{\tilde{\mathbf{u}}_k} \sum_{i=0}^{N_p-1} \|C\tilde{x}_{k+i|k}\|_{w_1}^p + \|\tilde{u}_{k+i|k}\|_{w_2}^p + \|\Delta\tilde{u}_{k+i|k}\|_{w_3}^p + \|z_{k+i|k}\|_{w_4}^p + \|\xi_{k+i|k}\|_{w_5}^p, \tag{6.19a}$$

subject to:

$$x_{k+i+1|k} = Ax_{k+i|k} + Bu_{k+i|k} + Ed_{k+i|k}, \tag{6.19b}$$
$$z_{k+1} = z_k + \frac{m}{L}(\alpha_1 u_{F,k} + \alpha_0), \tag{6.19c}$$
$$T_{ow,k+i|k} - T_{past,k+i|k} \geq \zeta + \xi_{k+i|k} \tag{6.19d}$$
$$\tilde{u}_{k-1} = u_{k-1} - u_s, \tag{6.19e}$$
$$\tilde{x}_k = \hat{x}_k - x_s, \tag{6.19f}$$
$$u_{min} \leq \tilde{u}_{k+i} + u_s \leq u_{max}, \tag{6.19g}$$
$$\Delta u_{min} \leq \Delta\tilde{u}_{k+i} \leq \Delta u_{max}, \tag{6.19h}$$
$$u_{k-1|k} \in \mathbb{U}, \tag{6.19i}$$
$$x_{k+i|k} \in \mathbb{X}, \tag{6.19j}$$

for all $i \in \mathbb{Z}_{[0,N_p-1]}$, $\Delta\tilde{u}_{k+i|k} = \tilde{u}_{k+i|k} - \tilde{u}_{k+i-1|k}$ are the input increments, Δu_{min} and Δu_{max} are minimum and maximum value of Δu, where it can be seen that the state and input are led to the targets x_s and u_s in (6.19f) and (6.19e), respectively. The role of this part is to steer the shifted states and inputs to zero. Thus, the capability of offset elimination strategy depends on the computation of the targets x_s and u_s. For

obtaining this optimal operating point, the following optimization problem is solved:

$$\min_{u_s,x_s} V_k \triangleq \{(y_{sp,k} - y_k^a)^T Q(y_{sp,k} - y_k^a) + (u_{s,k} - u_{sp,k})^T R(u_{s,k} - u_{sp,k})\}, \tag{6.20a}$$

subject to:

$$x_{s,k+1} = Ax_{s,k} + Bu_{s,k} + G_e\hat{e}_k, \tag{6.20b}$$

$$y_k^a \triangleq Cx_{s,k}, \tag{6.20c}$$

$$u_{min} \leq u_{s,k} \leq u_{max}, \tag{6.20d}$$

where $y_{sp,k}$ stands for the output set-points, and y_k^a is the achievable stationary output. Also, Q and R are positive definite weighting matrices. Following the strategy described in Figure 6.5, two optimization problems must be solved at each time instant k.

On the contrary, from (6.16), the states and disturbances presented by the observer satisfy

$$\hat{x}_{\bar{k}+1} = A\hat{x}_{\bar{k}} + B\hat{u}_{\bar{k}} + G_e\hat{e}_{\bar{k}}, \tag{6.21a}$$

$$y_{\bar{k}} = C\hat{x}_{\bar{k}}. \tag{6.21b}$$

Then, subtracting (6.20b) from (6.21a) will be

$$(\hat{x}_{\bar{k}+1} - x_{s,k+1}) = A(\hat{x}_{\bar{k}} - x_{s,k}) + B(\hat{u}_{\bar{k}} - u_{s,k}), \tag{6.22}$$

which relates to the original system considered by the target tracking optimization. The regulator will lead the states $\tilde{x}_k$ to zero, that is

$$(\hat{x}_{\bar{k}+1} - x_{s,k+1}) = 0. \tag{6.23}$$

Then, subtracting (6.20c) from (6.21b)

$$(y_{\bar{k}} - y_{sp}) = C(\hat{x}_{\bar{k}} - x_{s,k}). \tag{6.24}$$

Finally, from (6.23) and (6.24) leads to

$$y_{\bar{k}} = y_{sp}. \tag{6.25}$$

Therefore, both optimization problems should be solved simultaneously in the case of using an augmented model. However, in the single-layer health-aware MPC scheme, since the models of chemical processes are often complex and nonlinear, this leads to long solution times of the optimization problem. Moreover, long optimization horizons and many degrees of freedom increase the computational load. Hence, for chemical processes, one is faced with the trade-off between sub-optimality and computational effort.

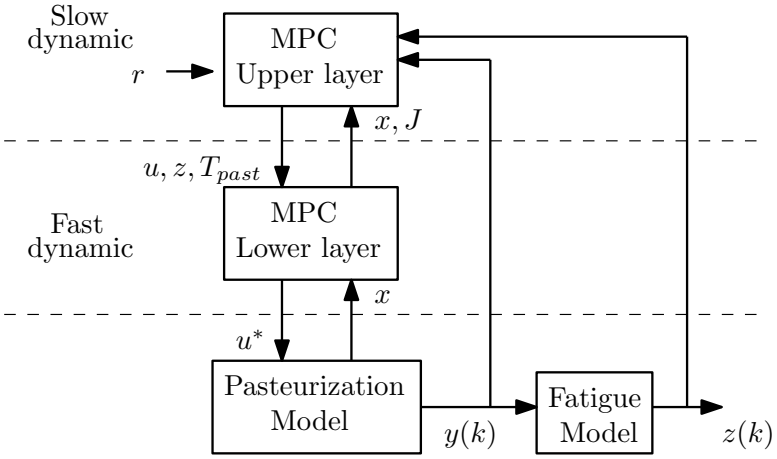

Figura 6.6: Representative block diagram of two-layer MPC with fatigue model.

6.4.2 Design of Multi-layer Health-aware MPC Controllers

In general, the design of multi-layer control architectures can be related to the diverse nature of the control objectives, which would not be able to be coupled into a single-layer architecture. In particular, the control objectives can be ranked in the following way:

- Foremost, the objectives of process operation are to maximize economic benefits and minimize the system degradation. Hence, the process operation is assessed by economic decision criteria and the health-aware objective, which are organized in the objective function of the upper layer optimization. For this reason, the degradation takes more time than the tracking trajectory for evaluation, the model considers the slow dynamics of the system.
- Furthermore, the goal of process control is to guarantee a stable operation under the effect of the degradation state and tracking the trajectory, which should be guaranteed by the lower-layer controllers that operate at fast dynamic model.

The control strategy addressed in this part is based on a multilayer (hierarchical) control structure that is shown in Figure 6.6. The proposed control system is a two-layer hierarchical architecture, where the solution of the dynamic optimization problem is calculated considering two different time-scales. In the upper layer, an optimization problem is solved with an economic cost function and a health-aware objective. The upper layer considers the slow dynamics of the system and uses larger sampling times than the low layer (slow time scale). Since the accumulation of damage cannot be assessed in a short period of time, the upper layer MPC has been implemented by using a longer prediction horizon, where the sampling time for the discretization of the system is larger

than the system in the lower layer. In the lower layer, the tracking controller receives the trajectory calculated by the upper layer and determines the setpoint trajectories for the base-layer control system by considering the faster dynamics of the plant (fast time scale). The current state values are required to provide initial conditions for dynamic real-time optimization (DRTO) and the tracking controller, that have to be estimated by means of measurements from the process. Thus, a time-scale separation of the measurements from the process must be performed, as the upper layer is operating at a lower sampling rate and should only take into account the slow trend in the measurements.

Upper-layer controller

In the optimization problem of the upper layer, the goal is to minimize accumulated damage by inserting (6.12) as a new state and a new objective in the MPC controller and a trajectory planner calculates a reachable reference y^r as close as possible to the exogenous reference signal r. At the same time, minimizing the economic objective that is the electrical power consumed by the heater is the second control goal of this layer.

Taking into account (6.12), the proposed approach relies on solving the following optimization problem at each time instant k:

$$\begin{aligned}\min_{\{u_k, Z_k, x_k^r, \xi_k\}} \sum_{i=0}^{N_{pu}-1} & \|r_{k+i+1|k} - y^r_{k+i|k}\|^p_{w_1} + \|u_{k+i|k}\|^p_{w_2} \\ & + \|\Delta u_{k+i|k}\|^p_{w_3} + \|z_{k+i|k}\|^p_{w_4} + \|\xi_{k+i|k}\|^p_{w_5},\end{aligned} \tag{6.26a}$$

subject to:

$$x^r_{k+i+1|k} = Ax^r_{k+i|k} + Bu_{k+i|k} + Ed_{k+i|k}, \tag{6.26b}$$

$$y^r_{k+i|k} = Cx^r_{k+i|k}, \tag{6.26c}$$

$$z_{k+1} = z_k + \frac{m}{L}(\alpha_1 u_{F,k} + \alpha_0), \tag{6.26d}$$

$$T_{ow(k+i|k)} - T_{past(k+i|k)} \geq \zeta + \xi_{k+i|k} \tag{6.26e}$$

$$u_{k+i|k} \in \mathbb{U}, \tag{6.26f}$$

$$x^r_{k+i|k} \in \mathbb{X}, \tag{6.26g}$$

for all $i \in \mathbb{Z}_{[0,N_{pu}-1]}$, and the new objective with the corresponding matrix weight w_4 is appended in the MPC cost function to minimize the accumulated damage. N_{pu} is the prediction horizon of the upper layer and the sampling time of the upper layer is t_u.

Lower-layer controller

The lower-layer controller is tracking the optimal trajectory under the influence of high frequency of the accumulated damage and is executed at sampling time t_l of the process.

In the lower-layer, the predictive controller is designed to track the calculated reference obtained from the upper layer. This generates from the following optimization problem:

$$\min_{u_k} \sum_{i=0}^{N_{pl}-1} \|e_{k+i|k}\|_{w_1}^p + \|\Delta u_{k+i|k}\|_{w_2}^p, \tag{6.27a}$$

subject to:

$$x_{k+i+1|k} = Ax_{k+i|k} + Bu_{k+i|k} + Ed_{k+i|k}, \tag{6.27b}$$

$$u_{k+i|k} \in \mathbb{U}, \tag{6.27c}$$

$$x_{k+i|k} \in \mathbb{X}, \tag{6.27d}$$

for all $i \in \mathbb{Z}_{[0,N_{pl}-1]}$, where N_{pl} is the prediction horizon of the lower layer. Moreover, $e_{k+i|k} = Cx^r_{k+i|k} - Cx_{k+i|k}$ is the error between the calculated references that are obtained from the upper layer and measured output. Since the accumulated damage should be assessed in a long prediction horizon, $N_{pl} < N_{pu}$ should be established and the sampling time of the upper layer should be greater than on from the lower layer, $t_u > t_l$.

6.5 Simulation Results

In this section, the performance of the proposed different health-aware MPC schemes is assessed with the pasteurization plant case study described in section 3.

6.5.1 Design of an MPC Controller with Health-aware Capabilities and Economic Objectives

In order to test the behavior of the proposed health-aware MPC scheme in two different manners, several simulations were carried out and the results obtained are presented in this part. The operating point for the hot-water flow is chosen as 200 ml/min. The behavior of the controlled temperature T_{past} from the pasteurization plant under the health-aware hierarchical MPC and single-layer MPC with and without the health-aware objective are presented in Figure 6.7 with its corresponding references, while the controlled variable T_{past} tracks the references. In Figure 6.8, an evolution of the accumulated damages obtained from multi-layer and single-layer MPC with and without a health-aware objective are provided.

Scenario 1 (Health-aware single-layer MPC)

The health-aware MPC is designed as described in Section 6.4.1, by adding the accumulated damage model presented before, as a new state introduced in (6.12). In addition,

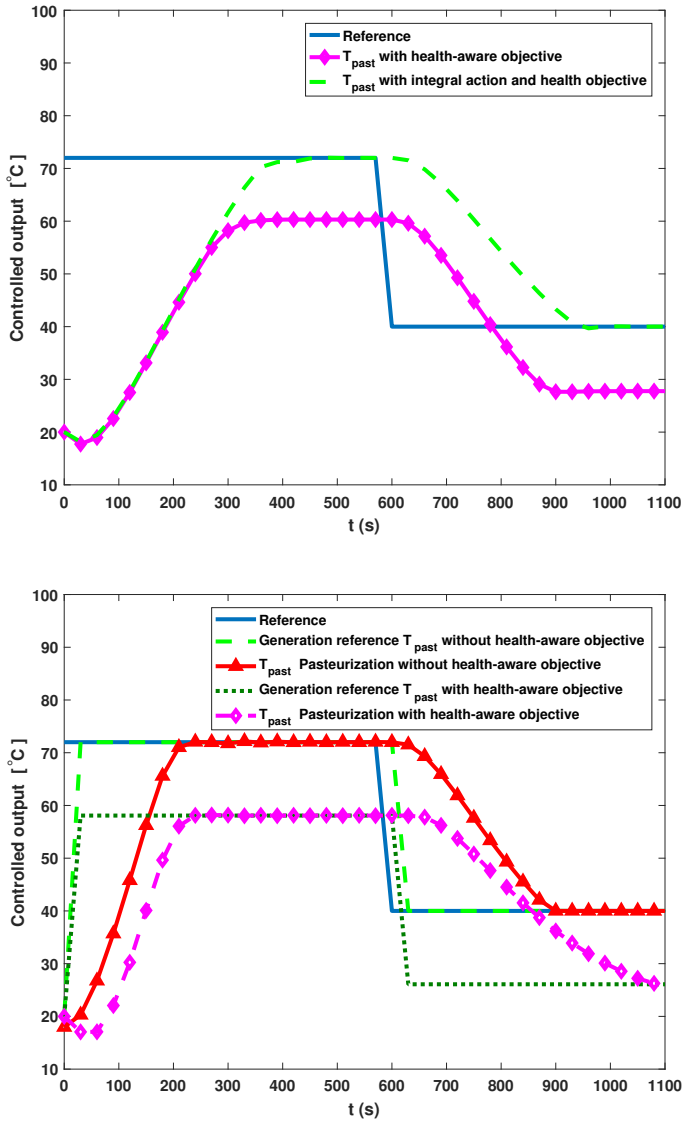

(a) Pasteurization temperature T_{past} in single-layer. (b) Pasteurization temperature T_{past} in multi-layer.

Figura 6.7: Evolution of pasteurization temperature T_{past} with and without the health-aware objective in the MPC.

to remove steady state offset that appears with the augmented model in the health-aware MPC is augmented again. Therefore, According to the complete model of the pasteurization system (3.2), the matrix E is utilized as disturbance in this chapter. Now with

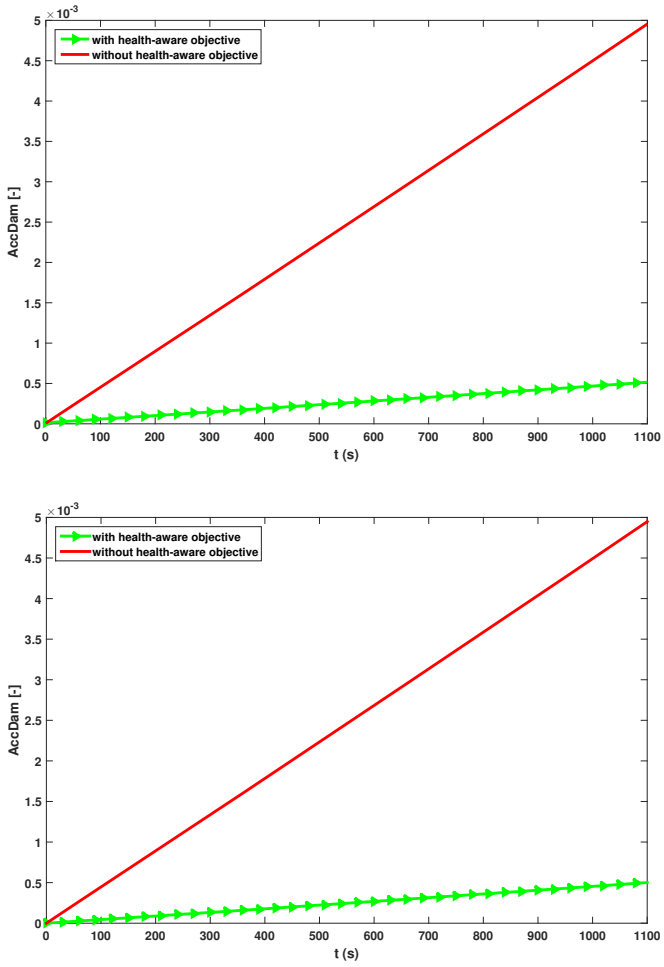

(a) Accumulated damages by single-layer structure. (b) Accumulated damages by multi-layer structure.

Figura 6.8: Evolution of accumulated damages with and without health-aware objective in the MPC.

the disturbance model as follows:

$$x_{n,k+1} = A_s x_{n,k} + B_s u_k + E_s d_k, \tag{6.28a}$$

$$y_{n,k} = C_s x_{n,k}, \tag{6.28b}$$

where A_s, B_s, C_s, and E_s are matrices of proper dimensions including accumulated damage and disturbance model given by (6.12) and (6.14a). The MPC controller has been implemented considering that the prediction horizon is chosen as $N_p = 400$ and the sampling time is 4 s. The control objective of the MPC controller for the pasteurization system is the pasteurization temperature T_{past} tracking the setpoint, while at the same time, the accumulated damage is evaluated as in (6.12) and the power of the electrical

heater P are minimized. From Figure 6.7a and Figure 6.8a, it can be seen that the cost and degradations are decreased while the temperature is tracking the references without steady-state offset.

Scenario 2 (Health-aware multi-layer MPC)

Alternatively, as discussed in Section 6.4.2, the health-aware MPC can be implemented using a two-layer hierarchical structure, where the solution of the optimization problem considered in the single-layer scheme is solved at different time scales. The two-layer MPC implemented in the new model is presented by

$$x_{n,k+1} = A_h x_{n,k} + B_h u_k + E_h d_k, \tag{6.29a}$$

$$y_{n,k} = C_h x_{n,k}, \tag{6.29b}$$

where the state and output vector are given by $x_n = [x; z]$ and $y_n = [y; z]$, respectively. Moreover, A_h, B_h, C_h, and E_h are state matrices of proper dimensions with included accumulated damage given by (6.12). The control objectives of the upper layer for the pasteurization system aim at minimizing the accumulated damage evaluated as (6.12) and reducing the power of the electrical heater as economic objective and at the same time. The appropriate pasteurization temperature T_{past} is calculated in order to save energy and avoid overheating the product. Due to the accumulation of damage can not be assessed in a short horizon, the upper layer MPC has been implemented by using prediction horizon $N_u = 300$, where the sampling time for the discretization of continues state-space model of the pasteurization plant(3.2) is 120 s. On the other hand, the control objective in the low layer MPC forces that the pasteurization temperature T_{past} is tracking the calculated appropriate pasteurization temperature in the upper layer. The prediction horizon is chosen $N_{pl} = 5$ and sampling time is 4 s. Figure 6.7b are the behavior of pasteurization temperature T_{past} with and without the health objective are presented. Moreover, the reduction of accumulated damage under multi-layer MPC scheme is presented in Figure 6.8b.

6.5.2 Results and Comparison Assessment

According to the results, it can be observed that the results of the inclusion of the fatigue objective in single-layer approach and two-layer approach are almost the same (see Figure 6.8). In particular, the accumulated damage is mitigated about 88% in both of them. However, from Figure 6.9 it can be seen the power of the electrical heater P from the multi-layer MPC is minimized more than in the single-layer MPC. This implies that the multi-layer health-aware MPC controller can achieve better results related to the economic cost objective. While there is some degree of flexibility playing with the temperature set-point for achieving the best result of minimizing accumulated damage in the multi-layer scheme. In order to have better cooperation between the two different control scheme, several simulation with different tunings have been implemented. Finally, the trade-off curves between the health objective and economic cost for single-layer and multi-layer schemes are presented in Figure 6.10. Moreover, Figure 6.10 shows

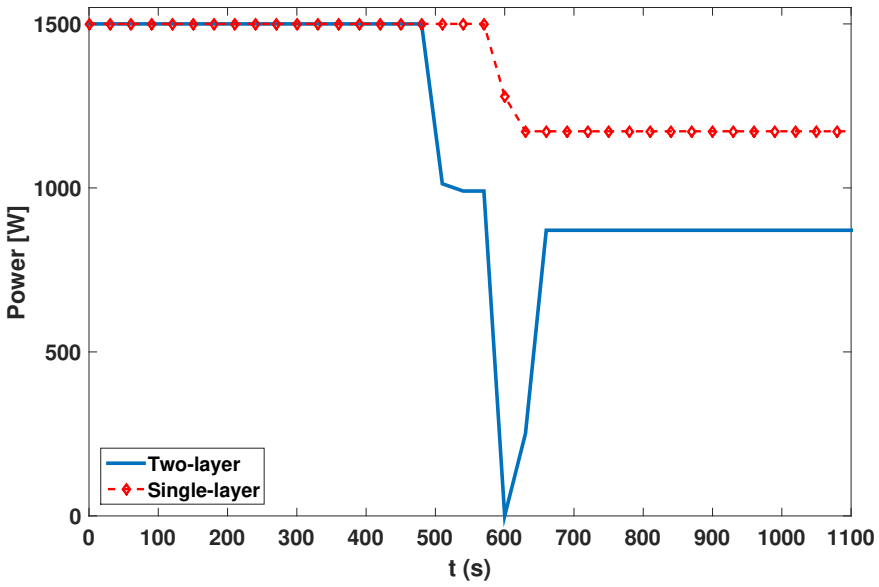

Figura 6.9: Evolution of power the electrical heater P in the single-layer and two-layer MPC.

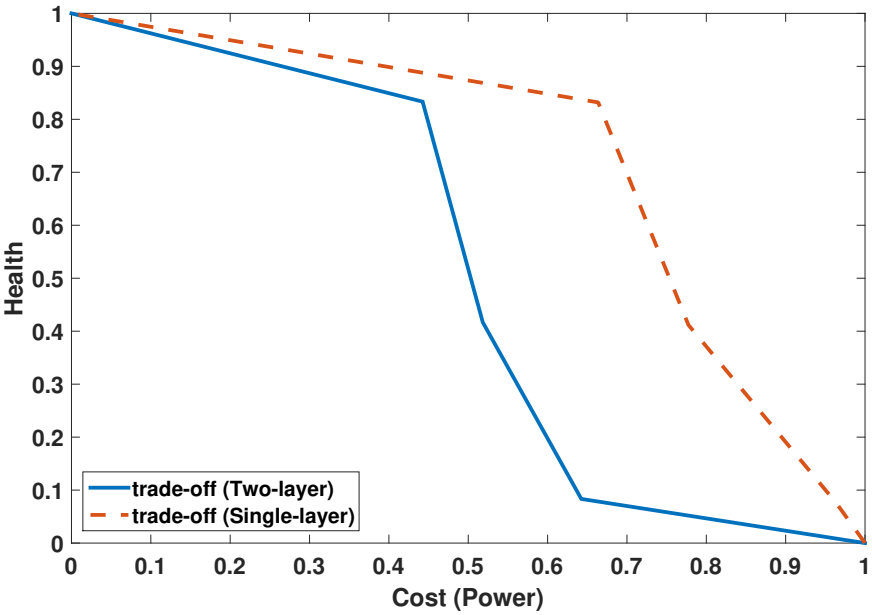

Figura 6.10: Trade-off between the health and cost in the single-layer and two-layer MPC over the normalization.

that independently of the tuning, the two-layer scheme is able to produce better results and it can be observed that the economic objective in single layer is not optimized as in the case of the multi-layer scheme.

6.6 Summary

In this chapter, the integration of MPC with fatigue-based prognosis to minimize the damage of components in a pasteurization plant and the optimization economic objective has been presented. The integration of a system health management module with MPC control has provided the pasteurization plant with a mechanism to operate safely and optimize the trade-off between components lifetime while saving energy, product and time. The MPC controller objective has been modified by adding an extra criterion that takes into account the accumulated damage plus including the economic objective. First, a single-layer health-aware MPC controller based on economic optimization by including integral action to eliminate steady state offset by adding extra criterion has proposed. Then, the single layer has been transformed to multi-layer scheme one taking into account the different dynamics of the objectives. The multi-layer health-aware MPC controller based on two optimization layer has been implemented with different time-scale. Both control schemes have been satisfactorily implemented using high-fidelity simulator of a utility-scale pasteurization plant. The results obtained show that there exists a trade-off between the minimization of the accumulated damage and tracking setpoint that manipulated for saving energy. Finally, these control schemes are compared and the results show that the multi-layer control scheme can minimize the economic cost more than the single layer and keeping the same degradation level for the components.

The content of this chapter was based on the following works:

F. Karimi Pour, V. Puig and C. Ocampo-Martinez. Multi-layer health-aware economic predictive control of a pasteurization pilot plant. *International Journal of Applied Mathematics and Computer Science*,28(1), 97-110), 2018.

F. Karimi Pour, V. Puig and C. Ocampo-Martinez. Health-aware model predictive control of pasteurization plant. *In Journal of Physics: Conference Series*,(Vol. 783, No. 1, p. 012030), 2017.

Capítol 7

Health-aware MPC-LPV based on system Reliability

This chapter addresses economic health-aware MPC-LPV controller for industrial systems; in particular, the economic health-aware model predictive control (MPC) for drinking water transport network, including an additional goal to extend the reliability of the components and system. The components and system reliability are incorporated in the MPC model using a Linear Parameter Varying (LPV) modelling approach. The proposed MPC-LPV control approach described in chapter 4 allows the controller to accommodate the parameter changes. Then, chance-constraint programming is used to compute an optimal water storage volume policy based on a desired risk acceptability level, managing to dynamically designate safety stocks in flow-based networks to satisfy varying flow demands. Finally, the proposed approach is applied to a part of a real drinking water transport network of Barcelona for demonstrating the performance of the method.

7.1 Introduction

Based on 3.2, Drinking Water Networks (DWNs) are critical infrastructures in urban environments. Also, the increasing complexity of the DWNs would generate some complications for the management under multiple objectives, such as economic operations, as well as safety, reliability and sustainability. MPC can provide appropriate techniques to perform the operational control of water systems to develop their performance since it allows to compute optimal control strategies ahead of time for all the flow and pressure control elements [36]. According to optimal control approaches for management water systems, MPC is not applied in a classical way because there is no reference to be tracked. Unlike conventional MPC, the common operational goal of many process industries, as DWNs, is the minimization of economic costs of the energy consumptions. To this aim, Economic MPC (EMPC) contributes a systematic approach for optimizing economic performance [99].

The application of control strategies by considering the system and components reliability becomes necessary to ensure the quality of service. In order to increase the system reliability, anticipate the appearance of faults, actuator health monitoring and reduce the operational costs must be considered. In fact, actuator health monitoring is focused on observing and estimating the safety and reliability of each actuator according to the actuator information. Recently, system reliability has been taken into account in system control process through a Prognosis and Health Management (PHM) framework [96]. In this context, the reliability is a standard procedure for estimating how long the system will perform its function exactly and can be used to predict future damages in the system given the state of its elements [168, 53]. On the other side, from control point of view and according to physical constraints and multi-objective cost functions, the MPC approach has been proved as an adequate strategy for implementing health-aware control (HAC) designs. In the HAC approach, the online prognostic information of the system or component is used to adjust the control actions or to develop the mission objective in order to maintain a high level of system health [97].

DWN reliability depends on several factors such as the quality and the quantity of the water available at the sources, the failure rates of the pumps and the valves failures, among others [102].The actuator reliability is usually modelled using an exponential function of the control input [53, 96]. On the other hand, the system reliability is determined from the combination of each actuator reliability taking into account the interconnection topology. In [164], the reliability analysis methodologies of water distribution systems are described based on tailor-made 'lumped supply–lumped demand' approach and Monte Carlo framework. In [43], a structure is proposed for devising a proactive risk-based integrity-monitoring approach for the control of urban water distribution networks. One significant disadvantage of the previous methods for reliability-based MPC is that they consider the reliability at the actuator level, not at the system level based on the interconnection topology, because of the non-linearity of the resulting constraints which would lead to the non-linear MPC. Moreover, Economic Nonlinear MPC (ENMPC) is usually computationally expensive and, in general, there is no guarantee that the solution of the optimization problem is the global optimum [98]. Another way of solving the optimization problem in case of a nonlinear system is translating the nonlinear problem into a quadratic problem by means of linearization approach. This approach has been recently improved by means of Linear Parameter Varying (LPV) models [30].

The main contribution of this chapter is to provide a health-aware MPC-LPV controller on the basis of PHM information provided by the on-line evaluation of the system reliability. The system reliability is integrated into the control algorithm using a LPV framework. The augmented model considering both the reliability and DWN models is interpreted as an LPV model. Moreover, an additional contribution of the chapter considers the use of chance constraints programming to compute an optimal water storage volume policy based on a desired acceptable risk level, system reliability and presenting the advantage of a given system and component reliability that is computed on-line in an MPC-LPV strategy is another contribution of this chapter. The first objective of this chapter is to present the interest of taking into account system and component reliability,

measured on-line in an MPC-LPV method. The second objective consists in designing a health-aware MPC-LPV strategy in order to formulate an optimization problem that exploits the functional dependency of scheduling variables and state vector. Moreover, using chance constraint programming to manage dynamically designated safety stocks in flow-based networks to satisfy time-varying demands and system reliability.Finally, the case study considered in this chapter to show the effectiveness of the proposed approach is based on a part of the DWN case study described in Chapter 3.

7.2 EMPC Formulation of DWN

In this chapter, the modeling approach based on flow introduced by the authors in [36, 37] is used. The pressure is not considered in this control-oriented model because the pressure is managed at distribution level of water network not transport network. The control-oriented model of DWN is considered as a set of linear discrete-time difference-algebraic equations (3.28).

The purpose of using MPC methods for controlling water distribution networks is to compute, ahead of time, the input commands to obtain the optimal performance of the network based on a set of control objectives [159]. The control objective can be formulated as the minimization of a convex multi-objective cost function that involves three operational goals for managing of DWN with different nature which mentioned in section 3.2.3. The controller should also operate actuators and tanks inside their bounds and extend the reliability of the system as will be presented later. The system is subject to hard input and state constraints provided by convex and closed polytopic sets defined as

$$x(k) \in \mathbb{X} := \{x \in \mathbb{R}^{n_x} | Gx \leq g\}, \tag{7.1a}$$

$$u(k) \in \mathbb{U} := \{u \in \mathbb{R}^{n_u} | Hu \leq h\}, \tag{7.1b}$$

for all $k \in \mathbb{Z}_{\geq 0}$, where $G \in \mathbb{R}^{m_x \times n_x}$, $g \in \mathbb{R}^{m_x}$, $H \in \mathbb{R}^{m_u \times n_u}$ and $h \in \mathbb{R}^{m_u}$ are vectors/matrices collecting the system constraints, signifying $m_u \in \mathbb{Z}_{\geq 0}$ and $m_x \in \mathbb{Z}_{\geq 0}$ the number of input and state constraints, respectively. Concerning the operation of the generalized flow-based networks, the following assumptions are used noticed in this chapter.

Assumption 7.1. *The demands in $d_m(k)$ and the states in $x(k)$ are observable at each time instant $k \in \mathbb{Z}_{\geq 0}$, also the pair (A, B) is stabilisable.*

Assumption 7.2. *The realization of demands at the current time instant $k \in \mathbb{Z}_{\geq 0}$ can be analyzed as*

$$d_m(k) = \overline{d}_m(k) + \widetilde{d}_m(k), \tag{7.2}$$

where $\overline{d}_m$ is the vector of expected disturbances and $\widetilde{d}_m$ is the vector of probabilistic independent forecasting errors with non-stationary uncertainty and a known (or approximated) quasi-concave probability distribution $\mathcal{D}\big(0, \sum(\overline{d}_{m,(j)}(k))\big)$, e.g., logistic, normal, exponential distribution, among others. Hence, the stochastic nature of each j-th row of

$d_m(k)$ is described by $\overline{d}_{m,(j)}(k)\mathcal{D}(j)\big(\overline{d}_{m,(j)}(k), \sum(\widetilde{d}_{m,(j)}(k))\big)$, where $\overline{d}_{m,(j)}(k)$ denotes its mean, and $\sum(\widetilde{d}_{m,(j)}(k))$ its variance.

Considering the network mathematical model (3.28) and three operational goals in the management of DWN that are introduced in subsection 3.2.3, the EMPC controller design is based on minimizing the finite horizon cost

$$J = \sum_{l=0}^{N_p-1} (\ell_e(l|k) + \ell_s(l|k) + \ell_{\Delta u}(l|k)), \tag{7.3}$$

where N_p is the prediction horizon. At each time instant, the optimization problem

$$\min_{\mathbf{u}(k),x(k),\boldsymbol{\xi}(k)} J(\mathbf{u}(k), x(k), \boldsymbol{\xi}(k)), \tag{7.4a}$$

subject to:

$$x(l+1|k) = Ax(l|k) + Bu(l|k) + B_d d_m(l|k),\ l = 0, \cdots, N_p - 1 \tag{7.4b}$$
$$0 = E_u u(l|k) + E_d d_m(k),\ l = 0, \cdots, N_p - 1 \tag{7.4c}$$
$$x(l|k) \geq x_s - \xi(l|k),\ l = 1, \cdots, N_p \tag{7.4d}$$
$$u(l|k) \in \mathbb{U},\ l = 0, \cdots, N_p - 1 \tag{7.4e}$$
$$x(l|k), \in \mathbb{X},\ l = 1, \cdots, N_p \tag{7.4f}$$
$$\xi(l|k) > 0,\ l = 0, \cdots, N_p \tag{7.4g}$$
$$x(0|k) = x(k), \tag{7.4h}$$

is solved online obtaining the optimal sequences $\mathbf{u}^*(k) = \{u(l|k)\}_{l\in\mathbb{Z}_{[0,N_p-1]}}$, $\mathbf{x}^*(k) = \{x(l|k)\}_{l\in\mathbb{Z}_{[1,N_p]}}$ and $\boldsymbol{\xi}^*(k) = \{xi(l|k)\}_{l\in\mathbb{Z}_{[1,N_p]}}$. Constraint (7.4g) is considered to guarantee the slack variable that is a positive value. Moreover, optimization problem is solved based on receding horizon philosophy that explained in chapter 2.

7.3 Chance-constrained Model Predictive Control

The different approaches to reliability analysis with MPC in the literature tend to produce a conservatism of the obtained control policy that effects negatively on the efficiency of the DWNs operation. Furthermore, in real applications, the boundedness assumption of disturbances might not hold, since, constraint violations are inescapable due to unexpected events, faults, etc, may appear. A more realistic qualification of uncertainty is the stochastic paradigm, which manages to produce less conservative control methods by incorporating explicit models of disturbances in the design of control laws and by transforming hard constraints into probabilistic constraints to cope with inevitable uncertainties, a stochastic strategy is a sophisticated theory in the field of optimization, but a revived consideration has been provided to the stochastic programming methods as powerful tools for control design, heading to the stochastic MPC, which has a particular alternative called Chance-Constrained MPC (CC-MPC) [31], a stochastic control

approach that represents robustness in terms of probabilistic(chance) constraints, and requires that the probability of violation of any operational condition or physical constraint is below a designated value. By placing this value suitably, the user/operator can deal with preservation against performance. Related works that address the CC-MPC approach in water systems can be found in [67, 165]. Some economic-oriented controller that respect to the reliability issue has been proposed [73], but without considering reliability at the system level and probabilistic constraints based on the reliability of the system.

If the stochastic nature of disturbances (demands) and reliability of components of the system is not explicitly considered, an optimal solution of (7.4) satisfying all constraints can not be found in real scenarios [173]. Therefore, in order to guarantee feasibility of the optimization problem (7.4), it is appropriate to relax the original constraints that involve stochastic elements with probabilistic statements in the form of *chance constraints*. In this manner, the constraints must be satisfied with predefined risk levels to manage the uncertainty and component reliability of the system. Chance-constrained programming is a technique of stochastic programming dealing with constraints of the general form as

$$\mathbb{P}[\mathrm{f}(v,\zeta) \leq 0] \geq 1 - \delta_{\zeta}, \tag{7.5}$$

where $\mathbb{P}$ indicates the probability operator, $v \in \mathbb{R}^{n_v}$ is the decision vector, $\zeta \in \mathbb{R}^{n_\zeta}$ a random variable and $\mathrm{f} : \mathbb{R}^{n_v} \times \mathbb{R}^{n_\zeta} \longrightarrow \mathbb{R}^{n_c}$ a constraint mapping. The level $\delta_\zeta \in (0,1)$ is user given and defines the preference for safety of the decision v. The constraint (7.5) means that we wish to take a decision v that satisfies the n_c-dimensional random inequality system $\mathrm{f}(v,\zeta) \geq 0$ with high enough probability. As demonstrated in [93], if $\mathrm{f}(.,.)$ is jointly convex in (v,ζ) and $\Phi \triangleq \mathbb{P}[.]$ is quasi-concave, then the feasible set

$$\Psi(\delta_\zeta) \triangleq \{v | \mathbb{P}[\mathrm{f}(v,\zeta) \leq 0] \geq 1 - \delta_\zeta\} \tag{7.6}$$

is convex for all $\delta_\zeta(0,1)$. All chance-constrained models need prior knowledge of the acceptable risk δ_ζ connected with the constraints. A lower risk acceptability proposes a harder constraint. In general, joint chance constraints lack from analytic expressions because they involve multivariate probability distribution [75]. In this chapter, by following the results in [75, 93], a uniform distribution of the joint risk is approximated by upper bounding the joint constraint and assuming a similar distribution of the joint risk amongst a set of *individual chance constraints* are transformed inside equivalent deterministic constraints.

By considering the general joint chance constraint (7.5), and defining $\mathrm{f}(v,\zeta) \triangleq \zeta - Fv$, with $F \in \mathbb{R}^{\zeta \times n_v}$, the additive stochastic element is separable and the following chance constraint is achieved:

$$\mathbb{P}[\zeta \leq Fv] \geq 1 - \delta_\zeta. \tag{7.7}$$

Then, by rewiring $\omega \triangleq Fv$, for any duple (ζ, ω), it follows that

$$\Phi_\zeta(\omega) = \mathbb{P}[\{\zeta_1 \leq \omega_1, ..., \zeta_{n_c} \leq \omega_{n_c}\}]. \tag{7.8}$$

Describing the events $C_i \triangleq \{\zeta_i \leq \omega_i\}, \forall i \in \mathbb{Z}_1^{n_c}$, which it can be assumed the events as faults that occurred in the accouters, it follows:

$$\Phi_\zeta(\omega) = \mathbb{P}[C_i \cap ... \cap C_{n_c}]. \tag{7.9}$$

Indicating the complements of the events C_i by $C_i^c \triangleq \{\zeta_i > \omega_i\}$, and it is obvious from probability theory that

$$C_1 \cap ... \cap C_n = (C_1^c \cup ... \cup C_{n_c}^c)^c, \tag{7.10}$$

and consequently

$$\begin{aligned} \Phi_\zeta(\omega) &= \mathbb{P}[C_i \cap ... \cap C_{n_c}] && \text{(7.11a)} \\ &= \mathbb{P}[(C_1^c \cup ... \cup C_{n_c}^c)^c] && \text{(7.11b)} \\ &= 1 - \mathbb{P}[(C_1^c \cup ... \cup C_{n_c}^c)^c] \leq 1 - \delta_\zeta. && \text{(7.11c)} \end{aligned}$$

By using the union bound, the Boole inequality allows bounding the result in (7.11c), declaring that for a countable set of events, the probability that at least one event occurs is not higher than the sum of the individual probabilities [75], so that

$$\mathbb{P}\Big[\cup_{i=1}^{n_c} C_i\Big] \leq \sum_{i=1}^{n_c} \mathbb{P}[C_i], \tag{7.12}$$

and, by applying (7.12) to 7.11c, it appears that

$$\sum_{i=1}^{n_c} \mathbb{P}[C_i^c] \leq \delta_\zeta \Longleftrightarrow \sum_{i=1}^{n_c} (1 - \mathbb{P}[C_i]) \leq \delta_\zeta. \tag{7.13}$$

Then, a set of constraints rises from previous results as sufficient conditions to enforce the joint chance constraint (7.7), by allotting the joint risk δ_ζ in n_c separate risks $\delta_{\zeta,i}, i \in \mathbb{Z}_i^{n_c}$. These constraints are described as follows

$$\begin{aligned} &\mathbb{P}[C_i] \geq 1 - \delta_{\zeta,i}, \qquad \forall i \in \mathbb{Z}_1^{n_c} && \text{(7.14a)} \\ &\sum_{i=1}^{n_c} \delta_{\zeta,i} \leq \delta_\zeta, && \text{(7.14b)} \\ &0 \leq \delta_{\zeta,i} \leq 1, && \text{(7.14c)} \end{aligned}$$

where (7.14a) produces the set of n_c effective individual chance constraints, which bounds the possibility that each inequality of the receding horizon problem maybe declines. Moreover, (7.14b) and (7.14c) are conditions forced to bound the new single risks in such a way that the joint risk bound is not breached. Each solution that satisfies the aforesaid constraints is guaranteed to provide (7.7).

Since the satisfaction of each individual constraint is an event $C_i, \forall i \in \mathbb{Z}_i^{n_c}$, a joint chance constraint requires that the connection of all the individual constraints is satisfied with the desired probability level such as:

$$\mathbb{P}\Big[\cap_{i=1}^{n_c} C_i\Big] \geq 1 - \delta_\zeta. \tag{7.15}$$

Considering that each individual constraint is probabilistically dependent, the level of conservatism can be derived by using the inclusion-exclusion principle for the union of finite events,$C_i, \forall i \in \mathbb{Z}_1^{n_c}$, which proves the following equality:

$$\begin{aligned}\mathbb{P}\Big[\cup_{i=1}^{n_c} C_i\Big] = &\sum_{i=1}^{n_c}\mathbb{P}[C_i] - \sum_{1\le i<j\le n_c}\mathbb{P}\Big[C_i\cap C_j\Big] \\ &+ \sum_{1\le i<j<k\le n_c}\mathbb{P}\Big[C_i\cap C_j\cap C_k\Big] - ... + (-1)^{n_c-1}\mathbb{P}\Big[\cap_{i=1}^{n_c} C_i\Big].\end{aligned} \tag{7.16}$$

It should be noted that, by introducing the event as a fault in the actuator, it can be observed (7.16) has similar as formulation as the one used for evaluating the system reliability based on the component reliability.

In a DWN, the constraints come from the model (7.4b)-(7.4d) that can be formulated as chance constraints statements taking into account the probabilities associated to the component reliability. Considering only faults in actuators, the reliability of the system is related to the system inputs $u_i(k)$. Hence, (7.5) can be formulated in case of the actuators as follows

$$\mathbb{P}[\mathrm{f}(u_i(k), \zeta_i(k)) \le 0] \ge 1 - \delta_{\zeta_i}, \tag{7.17}$$

where $\zeta(k) \in \{1, 0\}$ is input variable which considers if the actuator is one of two states $\{Available, Unavailable\}$ (or $\{1, 0\}$) defined as follows:

$$\zeta_i(k) = \begin{cases} 1, & R_i(k) \neq 0\ , \\ 0, & R_i(k) = 0, \end{cases} \tag{7.18}$$

where $R_i(k)$ is the reliability for each actuator. In case that $\zeta_i(k) = 1$ the input $u_i(k)$ associated to the i-th actuator is bounded by (7.1), otherwise an additional constraint setting $u_i(k)$ should be included. Furthermore, to determine the reliability associated to the system that associates a probability to the system model constraint (3.28), the joint-chance constraint probability calculation (7.16) should be used leading to the following probabilistic formulation for the MPC optimization problem (7.4)

$$\min_{\mathbf{u}(k),\mathbf{x}(k),\boldsymbol{\xi}(k)} J(\mathbf{u}(k), \mathbf{x}(k), \boldsymbol{\xi}(k)), \tag{7.19a}$$

subject to:

$$\mathbb{P}\Big[Ax(l|k) + B(\zeta_i)u(l|k) + B_d d_m(l|k), \tag{7.19b}$$

$$E_u(\zeta_i)u(l|k) + E_d d_m(k)\Big] \ge 1 - \delta, \quad l = 0, \cdots, N_p - 1 \tag{7.19c}$$

$$x(l|k) \ge x_s - \xi(l|k),\ l = 1, \cdots, N_p \tag{7.19d}$$

$$u(l|k) \in \mathbb{U},\ l = 0, \cdots, N_p - 1 \tag{7.19e}$$

$$x(l|k), \in \mathbb{X},\ l = 1, \cdots, N_p \tag{7.19f}$$

$$\xi(l|k) \ge 0,\ l = 0, \cdots, N_p \tag{7.19g}$$

$$x(0|k) = x(k). \tag{7.19h}$$

In this case, (7.19) depends on the probability distribution involved in the chance constraints. The main difficulty in solving this stochastic problem lies in computing the multivariate integration of the density function of the uncertain variables. In this chapter, the stochastic process of disturbances is addressed analytically and an uncertainty description given by a multivariate Gaussian distribution is chosen to use its properties and reformulate the chance constraints into a set of deterministic equivalents. The satisfaction of the probabilities of (7.19b) is associated with the reliability of the actuator and whole of the system. Hence, to evaluate these probabilities we can introduce the reliability of each actuator and the system in the model and guaranty the reliability of the model.

7.4 Reliability Assessment

7.4.1 Failure Rate and Reliability Concept

As mentioned before, the reliability is the ability of a system or component to perform its expected functions and it is described as Definition 2.2. Moreover, the definition of unreliability of actuators or a system is presented as Definition 2.3.

Many different functions have been accepted to describe the reliability functions of time. Some of the more general reliability functions consist the log-normal, exponential and Weibull distributions [89, 104]. In this chapter, the exponential distribution is used for modelling the component failure rate. In particular, engineering systems are organized to sustain varying amounts of loads where they can be expressed in terms of usage rate or occupied period. Revising the literature, it has been established that the function load strongly affects the component failure rate [100]. Therefore, it is necessary to consider the load versus failure rate relation when considering system reliability evaluation. In this work, failure rates are determined from actuators under different levels of load according to the applied control input. One of the commonly used relations is based on assuming that actuator fault rates vary with the load by the following exponential law

$$\lambda_i = \lambda_i^0 exp\Big(\beta_i u_i(t)\Big), \qquad i = 1, 2, ..., m. \tag{7.20}$$

where λ_i^0 indicates the baseline failure rate (nominal failure rate) and $u_i(t)$ is the control action at time t for the i^{th} actuator. β_i is a constant parameter that depends on the actuator characteristics.

In the useful period of life, elements can be characterized at a given time t by a baseline reliability measure $R_0(t)$. Then, $R_{0,i}(t)$ will denote the reliability of the i-th actuator obtained under nominal operating conditions

$$R_{0,i}(t) = exp\big(-\lambda_i^0 t\big), \qquad i = 1, 2, ..., m. \tag{7.21}$$

Hence, the component reliability of a system with the i-th component can be computed

by applying the exponential function and the baseline reliability level $R_{0,j}$ as follows

$$R_i(t) = R_{0,i}\ exp\Big(- \int_0^t \lambda_i(s)\ ds \Big), \qquad i = 1, 2, ..., m \tag{7.22}$$

In discrete-time, it can be rewritten as

$$R_i(k+1) = R_{0,i}(k)\ exp\Big(- T_s \sum_{s=0}^{k+1} \lambda_i(s) \Big), \qquad i = 1, 2, ..., m \tag{7.23}$$

where $\lambda_i(s)$ is the failure rate that is obtained from the i-th component under different levels of load and T_s is the sampling time.

7.4.2 Overall Reliability

The lifetime of a system can be quantified by the overall system reliability, denoted as $R_G(k)$. The overall system reliability is computed based on the reliabilities of elementary components (or subsystems). Therefore, $R_G(k)$ depends on the actuators' configuration which can generally be obtained from series and/or parallel combinations of subsystems (or components) [14]. However, there are some systems that do not follow the series, parallel or combination of series and parallel structures. To deal with the more general situation, a graph network model can be used in which it is possible to determine whether the system is working correctly by determining existance of a successful path in the system. A path for the graph network is a set of components, such that if all the components in the set are successful, the system will be successful. A minimal path P_s is a set of components that belongs to it, but the removal of any one component will generate the resulting set not to be a path [14]. Then, the overall system reliability $R_G(k)$ can be computed as

$$R_G(k) = 1 - \prod_{j=1}^{s} \Big(1 - \prod_{i \in P_{s,j}} R_i(k) \Big), \tag{7.24}$$

where $j = 1, .., s$ is minimal paths number. As mentioned above, there is indirect relationship between conservatism of probability and the overall system reliability. In fact, the formula obtained for overall reliability system (7.24) is consistent with the (7.16).

7.4.3 System Reliability Modeling

For the purpose of integrating the reliability function in the MPC model as a new state variable, a conversion is needed that allows to compute reliability in a linear-like form. The proposed transformation is based on applying the logarithm (7.24). As stated in (2.20), the (7.24) can be rewritten as

$$\log(Q_G(k)) = \log \Big(\prod_{j=1}^{s} \Big(1 - \prod_{i \in p_{s,j}} R_i(k) \Big) \Big), \tag{7.25}$$

and by introducing a change of variable

$$z_j(k) = 1 - \prod_{i \in p_{s,j}} R_i(k), \tag{7.26}$$

equation (7.25) leads to

$$\log(Q_G(k)) = \sum_{i \in p_{s,j}}^{s} \log(z_j(k)). \tag{7.27}$$

According to (7.26), the $\log(z_j(k))$ can be obtained as

$$\log(z_j(k)) = \frac{\log(z_j(k))}{\log(1 - z_j(k))} \sum_{i \in p_{s,j}} \log R_i(k). \tag{7.28}$$

Then, by renaming $\beta_j(k) = \frac{\log(z_j(k))}{\log(1-z_j(k))}$ in (7.28), (7.25) can be rewriten as

$$\log(Q_G(k)) = \sum_{i \in p_{s,j}}^{s} \beta_j(k) \sum_{i \in p_{s,j}} \log R_i(k). \tag{7.29}$$

Finally, the system unreliability can be estimated from the baseline system unreliability as follows:

$$\log(Q_G(k+1)) = \log(Q_G(k)) + \sum_{i \in p_{s,j}}^{s} \beta_j(k) \sum_{i \in p_{s,j}} \log R_i(k). \tag{7.30}$$

7.5 Economic health-aware MPC-LPV

7.5.1 General approach of economic health-aware MPC-LPV

This section presents the incorporation of reliability information in the predictive control law as a new state of the model. As mentioned in Section 7.4, the reliability of the DWN can be estimated using the control input (actuator commands) information. In order to include a new objective in the MPC that proposes to extend the system reliability, the reliability model is represented by means of the model (7.30). In fact, the new control model of DWN that includes the reliability and dynamic model of DWN is obtained based on the structure shown in Figure 7.1. Actually, there is a direct relationship between the dynamic model of DWN and its system reliability.

Thus, the new MPC model has the following structure

$$\begin{aligned} x_r(k+1) &= A_r x_r(k) + B_r u(k) + B_{r,d} d_m(k), \\ y_r(k) &= C_r x_r(k), \end{aligned} \tag{7.31}$$

where the state and output vector are given by $x_r = [x, \log(Q_G), \log(R_1), ..., \log(R_i)]^T$ and $y_r = [y, \log(Q_G)]^T$, respectively. The new matrices are defined as

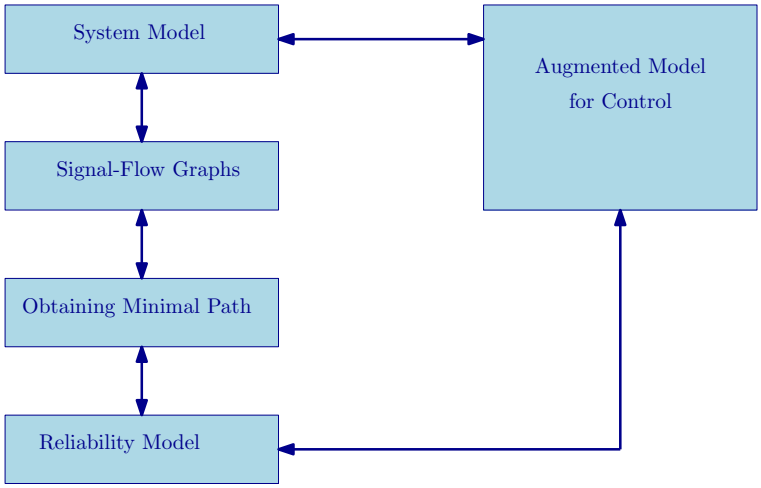

Figura 7.1: Digram of the new proposed control model approach.

$$A_r = \left[\begin{array}{c|c} A & 0_{n_x \times n_{i+1}} \\ \hline 0_{1\times n_x} & 1 \quad \sum_{i\in p_{s,j}}^{s} \beta_j(k) \\ \hline 0_{n_i \times n_x} & I_{n_i \times n_i} \end{array}\right], \qquad B_r = \left[\begin{array}{c} B_{n_u \times n_u} \\ \hline 0 \\ \hline -\lambda_i \times I_{n_i \times n_i} \end{array}\right],$$

$$B_{d,r} = \left[\begin{array}{c} B_{d,n_u \times n_u} \\ \hline 0_{n_{i+1} \times n_{B_d}} \end{array}\right], \qquad C_r = \left[\begin{array}{ccccc} C & 0 & 0 & \cdots & 0 \\ 0 & 1 & 0 & \cdots & 0 \end{array}\right]. \tag{7.32}$$

Therefore, the new MPC model (7.31) can be viewed as an LPV model that has as scheduling variable the control action $u_i(k)$ related to each state and actuator. The new MPC model (7.31) cannot be estimated before solving the optimization problem (7.4) since the future state sequence is not identified. In fact, $x(l|k)$ depends on the future control inputs $u(k)$ and scheduling parameters, where for general LPV models are not expected to be known but only to be measurable online at current time k. The idea is to obtain a solution to the problem (7.4) by solving an online optimization problem as a QP problem. The solution for this problem is to modify the exact MPC-LPV to a linear approximation of the MPC-LPV. This approximation uses an estimation of scheduling

variables, $\hat{\theta}$ instead of applying θ. Indeed, the scheduling variables in the prediction horizon are determined and used to update the matrices of the model adopted by the MPC controller. In fact, the same approach in chapter 4 is applied in this chapter for solving this problem. Hence, based on the optimal control sequence $\mathbf{u}(\mathbf{k})$, the sequence of states and predicted parameters may be obtained.

$$\mathbf{X}(k) = \begin{bmatrix} x(l+1|k) \\ x(l+2|k) \\ \vdots \\ x(N_p|k) \end{bmatrix} \in \mathbb{R}^{N_p,n_x}, \quad \Theta(k) = \begin{bmatrix} \hat{\theta}(l|k) \\ \hat{\theta}(l+1|k) \\ \vdots \\ \hat{\theta}(N_p-1|k) \end{bmatrix} \in \mathbb{R}^{N_p,n_\theta}. \tag{7.33}$$

Therefore, with slight abuse of notation f can be defined as: $\Theta(k) = f([x^T(k) \quad \mathbf{X}^T(k)], \mathbf{u}(k))$. The vector $\Theta(k)$ includes parameters from time k to $k+N_p-1$ whilst the state prediction is accomplished for time $k+1$ to $k+N_p$.

Hence, by using the definitions (7.33), the predicted states can be simply formulated as follows

$$\mathbf{X}(k) = \mathcal{A}(\Theta(k))x(k) + \mathcal{B}(\Theta(k))\mathbf{u}(k) + B_{r,d}d_m(k), \tag{7.34}$$

where $\mathcal{A} \in \mathbb{R}^{n_x \times n_x}$ and $\mathcal{B} \in \mathbb{R}^{n_x \times n_u}$ are given by (4.9) and (4.10).

By using (7.34) and augmented block diagonal weighting matrices $\tilde{w_1} = diag_{N_p}(w_1)$ and $\tilde{w_2} = diag_{N_p}(w_2)$, the cost function (7.3), with new additional objective to maximize the system reliability, can be rewritten in vector form as

$$\min_{\mathbf{u}(k),\boldsymbol{\xi}(k),\log Q_G(k)} \sum_{l=0}^{N_p} [\ell_e(l|k) + \ell_s(l|k) + \ell_{\Delta u}(l|k) - \ell_{Rg}(l|k)], \tag{7.35a}$$

subject to:

$$\mathbf{X}(k) = \mathcal{A}(\Theta(k))x(k) + \mathcal{B}(\Theta(k))\mathbf{u}(k) + B_{r,d}d_m(k), \tag{7.35b}$$
$$0 = E_u u(l|k) + E_d d_m(k), \tag{7.35c}$$
$$x(l+1|k) \geq x_s - \xi(l|k) \tag{7.35d}$$
$$\log Q_G(l+1|k) = \tilde{\mathbf{x}}_{nx+1}(l|k) \tag{7.35e}$$
$$u(l|k) \in \mathbb{U}, \ l = 0, \cdots, N_p - 1 \tag{7.35f}$$
$$x(l|k), \in \mathbb{X}, \ l = 1, \cdots, N_p \tag{7.35g}$$
$$\xi(l|k) \geq 0, \ l = 0, \cdots, N_p \tag{7.35h}$$
$$x(0|k) = x(k), \tag{7.35i}$$

where $\ell_{Rg}(k) \triangleq \log Q_G^\top w_3 \log Q_G$ is an additional objective with the corresponding weight w_3 into the EMPC-LPV cost function to maximize the system reliability. Since the predicted states $\Theta(k)$ in (7.34) are linear in control inputs $\mathbf{u}(k)$, the optimization problem can be solved as a QP problem, that is significantly further easier than solving a general nonlinear optimization problem.

7.5.2 Enhancing system reliability using chance constraints

Because of the stochastic nature of water demands, the DWN prediction model includes exogenous additive uncertainties. Therefore, the fulfillment of constraints for a given control input cannot be ensured. Hence, it is relevant to substitute the original constraints that include stochastic elements (7.1), by probabilistic statements in the frame of chance constraints (7.5). Regarding the Section 7.3 and the form of state constraint set $\mathbb{X}$, two types of chance constraints are existed. The form of a state joint chance constraint is described as

$$\mathbb{P}[G(r)x \leq g(r), \forall r \in \mathbb{Z}_{[1,m_x]}] \geq 1 - \delta_x, \tag{7.36}$$

where $\delta_x \in (0,1)$ is the risk acceptability level of constraint violation for the states, $G(r)$ and $g(r)$ indicate the rth row of G and g, respectively. This entails that all rows r have to be jointly satisfied with the probability $1 - \delta_x$. Also, the form of a state individual chance constraint is described as

$$\mathbb{P}[G(r)x \leq g(r)] \geq 1 - \delta_x, \qquad \forall r \in \mathbb{Z}_{[1,m_x]} \tag{7.37}$$

which requires that each rth row of the inequality has to be satisfied individually with the respective probability $1 - \delta_{x,r}$, where $\delta_{x,j} \in (0,1)$. Then, according to (7.14), the state constraints can be described as follows:

$$\mathbb{P}[G(r)x \leq g(r)] \geq 1 - \delta_{x,r}, \qquad \forall r \in \mathbb{Z}_{[1,m_x]} \tag{7.38a}$$

$$\sum_{r=1}^{m_x} \delta_{x,r} \leq \delta_x, \tag{7.38b}$$

$$0 \leq \delta_{x,r} \leq 1, \tag{7.38c}$$

and, as recommended in [154], specifying a constant and equal value of risk to each individual constraint, that is $\delta_{x,r} = \delta_x / m_x$ for all $r \in \mathbb{Z}_{[1,m_x]}$, then (7.38b) and (7.38c) are fulfilled.

By considering a known (or approximated) quasi-concave probabilistic distribution function for the efficacy of the stochastic disturbance in the dynamic model (3.28), it can follow that

$$\begin{aligned} \mathbb{P}[G(r)x(k+1) \leq g(r)] \geq 1 - \delta_{x,r} &\Leftrightarrow F_{G(r)B_d d_m(k)}(g(r) - G(r)(Ax(k) + Bu(k))) \geq 1 - \delta_{x,r} \\ &\Leftrightarrow G(r)(Ax(k) + Bu(k)) \leq g(r) - F^{-1}_{G(r)B_d d_m(k)}(1 - \delta_{x,r}), \end{aligned} \tag{7.39}$$

for all $r \in \mathbb{Z}_{[1,m_x]}$, where $F_{G(r)B_d d_m(k)}(.)$ and $F^{-1}_{G(r)B_d d_m(k)}(.)$ are the cumulative distribution and the left-quantile function of $G(r)B_d d_m(k)$, respectively. In order to guarantee a safety stock at each storage node of a flow-based network for decreasing the probability of stock-outs due to possible uncertainties in the network, a chance constraint strategy may be used. In this way, according to the (7.38a), the safety stocks are optimally assigned and designed by the constraint back-off effect caused by the term $F_{G(r)B_d d_m(k)}(1 - \delta_{x,r})$ in (7.36). Therefore, the original state constraint set $\mathbb{X}$ is adjusted by the effect of the

m_x deterministic equivalents in (7.39) and substituted by the stochastic feasibility set provided by

$$\begin{aligned}\mathbb{X}_s(k) :=& \{x(k) \in \mathbb{R}^{n_x} | \exists\ u(k) \in \mathbb{U}, \text{such that} \\ & G(r)(Ax(k) + Bu(k)) \leq g(r) - F^{-1}_{G(r)B_d d_m(k)}(1 - \delta_{x,r}) \quad \forall r \in \mathbb{Z}_{1,m_x} \\ & \text{and} \quad E_u u(k) + E_d \bar{d}(k) = 0\},\end{aligned} \tag{7.40}$$

where $\bar{d}(k) = \mathbb{E}[d_m]$ is the first moment of d_m for all $k \in \mathbb{Z}_{0\geq 0}$. The set $\mathbb{X}_s(k)$ is convex when non-empty for all $\delta_{x,r} \in (0, 1)$ in most distribution function, due to the convexity of $G(r)x(k + 1) \leq g(r)$ and the log-concavity assumption of the distribution. For some particular distributions, e.g., Gaussian, convexity is preserved for $\delta_{x,r} \in (0, 0.5]$ [75].

According to section 7.4, component and system reliability can be computed and maximized in the EMPC controller as states in the control model. Besides, (7.40) provides a new constraint set according to the deterministic equivalents in (7.39). However, (7.40) does not consider the states related to the component and system reliability of system hence, it is appropriate to adjust the constraint set (7.40) with probabilistic statements based on the component and system reliability states. Therefore, the system reliability is considered to be ruled by the probabilistic constraints.

In this way, according to general consent of chance constraints (7.5), (7.8) and (7.31) that it shows the system reliability is included in the state, the constraint set based on system reliability state by using the probabilistic statement can be proposed as:

$$x_{Rg}(k) \in \{x_{Rg} \in \mathbb{R}^{n_R} | \mathbb{P}[G_{Rg} x_{Rg} \geq g_{Rg}] \geq (1 - \delta_{Rg})\} \tag{7.41}$$

where $x_{Rg}(k) \in \mathbb{R}^{n_{Rg}}$ is system reliability state, $\delta_{Rg} \in (0, 1)$ is the risk acceptability level of constraint violation for the state. According to the above discussion and the effect of stochastic reliability in the model (7.31), (7.41) can be rewritten as follows

$$\begin{aligned}\mathbb{P}[G_{Rg} x_{Rg}(k + 1) \geq g_{Rg}] \geq (1 - \delta_{Rg}) &\Leftrightarrow F_{G_{Rg}\eta}(g_{Rg} - G_{Rg} x_{Rg}(k + 1)) \geq 1 - \delta_{Rg} \\ &\Leftrightarrow G_{Rg} x_{Rg}(k + 1) \geq g_{Rg} + F^{-1}_{G_{Rg}\eta}(1 - \delta_{Rg}),\end{aligned} \tag{7.42}$$

where η is a random vector whose components lie in a normal distribution, $F_{G_{Rg}\eta}(.)$ and $F^{-1}_{G_{Rg}\eta}(.)$ are the cumulative distribution and the left-quantile functions involved in the state and actuator-health deterministic equivalent constraints, respectively. The deficiency of reliability in the system can cause that the actuator operation compromise the network supply service, unless demands are reachable from other redundant flow paths or a fault-tolerant mechanism is activated. Hence, a preventive strategy can be performed to increase overall system reliability by guaranteeing that the system reliability at each time instant to remain above a safe threshold until a predefined maintenance horizon is reached. Thereupon, the probabilistic constraint (7.42) can be formulated in the predictive controller as

$$G_{Rg} x_{Rg}(k + N_p|k) \geq g_{Rg}(k) + F^{-1}_{G_{Rg}\eta}(1 - \delta_{Rg}), \tag{7.43a}$$

$$g_{Rg}(k) = x_{Rg,\,\min}(k) := x_{Rg}(k) + N_p \frac{R_{\text{tresh}} - x_{Rg}(k)}{k_M + N_p + k}, \tag{7.43b}$$

where $x_{Rg,\,\min}(k) \in \mathbb{R}^{n_{Rg}}$ is the vector of minimum reliability of the system allowed for time instant k and $R_{\text{tresh}} \in \mathbb{R}^{n_{Rg}}$ is the vector of threshold for the terminal system reliability at a maintenance horizon $k_M \in \mathbb{Z}_{\geq 0}$. The right-hand side of (7.43b) is an identical restriction of the remaining allowable system reliability ($R_{\text{tresh}} - x_{Rg}(k)$), that is updated at each time step, according to the applied control actions and guarantees that $x_{Rg}(k) \geq R_{\text{tresh}}$ for $k = k_M$.

Chance-constraints health-aware EMPC-LPV reformulation

First, the inclusion of system reliability in the control law as an additional state of the control model and discussing about how to use the probabilistic statements for state and especially reliability constraints and enforcing them to deterministic equivalent constraints. Next, the setting of the proposed economic health-aware MPC-LPV controller including deterministic equivalent constraints is shown, which consolidates into its optimization problem both the dynamic safety stocks and the system reliability theory, in order to improve the flow supply service level in a given network, handling demands uncertainty and equipment damage.

In this way, for a given sequence of demands d, predicted system reliability, acceptable risk levels δ_x and δ_{Rg}, the optimization problem associated with the deterministic equivalent for selected application at each time step k is expressed as follows:

$$\min_{\mathbf{u}(k),\boldsymbol{\xi}(k),\mathbf{x}(k)\mathbf{x_{Rg}}(k)} \sum_{k=0}^{N_p} [\ell_e(k) + \ell_s(k) + \ell_{\Delta u}(k) - \ell_{Rg}(k)], \tag{7.44a}$$

subject to:

$$\mathbf{X}(k) = \mathcal{A}(\Theta(k))x(k) + \mathcal{B}(\Theta(k))\mathbf{u}(k) + B_{r,d}d_m(k), \tag{7.44b}$$
$$0 = E_u u(l|k) + E_d d_m(k), \tag{7.44c}$$
$$x(r)(k+l+1|k) \leq x_{\max}(r) - \Phi^x_{k,r}(\delta_x), \tag{7.44d}$$
$$x(r)(k+l+1|k) \geq x_{\min}(r) + \Phi^x_{k,r}(\delta_x) \tag{7.44e}$$
$$G_{Rg}x_{Rg}(k+N_p|k) \geq x_{Rg,\,\min}(k) + \Phi^{x_{Rg}}_{k,\eta}(\delta_{Rg}), \tag{7.44f}$$
$$x(k+l+1|k) \geq x_s - \xi(k+l|k), \tag{7.44g}$$
$$\xi(k+l|k) \geq 0, \tag{7.44h}$$
$$x_{Rg}(l+1|k) = \tilde{\mathbf{x}_4}(k), \tag{7.44i}$$
$$u(k), u_{k+1}, ..., u_{k+N_p-1} \in \mathbb{U}, \tag{7.44j}$$
$$x(k|k), \bar{d}_m(k|k)) = (x(k), d_m(k)), \tag{7.44k}$$

for all $l \in \mathbb{Z}_{[0,N_p-1]}$ and all $r \in \mathbb{Z}_{[0,m_r]}$, where the terms $\Phi^x_{k,r}(\delta_x) = F^{-1}_{G(r)B_d d_m(k)}\big(1 - \frac{\delta_x}{n_x N_p}\big)$ and $\Phi^{x_{Rg}}_{k,\eta}(\delta_{Rg}) = F^{-1}_{G_{Rg}\eta}\big(1 - \frac{\delta_x}{N_p}\big)$ are the quantile functions involved in the states and system reliability deterministic equivalent constraints.

7.6 Application to the water network case study

In this section, two motivational examples are used to assess the implementation of the proposed economic health-aware MPC-LPV based on system reliability assessment using the water network case study described in details in Chapter 3. For both part, results were obtained using a 2.4 GHz and 12.00 Gb RAM Intel(R) Core(TM)i7-5500 CPU. Matlab and Yalmip toolbox were used to perform the simulations.

7.6.1 Water transport Network (3-Tanks)

In the first example, the proposed study concentrates on a small network based on the DWN case study. Two sources of water and four demand sector which is represented the district metered area (DMA), are considered (see Figure 7.2). It is assumed that the demand forecast (d_m) at each demand sector is known and that every single source can provide this water demand (Figure 7.3). First, system components must be identified. In this case, there are 3 pumps, 3 valves, 2 sources, 3 tanks, 2 intersection nodes, and several pipes. Afterwards, according the definition of minimal path P_s in subsection 7.4.2 the minimal path sets is determined for the water network, while the P_s is determined based on the relation and the possible connection between the each source and demand sector. By considering all the paths from all the sources to the demand sector, the combination of all flow paths should follow the functional requirements necessary to satisfy the consumer demands. A minimal path set is composed by those elements which allow a flow path between sources and demand sector, such as pipes, tanks, pumps and valves. Based on this analysis, the following list of each minimal paths is presented in Table 7.1. There are five minimal path sets in the system of Figure 7.2. The reliability of each minimal path set depends on the reliability of its components. Tanks and pipes are supposed to be perfectly reliable. However, sources are involved in the minimal path

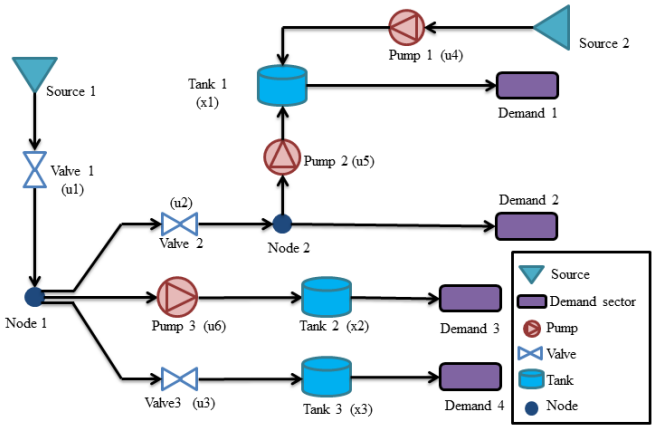

Figura 7.2: Drinking water network diagram (Three-tanks).

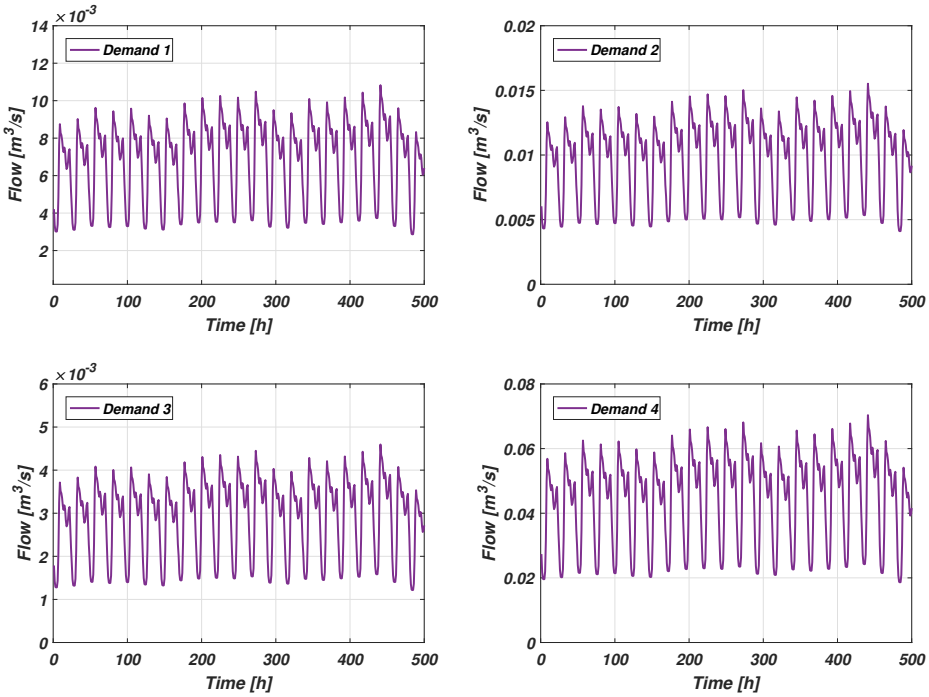

Figura 7.3: Drinking water demand for the three tanks example.

sets only for illustrative purposes of the proposed procedure. Table 7.2 provides the simulation parameters used.

Figure 7.4 shows the evolution of the valves and pumps behaviors that were obtained using the new approach of the health-aware MPC-LPV in the three tanks example with and without the health-aware objective. As it can be seen in Figure 7.4, the behaviour of

Taula 7.1: Success minimal paths of the water transport network of Barcelona (3-Tanks) .

Path	Component Set
P_1	$\{Source1,\ Valve1,\ Valve3,\ Demand4\}$
P_2	$\{Source1,\ Valve1,\ Pump3,\ Demand3\}$
P_3	$\{Source1,\ Valve1,\ Valve2,\ Demand2\}$
P_4	$\{Source1,\ Valve1,\ Valve2,\ Pump2,\ Demand1\}$
P_5	$\{Source2,\ Pump1,\ Demand1\}$

Taula 7.2: Simulation parameters.

Parameter	Value									
Np	24									
$T_s[h]$	1									
$T_m[h]$	200									
α_1	α_1	α_2	α_3	α_4	α_5	α_6				
	0.123	0	0	0.054	0	0				
u_{min} $[m^3/s]$	u_1	u_2	u_3	u_4	u_5	u_6				
	0	0	0	0	0	0				
u_{max} $[m^3/s]$	u_1	u_2	u_3	u_4	u_5	u_6				
	1.297	0.05	0.12	0.015	0.0317	0.022				
$\lambda_0[h^{-1} \times h^{-4}]$	λ_1	λ_2	λ_3	λ_4	λ_5	λ_6				
	1.2	3.45	6.3	9.5	1	1				
x_{min} $[m^3]$	x_1	x_2	x_3	x_4	x_5	x_6	x_7	x_8	x_9	x_{10}
	0	0	0	0	0	0	0	0	0	0
x_{max} $[m^3]$	x_1	x_2	x_3	x_4	x_5	x_6	x_7	x_8	x_9	x_{10}
	470	960	3100	1	1	1	1	1	1	1
x_0 $[m^3]$	x_1	x_2	x_3	x_4	x_5	x_6	x_7	x_8	x_9	x_{10}
	0.75	0.62	0.34	0	1	1	1	1	1	1

control actions that related to the valves is different from the pumps actuators. However, in all of them, the behaviours of control actions in both scenarios are almost the same. Considering the health-aware objective does not significantly affect the behaviour of the valves and pumps. The comparison of the volume evolution of three tanks based on the health-aware MPC-LPV with and without the health-aware objective is presented in Figure 7.5. The safety volumes of the tanks are satisfied hence, the pressure of the network may be guaranteed, subsequently ensuring the hydraulic performance. The system reliability prediction of the DWN that is obtained when using proposed controller with and without the health-aware objective is presented in Figure 7.6. According to these results, it can be observed that with the use of health-aware objective in the MPC, the network reliability is better preserved compared to the case that the reliability is not considered in the MPC objectives. However, the responses of water tanks are similar in both scenarios. The trade-off between the decreasing operating cost and increasing system reliability can be observed in Figure 7.6. Note that the differences in the amount of the operational cost using the proposed approach is similar to the EMPC controller without reliability objective. Figure 7.6 shows that the system reliability is increased from 0.9071 to 0.9891 and that is about 9.06% of improvement, while the accumulated cost is increased from 114.6 to 116.7 that is about 1.74% of increment.

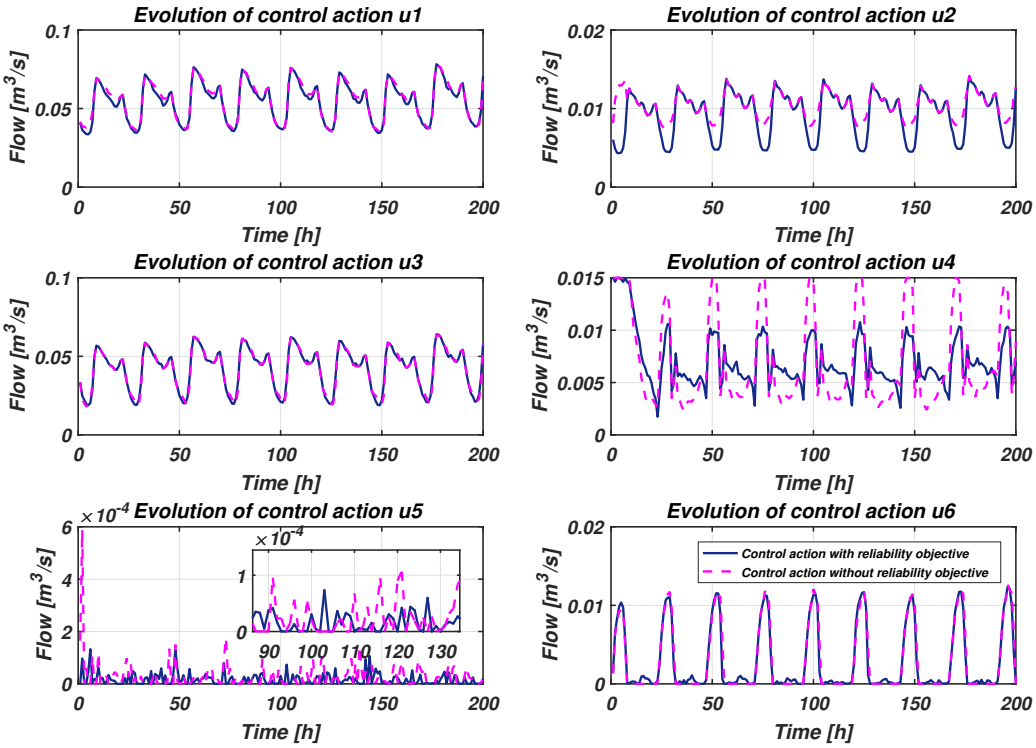

Figura 7.4: Evaluation of the control actions results of 3-tanks.

7.6.2 Chance-constraints health-aware EMPC-LPV for water transport network of Barcelona (17-Tanks)

Now, a more complex and realistic example also based on the DWN case study is considered as a case study. This case includes 17 tanks and 9 sources, consisting of five underground and four surface sources, which currently provide an inflow of about 2 m^3/s. The case study also includes 61 actuators (valves and pumps), 12 nodes and 25 demands. Figure 7.7 presents the general topology of the network, showing a complex system in terms of its elements and the relationships and connections between them. Figure 7.8 presents the graph obtained from this network; the nodes correspond to reservoirs or pipe merging/splitting nodes and the arcs correspond to actuators (pumps and valves).The graph of the water network is obtained from the state space representation of the system where this approach are explained with more detail in [203].

As in the previous example, demand sectors, sources, pipelines and tanks are considered perfectly reliable whereas actuators are not [218]. Moreover, it is expected that the demand forecast (d_m) at each demand sectors is known and that every single source

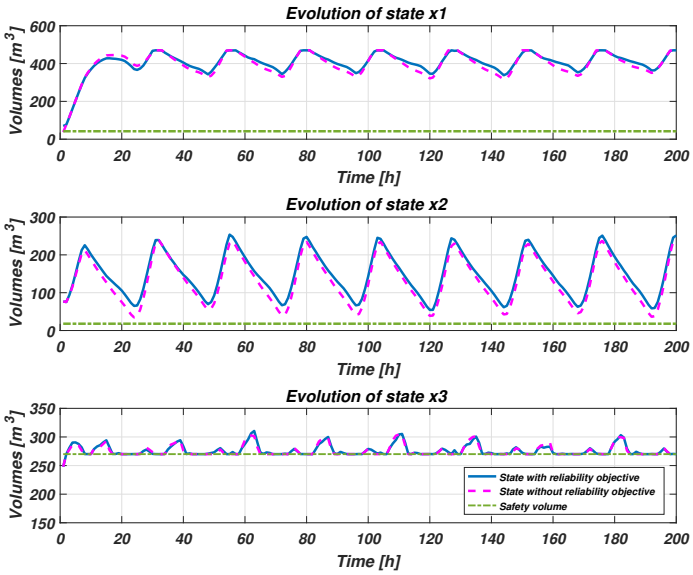

Figura 7.5: Results of the evolutions of storage tanks for 3-tanks.

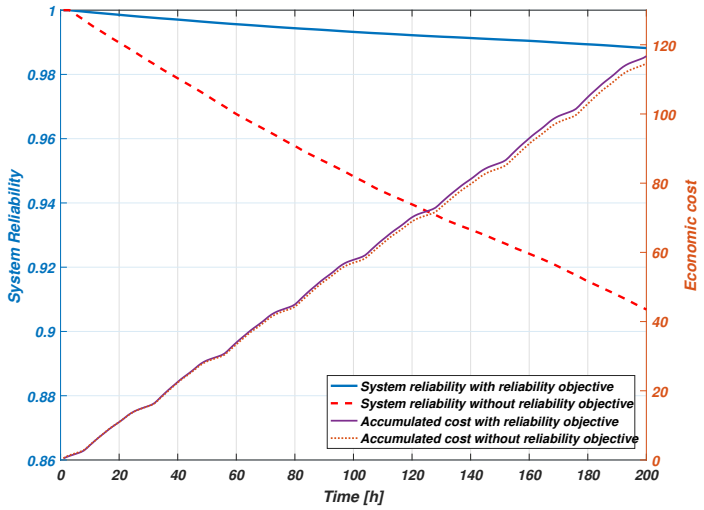

Figura 7.6: Evaluation of system reliability and accumulated economic cost for 3-tanks.

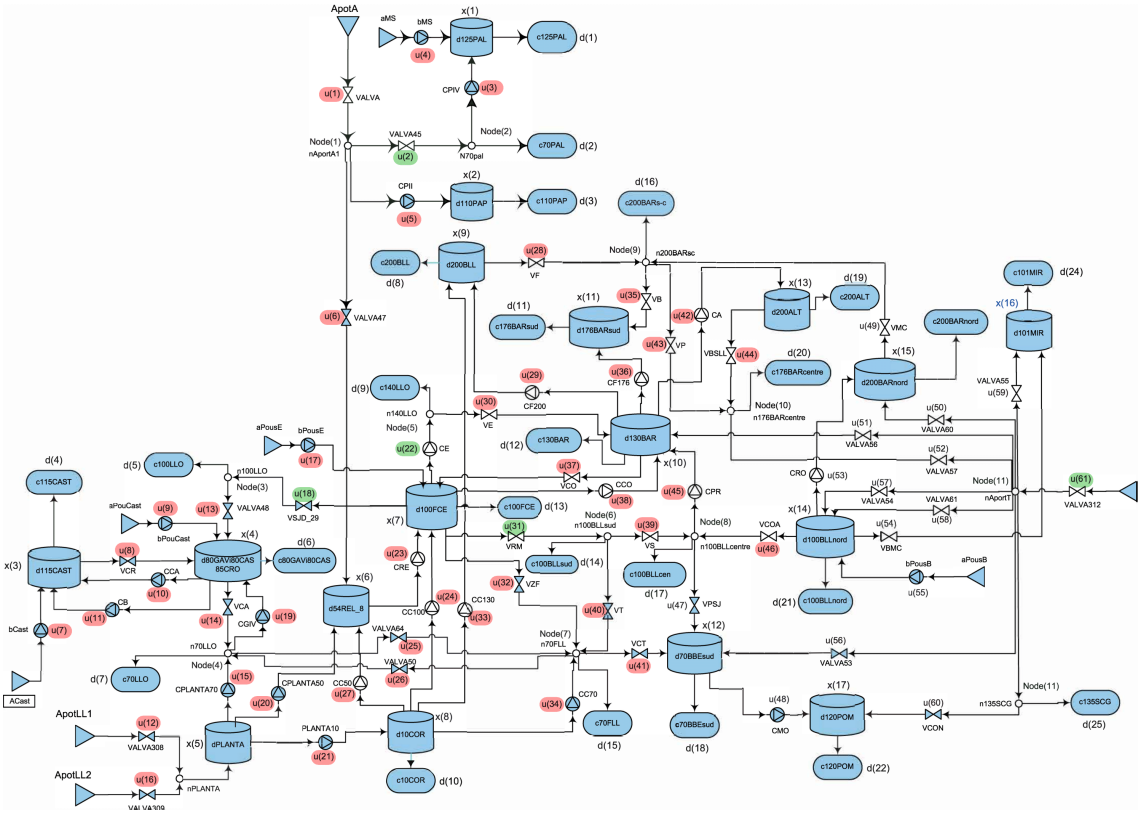

Figura 7.7: Barcelona drinking water network (17-Tanks).

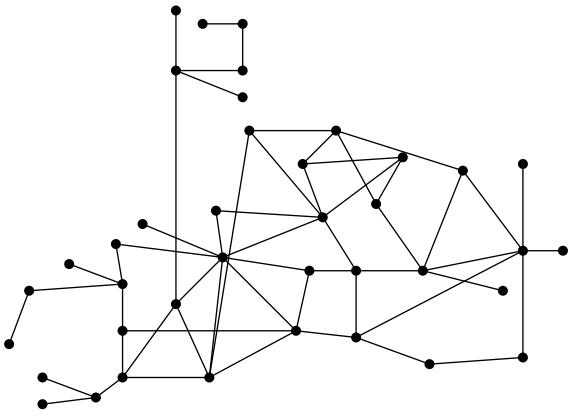

Figura 7.8: Case study based on the DWN case study.

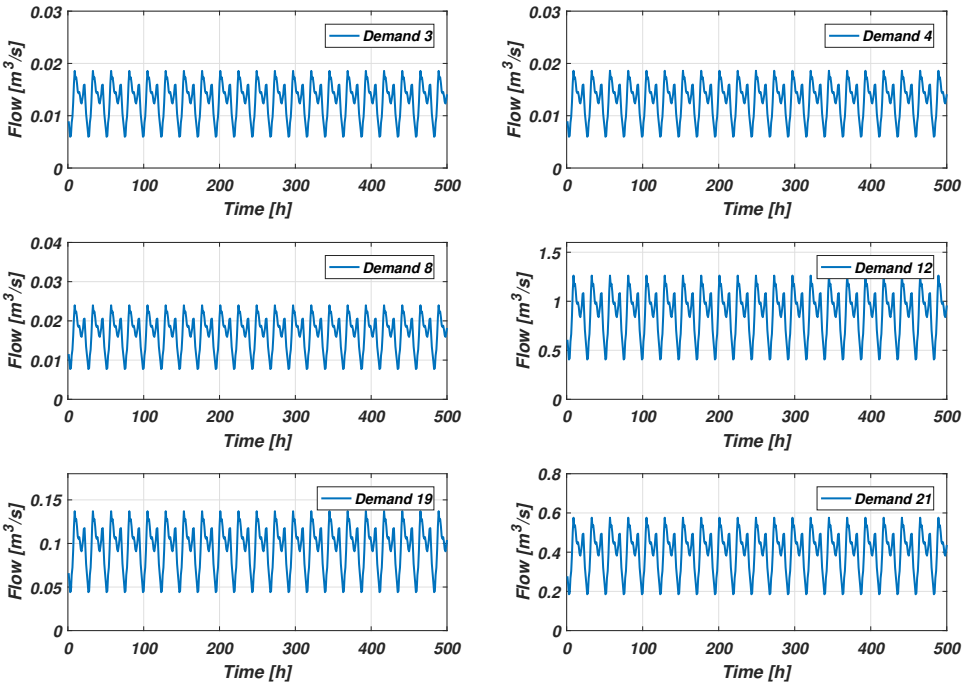

Figura 7.9: Drinking water demand for several sinks.

can supply the required water demand (see some demand sectors in Figure 7.9). The economic health-aware MPC-LPV formulation proposed in previous section has been applied to a simulation model of DWN presented in Figure 7.9.

From the reliability analysis, it could be obtained which states are structurally controllable, since the path computation analysis provides all possible paths from a source to target sectors. Moreover, for each path, an approximate operational cost (according to the electricity cost of each element) and a maximal water flow (according to the physical constraints of the actuators) can also be derived.

Tables 7.3 and 7.4 present important number of crucial actuators within the network, according to the topology and the way network elements are linked, as most actuators (pumps or valves) have only one connection between tanks and demands. Subsequently, if an actuator fails, then the corresponding demand will not be satisfied. Note that the information presented in Tables 7.3 and 7.4 is particularly significant for an operator because it shows the critical elements in the network for monitoring/improvement policies to be performed in the event of element damage. Considering to the DWN (Figures 7.7), Tables 7.3 and 7.4 and the study of the success minimal path of the water network, 607 minimal path sets are specified inside the system. A representation of the success

Taula 7.3: Structural actuators (towards tanks).

No.	Name	No.	Name	No.	Name	No.	Name
u_1	VALVA	u_{16}	VALVA309	u_{33}	CC130	u_{47}	VPSJ
u_3	CPIV	u_{17}	bPousE	u_{34}	CC70	u_{48}	CMO
u_4	bMS	u_{19}	CGIV	u_{35}	VB	u_{49}	VMC
u_5	CPII	u_{20}	CPLANTA50	u_{36}	CF176	u_{50}	VALVA60
u_6	VALVA47	u_{21}	PLANTA10	u_{37}	VCO	u_{51}	VALVA56
u_7	bCast	u_{23}	CRE	u_{38}	CCO	u_{52}	VALVA57
u_8	VCR	u_{24}	CC100	u_{39}	VS	u_{53}	CRO
u_9	bPouCast	u_{25}	VALVA64	u_{40}	V	u_{54}	VBMC
u_{10}	CCA	u_{26}	VALVA50	u_{41}	VCT	u_{55}	bPousB
u_{11}	CB	u_{27}	CC50	u_{42}	CA	u_{56}	VALVA53
u_{12}	VALVA308	u_{28}	VF	u_{43}	VP	u_{57}	VALVA54
u_{13}	VALVA48	u_{29}	CF200	u_{44}	VBSLL	u_{58}	VALVA61
u_{14}	VCA	u_{30}	VE	u_{45}	CPR	u_{59}	VALVA55
u_{15}	CPLANTA70	u_{32}	VZF	u_{46}	VCOA	u_{60}	VCON

Taula 7.4: Structural actuators (towards demands).

No.	Name	No.	Name	No.	Name	No.	Name
u_2	VALVA45	u_{18}	VSJD-29	u_{22}	CE	u_{31}	VRM
u_{61}	VALVA312						

Taula 7.5: Success minimal paths of the DWN case study.

Path	Component Set
P_1	$\{aMS,\ bMS,\ c125PAL\}$
P_2	$\{AportA,\ VALVA,\ VALVA45,\ c70PAL\}$
P_3	$\{AportA,\ VALVA,\ VALVA47,\ CPIV,\ c125PAL\}$
P_4	$\{AportA,\ VALVA,\ CPII,\ c110PAP\}$
P_5	$\{ACast,\ bCast,\ c115CAST\}$
$\vdots$	$\vdots$
P_{607}	$\{AportT,\ VALVA312,\ c135SCG\}$

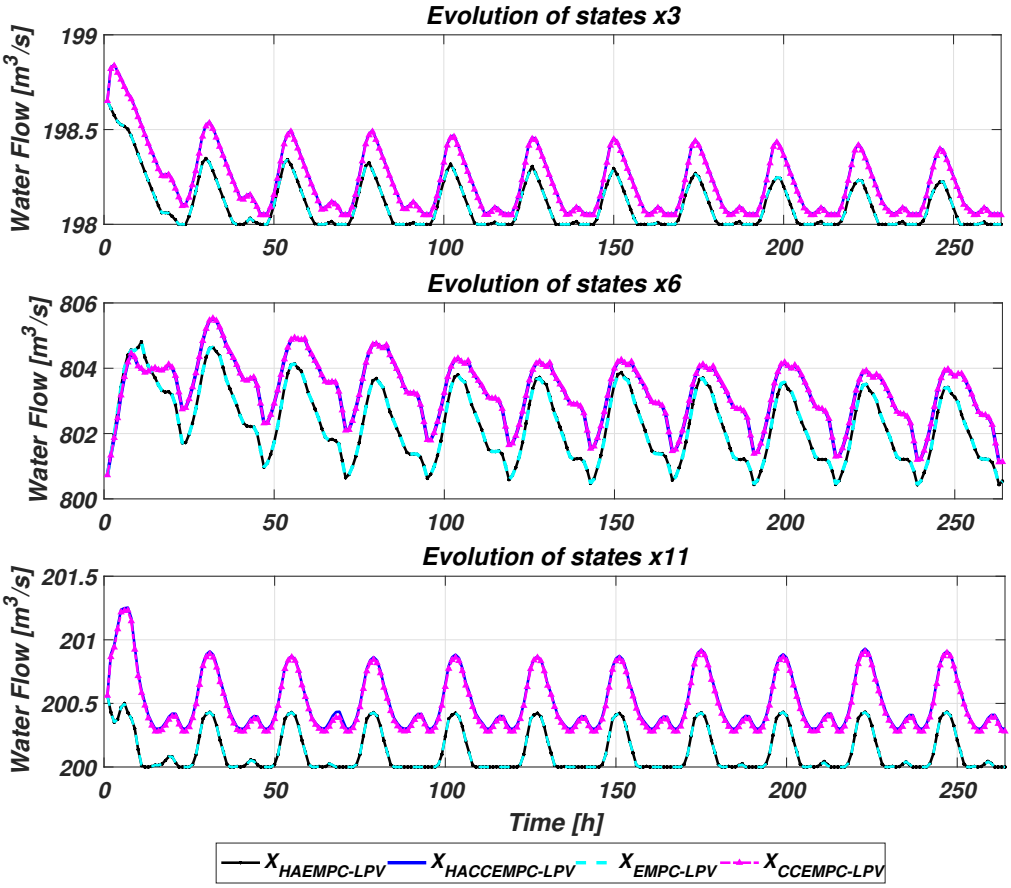

Figura 7.10: Evaluation of the control actions results.

minimal paths from the water network is presented in Table 7.5. The reliability of each minimal path set depends on the reliability of its components. Tanks and pipes are supposed perfectly reliable. However, sources are involved in the minimal path sets only for illustrative purposes of the procedure. The objective of the MPC is to minimize the multi-objective cost function (7.44). The prediction horizon is 24 hours because the system and also the electrical tariff have periodicity of 1 day. The analysis is exhibited a time period of 11 day (264hours) with sampling time of 1 hour. The weights of the cost function (7.44a) are $W_e = 100$, $W_s = 1$, $W_{\Delta_u} = 1$ and $W_{R_g} = 10$. The weighting matrices are founded by iterative tuning until the desired performance is achieved. The tuning of these parameters is arranged based on that the objective with the highest preference is the economic cost, which must be minimized maintaining proper levels of safety volumes and control action smoothness and the same time should maximize the system reliability.

In order to analyze and assess the benefits of the proposed economic Health-aware

MPC-LPV approach, a comparison with respect to baseline control strategies described in the literature of chapter 2 for the same case study is considered. Especially, the evaluated methods are the following:

Health-aware economic MPC-LPV with chance-constraints (HACCEMPC-LPV): This is the approach proposed in this chapter, that depends on solving Problem (7.44). This approach takes into account time-varying stochastic demand uncertainty and stochastic whole reliability of the system. Therefore, the base stock constraint, the hard bounds of the states and the terminal constraint of the system reliability are in the form of chance constraints.

Economic MPC-LPV (EMPC-LPV): This approach is based on the new control model of the network while the reliability objective is not considered in the cost functions. Moreover, it does not consider the stochastic demand uncertainty, chance-constraints or terminal constraint of the system reliability of the network.

Chance-constrained economic MPC-LPV (CCEMPC-LPV): This approach includes robustness only for demand uncertainty by replacing the state deterministic constraints with chance-constraints. Moreover, the CCEMPC-LPV controller includes neither the reliability objective nor the terminal constraint of the system reliability of the network.

Health-aware economic MPC-LPV (HAEMPC-LPV): This approach relies on solving problem (7.35). In this approach, an additional goal is included to the controller in order to extend the components and system reliability. The HAEMPC-LPV does not consider stochastic demand uncertainty and chance constraints.

Table 7.6 exhibits the numeric assessment of the above-mentioned controllers through different key performance indicators (KPIs), which are detailed below:

$$KPI_e := \frac{1}{n_s+1}\sum_{k=0}^{n_s}\alpha^\top(k)u_k\Delta_t, \tag{7.45a}$$

$$KPI_{\Delta_u} := \frac{1}{n_s+1}\sum_{i=1}^{n_u}\sum_{k=0}^{n_s}(\Delta_u(i,k))^2, \tag{7.45b}$$

$$KPI_s := \sum_{i=1}^{n_x}\sum_{k=0}^{n_s}\max\{0, x_s(i,k)-x(i,k)\}, \tag{7.45c}$$

$$KPI_R := x_{Rg}(k), \tag{7.45d}$$

$$KPI_t := t_{opt}(k), \tag{7.45e}$$

where KPI_e denotes the average economic performance of the water network, KPI_{Δ_u} evaluates the smoothness of the control actions, KPI_s comprises the quantity of water utilized from safety stocks, KPI_R denotes the value of the whole system reliability of the DWN and KPI_t defines the difficulty to solve the optimization tasks associated with each approach accounting $t_{opt}(k)$ as the average time that gets to solve the corresponding FHOP. In $KPI_e, KPI_{\Delta_u}, KPI_s$ and KPI_t lower values signify better performance results. However, a higher KPI_R value shows better performance in system reliability of the DWN. Furthermore, Table 7.7 presents details of the production and operational

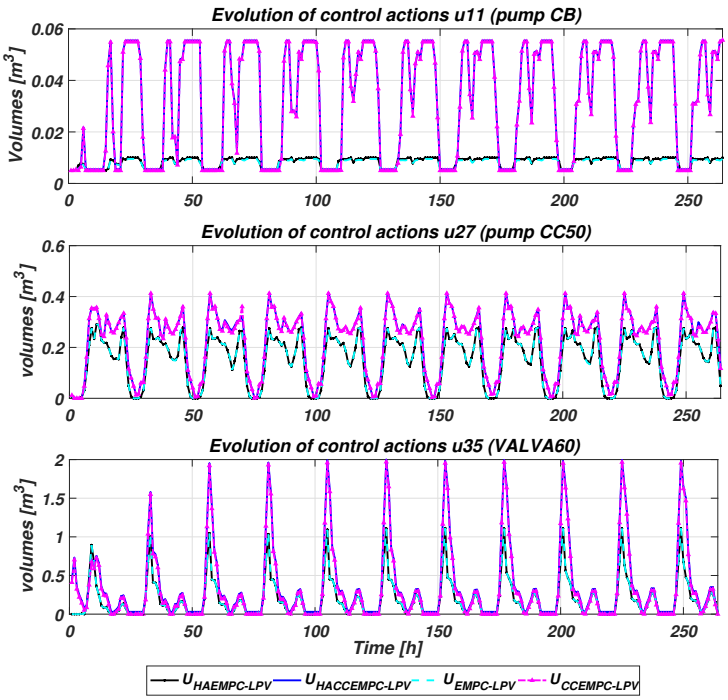

Figura 7.11: Results of the evolutions of control action.

costs associated with each approach, which are one of the most important objectives for the DWN managers.

Figures 7.11 and 7.10 show the evolution of the valves and pumps commands and tank volumes for comparison of different considered MPC approaches for DWN, respectively. Figure 7.11 shows that pumps always try to operate at the minimum cost, i.e., when the electrical tariff is cheaper. Moreover, 7.12 shows the comparison of evolution of the valves and pumps commands during the 48 hours. Figure 7.10 shows the proper replenishment planning that the predictive controller dictates according to the cyclic behavior of demands. Note that the net demand of each tank is properly satisfied along the simulation horizon.

Although the behavior of the control inputs (valve and pump commands) (see Figure 7.11) and selected storage tanks (see Figure 7.10) are very similar in all the approaches, Figure 7.13 shows comparison of the system reliability predictions and accumulated economic cost of the DWN that obtained from the different MPC approaches.

As shown in Figure 7.11, the behavior of the valves and pumps in CCEMPC-LPV and HACCEMPC-LPV approaches are almost the same while the amount of the inputs at HACCEMPC-LPV method is increased. On the other hand, the evaluation of the valves and pumps in EMPC-LPV and HAEMPC-LPV methods are the same. Simultaneously,

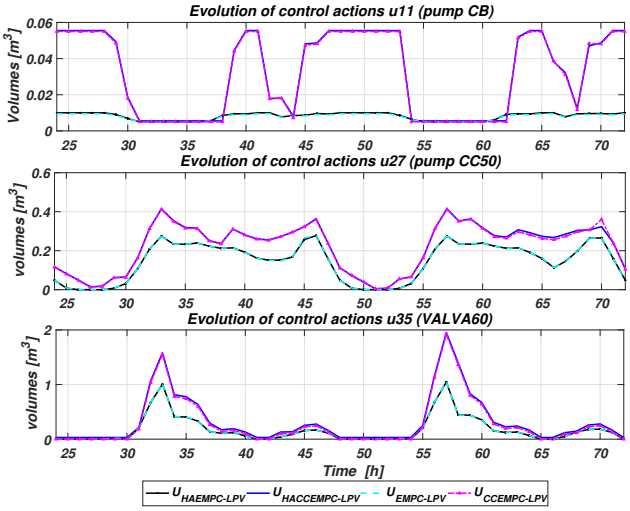

Figura 7.12: Results of the evolutions of control action in 48 h.

this situation has appeared in the evolutions of selected storage tanks that are presented in Figure 7.10. According to these results and reviewing the results in Tables 7.6 and 7.7, it can be observed that the robustness enhancements of the HACCEMPC-LPV approach is outperform the other controllers in terms of reliability. The EMPC-LPV controller has low values in most of the KPI_e but, the guarantee of reliability and robust or problematic feasibility is not considered. The main disadvantage of this controller is that control actions are computed based on economic criteria. In this case the controller overexploits those actuators that have lower operational costs, quickening their damage and hazarding the service reliability. The HAEMPC-LPV strategy reached the lowest KPI_e with the EMPC-LPV controller by including the reliability objective in the control law. However, the stochastic demand uncertainty and stochastic uncertainty of the system reliability is not recognized.

In order to manage the stochastic demand uncertainty, CCEMPC-LPV and HACCEMPC-LPV controllers incorporated the robustness for demand uncertainty by replacing the state deterministic constraints with chance constraints. Generally, chance constraints create an optimal back-off from real constraints as a risk-averse mechanism to face the non-stationary uncertainty included in the prediction of states.

Table 7.7 presents the details of water production and electricity cost of each approach. The HACCEMPC-LPV approach has quite similar costs to those of the baseline CCEMPC-LPV approach, but with the advantage of a better handling of constraints and considering the system reliability into the control law. Generally, the proposed HACCEMPC-LPV approach leads to a higher total closed-loop operational cost if considering only the water and electric costs as signs for economic performance. This is the trade-off for increasing the reliability of the system.

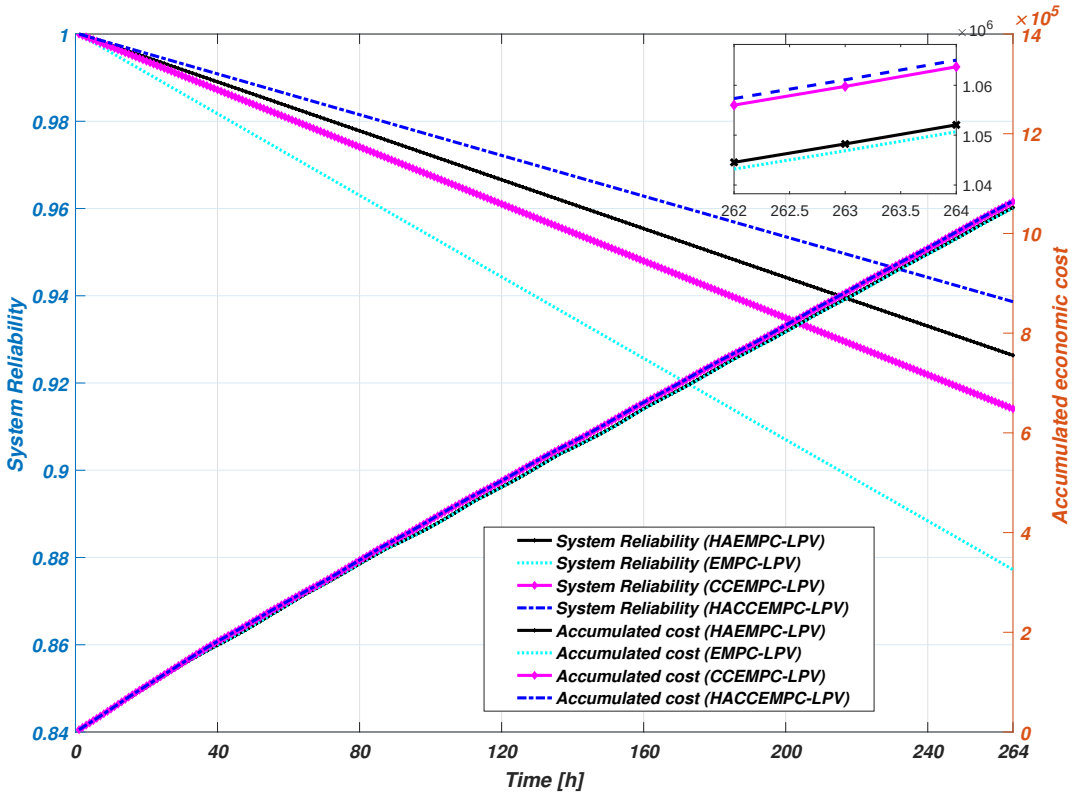

Figura 7.13: Evaluation of system reliability and accumulated economic cost.

Taula 7.6: Comparison of control performance.

Controller	KPI_e	KPI_{Δ_u}	KPI_s	KPI_R	KPI_t	Simulation Time
EMPC-LPV	3779.81	0.5271	28951.72	0.8772	1.5628	412.599
CCEMPC-LPV	4029.09	0.4910	28955.69	0.9186	1.9051	502.952
HAEMPC-LPV	3980.07	0.5317	28952.62	0.9263	1.78348	470.841
HACCEMPC-LPV	4029.19	0.4903	28955.90	0.9386	1.9664	519.147

7.7 Summary

In this chapter, an economic health-aware MPC-LPV strategy based on the system reliability for water transport network has been proposed to deal with the management of

Taula 7.7: Comparison of daily average costs of the MPC approaches.

MPC Approach	Water Average Cost (e.u./day)	Electric Average Cost (e.u./day)	Daily Average Cost (e.u./day)
EMPC-LPV	44162.44	3053.08	47215.53
CCEMPC-LPV	51237.98	3262.43	54500.42
RHEMPC-LPV	44369.90	3121.84	47491.75
RHCCEMPC-LPV	51438.13	3262.64	54700.77

flow-based networks, considering both demand uncertainty and system reliability with probabilistic constraints. The considered control-oriented model of the water transport network is based on flows. By considering chance constraints programming to compute an optimal tank policy based on a desired risk acceptability level, the system reliability is introduced as state variables inside the control model, which involves a nonlinear term. This is changed in to a linear-like form through the LPV structure. The scheduling parameters at each time instant are updated with the state vector value at that time. The new health-aware MPC-LPV method is solved iteratively by a series of QP problems and the MPC model is updated through the scheduling parameters estimated at each time instant. Moreover, varying flow demands and system reliability are satisfied by considering chance-constraint programming. The results obtained show that the system reliability of the DWN network is maximized with the proposed controller while the cost increases. The level of resultant back-off is variable and belongs to the volatility of the forecasted demand and system reliability at each prediction step and the agreement of the probabilistic distributions employed to model uncertainties. The reality of unbounded disturbances in the system prevents the guarantee of robust feasibility with these schemes. Therefore, the strategy proposed in this chapter is based on a service-level guarantee and a probabilistic feasibility.

The content of this chapter was based on the following works:

F. Karimi Pour, V. Puig, and G. Cembrano. Economic Health-Aware LPV-MPC Based on System Reliability Assessment for Water Transport Network. *Energies, 12(15), 3015*,2019.

F. Karimi Pour, V. Puig, and G. Cembrano. Economic Health-aware MPC-LPV based on DBN Reliability model for Water Transport Network. 6^{th} *International Conference on Control, Decision and Information Technologies (CoDIT)*,(pp. 1408-1413). IEEE, France,2019.

F. Karimi Pour, V. Puig, and G. Cembrano. Health-aware LPV-MPC based on system reliability assessment for drinking water networks. *IEEE Conference on Control Technology and Applications (CCTA)*,(pp. 187-192). IEEE, Denmark, 2018.

F. Karimi Pour, V. Puig, and G. Cembrano. Health-aware LPV-MPC based on a reliability-based remaining useful life assessment. 10^{th} *IFAC Symposium on Fault Detection, Supervision and Safety for Technical Processes, (SAFEPROCESS)*,IFAC-Papers OnLine,51(24), 1285-1291, Poland, 2018.

F. Karimi Pour, V. Puig, and G. Cembrano. Economic MPC-LPV Control for the Operational Management of Water Distribution Networks. *IFAC Workshop on Control Methods for Water Resource Systems (CMWRS 2019)*, IFAC-PapersOnLine, 52(23), 88-93, Netherlands, 2019.

F. Karimi Pour, V. Puig, and G. Cembrano. Economic Reliability-Aware MPC-LPV for Operational Management of Flow-based Water Networks including Chance-Constraints Programming. *Processes, 8(1), p.60.*

F. Karimi Pour and V. Puig. Economic Reliability-Aware MPC-LPV based on Chance-Constraints Programming for Water Networks. Accepted in "European Control Conference (ECC)", 2020.

Capítol 8

Health-aware optimization-based control design for autonomous racing vehicle

The accurate estimation of the State of Charge (SOC) and an acceptable prediction of the Remaining Useful Life (RUL) of batteries in autonomous vehicles are essential for safe and lifetime optimized operation. The estimation of the expected RUL is quite helpful to reduce maintenance cost, safety hazards, and operational downtime. This chapter proposes an innovative health-aware control approach for autonomous racing vehicles to simultaneously control it to the driving limits and to follow the desired path based on maximization of the battery RUL. To deal with the non-linear behaviour of the vehicle, a Linear Parameter Varying (LPV) model is developed. Based on this model, a robust controller is designed and synthesized by means of the Linear Matrix Inequality (LMI), where the general objective is to maximize progress on the track subject to win racing and saving energy. The main contribution is to preserve the lifetime of battery while optimizing a lap time to achieve the best path of a racing vehicle. The control design is divided into two layers with different time scale, path planner and controller. The first optimization problem is related to the path planner where the objective is to optimize the lap time and to maximize the battery RUL to obtain the best trajectory under the constraints of the circuit. The proposed approach is formulated as an optimal on-line robust LMI based Model Predictive Control (MPC) that steered from Lyapunov stability. The second part is focused on a controller gain synthesis solved by LPV based on Linear Quadratic Regulator (LPV-LQR) problem in LMI formulation with integral action for tracking the trajectory. The proposed approach is evaluated in simulation and results show the effectiveness of the proposed planner for optimizing the lap time and especially for maximizing the battery RUL.

8.1 Introduction

In the last decades, autonomous driving technology has become a significant focus in automotive industry. Autonomous driving technology is anticipated to decrease driver errors, prevent possibly dangerous situations and simplify the driver's work [155]. The advanced driver assistance systems (ADAS) or even autonomous driving are fast developing field, with interest in both industry and academia. ADAS can be found nowadays in many commercial vehicles such as cruise control or lane keeping which are based on classic control strategies [26]. However, lateral control of an autonomous vehicle still needs to be more investigated because of the difficulties it poses

The recent research on autonomous driving incorporates different fields, containing perception, planning, and control. The purpose of perception is to acquire information for autonomous vehicles from their situations. The goal of control is to obtain the suitable parameters for systems to follow the planned path and planning is the decision-making frame between perception and control [83]. The specific object of planning is to steer vehicles with a safe path, without collision, to their destinations, considering vehicle dynamics and road lines. Path planning has been widely investigated in mobile robotics applications [50]. In [224], the grid-based approach is used for dynamic path planning where the environment is planned to a set of cells and each cell describes the behaviour of an obstacle at that situation in the environment. A hierarchical path planning approach for mobile robot navigation in complex situations is presented in [199]. Both approaches perform well for path planning in low-speed applications but are not proper for high-speed driving. The control goal is to follow the references generated by the trajectory generator. This is a complicated task that must guarantee certain levels of performance and ensure vehicle stability. The trajectory-tracking problem is very crucial for autonomous racing vehicles, and many control algorithms have been proposed such as fuzzy controller [52], Linear Quadratic Regulator (LQR) [61] and Model Predictive Control (MPC) [180]. In [88], authors propose a model predictive path tracking controller according to the vehicle dynamics and actuators conditions in its path tracking. However, it is feasible that the planned path is not available to be tracked by the vehicle since the vehicle dynamics and its constraints are not included in path generation [57]. A path tracking scheme for a mobile robot based on neural predictive control is introduced in [76], where a multi-layer back propagation neural network is employed to model kinematics of the robot.

In general, the main objective of the autonomous racing is to make the lap in the shortest possible time while maintaining a smooth driving behaviour [103]. However, if the objective is the minimization of the lap time, the controller has to plan the trajectory on an adequately time horizon to avoid steering the vehicle outside the track [187]. In this area, there are some research such as in [28] that propose an adaptive MPC approach for solving lane keeping problem. In [212], a real-time MPC control scheme is introduced that solves the racing problem and test it in miniature race cars. Also, the Learning MPC is proposed to provide a solution to the racing problem in [187]. To minimize the time in a circuit implies going as fast as possible without exceeding circuit limits. But, it also affects the energy consumption of the vehicle and a trade-off between these two

objectives have received great interest in recent years, particularly in the area of car racing. Several studies solve this problem by using an optimal control technique, [27] and [212]. However, the considered control framework requires the use of safe energy mechanisms which still have not been considered in scientific literature. In this chapter, we propose to develop a framework for optimal compromise between control and energy management increasing enlarging the autonomous operation of the vehicle.

The increasing requirement for considering the reliability and availability of autonomous vehicles has led to the improvement and integration of prognostics and health management (PHM) techniques with automated systems [95]. The remaining useful life (RUL) is defined as the remaining time that a component (or system) will be able to perform its expected operation. This time regularly depends on the ageing of the components and the operating conditions. Regularly, the energy source of an autonomous racing vehicle is based on a battery. Obtaining more information about battery lifetime behaviour would result in the construction of cost-effective and long-lasting batteries. The performance of the racing vehicle is progressively reduced over time because of the battery ageing. The effect of ageing is characterized by losing power. This deterioration is caused by several factors such as high-rate cycling, overburden and overdischarge [217]. To avoid damages and decrease the ageing rate during the charge/discharge cycles of the battery, it is required to monitor the State of Charge (SoC). The SoC is the proportion of the possible charge, compared to the total charge available when the battery is fully charged at a specific time.

A recent summary of methods for battery diagnosis can be found in [228]. The battery RUL prediction and the uncertainty management by using the particle filter (PF) approach (applying the practical degradation model to create a state transition equation) are provided in [193]. An integrated method based on a mixture of Gaussian process model and PF for battery SoH estimation is presented in [127]. Using the model-based tracking approach is a general way to obtain suitable results [228]. The usage of Kalman filtering for monitoring the SoC was reported in a lot of studies, e.g.[172, 194]. On the other side, motion control actions are observed as a source of stress degradation such as [96]. In [185] the authors proposed an approach to estimate RUL based on assuming a decisive relation between the degradation and the control input. To the knowledge of the authors, there is no study detected to consider SoC and RUL battery inside the model of the racing vehicle. In this work, we propose a health-aware control approach for a racing vehicle as a novel approach to solve driving control problems and at the same time to maintain and minimize the consumption of the battery energy.

The main contribution of this chapter is to provide a health-aware control design for a racing vehicle that generates an optimal path for the racing by optimizing the lap time and maximizing the RUL of the battery in the planner. The control design is divided into two layers (path planner and controller) with different time scales. The first layer included a path planner whose objective is to optimize the lap time and maximize the battery RUL to obtain the best trajectory under the constraints of the circuit. The second layer is focused on a controller gain with integral action for tracking the trajectory obtained by the planner. Both optimization problems are solved using

Linear Matrix Inequality (LMI) approach for MPC considering an LPV model of the vehicle and the input and output constraints. Several reasons justify the use of LMIs [24]. In fact, the resulting LMI-based optimization problems can be solved in polynomial time, using interior-point methods and the optimal solution is global [11]. Finally, the proposed approach is assessed in simulation and results show the effectiveness of the proposed planner for optimizing the lap time while at the same maximizing the RUL of the battery.

8.2 System Modeling

In this chapter, the vehicle model (3.38) is modified to (8.1) by including the disturbances and noise. Then, the vehicle model is concisely expressed in state space representation as

$$\dot{x}(t) = f(x(t), u(t), w_d(t), v_n(t)), \tag{8.1}$$

where at time t the vectors x, u, w and v represent the state, input, disturbances and noise

$$x = [v_x \; v_y \; \omega \; e_y \; e_\theta]^\top, \quad u = [\delta \; \alpha]^\top, \tag{8.2}$$

and v_n is the measurement noise that is applied into measurable states and w_d is the friction force disturbances that is considered as a variation of the nominal $F_{friction} = \mu mg$.

In order to achieve the best trajectory where the lap time is optimized, the time (t) should be considered as a state variable. This is achieved by formulating kinematic model (3.37) in the space domain considering the time (t) as a state variable which will be used for optimizing the lap time. Furthermore, because of the problem consists on computing the best path, the curvature (κ) has to be implemented in terms of the driven distance, since the time evolution is unknown at the beginning of the optimization. By considering $x_c = [e_y, \; e_\theta, \; s]^\top$ as the state vector of kinematic model (3.37), then, a new state vector $\tilde{x}_c = [\tilde{e}_y, \; \tilde{e}_\theta, \; t]^\top$ is determined by applying

$$\tilde{\dot{x}}_c = \frac{dx_c}{ds} = \frac{dx_c}{dt}.\frac{dt}{ds} = \dot{x}_c \frac{1}{\dot{s}}. \tag{8.3}$$

Then, the following kinematic model equation is obtained when the time is considered as a state in the model

$$\begin{aligned} \tilde{\dot{e}}_y &= \sin(e_\theta)v_x + \cos(e_\theta)v_y, \\ \tilde{\dot{e}}_\theta &= \frac{\omega}{\dot{s}} - \kappa, \\ \dot{t} &= \frac{1}{\dot{s}}. \end{aligned} \tag{8.4}$$

The main goal is to maximize the Remaining Useful Life (RUL) of the battery vehicle that has a direct connection by reducing vehicle energy consumption as low as

possible considering that the energy is stored in the battery. In order to minimize the vehicle energy and maximize the RUL, the state of charge (SoC) of the battery must be considered as a state variable. The SoC of a battery at a given time is the proportion of the charge available, compared to the total charge available when it is fully charged. The range of $SoC \in [0, 1]$, where 0 denotes the battery is fully discharge, and 1 corresponds to 100% of the charge, i.e., that, the battery is fully charged. Based on the previous study [194], the most common used approach to compute the SoC is described as follows:

$$SoC(t) = SoC(t_0) - \frac{1}{C_T} \int_{t_0}^{t} I_{batt}(t)dt, \tag{8.5}$$

where t_0 presents the initial time and C_T is total capacity of the battery. However, to include the SoC of the battery in the vehicle model, the SoC can be expressed as a function of the velocity of the vehicle. Then, the SoC in the battery can be modeled as follows

$$\begin{aligned} SoC(t) &= SoC(t_0) - \ P_{batt}(t), \\ P_{batt}(t) &= P_{move}(t) + P_{friction}(t), \\ P_{batt}(t) &= \frac{1}{2} C_d \rho A_r v_x^2 + \mu m g v_x, \end{aligned} \tag{8.6}$$

where C_d is drag coefficient for the wheel, A_r indicates the vehicle front area and ρ is the air density at $25°C$.

Therefore, based on the (3.34) and (8.3)-(8.6), , Eq.(8.1) can be expressed as:

$$\dot{\tilde{x}}(t) = \tilde{f}(\tilde{x}(t), u(t), w(t), v(t)), \tag{8.7}$$

where the augmented vector of states is defined as follows

$$\tilde{x}(t) = [v_x,\ v_y,\ \omega,\ \tilde{e}_y,\ \tilde{e}_\theta,\ t,\ SoC]^\top. \tag{8.8}$$

8.2.1 LPV modeling

Given vehicle nonlinear characteristics, time-varying parameters and parametric uncertainties, vehicle steering control systems regularly exhibit strong nonlinearities. The previous vehicle non-linear model will be transformed into an LPV representation by embedding the nonlinearities inside model parameters. As a result, there parameters are expressed in terms of some system variables called scheduling variables that vary in a known bounded interval. This procedure leads to the following LPV model in discrete-time

$$\begin{aligned} \tilde{x}(k+1) &= A(\theta(k))\tilde{x}(k) + B(\theta(k))u(k) + Ew(k) \\ \tilde{y}(k) &= C\tilde{x}(k) + Dv(k), \end{aligned} \tag{8.9}$$

where the discrete time is denoted by $k \in \mathbb{Z}$, and $v \in \mathbb{R}^{n_y}$ is The matrices A, B, C and E are obtained as:

$$A(\theta(k)) = \begin{bmatrix} a_{11} & a_{12} & a_{13} & 0 & 0 & 0 & 0 \\ 0 & a_{22} & a_{23} & 0 & 0 & 0 & 0 \\ 0 & a_{32} & a_{33} & 0 & 0 & 0 & 0 \\ 0 & 1 & 0 & 0 & a_{45} & 0 & 0 \\ 0 & a_{52} & a_{53} & 0 & 1 & 0 & 0 \\ a_{61} & a_{62} & 0 & 0 & 0 & 0 & 0 \\ a_{71} & 0 & 0 & 0 & 0 & 0 & 1 \end{bmatrix}, \; B(\theta(k)) = \begin{bmatrix} b_{11} & 1 \\ b_{21} & 0 \\ b_{31} & 0 \\ 0 & 0 \\ 0 & 0 \\ 0 & 0 \\ 0 & 0 \end{bmatrix}, \; E = \begin{bmatrix} 1/m \\ 0 \\ 0 \\ 0 \\ 0 \\ 0 \\ 0 \end{bmatrix},$$

$$C = \begin{bmatrix} 1 & 0 & 0 & 0 & 0 & 0 \\ 0 & 1 & 0 & 0 & 0 & 0 \\ 0 & 0 & 1 & 0 & 0 & 0 \end{bmatrix}. \tag{8.10}$$

where the matrix values are presented in Appendix A. (B.1). Vector $\theta(k) := [\theta_{1,k}, \theta_{2,k}, ..., \theta_{N,k}]^T \in \mathbb{R}^N$ is the vector of scheduling parameters and each variable, θ_j is known and varies in a defined interval $\theta_j \in [\underline{\theta_j}, \overline{\theta_j}] \; \forall j \in [1, ..., N]$, which belongs to a convex polytope Θ defined by (2.10). Clearly, as $\theta(k)$ varies inside the convex polytope Θ, the matrices of the system (8.9) vary inside a corresponding polytope Ψ, which is defined (2.11) and the matrices of the system (8.9) can be rewritten as (2.12).

8.3 Problem Statements

The main control goal for the vehicle is to obtain the best path trajectory according to the vehicle dynamics and its limits for racing. Then, the controller forces the vehicle to track the trajectory obtained online by the planner. However, if the objective is only the minimization of the lap time, the controller has to plan the trajectory on an adequately time horizon to avoid steering the vehicle outside the track. However, this plan also affects the energy consumption of the vehicle. Thus, the management of the trade-off between these two objectives is an open problem in the area of car racing. Therefore, in addition to obtaining a planned trajectory with optimal lap time, the energy consumption of the vehicle that depends on the battery RUL should be considered into the optimization problem solved by the planner.

Generally, the design of multi-layer control structures can be related to the different type of control objectives, which would are not adequately solved in a one layer architecture[100]. Specifically, the control objectives can be arranged in the following way:

- The objectives of planner operation are to optimize time and maximize lifetime. Since, assessing the battery SoC requires more time than the tracking trajectory evaluation, the planner operates at a slower time scale than the controller.

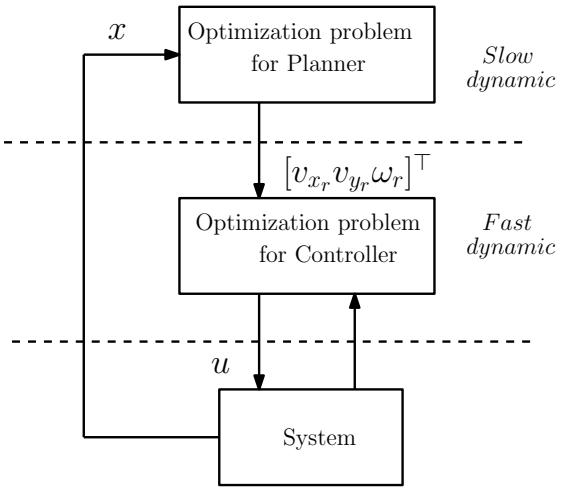

Figura 8.1: Block diagram of control approach

- The objectives of controller are to guarantee a stable operation of the vehicle while tracking the trajectory provided by the planner.

The control strategy presented in this chapter is based on a multilayer (hierarchical) control structure including the energy management. This structure, conceptualized in Figure 8.1, is a two-layer hierarchical architecture, where the solution of the problem is obtained by decoupling the problem into two different time-scales. In the upper layer, the planner solves an optimization problem that has a objective to provide the optimal path (reference that is shown by index r in Figure.8.1) to the automatic control (low layer). In the lower layer, the tracking controller receives the path trajectory calculated by the upper layer and determines the best trajectories for the controller-layer control system by considering the faster dynamics of the plant, which is operated by pole placement method.

8.4 Proposed approach

8.4.1 LPV MPC Planner

The main goal of the planner part is to find the path within the circuit and provide such information to the automatic control. In general, the path trajectory is obtained according to the body frame velocities of the vehicle. In this chapter, for solving these optimization problems to obtain the best path, a robust LMI-based MPC controller, which is robust against parametric uncertainties and velocity-varying according to constraints is presented. Hence, the optimal control problem can be restated as the following robust LMI-based MPC [116], which minimizes the infinite horizon quadratic objective

function:

$$J_\infty(k) = \sum_{i=0}^{\infty}(\| \tilde{x}(k+i|k) \|_{Q_1} + \| \tilde{u}(k+i|k) \|_R), \tag{8.11}$$

where $\tilde{u} = [\delta \ \alpha]^\top$ is the control input generated by the planner. Moreover, $\tilde{x}(k+i|k)$ and $\tilde{u}(k+i|k)$ denote the state predicted based on the measurements and the control input at time $k+i$, computed at time k, respectively. $\tilde{x}(k) = \tilde{x}(k|k)$ and $\tilde{u}(k) = \tilde{u}(k|k)$ denote the measured state and control input applied to the system plant at time k, respectively. Besides, $Q_1 = Q_1^\top > 0$ and $R^\top > 0$ are positive definite weighing matrices.

The control law is obtained by minimizing cost function (8.11) with respect to the control moves, that is:

$$\min_{\tilde{u}(k+i|k), i\geq 0} \ \max_{[A(k+i), B(k+i)]\in\Psi, i\geq 0} J_\infty(k), \tag{8.12}$$

where the maximization in (8.12) is taken over the set Ψ of uncertain systems. The solution of leads to a state feedback law for the planner given by:

$$\tilde{u}(k+i|k) = K(\theta(k))\tilde{x}(k+i|k), \tag{8.13}$$

where the state feedback gain is given by

$$K(\theta(k)) = \sum_{j=1}^{N} \mu_j(\theta(k))K_j. \tag{8.14}$$

8.4.2 LMI control design of Planner including health management

One of the motivations in this work is to integrate the information about the battery SoC in the planner and controller design. Accordingly, the battery lifetime will be estimated by means of the RUL computed using an approach based on the SoC.

RUL computation via SoC assessment

Once the battery SoC is calculated for the racing vehicle, an approach to evaluate RUL function is introduced.

Proposition 8.1. *Considering that RUL is computed when the state of charge behaviour reaches or exceed the state of charge thresholded value which noted SoC_{thresh}. Therefore the expected RUL is given by*

$$RUL(k) = \frac{SoC_{thresh} - SoC(k)}{-u_b(k)}, \tag{8.15}$$

where u_b is the battery input.

Demostració. The derivative of the state of charge of the battery is given by

$$\frac{d(SoC)}{dt} = u_{discharge}(t), \tag{8.16}$$

or, equivalently in discrete-time can be rewritten as follows

$$\frac{SoC(k+1) - SoC(k)}{\Delta t} = u_{discharge}(k). \tag{8.17}$$

Assuming the $SoC(k+1)$ reaches the SoC threshold (SoC_{thresh}), where SoC threshold is the point at which the battery would no longer reliably provide energy for moving the vehicle. Then, (8.17) can be rewritten as:

$$\frac{SoC_{tresh} - SoC(k)}{\Delta t} = u_{discharge}(k) \tag{8.18}$$

According to (8.18), the definition of the RUL and considering that Δt provides an estimation of the RUL yields to:

$$RUL(k) = \frac{SoC_{thresh} - SoC(k)}{u_{discharge}(k)}, \tag{8.19}$$

where, $u_{discharge}$ is considered the negative value of the battery input which dented $-u_b$. □

LMI control design based RUL objective

The LMI control design for the planner based on the optimizing the lap time and RUL objectives is now proposed for the racing vehicle. The objective of the trajectory planner is modified to find the best path within the circuit that optimizes the lap time t and at the same time maximize the lifetime of the system. In order to increase the RUL of the battery and optimizing the lap time, the optimization planner objective (8.11) should be modified according to the new objectives. According to the (8.15), there is a relation between the RUL and battery SoC and control input. Moreover, the SoC model (8.6) and (8.4) are considered as new states in the vehicle model. Hence, the optimization planner can be updated based on the RUL and lap time and the robust LMI optimization problem of the planner (8.11) is reformulated as follows:

$$\min_{\tilde{u}(k+i|k), i\geq 0} \max_{[A(k+i), B(k+i)]\in\Psi, i\geq 0} J_{g,\infty}(k) = \sum_{i=0}^{\infty} (\| t \|^2_{\lambda_1} + \| \frac{1}{RUL} \|^2_{\lambda_2}), \tag{8.20}$$

where λ_1 and λ_2 are positive definite weighing matrices.

Given that t is a state of the model and the RUL is estimated based on the SoC which is another state of vehicle model, the optimization problem (8.20) can be solved

as a LQR problem based on the robust LMI similarly to (8.12) with some new condition. Therefore, the state feedback control law can be formulated for the LPV planner model as follows:

$$\tilde{u}(k+i|k) = K_g(\theta(k))\tilde{x}(k+i|k), \tag{8.21}$$

where the state feedback gain matrix is given by

$$K_g(\theta(k)) = \sum_{j=1}^{N} \mu_j(\theta(k))K_j, \tag{8.22}$$

that is obtained using the following theorem based on the [116], but adapted to the racing vehicle and using the new objective function (8.20). Before presenting the theorem let's consider some Lemmas such as:

Lemma 8.1. *[51] Consider A as a symmetric matrix. Then*

$$\lambda_{max}(A) \leq \Longleftrightarrow \gamma A - \gamma I \leq 0. \tag{8.23}$$

Lemma 8.2. *[51] consider A a matrix of appropriate dimensions, and γ a positive scalar. Hence,*

$$A^\top A - \gamma^2 I \leq 0 \Longleftrightarrow \begin{bmatrix} -\gamma I & A \\ A^\top & -\gamma I \end{bmatrix} \leq 0. \tag{8.24}$$

Lemma 8.3. *(Schur complement lemma)*

$$\begin{bmatrix} Q(x) & S(x) \\ S^\top(x) & R(x) \end{bmatrix} > 0, \tag{8.25}$$

where $Q(x) = Q^\top(x)$, $R(x) = R^\top(x)$ and $S(x)$ is the affine function of x. Then,(8.25) *is equivalent to the following conditions:*

$$\begin{aligned} &Q(x) > 0,\ R(x) - S^\top(x)Q^{-1}(x)S(x) > 0, \\ &R(x) > 0,\ Q(x) - S(x)R^{-1}(x)S^\top(x) > 0. \end{aligned} \tag{8.26}$$

Theorem 8.1. *Considering $\tilde{x}(k|k)$ is the state of the system* (8.9) *measured at each sampling time k and there are constraints on the output and control input where $\tilde{u}_{max}$ and $\tilde{y}_{max}$ are the maximum values of control input and output of vehicle. The state feedback matrix K_g in the control law $\tilde{u}(k+i|k) = K_g(\theta(k))\tilde{x}(k+i|k)$ that minimizes the upper bound on the performance objective function at sampling time k_g given by $K_g = YQ^{-1}$ can be found, if there exist K_g, Q, γ and $\gamma \in \mathbb{R}^{1\times 1} > 0$, $Q = Q^\top \in \mathbb{R}^{7\times 7} > 0$, $Y \in \mathbb{R}^{2\times 7}$ where Q and Y are obtained from the solution of the following linear objective minimization problem*

$$\min_{\gamma,Q,Y} \gamma \tag{8.27}$$

subject to,

$$\begin{bmatrix} 1 & \tilde{x}(k)^\top \\ \tilde{x}(k) & Q \end{bmatrix} \geq 0, \tag{8.28}$$

$$\begin{bmatrix} Q & * & * & * \\ A_jQ + B_jY & Q & 0 & 0 \\ Q_1^{1/2}Q & 0 & \gamma I & 0 \\ R^{1/2}Y & 0 & 0 & \gamma I \end{bmatrix} > 0, \tag{8.29}$$

$$\begin{bmatrix} -\gamma I & (-1/RUL(k)) \\ (-1/RUL(k))^\top & -\gamma I \end{bmatrix} \leq 0, \tag{8.30}$$

$$\begin{bmatrix} u_{max}^2 I & Y \\ Y^\top & Q \end{bmatrix} \geq 0, \tag{8.31}$$

$$\begin{bmatrix} Q & (A_jQ + B_jY)^\top C^\top \\ C(A_jQ + B_jY) & \tilde{y}_{max}^2 \end{bmatrix} \geq 0, \tag{8.32}$$

Demostració. The proof is obtained in following few steps:

(1) Proof for the stability and optimization.

By considering a quadratic Lyapunov-Krasovskii function $V(x(k)) = \tilde{x}^\top(k)P\tilde{x}(k) > 0$, where $P > 0$ is a symmetrical positive-definite matrix, the upper bound on the objective function J_∞ is obtained.

To guarantee the existence of the upper bound on the performance at sampling time k, the following inequalities must be satisfied

$$\begin{aligned} &V(\tilde{x}(k+i+1|k)) - V(\tilde{x}(k+i|k)) \leq -J_{g,\infty}(k) \\ &\forall [A(k+i), B(k+i)] \in \Psi, i \geq 0 \end{aligned} \tag{8.33}$$

Then, by requiring $\tilde{x}(\infty|k) = 0$ such that $V\tilde{x}((\infty|k)) = 0$ and summing (8.33) from $i = 0$ to $i = \infty$, it can be obtained

$$\max_{[A(k+i),B(k+i)]\in\Psi, i\geq 0} J_\infty \leq V(\tilde{x}(k|k)). \tag{8.34}$$

Minimizing of $V(\tilde{x}(k)) = \tilde{x}(k)^\top P\tilde{x}(k), P > 0$ is equivalent to

$$\begin{aligned} &\min_{\gamma,P} \gamma \\ \text{s.t} \quad &\tilde{x}(k)^\top P\tilde{x}(k) \leq 0. \end{aligned}$$

Defining $Q = \gamma P^{-1} > 0$ and using the Schur-complement [51], equation (8.28) is established. Then, by substituting (8.21) and (8.9), inequality (8.33) becomes:

$$\begin{aligned} \tilde{x}(k+i|k)^\top \big(&(A(k+i) + B(k+i)K_g)^\top P(A(k+i) + B(k+i)K_g) - P \\ &+ K_g^\top RK_g + Q_1 \big) \tilde{x}(k+i|k) \leq 0. \end{aligned}$$

and it is defined in $[A(k+i), B(k+i)]$. Then, it is satisfied for all $[A(k+i), B(k+i)] \in \Psi$. Hence, by substituting $P = \gamma Q^{-1},\ Q > 0,\ Y = K_g Q$, pre - and post- multiplying by Q and using Lemma 8.3, equation (8.29) is obtained.

(2) Proof for maximizing the RUL of battery. According to objective (8.20) and definition of $\| (1/RUL) \|^2$, we have

$$\| (1/RUL) \|^2 = (\lambda_{max}((1/RUL)^\top (1/RUL)))^{\frac{1}{2}}.$$

Then, by using Lemmas (8.1) and (8.2), for $\gamma > 0$

$$\begin{aligned}
&\| (1/RUL) \|^2 \leq \gamma \\
&\iff \lambda_{max}((1/RUL)^\top (1/RUL)) \leq \gamma^2, \\
&\iff (1/RUL)^\top (1/RUL) - \gamma^2 \leq 0, \\
&\iff \begin{bmatrix} -\gamma I & (-1/RUL(k)) \\ (-1/RUL(k))^\top & -\gamma I \end{bmatrix} \leq 0.
\end{aligned}$$

(3) Proof for output and input constraints.

Consider the Euclidean norm bound and maximum bound on the constraints of input

$$\|\tilde{u}(k+i|k)\|_2 \leq u_{max}.$$

Following [116],

$$\begin{aligned}
V(\tilde{x}(k+i|k)) &= \tilde{x}(k+i|k)^\top Q^{-1} \tilde{x}(k+i|k) \\
&\leq \tilde{x}(k|k)^\top Q^{-1} \tilde{x}(k|k) \leq 1,
\end{aligned} \tag{8.35}$$

is state-invariant ellipsoid. Therefore, it can be obtained

$$\begin{aligned}
\max_{i \geq 0} \|\tilde{u}(i|k)\|_2^2 &= \max_{i \geq 0} \|YQ^{-1}\tilde{x}(i|k)\|_2^2 \\
&\leq \lambda_{max}(Q^{-1/2} Y^\top Y Q^{-1/2}) \geq u_{max}^2
\end{aligned}$$

where λ_{max} denotes the largest generalized eigenvalue and by using Lemma 8.3, the (8.31) is established.

The output constraints (8.32) is satisfied based on the

$$\|y(k+i|k)\|_2 \leq y_{max}.$$

Thus,

$$\begin{aligned}
\max_{i \geq 1} \|y(i|k)\|_2 &= \max_{i \geq 0} \|[C\ 0](A_g + B_g K_g)\tilde{x}(i|k)\|_2 \\
&\leq \lambda_{max}([C\ 0](A_g + B_g K_g) Q^{1/2}) \leq y_{max}
\end{aligned}$$

Then, by multiplying on the left and right by $Q^{1/2}$

$$Q^{1/2}((A_g + B_g K_g)[C\ 0]^\top [C\ 0](A_g + B_g K_g))Q^{1/2} \leq y_{max}^2 I$$

such that by using using Lemma 8.3, the inequality (8.32) is satisfied. □

8.4.3 Tracking Controller

The controller objective is to track the reference that is generated by the planner considering the same constraints on inputs and states. The controller is designed by pole placement and augmenting the plant with an integrator to remove steady state errors. The integrator can be including the following equation in the state space model of the vehicle

$$z(k+1) = z(k) + (y_r(k) - C\tilde{x}(k)), \tag{8.38}$$

where y_r is the references that are obtained by the planner such that the augmented system (8.9) with integrator is

$$\begin{aligned} \begin{bmatrix} \tilde{x}(k+1) \\ z(k+1) \end{bmatrix} &= \begin{bmatrix} A(\theta(k)) & 0 \\ -T_s C & I \end{bmatrix} \begin{bmatrix} \tilde{x}(k) \\ z(k) \end{bmatrix} + \begin{bmatrix} B(\theta(k)) \\ 0 \end{bmatrix} u(k) + \begin{bmatrix} 0 \\ T_s I \end{bmatrix} y_r(k) + \begin{bmatrix} E \\ 0 \end{bmatrix} w(k) \\ y(k) &= \begin{bmatrix} C & 0 \end{bmatrix} \begin{bmatrix} \tilde{x}(k) \\ z(k) \end{bmatrix} \end{aligned} \tag{8.39}$$

Then, the feedback control law can be formulated as follows using state feedback

$$u(k) = [K_c(\theta(k))] \begin{bmatrix} \tilde{x}(k) \\ z(k) \end{bmatrix}, \tag{8.40}$$

where $K_c = [K_{c1} K_{c2}]$ is the feedback gain matrix obtained using the following proposition which presents a LMI based formulation for solving the LPV LQR problem via an H_2 problem.

For obtaining a faster dynamics in the lower layer than in the upper layer, the position of poles should be forced close to zero and inside the unit circle region. To determine and analyze the stability and location of poles in the low layer optimization can be used $\mathcal{D}$-stability. By using the definition of the $\mathcal{D}$-stability based on the region and [42], which is a subset $\mathcal{D}$ of the complex plane determined for a symmetric matrix $a = [a_{kl}] \in \mathbb{R}^{m \times m}$ and a matrix $b = [b_{kl}] \in \mathbb{R}^{m \times m}$such that:

$$\mathcal{D} = \{g \in \mathbf{C} : f_g < 0\},$$

where $f_D(g)$ is the characteristic function, defined as:

$$f_D(g) = a + gb + g^* b = [a_{kl} + g b_{kl} + g^* b_{kl}]_{1 \leq k,l \leq m} \tag{8.41}$$

and g^* denotes the complex conjugate of g.

By considering the close-loop mode, therefore the $\mathcal{M}$ can be described by:

$$\mathcal{M} = \{(A_j + B_j K_j) : eig\ (A_j + B_j K_j) \in \mathcal{D}\}. \tag{8.42}$$

Therefore, by following the [42], the close-loop mode is quadratically $\mathcal{D}$-stable if there exists a symmetric matrix $P > 0$ such that:

$$a \otimes P + b \otimes (A_j + B_j K_j)P + b^\top \otimes ((A_j + B_j K_j)P)^\top < 0, \tag{8.43}$$

then, by substituting $W_j = K_j P$ and to assess that all the poles of closed-loop are inside the circular region centered in $(q, 0)$ with radius r, it can be shown that:

$$\begin{bmatrix} -rP & qP + A_j P + B_j W_j \\ qP + PA_j^\top + W_j^\top B_j^\top & -rP \end{bmatrix} < 0. \tag{8.44}$$

Therefore, by considering (8.44) and the dimensions of the system (8.8), the following proposition based on [51] can be modified considering the vehicle LPV model.

Proposition 8.2. *[24] Given the LQR parameters $Q = Q^\top \in \mathbb{R}^{7\times 7} > 0$, $Y \in \mathbb{R}^{2\times 7}$, a state feedback control in the form of $u(k) = K_c(\theta(k))[\tilde{x}(k), z(k)]^\top$ exists such that $\gamma > 0$, if and only if there exist $P \in \mathbb{R}^{7\times 7}$, $Y \in \mathbb{R}^{2\times 7}$ and $W_j \in \mathbb{R}^{2\times 7}$ satisfying*

$$(A_j P + B_j W_j) + (A_j P + B_j W_j)^\top + \tilde{x}_0 \tilde{x}_0^\top < 0, \tag{8.45}$$

$$trace\left(Q^{1/2} X (Q^{1/2})^\top\right) + trace(Y) < \gamma, \tag{8.46}$$

$$\begin{bmatrix} -Y & R^{1/2} W_j \\ (R^{1/2} W_j)^\top & -P \end{bmatrix} < 0, \tag{8.47}$$

$$\begin{bmatrix} -rP & qP + A_j P + B_j W_j \\ qP + PA_j^\top + W_j^\top B_j^\top & -rP \end{bmatrix} < 0. \tag{8.48}$$

where a feedback gain is given by $K_{c,j} = W_j P^{-1}$.

Remark 8.1. It is important to note that the optimal solution from the planner in online mode may fail to exist. For such cases, the planner and controller optimization problems are solved separately. It means that the robust LMI problem is solved by an optimal offline trajectory planner that calculates the best trajectory under the constraints of the circuit. Then, the controller part using that trajectory as references for tracking the best path under the same constraints.

8.5 Simulation results and discussion

The performance of the proposed approach involving a planner that includes battery energy management and tracking controller is assessed with a case study based on the

Berkeley autonomous racing vehicle. This vehicle can be modelled using the non-linear model (3.34)-(3.36) with the parameters presented in Table 8.1.

An *oval* circuit is chosen for assessing the proposed strategy that endeavors to cover various driving conditions as acceleration platforms and speed loss on curves also driving on different road situations. Therefore, there exist the unknown friction forces related to the different situations which is considered as disturbances. According to the different velocity and circuit shape, a trajectory planner has responsibility for creating a feasible trajectory by using a polynomial curve production method [15]. In addition, computing consecutive and differentiable curves (accelerations and velocities) under an overall constrained vehicle acceleration are consisted. Hence, in an on-line mode, the planner algorithm including the health management creates the linear and angular velocity references plus requested positions and orientations for the control loop.

The planner tuning is based on finding a best trade-off between maximizing the battery RUL and minimizing lap time In order to achieve the best performance, the small values of LQR parameters $(Q1, R)$ are considered inside the planner optimization problem presented in Table 8.1.

Figure 8.2 presents the trajectory path that obtained using the planner based on the *oval* circuit shape with and without considering maximization of the RUL objective (8.30) inside the robust LMI problem of planner. From Figure 8.2, it can observed that

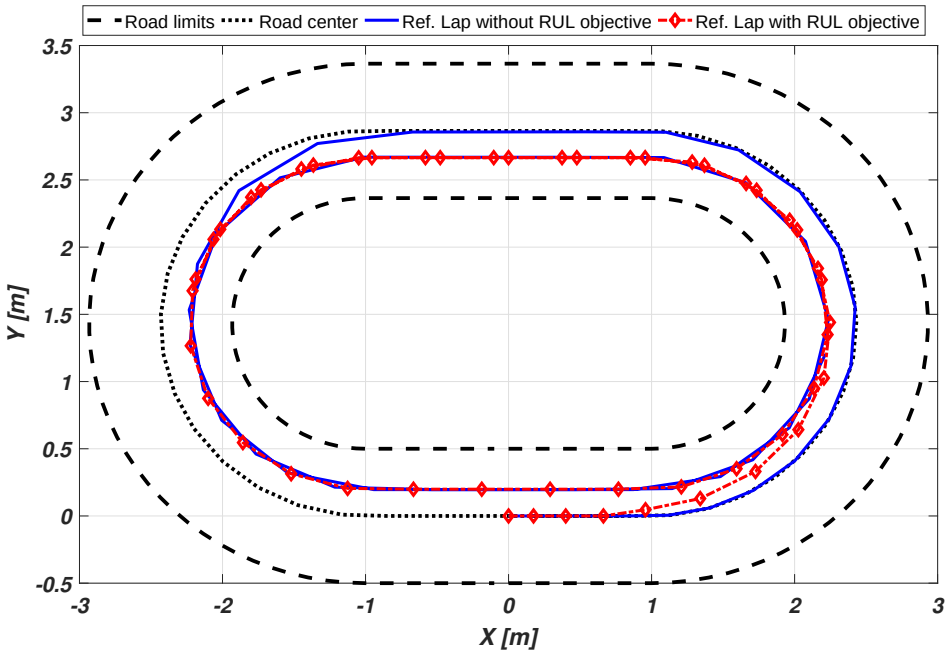

Figura 8.2: Comparison of planner racing laps with and without RUL objective.

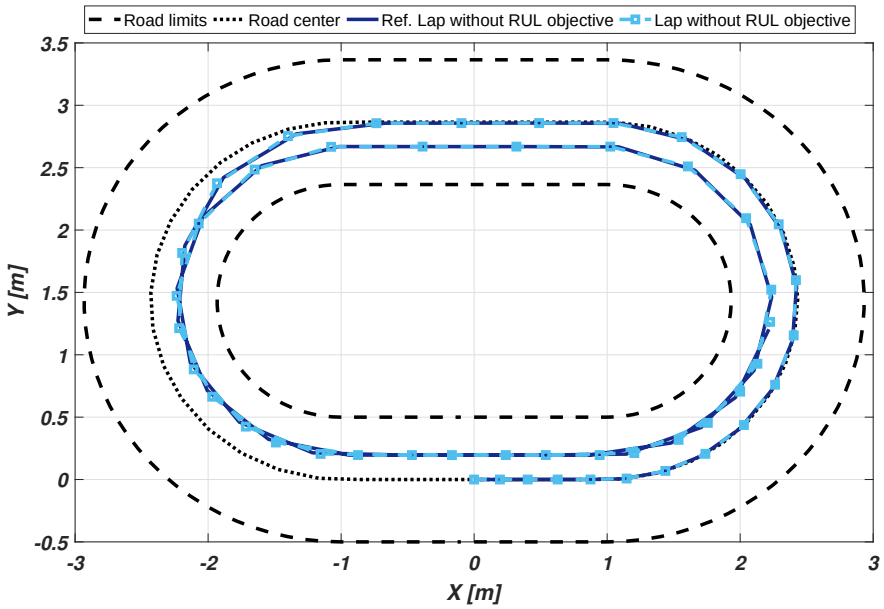

Figura 8.3: The reference and response of racing lap without RUL objective.

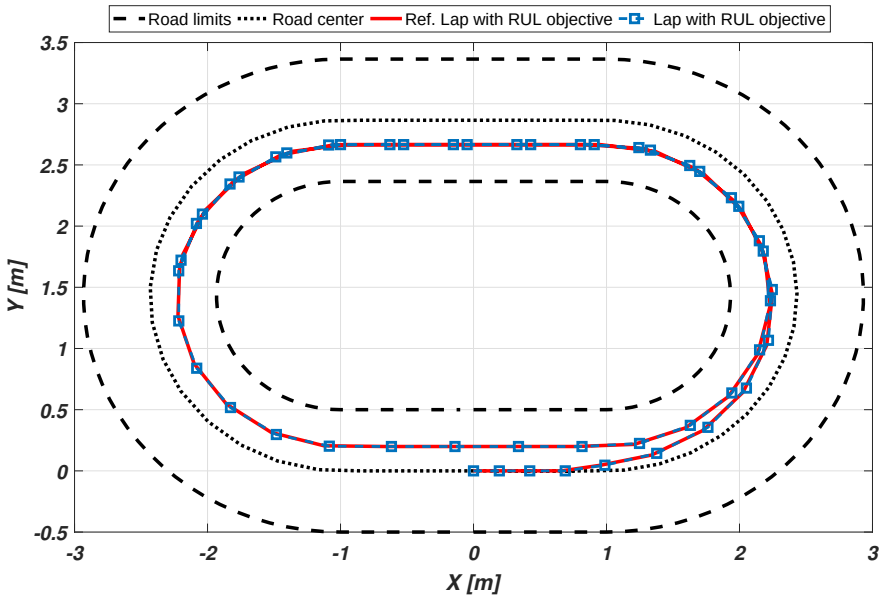

Figura 8.4: The reference and response of racing lap with RUL objective.

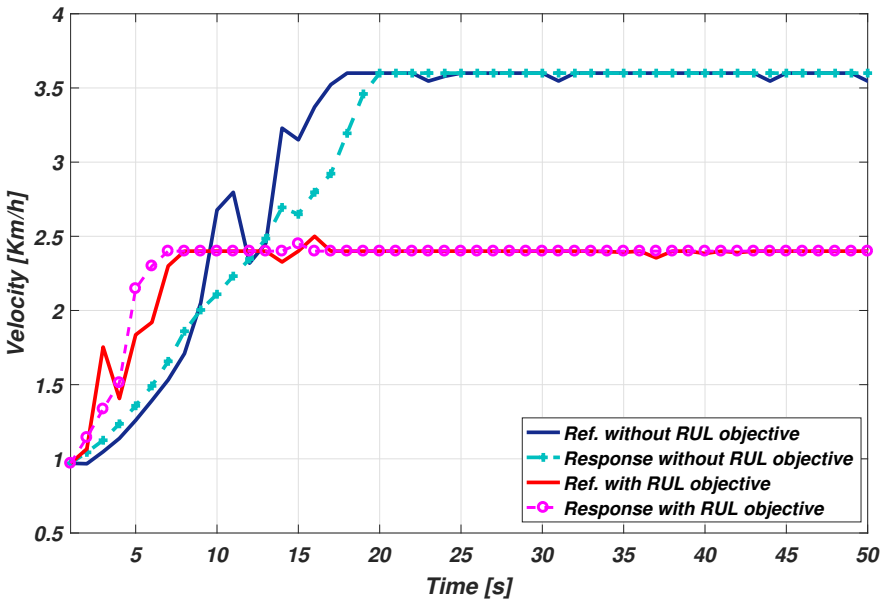

Figura 8.5: Comparison of the velocity with and without the RUL objective.

the racing trajectory of the planner in the case of the RUL objective after some iteration goes to close to the lower bound of the circuit for saving the energy of battery. However, at the same time the trajectory lap is shorter than without the RUL criteria which makes a small trade-off between maximizing the battery RUL and optimizing the time.

According to the general control approach Figure 8.1, the solution of the planner optimization problem (upper layer) will be used as reference variables for the controller optimization problem (low layer). In the control optimization, the tuning aims to minimize the velocity and lateral errors while computing smooth control actions for the vehicle. The weighting matrices are founded by iterative tuning until the desired performance is achieved. The values of the parameters is used in the simulation are presented in Table 1.

Figures 8.3 and 8.4 show the optimal results of the tracking of the trajectory path that achieved, in an online mode, by the planner without and with considering the RUL objective, respectively. According to these figures, it can observed that the controller is able perfectly to track the optimal trajectory provided by the planner in both cases.

Figure 8.5 presents the reference and the response of the longitudinal velocity profile in both scenario of the RUL objective. From this figure, it can be observed that in the scenario with RUL criteria, the response of velocity from the planner is modified based on the RUL and it is less than the velocity without the RUL criteria. In both scenarios, the results from the controller tracking part are quite good and the response of velocity

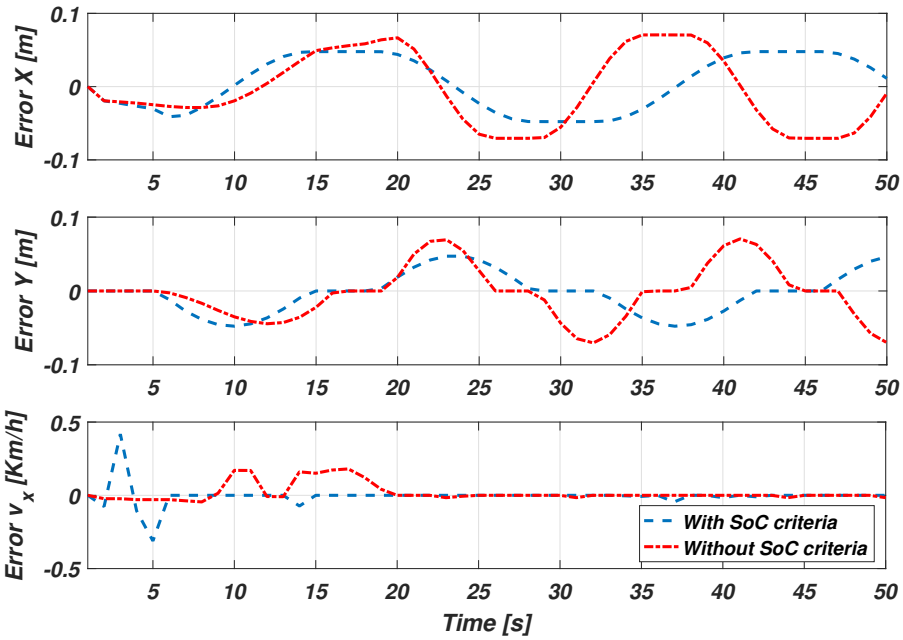

Figura 8.6: Error achieved during the simulation racing laps.

have tracked the reference from the planner.

The good performance of the controller tracking is shown in Figure 8.6. It can be perceived that the controller is able to reduce the errors to zero in spite of the complexity of driving in a high lateral acceleration situation. The comparison of the RUL of battery is presented in the Figure 8.7, where it can be seen the battery RUL is increased 11.71 according to the solving the robust LMI of planner without the RUL objective.

To evaluate the effectiveness and RUL efficiency of the presented approach based on the robust LMI problem, the response of the tracking controller from the system model including the friction force disturbance and measurement noise with the system model without them are compared in Figure 8.8. Moreover, Figure 8.9 depicts the response of the longitudinal velocity profile in both scenario of the friction force disturbance and measurement noise where the level of noise considered as random value of 20% of steady-state level of velocity and friction force disturbance is shown in Figure 8.10.

Furthermore, to show the differences of time scale between the upper layer and lower layer, the position of closed loop poles from both layers in a specific operating point are illustrated in Figure 8.11. From this figure, it can be observed that the poles of both loops satisfy the stability of the system behaviors. According to using LPV framework model and varying of the linear models can not be used fixed eigenvalue in closed loop but, in every iteration try to force and obtain the poles near to zero. Moreover, the

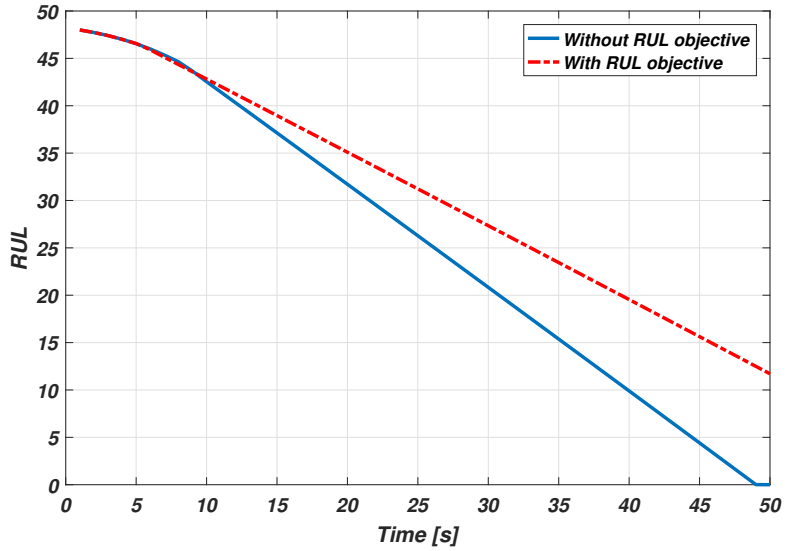

Figura 8.7: Comparison of the battery RUL.

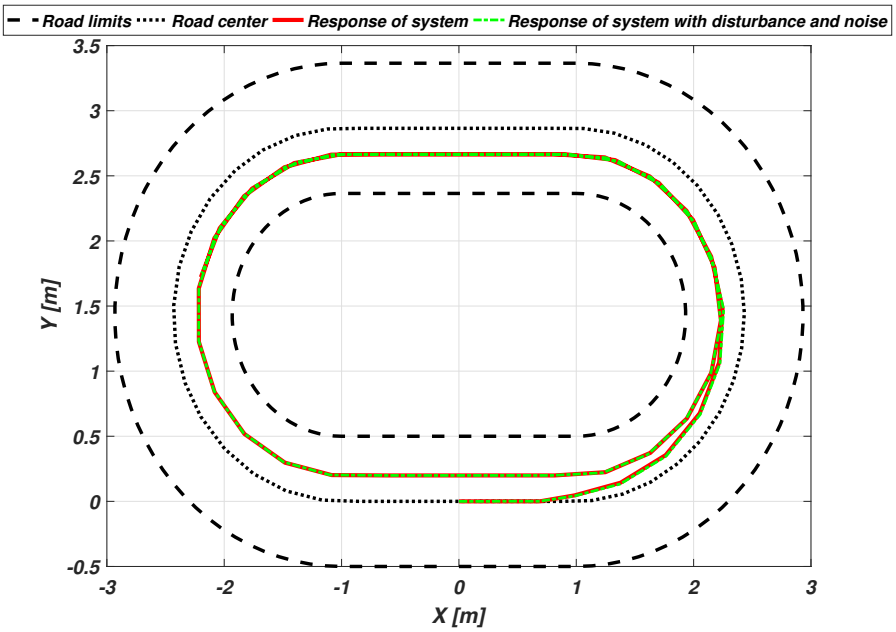

Figura 8.8: Comparison of the Response with and without the disturbance and noise with RUL objective

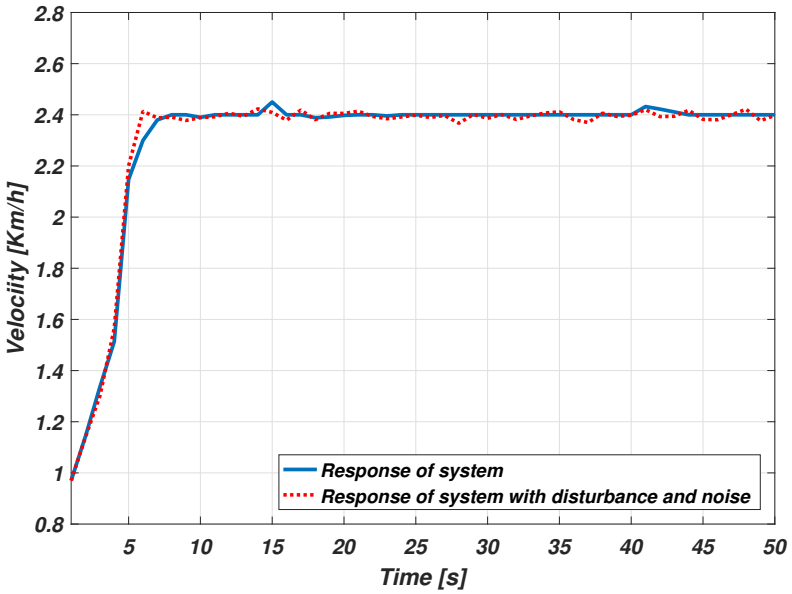

Figura 8.9: Comparison of the velocity with and without the disturbance and noise with RUL objective.

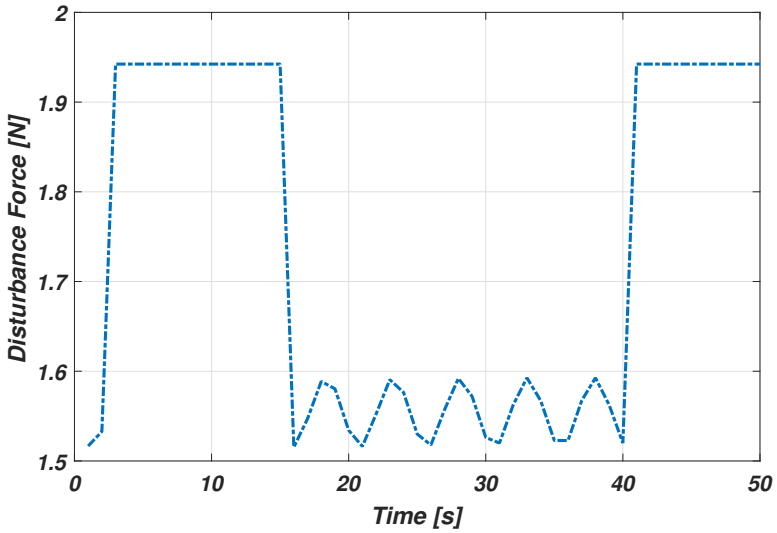

Figura 8.10: Friction force disturbance.

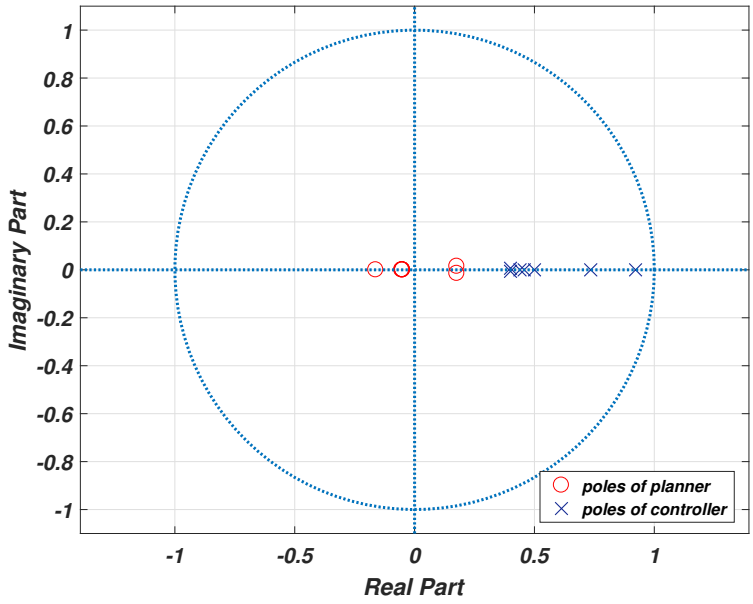

Figura 8.11: Poles positions of the planner and controller in a particular operating point.

Taula 8.1: Model parameters value.

Parameter	Value	unit
l_f	0.125	m
l_r	0.125	m
C_f	68	N/rad
C_r	71	N/rad
C_d	0.36	N/rad
I	0.03	kg/m^2
m	1.98	kg
μ	0.5	N/rad
ρ	1.184	kg/m^3
A_r	1.91	m^2
T_s	0.1	s
$SoC_{threshold}$	0.1	

poles position from the two layers are shows the dynamic behaviour of low layer is faster than upper layer.

8.6 Summary

This chapter has proposed methodology for autonomous steering a vehicle based on the robust LMI-based MPC approach. The nonlinear model of vehicle is modified by including the time and the battery model as states into the vehicle model. Then, to take into account the nonlinearities of the vehicle, the nonlinear model is transformed into an LPV model using a polytopic approach. The proposed approach is designed to solve driving control problems and at the same time to maintain and minimize the consumption of the battery energy. The proposed solution is divided into two layers with different time scale: path planner and controller. The pole placement approach is used dynamic decoupling between both layers. The optimal planning algorithm minimizes the lap time while at the same time maximizes the lifetime of battery. The controller is designed using a LPV-LQR approach using LMI formulation. The model of the controller is augmented with integral action for improving the trajectory tracking obtained on-line by the planner. To evaluate the effectiveness and RUL efficiency of the presented approach, the force friction disturbance and noise is considered inside the system. The strategies are tested in simulation using the Berkeley autonomous vehicle with different scenarios including the comparison of system behaviours and battery RUL. The results show that the RUL of the battery is maximized in all scenarios. For future research, it would be interesting to consider the fault in the system and implementing the proposed approach on the real benchmark of the vehicle.

The content of this chapter was based on the following works:

F. Karimi Pour, D. Theilliol, V. Puig, and G. Cembrano. Health-aware Optimization-based Control Design: Application to Autonomous Racing based State of Charge. 4^{th} *In 2019 4th Conference on Control and Fault Tolerant Systems (SysTol)*, (pp. 244-249), IEEE. Morocco, 2019.

F. Karimi Pour, D. Theilliol, V. Puig, and G. Cembrano. Health-aware Control Design based on Remaining Useful Life Estimation for Autonomous Racing Vehicle. Accepted in *ISA Transactions*.

Part IV

Conclusions and perspectives

Capítol 9

Concluding Remarks

As a concluding remark, the objectives proposed in the beginning of the thesis were fulfilled. Furthermore, during the thesis development new objectives and tasks have appeared that enrich the proposed approaches and have complemented the obtained results. Therefore, this chapter summarizes the main contributions of the thesis. It is worth mentioning that these contributions were reported at each corresponding chapter. Furthermore, the proposal of future ways to continue the research developed in the thesis will be pointed out in this chapter.

9.1 Conclusions

In the following, the contributions related to the different proposed objectives are summarized.

- Develop an economic MPC strategy for nonlinear systems
  - The nonlinear systems have been transformed into quasi-LPV/TS models
  - The optimization problem has been exploited as a functional dependency of scheduling variables and state vector to develop a prediction strategy with a numerically suitable solution.
  - the economic optimization problem is solved by using a series of QP problems at each time instant.
  - The stability of the proposed approach has been certified and investigated.
  - The rigorous analysis of using terminal penalties and terminal regions instead of a terminal equality constraint for guarantying the stability of EMPC control scheme based on the LPV/TS models has been provided.
  - The comparison between standard EMPC and the proposed approach has been performed in order to show the proposed approach is less conservative and computationally quite effective.

  - The proposed algorithm for EMPC strategy based on the quasi-LPV/TS has been illustrated through a pasteurization plant as a case study while it is described by a quasi-LPV model/ TS models.

- Design a MPC controller for nonlinear system with varying delays affecting states and inputs by using LPV framework.

  - The new MPC strategy based on LPV models with varying delays affecting states and inputs has been provided.
  - The proposed control approach allows the controller to accommodate the scheduling parameters and delay change.
  - By computing the prediction of the state variables and delay along a prediction time horizon, the system model can be modified according to the evaluation of the estimated state and delay at each time instant.
  - The prediction of the state variables and delay have been computed along a prediction time horizon.
  - The system model has been modified according to the evaluation of the estimated state and delay at each time instant.
  - A pasteurization plant system has been used as a case study to demonstrate the effectiveness of the proposed approach.

- Modeling the degradation of actuators and reliability of system/actuators as a function of affected by control actions.

  - The damage is assessed with the rainflow-counting algorithm that allows to estimate the components fatigue.
  - The accumulated damage has been obtained as a function of time instead of the number of cycles.
  - The MPC controller objective has been modified by adding an extra criterion that takes into account the accumulated damage plus including the economic objective.
  - Two different health-aware economic predictive control strategies have been proposed that aims minimizing the damage of components.
  - The single-layer predictive controller by including integral action to eliminate steady state offset by adding extra criterion has been provided.
  - The multi-layer health-aware MPC controller based on two optimization layer has implemented with different time-scale.
  - To achieve the advisable trade-off between minimal accumulated damage and operational costs, both control strategies have been compared.
  - Both control schemes have been satisfactorily implemented using high-fidelity simulator of a utility-scale pasteurization plant.

- Develop a health-aware MPC for a complex system

  - a health-aware MPC-LPV controller on the basis of PHM information has been provided by the on-line evaluation of the system reliability.
  - The actuator reliability has been modelled using an exponential function of the control input.
  - The system reliability is determined from the combination of each actuator reliability taking into account the interconnection topology.
  - The system reliability has been introduced as state variables inside the control model, which includes nonlinear term and it have been changed in a linear-like form through the LPV structure.
  - The proposed health-aware MPC-LPV control approach has been effectually solved iteratively by a series of QP problems that applies an update MPC model updated through the scheduling parameters estimated at each time instant.
  - The economic health-aware MPC for a complex system has been developed to extend the components and system reliability based on a finite horizon stochastic optimization problem with joint probabilistic (chance) constraints in order to manage dynamically designate safety stocks in the system.
  - The proposed approach has been applied to a part of a real drinking water transport network of Barcelona for demonstrating the performance of the method.

- Design and develop health-aware control strategy based on remaining useful life estimation using a LPV-LQR approach.

  - The health-aware control design has been provided for a racing vehicle that generates an optimal path for the racing by optimizing the lap time and maximizing the RUL of the battery in the planner.
  - A new control has been designed to solve driving control problems and at the same time to maintain and minimize the consumption of the battery energy.
  - The Remaining Useful Life (RUL) of the battery has been obtained according to estimate the state of charge (SoC) of the battery.
  - The new model of the vehicle has been presented by including the lap time and SoC of battery.
  - The control design has been divided into two layers with different time scale, path planner and controller.
  - The optimization problem of path planner has been solved where the objective is to optimize the lap time and maximize the battery RUL to obtain the best trajectory under the constraints of the circuit.
  - The second optimization problem of controller gain with integral action for tracking the trajectory has been obtained by an optimal on-line from the planner.
  - Both optimization problems are solved via a set of robust Linear Matrix Inequality (LMI) based on the MPC for LPV model of vehicle by subject to input and output constraints.

9.2 Future Research

There are still some open problems regarding the role of evolutionary health aware controller for the industrial systems. Some suggested ideas for future directions are outlined next:

- The stability results for EMPC controller based on the LPV models have been obtained. It is still an open problem to proof the stability and feasibility of proposed approach for the system with varying delay in state and input.
- The contributions regarding the design of MPC-LPV controller have been presented for systems without the disturbance and noise. It would be interesting to extend the design methodologies for system by considering the uncertainty and sensitivity of disturbance in the model.
- The health-aware MPC control approach has been applied in systems which work in healthy operation. It would be interesting to investigate the proposed approach based on enhancing the sensitivity of faults in actuators or system.
- The contributions regarding predication of the reliability have been proposed based on the exponential function model. The prediction of the reliability of component or system can be obtained based on other approach and it would be investigating the results of their comparison.
- The health-aware control have been used based on the model of the degradation or reliability and subsequently RUL. It would be interesting to use the data of the system degradation or reliability and use machine-learning for modeling the system degradation or reliability.

Part V

Appendices

Appendix A

Pasteurization Plant

Taula A.1: Time constants and gains of the hot-water tank

	Parameters			
F_h(ml/min)	τ_1(s)	τ_2(s)	K_1	K_2
150	0.6268	0.0597	1636	1638
230	0.7213	0.0448	1219	1219
300	0.7707	0.0367	993	993
400	0.8176	0.0292	784	784
550	0.8585	0.0223	593	593

Taula A.2: Time constants of the G_{ij} transfer functions

	Parameters	
F_h(ml/min)	τ_1(s)	τ_2(s)
F_h(ml/min)	τ_{21}(s)	
155	14	53
180	21	40
230	25	26
305	28	18
410	25	14
557	29	13
694	9	9

For obtaining the pasteurization model, physical principle based fundamental laws

Taula A.3: Gains of the G_{ij} transfer functions

	Gains		
$R = F_h/F_c$	K_{22}	K_{21}	K_{12}
0.238	0.757	0.243	0.926
0.46	0.533	0.435	0.87
1.11	0.317	0.68	0.606
1.22	0.35	0.65	0.57
1.57	0.27	0.729	0.47
1.61	0.257	0.742	0.468
1.66	0.246	0.753	0.455
1.8	0.15	0.849	0.476
1.88	0.154	0.845	0.46
1.94	0.197	0.8	0.428
2.17	0.183	0.816	0.388
2.7	0.165	0.834	0.34
3.85	0.068	0.928	0.257
4.06	0.055	0.94	0.25

Taula A.4: The adjusted parameters

Parameter	Value	Parameter	Value
α_1	2.2×10^{-4}	α_{14}	4×10^{-4}
α_2	1.6×10^{-4}	α_{15}	3.96×10^{-1}
α_3	3.74×10^{-3}	α_{16}	16.8154
α_4	10^{-4}	α_{17}	6.814×10^{-2}
α_5	3.09×10^{-2}	α_{18}	2.68×10^{-1}
α_6	1.44×10^{-1}	α_{19}	16.3567
α_7	1.8×10^{-3}	α_{20}	9.62×10^{-4}
α_8	4.8×10^{-4}	α_{21}	4
α_9	6.54×10^{-2}	α_{22}	1.87×10^{-1}
α_{10}	5.18×10^{-3}	α_{23}	11.81
α_{11}	2.5×10^{-3}	α_{24}	269.44
α_{12}	22×10^{-2}	α_{25}	5.8×10^{-4}
α_{13}	1.16×10^{-3}		

such as energy balances and heat exchanger design are utilized to describe the main

processes of the plant. Therefore, Energy balance and Bernoulli's law give

$$\begin{aligned}\frac{dT_1}{dt} =& \frac{2}{M_1 C_P}(-UA\frac{T_1(t)+T_4(t-\tau)}{2} - T_a) \\ & - F_1 C_p(T_1(t) - T_4(t-\tau)) - \frac{dT_4(t-\tau)}{dt}\end{aligned} \tag{A.1a}$$

$$\begin{aligned}\frac{dT_2}{dt} =& \alpha_1 P(t) - F_2 C_p(T_2(t) - T_2 r(t)) \\ & - \alpha_2 T_2(t) + \alpha_3\end{aligned} \tag{A.1b}$$

$$\begin{aligned}\frac{dT_{2r}}{dt} =& F_1(T_4(t) - T_{in}(t)) + \alpha_4 F_2(T_2(t) - T_{2r}(t)) \\ & - \alpha_5(T_2(t) - T_a) - \alpha_6 - \alpha_7 N_1(t) \\ & (T_4(t) - T_{in}(t)) + \alpha_8 N_2(t)(T2(t) - T_{2r}(t)) \\ & - \alpha_9(T_4(t) - T_{in}(t)) + \alpha_{10}(T_2(t) - T_{2r}(t))\end{aligned} \tag{A.1c}$$

$$\begin{aligned}\frac{dT_4}{dt} =& - F1(T_4(t) - Tin(t)) + \alpha_{11} F_2(T_2(t) - T2r(t)) \\ & - \alpha_{12} - \alpha_{13} N_1(t)(T_4(t) - Tin(t)) \\ & + \alpha_{14} N_2(t)(T_2(t) - T2r(t))\end{aligned} \tag{A.1d}$$

$$\frac{dT_{in}}{dt} = \frac{\alpha_{15}(N_1(t) - \alpha_{16})(T_1(t) - T_{in}(t))}{M_2} \tag{A.1e}$$

where

$$\begin{aligned}F_1 &= \alpha_{17}(N_1(t) - \alpha_{16}), \\ F_2 &= \alpha_{18}(N_2(t) - \alpha_{19}),\end{aligned}$$

and the delay of system is

$$\begin{aligned}\tau(t) =& - \alpha_{20} - \alpha_{21}(N_1(t))^3 + \alpha_{22}(N_1(t))^2 \\ & - \alpha_{23} N_1(t) + \alpha_{24}.\end{aligned}$$

The value of arrays of state-space matrices for the controller used in the pasteurization model 2 are presented below.

$$
\begin{aligned}
a_{11} &= \frac{-UA}{M_1 C_p} - F_1 C_p \\
a_{22} &= -F_2 C_p - \alpha_2 \\
a_{23} &= F_2 C_p \\
a_{32} &= F_2 \alpha_4 + N_2(k)\alpha_8 + \alpha_{10} - \alpha_5 \\
a_{33} &= -F_2 \alpha_4 - N_2(k)\alpha_8 - \alpha_{10} \\
a_{34} &= -N_1(k)\alpha_7 + F_1 - \alpha_9 \\
a_{35} &= N_1(k)\alpha_7 - F_1 + \alpha_9 \\
a_{42} &= F_2 \alpha_{11} + N_2(k)\alpha_{14} \\
a_{43} &= -F_2 \alpha_{11} - N_2(k)\alpha_{14} \\
a_{44} &= -N_1(k)\alpha_{13} - F_1 \\
a_{45} &= N_1(k)\alpha_{13} + F_1 \\
a_{53} &= \frac{\alpha_{15}(N_1(k) - \alpha_{16})}{M_2} \\
a_{55} &= \frac{-\alpha_{15}(N_1(k) - \alpha_{16})}{M_2} \\
b_{11} &= -\alpha_{17} C_p (T_1(k) - T_4(k-\tau)) \\
b_{22} &= -\alpha_{18} C_p (T_2(k) - T_{2r}(k)) \\
b_{23} &= \alpha_1 \\
b_{31} &= (\alpha_{17} - \alpha_7)(T_4(k) - T_{in}(k)) \\
b_{32} &= (\alpha_{18}\alpha_{14} + \alpha_8)(T_2(k) - T_{2r}(k)) \\
b_{41} &= (-\alpha_{17} - \alpha_7)(T_4(k) - T_{in}(k)) \\
b_{42} &= (\alpha_{18}\alpha_{11} + \alpha_{14})(T_2(k) - T_{2r}(k)) \\
b_{51} &= \frac{\alpha_{15}(T_{2r}(k) - T_{in}(k))}{M_2} \\
b_{d,11} &= \alpha_{25} T_a \\
b_{d,21} &= \alpha_3 \\
b_{d,31} &= \alpha_5 T_a - \alpha_6 \\
b_{d,41} &= \alpha_{12} \\
a_{\tau,12} &= -F_2 \alpha_{11} - N_2(k)\alpha_{14} \\
a_{\tau,13} &= F_2 \alpha_{11} + N_2(k)\alpha_{14} \\
a_{\tau,14} &= \frac{UA}{M_1 C_p} + F_1 C_p + F_1 + \alpha_{13} N_1(k) \\
a_{\tau,15} &= \alpha_{13} N_1(k) - F_1 \\
b_{\tau,11} &= (\alpha_{17} + \alpha_{13})(T_4(k-\tau) - T_{in}(k-\tau)) \\
b_{\tau,12} &= (-\alpha_{11}\alpha_{18} - \alpha_{14})(T_2(k-\tau) - T_{2r}(k-\tau))
\end{aligned}
\tag{A.2}
$$

Appendix B

Racing Vehicle

The value of arrays of state-space matrices for the controller used in the racing vehicle model are presented below.

$$
\begin{aligned}
a_{11} &= \frac{-\mu g}{v_x}, & a_{13} &= \frac{C_f l_f \sin(\delta)}{m v_x} + v_y, \\
a_{12} &= \frac{C_f \sin(\delta)}{m v_x}, & a_{22} &= -\frac{C_r + C_f \cos(\delta)}{m v_x}, \\
a_{23} &= -\frac{C_f l_f \cos(\delta) - C_r l_r}{m v_x} - v_x, & a_{32} &= -\frac{C_f l_f \cos(\delta) - C_r l_r}{I v_x}, \\
a_{33} &= -\frac{C_f l_f^2 \cos(\delta) + C_r l_r^2}{I v_x}, & a_{45} &= v_x, \\
a_{52} &= -\frac{\kappa}{1 - e_y \kappa}, & a_{53} &= \frac{\kappa \sin(e_\theta)}{1 - e_y \kappa}, \\
a_{61} &= \frac{\cos(e_\theta)}{1 - e_y \kappa}, & a_{62} &= -\frac{\sin(e_\theta)}{1 - e_y \kappa}, \\
a_{71} &= -\frac{1}{2} C_d \rho A_r - \mu m g, & b_{11} &= -\frac{1}{m} \sin(\delta) C_f, \\
b_{21} &= \frac{1}{m} \cos(\delta) C_f, & b_{31} &= \frac{1}{m} \cos(\delta) C_f l_f.
\end{aligned}
\tag{B.1}
$$

Appendix C

Some Lemma

Lemma C.1. *(cf. [25]) Let $F_0, F_0, ..., F_p$ be quadratic functions of the variable $\omega \in \mathbb{R}_{n_x}$, i.e.*

$$F_i(\omega) \triangleq \omega^\top M_i \omega + 2y_i^\top + z_i,$$

for all $i \in \mathbb{I}_{1,p}$, while $y_i \in \mathbb{R}_{n_x}, M_i^\top = M_i \in \mathbb{R}^{n_x \times n_x}$ and $z_i \in \mathbb{R}$. If there exists a scalar $\omega > 0$, such that for ω

$$F_0(\omega) - \sum_{i=1}^{p} \omega F_i(\omega) \leq 0,$$

hence, $F_0(\omega) \leq 0$ for all ω such that $F_i(\omega) \leq 0$ for all $i \in \mathbb{I}_{1,p}$.

Lemma C.2. *(cf. [225]) Let $M \in \mathbb{R}^{n_x \times n_x}, y \in \mathbb{R}$ and $z \in \mathbb{R}$. The inequality*

$$x^\top M x + 2y^\top + c \leq 0$$

is proved for all $x \in \mathbb{R}^{n_x}$ if and only if

$$\begin{bmatrix} M & y \\ y^\top & z \end{bmatrix} \preceq 0.$$

Bibliografia

[1] P. Aadaleesan, N. Miglan, R. Sharma, and P. Saha. Nonlinear system identification using Wiener type Laguerre–Wavelet network model. *Chemical Engineering Science*, 63(15):3932–3941, 2008.

[2] J. Abonyi, L. Nagy, and F. Szeifert. Fuzzy model-based predictive control by instantaneous linearization. *Fuzzy Sets and Systems*, 120(1):109–122, 2001.

[3] R. Ahmad and S. Kamaruddin. An overview of time-based and condition-based maintenance in industrial application. *Computers & Industrial Engineering*, 63(1):135–149, 2012.

[4] F. Ahmadzadeh and J. Lundberg. Remaining useful life estimation. *International Journal of System Assurance Engineering and Management*, 5(4):461–474, 2014.

[5] C. F. Alastruey, M. De la Sen, and M. García-Sanz. Modelling and identification of a high temperature short time pasteurization process including delays. In *Proceedings of the 7th Mediterranean Conference on Control and Automation*, pages 28–30, Israel, 1999.

[6] E. Alcala, V. Puig, J. Quevedo, and T. Escobet. Gain-scheduling lpv control for autonomous vehicles including friction force estimation and compensation mechanism. *IET Control Theory & Applications*, 12(12):1683–1693, 2018.

[7] R. N. Allan et al. *Reliability evaluation of power systems*. Springer Science & Business Media, 2013.

[8] R. Amrit, J. B. Rawlings, and D. Angeli. Economic optimization using model predictive control with a terminal cost. *Annual Reviews in Control*, 35(2):178–186, 2011.

[9] A. Angeli, D.and Casavola and F. Tedesco. On average performance of economic model predictive control with time-varying cost and terminal constraints. In *American Control Conference (ACC), 2015*, pages 2974–2979. IEEE, 2015.

[10] D. Angeli, R. Amrit, and J. B. Rawlings. On average performance and stability of economic model predictive control. *IEEE transactions on automatic control*, 57(7):1615–1626, 2012.

[11] H. X. Araújo, A. G. Conceição, G. H. Oliveira, and J. Pitanga. Model predictive control based on lmis applied to an omni-directional mobile robot. *IFAC Proceedings Volumes*, 44(1):8171–8176, 2011.

[12] Armfield. *Process Plant trainer PTC23-MKII, Instruction Manual.* 2015.

[13] G. Awuah, H. Ramaswamy, and A. Economides. Thermal processing and quality: Principles and overview. *Chemical Engineering and Processing: Process Intensification*, 46(6):584–602, 2007.

[14] G. B. Baecher and J. T. Christian. *Reliability and statistics in geotechnical engineering.* John Wiley & Sons, 2005.

[15] C. L. Bianco, A. Piazzi, and M. Romano. Velocity planning for autonomous vehicles. In *IEEE Intelligent Vehicles Symposium, 2004*, pages 413–418. IEEE, 2004.

[16] F. Bicking, P. Weber, and D. Theilliol. Reliability importance measures for fault tolerant control allocation. In *Control and Fault-Tolerant Systems (SysTol), 2013 Conference on*, pages 104–109. IEEE, 2013.

[17] F. Bicking, P. Weber, D. Theilliol, and C. Aubrun. Control allocation using reliability measures for over-actuated system. In *Intelligent Systems in Technical and Medical Diagnostics*, pages 487–497. Springer, 2014.

[18] R. B. Billings and C. V. Jones. *Forecasting urban water demand.* American Water Works Association, 2011.

[19] J. D. Birdwell, D. A. Castanon, and M. Athans. On reliable control system designs. *IEEE transactions on systems, man, and cybernetics*, 16(5):703–711, 1986.

[20] W. R. Blischke and D. P. Murthy. *Reliability: modeling, prediction, and optimization*, volume 767. John Wiley & Sons, 2011.

[21] C. M. Böhm. *Predictive control using semi-definite programming-efficient approaches for periodic systems and Lur'e systems.* Logos-Verlag, 2011.

[22] J. Bon, G. Clemente, H. Vaquiro, and A. Mulet. Simulation and optimization of milk pasteurization processes using a general process simulator (prosimplus). *Computers & chemical engineering*, 34(3):414–420, 2010.

[23] S. Bououden, M. Chadli, L. Zhang, and T. Yang. Constrained model predictive control for time-varying delay systems: application to an active car suspension. *International Journal of Control, Automation and Systems*, 14(1):51–58, 2016.

[24] S. Boyd, L. El Ghaoui, E. Feron, and V. Balakrishnan. *Linear matrix inequalities in system and control theory*, volume 15. Siam, 1994.

[25] S. Boyd, L. El-Ghaoui, E. Feron, V. Balakrishnan, and E. Yaz. Linear matrix inequalities in system and control theory. *Proceedings of the IEEE*, 85(4):698–699, 1997.

[26] K. A. Brookhuis, D. De Waard, and W. H. Janssen. Behavioural impacts of advanced driver assistance systems–an overview. *European Journal of Transport and Infrastructure Research*, 1(3), 2019.

[27] M. Brunner, U. Rosolia, J. Gonzales, and F. Borrelli. Repetitive learning model predictive control: An autonomous racing example. In *2017 IEEE 56th Annual Conference on Decision and Control (CDC)*, pages 2545–2550. IEEE, 2017.

[28] M. Bujarbaruah, X. Zhang, H. E. Tseng, and F. Borrelli. Adaptive mpc for autonomous lane keeping. *arXiv preprint arXiv:1806.04335*, 2018.

[29] P. Bumroongsri. An offline formulation of MPC for LPV systems using linear matrix inequalities. *Journal of Applied Mathematics*, pages 1–13, 2014.

[30] P. Bumroongsri and S. Kheawhom. MPC for LPV systems based on parameter-dependent Lyapunov function with perturbation on control input strategy. *Engineering Journal*, 16(2):61–72, 2012.

[31] G. C. Calafiore, F. Dabbene, and R. Tempo. Research on probabilistic methods for control system design. *Automatica*, 47(7):1279–1293, 2011.

[32] E. F. Camacho and C. Bordons. *Model Predictive Control*. Springer-Verlag, Germany, 2004.

[33] Y.-Y. Cao and P. M. Frank. Stability analysis and synthesis of nonlinear time-delay systems via linear takagi–sugeno fuzzy models. *Fuzzy sets and systems*, 124(2):213–229, 2001.

[34] B. Capron, M. Uchiyama, and D. Odloak. Linear matrix inequality-based robust model predictive control for time-delayed systems. *IET control theory & applications*, 6(1):37–50, 2012.

[35] A. Casavola, D. Famularo, and G. Franze. A feedback min-max MPC algorithm for LPV systems subject to bounded rates of change of parameters. *IEEE Transactions Automatic Control*, 47(7):1147–1153, 2002.

[36] G. Cembrano, J. Quevedo, V. Puig, R. Pérez, J. Figueras, J. Verdejo, I. Escaler, G. Ramón, G. Barnet, P. Rodríguez, et al. Plio: a generic tool for real-time operational predictive optimal control of water networks. *Water Science and Technology*, 64(2):448–459, 2011.

[37] G. Cembrano, J. Quevedo, M. Salamero, V. Puig, J. Figueras, and J. Martı. Optimal control of urban drainage systems. a case study. *Control engineering practice*, 12(1):1–9, 2004.

[38] D. Chen, W. Zhao, J. C. Sprott, and X. Ma. Application of takagi–sugeno fuzzy model to a class of chaotic synchronization and anti-synchronization. *Nonlinear Dynamics*, 73(3):1495–1505, 2013.

[39] X. Chen, M. Heidarinejad, J. Liu, and P. D. Christofides. Distributed economic mpc: Application to a nonlinear chemical process network. *Journal of Process Control*, 22(4):689–699, 2012.

[40] Z. Chen and S. Zheng. Lifetime distribution based degradation analysis. *IEEE Transactions on Reliability*, 54(1):3–10, 2005.

[41] H. Cheng and A. Friis. Operability and flexibility of a milk production line. *Food and Bioproducts Processing*, 85(4):372–380, 2007.

[42] M. Chilali and P. Gahinet. H/sub/spl infin//design with pole placement constraints: an lmi approach. *IEEE Transactions on automatic control*, 41(3):358–367, 1996.

[43] S. E. Christodoulou. Water network assessment and reliability analysis by use of survival analysis. *Water resources management*, 25(4):1229–1238, 2011.

[44] P. S. Cisneros, S. Voss, and H. Werner. Efficient nonlinear model predictive control via quasi-lpv representation. In *Decision and Control (CDC), 2016 IEEE 55th Conference on*, pages 3216–3221. IEEE, 2016.

[45] D. Davis. An analysis of some failure data. *Journal of the American Statistical Association*, 47(258):113–150, 1952.

[46] J. V. De Oliveira and J. M. Lemos. Long-range predictive adaptive fuzzy relational control. *Fuzzy Sets and Systems*, 70(2-3):337–357, 1995.

[47] M. Diehl, R. Amrit, and J. B. Rawlings. A lyapunov function for economic optimizing model predictive control. *IEEE Transactions on Automatic Control*, 56(3):703–707, 2011.

[48] B. Ding. Dynamic output feedback predictive control for nonlinear systems represented by a takagi–sugeno model. *IEEE Transactions on Fuzzy Systems*, 19(5):831–843, 2011.

[49] B. Ding, Y. Xi, M. T. Cychowski, and T. Mahony. A synthesis approach for output feedback robust constrained model predictive control. *Automatica*, 44(1):258–264, 2008.

[50] D. Dolgov, S. Thrun, M. Montemerlo, and J. Diebel. Path planning for autonomous vehicles in unknown semi-structured environments. *The International Journal of Robotics Research*, 29(5):485–501, 2010.

[51] G.-R. Duan and H.-H. Yu. *LMIs in control systems: analysis, design and applications*. CRC press, 2013.

[52] A. El Hajjaji and S. Bentalba. Fuzzy path tracking control for automatic steering of vehicles. *Robotics and Autonomous Systems*, 43(4):203–213, 2003.

[53] H. M. Elattar, H. K. Elminir, and A. Riad. Prognostics: a literature review. *Complex & Intelligent Systems*, 2(2):125–154, 2016.

[54] M. Ellis and P. D. Christofides. Real-time economic model predictive control of nonlinear process systems. *AIChE Journal*, 61(2):555–571, 2015.

[55] M. Ellis, H. Durand, and P. D. Christofides. A tutorial review of economic model predictive control methods. *Journal of Process Control*, 24(8):1156–1178, 2014.

[56] T. Endo, K. Mitsunaga, and H. Nakagawa. Fatigue of metals subjected to varying stress?-prediction of fatigue lives. In *Preliminary Proceedings of the Chugoku-Shikoku District Meeting, Japanese Society of Mechanical Engineers, Tokyo*, 1967.

[57] S. M. Erlien. *Shared vehicle control using safe driving envelopes for obstacle avoidance and stability*. PhD thesis, Stanford University, 2015.

[58] T. Escobet, V. Puig, and F. Nejjari. Health aware control and model-based prognosis. In *Control & Automation (MED), 2012 20th Mediterranean Conference on*, pages 691–696. IEEE, 2012.

[59] T. Escobet, V. Puig, J. Quevedo, and D. Garcia. A methodology for incipient fault detection. In *Control Applications (CCA), 2014 IEEE Conference on*, pages 104–109. IEEE, 2014.

[60] T. Escobet, J. Quevedo, V. Puig, and F. Nejjari. Combining health monitoring and control. In *Diagnostics and prognostics of engineering systems: methods and techniques*, pages 230–255. IGI Global, 2013.

[61] Z. Fan and H. Chen. Study on path following control method for automatic parking system based on lqr. *SAE International Journal of Passenger Cars-Electronic and Electrical Systems*, 10(2016-01-1881):41–49, 2016.

[62] C. Fantuzzi and R. Rovatti. On the approximation capabilities of the homogeneous takagi-sugeno model. In *Fuzzy Systems, 1996., Proceedings of the Fifth IEEE International Conference on*, volume 2, pages 1067–1072. IEEE, 1996.

[63] A. Ferramosca, D. Limon, and E. F. Camacho. Economic mpc for a changing economic criterion for linear systems. *IEEE Transactions on Automatic Control*, 59(10):2657–2667, 2014.

[64] M. S. Finkelstein. A note on some aging properties of the accelerated life model. *Reliability Engineering & System Safety*, 71(1):109–112, 2001.

[65] E. Garone and A. Casavola. Receding horizon control strategies for constrained LPV systems based on a class of nonlinearly parameterized Lyapunov functions. *IEEE Transactions on Automatic Control*, 57(9):2345–2360, 2012.

[66] Y. Ge, J. Wang, and C. Li. Robust stability conditions for dmc controller with uncertain time delay. *International Journal of Control, Automation and Systems*, 12(2):241–250, 2014.

[67] A. Geletu, M. Klöppel, H. Zhang, and P. Li. Advances and applications of chance-constrained approaches to systems optimisation under uncertainty. *International Journal of Systems Science*, 44(7):1209–1232, 2013.

[68] I. Gertsbakh. *Reliability theory: with applications to preventive maintenance.* Springer, 2013.

[69] A. Ginart, I. Barlas, J. L. Dorrity, P. Kalgren, and M. J. Roemer. Self-healing from a phm perspective. In *Autotestcon, 2006 IEEE*, pages 697–703. IEEE, 2006.

[70] A. González, E. Adam, and J. Marchetti. Conditions for offset elimination in state space receding horizon controllers: A tutorial analysis. *Chemical Engineering and Processing: Process Intensification*, 47(12):2184–2194, 2008.

[71] N. Gorjian, L. Ma, M. Mittinty, P. Yarlagadda, and Y. Sun. A review on degradation models in reliability analysis. In *Engineering Asset Lifecycle Management*, pages 369–384. Springer, 2010.

[72] K. Grijspeerdt, L. Mortier, J. De Block, and R. Van Renterghem. Applications of modelling to optimise ultra high temperature milk heat exchangers with respect to fouling. *Food Control*, 15(2):117–130, 2004.

[73] J. M. Grosso, C. Ocampo-Martínez, and V. Puig. A service reliability model predictive control with dynamic safety stocks and actuators health monitoring for drinking water networks. In *Decision and Control (CDC), 2012 IEEE 51st Annual Conference on*, pages 4568–4573. IEEE, 2012.

[74] J. M. Grosso, C. Ocampo-Martinez, and V. Puig. Reliability–based economic model predictive control for generalised flow–based networks including actuators? health–aware capabilities. *International Journal of Applied Mathematics and Computer Science*, 2016.

[75] J. M. Grosso, P. Velarde, C. Ocampo-Martinez, J. M. Maestre, and V. Puig. Stochastic model predictive control approaches applied to drinking water networks. *Optimal Control Applications and Methods*, 38(4):541–558, 2017.

[76] D. Gu and H. Hu. Neural predictive control for a car-like mobile robot. *Robotics and Autonomous Systems*, 39(2):73–86, 2002.

[77] F. Guenab, P. Weber, D. Theilliol, and Y. Zhang. Design of a fault tolerant control system incorporating reliability analysis and dynamic behaviour constraints. *International Journal of Systems Science*, 42(1):219–233, 2011.

[78] D. He, J. Sun, and L. Yu. Economic mpc with a contractive constraint for nonlinear systems. *International Journal of Robust and Nonlinear Control*, 26(18):4072–4087, 2016.

[79] M. Heidarinejad, J. Liu, and P. D. Christofides. Economic model predictive control of nonlinear process systems using lyapunov techniques. *AIChE Journal*, 58(3):855–870, 2012.

[80] A. Heng, S. Zhang, A. C. Tan, and J. Mathew. Rotating machinery prognostics: State of the art, challenges and opportunities. *Mechanical systems and signal processing*, 23(3):724–739, 2009.

[81] C. Hoffmann and H. Werner. A survey of linear parameter-varying control applications validated by experiments or high-fidelity simulations. *IEEE Transactions on Control Systems Technology*, 23(2):416–433, 2015.

[82] D. Hrovat, S. Di Cairano, H. E. Tseng, and I. V. Kolmanovsky. The development of model predictive control in automotive industry: A survey. In *IEEE International Conference on Control Applications (CCA)*, pages 295–302, 2012.

[83] X. Hu, L. Chen, B. Tang, D. Cao, and H. He. Dynamic path planning for autonomous driving on various roads with avoidance of static and moving obstacles. *Mechanical Systems and Signal Processing*, 100:482–500, 2018.

[84] J. Ibarrola, J. Guillén, J. Sandoval, and M. García-Sanz. Modelling of a high temperature short time pasteurization process. *Food Control*, 9(5):267–277, 1998.

[85] J. J. Ibarrola, J. M. Sandoval, M. Garcia-Sanz, and M. Pinzolas. Predictive control of a high temperature–short time pasteurisation process. *Control Engineering Practice*, 10(7):713–725, 2002.

[86] A. K. Jardine, D. Lin, and D. Banjevic. A review on machinery diagnostics and prognostics implementing condition-based maintenance. *Mechanical systems and signal processing*, 20(7):1483–1510, 2006.

[87] S. C. Jeong and P. Park. Constrained mpc algorithm for uncertain time-varying systems with state-delay. *IEEE Transactions on Automatic Control*, 50(2):257–263, 2005.

[88] J. Ji, A. Khajepour, W. W. Melek, and Y. Huang. Path planning and tracking for vehicle collision avoidance based on model predictive control with multiconstraints. *IEEE Transactions on Vehicular Technology*, 66(2):952–964, 2016.

[89] R. Jiang and A. K. Jardine. Health state evaluation of an item: A general framework and graphical representation. *Reliability Engineering & System Safety*, 93(1):89–99, 2008.

[90] T. A. Johansen, R. Shorten, and R. Murray-Smith. On the interpretation and identification of dynamic takagi-sugenofuzzy models. *IEEE Transactions on Fuzzy systems*, 8(3):297–313, 2000.

[91] M. Jungers, R. C. Oliveira, and P. L. Peres. MPC for LPV systems with bounded parameter variations. *International Journal of Control*, 84(1):24–36, 2011.

[92] S. Kadry. *Diagnostics and Prognostics of Engineering Systems: Methods and Techniques: Methods and Techniques*. IGI Global, 2012.

[93] P. Kall, J. Mayer, et al. *Stochastic linear programming*, volume 7. Springer, 1976.

[94] F. Karimi Pour, C. Ocampo-Martinez, and V. Puig. Output-feedback model predictive control of a pasteurization pilot plant based on an lpv model. In *Journal of Physics: Conference Series*, volume 783, page 012029. IOP Publishing, 2017.

[95] F. Karimi Pour, V. Puig, and G. Cembrano. Health-aware lpv-mpc based on a reliability-based remaining useful life assessment. *IFAC-PapersOnLine*, 51(24):1285–1291, 2018.

[96] F. Karimi Pour, V. Puig, and G. Cembrano. Health-aware lpv-mpc based on system reliability assessment for drinking water networks. In *2018 IEEE Conference on Control Technology and Applications (CCTA)*, pages 187–192. IEEE, 2018.

[97] F. Karimi Pour, V. Puig, and G. Cembrano. Economic health-aware lpv-mpc based on system reliability assessment for water transport network. *Energies*, 12(15):3015, 2019.

[98] F. Karimi Pour, V. Puig, and G. Cembrano. Economic mpc-lpv control for the operational management of water distribution networks. *IFAC-PapersOnLine*, 52(23):88–93, 2019.

[99] F. Karimi Pour, V. Puig, and C. Ocampo-Martinez. Economic predictive control of a pasteurization plant using a linear parameter varying model. In *Computer Aided Chemical Engineering*, volume 40, pages 1573–1578. Elsevier, 2017.

[100] F. Karimi Pour, V. Puig, and C. Ocampo-Martinez. Multi-layer health-aware economic predictive control of a pasteurization pilot plant. *International Journal of Applied Mathematics and Computer Science*, 28(1):97–110, 2018.

[101] F. Karimi Pour, V. Puig, and C. Ocampo-Martinez. Model predictive control based on lpv models with parameter-varying delays. In *2019 18th European Control Conference (ECC)*, pages 3644–3649. IEEE, 2019.

[102] F. Karimi Pour, V. Puig Cayuela, and C. Ocampo-Martínez. Health-aware model predictive control of pasteurization plant. In *ACD'16-13th European Workshop on Advanced Control and Diagnosis 17-18 November 2016, Lille, France*, 2016.

[103] F. Karimi Pour, D. Theilliol, V. Puig, and G. Cembrano. Health-aware optimization-based control design: Application to autonomous racing based state of charge. In *2019 4th Conference on Control and Fault Tolerant Systems (SysTol)*, pages 244–249. IEEE, 2019.

[104] F. K. Karimi Pour, V. Puig, and G. Cembrano. Economic health-aware mpc-lpv based on dbn reliability model for water transport network. In *2019 6th International Conference on Control, Decision and Information Technologies (CoDIT)*, pages 1408–1413. IEEE, 2019.

[105] K. Kavsek-Biasizzo, I. Skrjanc, and D. Matko. Fuzzy predictive control of highly nonlinear ph process. *Computers & chemical engineering*, 21:S613–S618, 1997.

[106] S. Kawamoto, K. Tada, A. Ishigame, and T. Taniguchi. An approach to stability analysis of second order fuzzy systems. In *Fuzzy Systems, 1992., IEEE International Conference on*, pages 1427–1434. IEEE, 1992.

[107] V. Kechichian, G. P. Crivellari, J. A. Gut, and C. C. Tadini. Modeling of continuous thermal processing of a non-newtonian liquid food under diffusive laminar flow in a tubular system. *International Journal of Heat and Mass Transfer*, 55(21-22):5783–5792, 2012.

[108] C. M. Kellett. A compendium of comparison function results. *Mathematics of Control, Signals, and Systems*, 26(3):339–374, 2014.

[109] M. T. Khadir and J. Ringwood. Linear and nonlinear model predictive control design for a milk pasteurisation plant. *Control and intelligent systems*, 31(1), 2003.

[110] A. Khelassi, J. Jiang, D. Theilliol, P. Weber, and Y. Zhang. Reconfiguration of control inputs for overactuated systems based on actuators health. In *Proceedings of 18th IFAC World Congress*, 2011.

[111] A. Khelassi, D. Theilliol, and P. Weber. Reconfigurability analysis for reliable fault-tolerant control design. *International Journal of Applied Mathematics and Computer Science*, 21(3):431–439, 2011.

[112] A. Khelassi, D. Theilliol, P. Weber, and J.-C. Ponsart. Fault-tolerant control design with respect to actuator health degradation: An lmi approach. In *Control Applications (CCA), 2011 IEEE International Conference on*, pages 983–988. IEEE, 2011.

[113] A. Khelassi, D. Theilliol, P. Weber, and D. Sauter. A novel active fault tolerant control design with respect to actuators reliability. In *Decision and Control and European Control Conference (CDC-ECC), 2011 50th IEEE Conference on*, pages 2269–2274. IEEE, 2011.

[114] M. Killian, B. Mayer, A. Schirrer, and M. Kozek. Cooperative fuzzy model-predictive control. *IEEE Transactions on Fuzzy Systems*, 24(2):471–482, 2016.

[115] M. V. Kothare, V. Balakrishnan, and M. Morari. Robust constrained model predictive control using linear matrix inequalities. *Automatica*, 32(10):1361–1379, 1996.

[116] M. V. Kothare, V. Balakrishnan, and M. Morari. Robust constrained model predictive control using linear matrix inequalities. *Automatica*, 32(10):1361–1379, 1996.

[117] K. Kunz, S. M. Huck, and T. H. Summers. Fast model predictive control of miniature helicopters. In *Control Conference (ECC), 2013 European*, pages 1377–1382. IEEE, 2013.

[118] H. Kwakernaak and R. Sivan. *Linear optimal control systems*, volume 1. Wiley-interscience New York, 1972.

[119] A. Kwiatkowski, M.-T. Boll, and H. Werner. Automated generation and assessment of affine lpv models. In *Decision and Control, 2006 45th IEEE Conference on*, pages 6690–6695. IEEE, 2006.

[120] M. P. Lafmejani. *Evaluation of Damage-based Material Models for Carbon Fiber-reinforced Polymer Composite Laminate Under Mixed-mode Bending*. PhD thesis, Universiti Teknologi Malaysia, 2014.

[121] Y. Langeron, A. Grall, and A. Barros. Actuator health prognosis for designing lqr control in feedback systems. *Chemical Engineering Transactions*, 33:979–984, 2013.

[122] J. Lawless and M. Crowder. Covariates and random effects in a gamma process model with application to degradation and failure. *Lifetime Data Analysis*, 10(3):213–227, 2004.

[123] S. Lee, S. Jeong, D. Ji, and S. Won. Robust model predictive control for lpv systems with delayed state using relaxation matrices. In *American Control Conference (ACC), 2011*, pages 716–721. IEEE, 2011.

[124] S. M. Lee, J. H. Park, D. H. Ji, and S. C. Won. Robust model predictive control for LPV systems using relaxation matrices. *IET Control Theory & Applications*, 1(6):1567–1573, 2007.

[125] Y. L. Lee. *Fatigue testing and analysis: theory and practice*, volume 13. Butterworth-Heinemann, 2005.

[126] D. Li and Y. Xi. The feedback robust MPC for LPV systems with bounded rates of parameter changes. *IEEE Transactions on Automatic Control*, 55(2):503–507, 2010.

[127] F. Li and J. Xu. A new prognostics method for state of health estimation of lithium-ion batteries based on a mixture of gaussian process models and particle filter. *Microelectronics Reliability*, 55(7):1035–1045, 2015.

[128] N. Li, S.-Y. Li, and Y.-G. Xi. Multi-model predictive control based on the takagi–sugeno fuzzy models: a case study. *Information Sciences*, 165(3-4):247–263, 2004.

[129] F. Liao, J. L. Wang, and G.-H. Yang. Reliable robust flight tracking control: an lmi approach. *IEEE Transactions on Control Systems Technology*, 10(1):76–89, 2002.

[130] F. V. Lima. *Interval Operability: A tool to design the feasible output constraints for non-square model predictive controllers*. ProQuest, USA, 2007.

[131] J. Lofberg. Yalmip: A toolbox for modeling and optimization in MATLAB. In *Computer Aided Control Systems Design, 2004 IEEE International Symposium on*, pages 284–289. IEEE, 2004.

[132] C. J. Lu and W. O. Meeker. Using degradation measures to estimate a time-to-failure distribution. *Technometrics*, 35(2):161–174, 1993.

[133] Q. Lu, P. Shi, H.-K. Lam, and Y. Zhao. Interval type-2 fuzzy model predictive control of nonlinear networked control systems. *IEEE Trans. Fuzzy Systems*, 23(6):2317–2328, 2015.

[134] Y. Lu and Y. Arkun. Quasi-min-max MPC algorithms for LPV systems. *Automatica*, 36(4):527–540, 2000.

[135] Y. Lu and Y. Arkun. Quasi-min-max mpc algorithms for lpv systems. *Automatica*, 36(4):527–540, 2000.

[136] Y. Lu and Y. Arkun. A quasi-min-max MPC algorithm for linear parameter varying systems with bounded rate of change of parameters. In *American Control Conference*, volume 5, pages 3234–3238, USA, 2000.

[137] F. Machuca and O. Urresta. Educational software for the teaching of the dynamics and control of shell and tube heat exchangers. *Revista Facultad de Ingeniería Universidad de Antioquia*, (44):52–60, 2008.

[138] J. M. Maciejowski. *Predictive control: with constraints*. Pearson education, USA, 2002.

[139] M. Maeda, M. Shimakawa, and S. Murakami. Predictive fuzzy control of an autonomous mobile robot with forecast learning function. *Fuzzy Sets and Systems*, 72(1):51–60, 1995.

[140] J. M. Maestre, R. R. Negenborn, et al. *Distributed model predictive control made easy*, volume 69. Springer, 2014.

[141] A. Marcos and G. J. Balas. Development of linear-parameter-varying models for aircraft. *Journal of Guidance, Control, and Dynamics*, 27(2):218–228, 2004.

[142] J. C. Marin, A. Barroso, F. Paris, and J. Canas. Study of damage and repair of blades of a 300kW wind turbine. *Energy*, 33(7):1068–1083, 2008.

[143] D. Q. Mayne. Model predictive control: Recent developments and future promise. *Automatica*, 50(12):2967–2986, 2014.

[144] D. Q. Mayne, J. B. Rawlings, C. V. Rao, and P. O. Scokaert. Constrained model predictive control: Stability and optimality. *Automatica*, 36(6):789–814, 2000.

[145] L. Mays. *Urban stormwater management tools*. McGraw Hill Professional, 2004.

[146] W. Q. Meeker, L. A. Escobar, and C. J. Lu. Accelerated degradation tests: modeling and analysis. *Technometrics*, 40(2):89–99, 1998.

[147] J. Mohammadpour and C. W. Scherer. *Control of linear parameter varying systems with applications*. Springer Science & Business Media, 2012.

[148] W. Mokhtar, F. S. Taip, N. Aziz, and S. Noor. Process control of pink guava puree pasteurization process: Simulation and validation by experiment. *International Journal on Advanced Science, Engineering and Information Technology*, 2(4):302–305, 2012.

[149] M. Musallam and C. M. Johnson. An efficient implementation of the rainflow counting algorithm for life consumption estimation. *IEEE Transactions on reliability*, 61(4):978–986, 2012.

[150] K. R. Muske and T. A. Badgwell. Disturbance modeling for offset-free linear model predictive control. *Journal of Process Control*, 12(5):617–632, 2002.

[151] K. R. Muske and J. B. Rawlings. Model predictive control with linear models. *AIChE Journal*, 2(39):262–287, 1993.

[152] S. Nahmias and Y. Cheng. *Production and operations analysis*, volume 6. McGraw-hill New York, 2009.

[153] A. Negiz, P. Ramanauskas, A. Çinar, J. E. Schlesser, and D. J. Armstrong. Modeling, monitoring and control strategies for high temperature short time pasteurization systems?3. statistical monitoring of product lethality and process sensor reliability. *Food control*, 9(1):29–47, 1998.

[154] A. Nemirovski and A. Shapiro. Convex approximations of chance constrained programs. *SIAM Journal on Optimization*, 17(4):969–996, 2006.

[155] J. Ni and J. Hu. Dynamics control of autonomous vehicle at driving limits and experiment on an autonomous formula racing car. *Mechanical Systems and Signal Processing*, 90:154–174, 2017.

[156] A. Niesłony. Determination of fragments of multiaxial service loading strongly influencing the fatigue of machine components. *Mechanical Systems and Signal Processing*, 23(8):2712–2721, 2009.

[157] R. Ocampo. Fatigue failures in pumps-part 1. *World Pumps*, 2008(500):42–45, 2008.

[158] C. Ocampo-Martínez, V. Puig, G. Cembrano, R. Creus, and M. Minoves. Improving water management efficiency by using optimization-based control strategies: the barcelona case study. *Water science and technology: water supply*, 9(5):565–575, 2009.

[159] C. Ocampo-Martinez, V. Puig, G. Cembrano, and J. Quevedo. Application of predictive control strategies to the management of complex networks in the urban water cycle [applications of control]. *IEEE Control Systems*, 33(1):15–41, 2013.

[160] H. Ohtake, K. Tanaka, and H. O. Wang. Fuzzy modeling via sector nonlinearity concept. *Integrated Computer-Aided Engineering*, 10(4):333–341, 2003.

[161] S. Osaki and T. Nakagawa. Bibliography for reliability and availability of stochastic systems. *IEEE Transactions on Reliability*, 25(4):284–287, 1976.

[162] C. C. Osgood. *Fatigue Design: International Series on The Strength and Fracture of Materials and Structures*. Elsevier, 2013.

[163] C. I. Ossai, B. Boswell, and I. J. Davies. A markovian approach for modelling the effects of maintenance on downtime and failure risk of wind turbine components. *Renewable Energy*, 96:775–783, 2016.

[164] A. Ostfeld. Reliability analysis of water distribution systems. *Journal of Hydroinformatics*, 6(4):281–294, 2004.

[165] T. Ouarda and J. Labadie. Chance-constrained optimal control for multireservoir system optimization and risk analysis. *Stochastic environmental research and risk assessment*, 15(3):185–204, 2001.

[166] H. Pacejka. *Tire and vehicle dynamics*. Elsevier, 2005.

[167] P. Park and S. C. Jeong. Constrained RHC for LPV systems with bounded rates of parameter variations. *Automatica*, 40(5):865–872, 2004.

[168] M. Pecht. Prognostics and health management of electronics wiley-intersicence. *New York, NY*, 2008.

[169] M. Pecht. Prognostics and health management of electronics. *Encyclopedia of Structural Health Monitoring*, 2009.

[170] M. Pecht and S. Kumar. Data analysis approach for system reliability, diagnostics and prognostics. In *Pan pacific microelectronics symposium, Kauai, Hawaii, USA*, pages 22–24, 2008.

[171] E. B. Pereira, R. Galvao, and T. Yoneyama. Model predictive control with contraints on accumulated degradation of actuators. In *ABCM Symposium Series in Mechatronics*, pages 394–402, 2010.

[172] G. L. Plett. Sigma-point kalman filtering for battery management systems of lipb-based hev battery packs: Part 1: Introduction and state estimation. *Journal of Power Sources*, 161(2):1356–1368, 2006.

[173] F. K. Pour, V. Puig, and G. Cembrano. Economic reliability-aware mpc-lpv for operational management of flow-based water networks including chance-constraints programming. *Processes*, 8(1):60, 2020.

[174] M. Pourasghar, V. Puig, and C. Ocampo-Martinez. Comparison of set-membership and interval observer approaches for state estimation of uncertain systems. In *2016 European Control Conference (ECC)*, pages 1111–1116. IEEE, 2016.

[175] C. Poussot-Vassal, O. Sename, L. Dugard, P. Gaspar, Z. Szabo, and J. Bokor. A new semi-active suspension control strategy through lpv technique. *Control Engineering Practice*, 16(12):1519–1534, 2008.

[176] C. Poussot-Vassal, O. Sename, L. Dugard, P. Gaspar, Z. Szabo, and J. Bokor. Attitude and handling improvements through gain-scheduled suspensions and brakes control. *Control Engineering Practice*, 19(3):252–263, 2011.

[177] V. Puig, C. Ocampo-Martinez, and S. M. De Oca. Hierarchical temporal multi-layer decentralised mpc strategy for drinking water networks: application to the barcelona case study. In *Control & Automation (MED), 2012 20th Mediterranean Conference on*, pages 740–745. IEEE, 2012.

[178] S. J. Qin and T. A. Badgwell. An overview of industrial model predictive control technology. *In AIChE Symposium Series*, 93(316):232–256, 1996.

[179] S. J. Qin and T. A. Badgwell. A survey of industrial model predictive control technology. *Control engineering practice*, 11(7):733–764, 2003.

[180] G. V. Raffo, G. K. Gomes, J. E. Normey-Rico, C. R. Kelber, and L. B. Becker. A predictive controller for autonomous vehicle path tracking. *IEEE transactions on intelligent transportation systems*, 10(1):92–102, 2009.

[181] J. B. Rawlings, D. Angeli, and C. N. Bates. Fundamentals of economic model predictive control. In *CDC*, pages 3851–3861, 2012.

[182] J. B. Rawlings, D. Bonné, J. B. Jorgensen, A. N. Venkat, and S. B. Jorgensen. Unreachable setpoints in model predictive control. *IEEE Transactions on Automatic Control*, 53(9):2209–2215, 2008.

[183] J. B. Rawlings and D. Q. Mayne. *Model predictive control: Theory and design*. Nob Hill Pub., 2009.

[184] J. V. Ringwood and S. Simani. Overview of modelling and control strategies for wind turbines and wave energy devices: Comparisons and contrasts. *Annual Reviews in Control*, 40:27–49, 2015.

[185] D. J. Rodriguez, J. J. Martinez, and C. Berenguer. An architecture for controlling the remaining useful lifetime of a friction drive system. *IFAC-PapersOnLine*, 51(24):861–866, 2018.

[186] A. Rosich and C. Ocampo-Martinez. Real-time experimental implementation of predictive control schemes in a small-scale pasteurization plant. In *Developments in Model-Based Optimization and Control*, pages 255–273. Springer, 2015.

[187] U. Rosolia, A. Carvalho, and F. Borrelli. Autonomous racing using learning model predictive control. In *2017 American Control Conference (ACC)*, pages 5115–5120. IEEE, 2017.

[188] D. Rotondo, F. Nejjari, and V. Puig. Quasi-LPV modeling, identification and control of a twin rotor MIMO system. *Control Engineering Practice*, 21(6):829–846, 2013.

[189] D. Rotondo, F. Nejjari, and V. Puig. Quasi-lpv modeling, identification and control of a twin rotor mimo system. *Control Engineering Practice*, 21(6):829–846, 2013.

[190] J. A. Roubos, S. Mollov, R. Babuška, and H. B. Verbruggen. Fuzzy model-based predictive control using takagi–sugeno models. *International Journal of Approximate Reasoning*, 22(1-2):3–30, 1999.

[191] W. J. Rugh and J. S. Shamma. Research on gain scheduling. *Automatica*, 36(10):1401–1425, 2000.

[192] M. S. Sadeghi, N. Vafamand, and M. H. Khooban. Lmi-based stability analysis and robust controller design for a class of nonlinear chaotic power systems. *Journal of the Franklin Institute*, 353(13):2835–2858, 2016.

[193] B. Saha and K. Goebel. Modeling li-ion battery capacity depletion in a particle filtering framework. In *Proceedings of the annual conference of the prognostics and health management society*, pages 2909–2924, 2009.

[194] R. Schacht-Rodriguez, G. Ortiz-Torres, C. Garcia-Beltran, C. Astorga-Zaragoza, J.-C. Ponsart, and D. Theilliol. Soc estimation using an extended kalman filter for uav applications. In *2017 International Conference on Unmanned Aircraft Systems (ICUAS)*, pages 179–187. IEEE, 2017.

[195] J. S. Shamma. *Analysis and design of gain scheduled control systems*. PhD thesis, Massachusetts Institute of Technology, 1988.

[196] J. S. Shamma. An overview of lpv systems. In *Control of linear parameter varying systems with applications*, pages 3–26. Springer, 2012.

[197] K. Shi, B. Wang, L. Yang, S. Jian, and J. Bi. Takagi–sugeno fuzzy generalized predictive control for a class of nonlinear systems. *Nonlinear Dynamics*, 89(1):169–177, 2017.

[198] T. Shi and H. Su. Sampled-data MPC for LPV systems with input saturation. *IET Control Theory & Applications*, 8(17):1781–1788, 2014.

[199] A. Shum, K. Morris, and A. Khajepour. Direction-dependent optimal path planning for autonomous vehicles. *Robotics and Autonomous Systems*, 70:202–214, 2015.

[200] X.-S. Si, W. Wang, C.-H. Hu, and D.-H. Zhou. Remaining useful life estimation–a review on the statistical data driven approaches. *European journal of operational research*, 213(1):1–14, 2011.

[201] D. Siljak. On reliability of control. In *Decision and Control including the 17th Symposium on Adaptive Processes, 1978 IEEE Conference on*, volume 17, pages 687–694. IEEE, 1979.

[202] D. D. Šiljak. Reliable control using multiple control systems. *International Journal of Control*, 31(2):303–329, 1980.

[203] D. D. Siljak. *Decentralized control of complex systems*. Courier Corporation, 2011.

[204] R. Sivakumar, K. S. Manic, V. Nerthiga, R. Akila, and K. Balu. Application of fuzzy model predictive control in multivariable control of distillation column. *International Journal of Chemical Engineering and Applications*, 1(1):38, 2010.

[205] P. Sopasakis, A. K. Sampathirao, A. Bemporad, and P. Patrinos. Uncertainty-aware demand management of water distribution networks in deregulated energy markets. *Environmental Modelling & Software*, 101:10–22, 2018.

[206] T. Takagi and M. Sugeno. Fuzzy identification of systems and its applications to modeling and control. *IEEE transactions on systems, man, and cybernetics*, (1):116–132, 1985.

[207] K. Tanaka and H. O. Wang. *Fuzzy control systems design and analysis: a linear matrix inequality approach*. John Wiley & Sons, 2004.

[208] S. Terradellas Balaguer. Small-scale pasteurization plants: modeling and real-time control. Master's thesis, Universitat Politècnica de Catalunya, 2016.

[209] M. Tortorella. Reliability theory: With applications to preventive maintenance, 2001.

[210] K. L. Tsui, N. Chen, Q. Zhou, Y. Hai, and W. Wang. Prognostics and health management: A review on data driven approaches. *Mathematical Problems in Engineering*, 2015, 2015.

[211] J. Van Noortwijk. A survey of the application of gamma processes in maintenance. *Reliability Engineering & System Safety*, 94(1):2–21, 2009.

[212] R. Verschueren, M. Zanon, R. Quirynen, and M. Diehl. Time-optimal race car driving using an online exact hessian based nonlinear mpc algorithm. In *2016 European Control Conference (ECC)*, pages 141–147. IEEE, 2016.

[213] M. Vidyasagar and N. Viswanadham. Reliable stabilization using a multi-controller configuration. *Automatica*, 21(5):599–602, 1985.

[214] G. W. Vogl, B. A. Weiss, and M. Helu. A review of diagnostic and prognostic capabilities and best practices for manufacturing. *Journal of Intelligent Manufacturing*, pages 1–17, 2016.

[215] N. Wada, K. Saito, and M. Saeki. Model predictive control for linear parameter varying systems using parameter dependent Lyapunov function. *IEEE Transactions on Circuits and Systems II: Express Briefs*, 53(12):1446–1450, 2006.

[216] L. Wang. *Model predictive control system design and implementation using MATLAB*. Springer, Germany, 2009.

[217] N. Watrin, B. Blunier, and A. Miraoui. Review of adaptive systems for lithium batteries state-of-charge and state-of-health estimation. In *2012 IEEE Transportation Electrification Conference and Expo (ITEC)*, pages 1–6. IEEE, 2012.

[218] P. Weber, C. Simon, D. Theilliol, and V. Puig. Fault-tolerant control design for over-actuated system conditioned by reliability: a drinking water network application. In *8th IFAC Symposium on Fault Detection, Supervision and Safety of Technical Processes, SAFEPROCESS 2012*, page CDROM, 2012.

[219] W. Weibull. Wide applicability. *Journal of applied mechanics*, 103(730):293–297, 1951.

[220] A. P. White, G. Zhu, and J. Choi. *Linear parameter-varying control for engineering applications*. Springer, 2013.

[221] C. Wong, S. L. Shah, M. M. Bourke, and D. G. Fisher. Adaptive fuzzy relational predictive control. *fuzzy Sets and systems*, 115(2):247–260, 2000.

[222] F. Wu and K. M. Grigoriadis. Lpv systems with parameter-varying time delays: analysis and control. *Automatica*, 37(2):221–229, 2001.

[223] N. E. Wu, X. Wang, M. Smapath, and G. Kott. An operational approach to budget-constrained reliability allocation. In *15th IFAC World Congress, Barcelona, Spain*, pages 199–204, 2002.

[224] W. Xu, J. Pan, J. Wei, and J. M. Dolan. Motion planning under uncertainty for on-road autonomous driving. In *2014 IEEE International Conference on Robotics and Automation (ICRA)*, pages 2507–2512. IEEE, 2014.

[225] S. Yu, C. Böhm, H. Chen, and F. Allgöwer. Finite horizon model predictive control with ellipsoid mapping of uncertain linear systems. *IET Control Theory & Applications*, 6(18):2820–2828, 2012.

[226] S. Yu, C. Böhm, H. Chen, and F. Allgöwer. Model predictive control of constrained LPV systems. *International Journal of Control*, 85(6):671–683, 2012.

[227] K. Zeng, N.-Y. Zhang, and W.-L. Xu. A comparative study on sufficient conditions for takagi-sugeno fuzzy systems as universal approximators. *IEEE Transactions on fuzzy systems*, 8(6):773–780, 2000.

[228] J. Zhang and J. Lee. A review on prognostics and health monitoring of li-ion battery. *Journal of Power Sources*, 196(15):6007–6014, 2011.

[229] L. Zhang, W. Xie, Z. Zhong, and J. Wang. Robust model predictive control synthesis for state-delayed systems with randomly occurring input saturation nonlinearities. *Transactions of the Institute of Measurement and Control*, 40(1):179–190, 2018.

[230] T. Zhang, G. Feng, and J. Lu. Fuzzy constrained min-max model predictive control based on piecewise lyapunov functions. *IEEE Transactions on Fuzzy Systems*, 15(4):686–698, 2007.